Study on osteoarthritic joint: regenerative potential and disease markers

Alice Tirnoveanu
BSc (Hons)

Submitted in fulfilment of requirements for the degree of Doctor of Philosophy (PhD)

Faculty of Science, Engineering and Social Sciences, School of Psychology and Life Sciences, Department of Life Sciences

Canterbury Christ Church University

Canterbury

March 2022

Abstract

Osteoarthritis (OA) is the most predominant form of arthritis. It is characterised by joint chronic pain and severe tissue degeneration that ultimately can lead to disability. Although scientists together with clinicians have identified the risk factors for the development of OA, the underlying cause has not been elucidated yet. The current treatment options for OA are focused on symptom relief rather than the prevention or reverse of degeneration. Ultimately, the afflicted joint will have to be surgically replaced with medical-grade prosthesis to restore full function.

In this study we focus on tissue regeneration of bone and cartilage in joints by modulation of the resident population of stem/progenitor cells, as a new approach in the treatment of musculo-skeletal injury and degeneration.

The work presented in this study addresses the presence of neurotrophins receptor OA animal model, the effect of Neurotrophin-3 (NT-3) on the proliferation and differentiation of primary stem/progenitors from human hip joints affected by OA compared with stem/progenitors from healthy bone marrow, and an extensive proteomic analysis of the proteins in the EVs secreted by the previously mentioned human cell populations.

The results obtained in this research project indicate that 1. OA induces a decrease in the incidence of neurotrophin receptors in the cells of the joint, 2. NT-3 has the potential to accelerate the bone tissue healing process, by stimulation of osteogenesis, and 3. the proteomic content of EVs derived from tissue with OA it can serve as indicator of the disease.

Table of Contents

List of Tables

List of Figures

Acknowledgements

Author's Declaration

I, Alice N. Tirnoveanu, declare that the work included in this thesis is entirely my own. Where information has been derived from other sources, I confirm that this has been indicated.

Chapter 1: Introduction

1.1. Human Skeletal Joint

A joint or an articulation is defined as a complex structure that connects the bones of human skeleton and links the skeletal system into a functional entity.

In foetal life, the development of the skeletal system is derived from the embryonic mesoderm via the limb bud. The formation of the limbs begins in the week four of the gestation and is initiated through the Apical Ectodermal Ridge (AER) and the Zone of Polarization Activity (ZPA). AER directs the longitudinal growth and together with the rapidly dividing mesodermal cells from the progression zone is involved in the limb elongation (Gilbert SF, 2000). The dorsal/ventral growth is controlled by the Wnt signalling pathway. The anterior-posterior limb growth is control by ZAP and together with the mesodermal stroma cells determine the formation of the digits (Geetha-Loganathan, Nimmagadda and Scaal, 2008). For the healthy limb formation, bi-directional growth has to happen at the same time. Growth factor such as FGF-4 and FGF-8 are vital in this process (Boulet *et al.*, 2004). They simultaneously initiate the Wnt signalling pathway in both, AER and ZAP. Upregulation and downregulation of FGF-4 and FGF-8 during limb development result into conditions such as conditional amputation and polydactyly (Lu, Minowada and Martin, 2006). On the other hand, the development of cranial bones and the joints between them derive from the neural crest cells. In the early development, the primary skeleton is cartilaginous (Knight and Schilling, 2013). The bone tissue forms through direct development where MSCs differentiate direct into cells that induce intramembranous ossification or through indirect development where MSCs first differentiate into hyaline cartilage templates for future bones. These cartilaginous templates are progressively replaced by the bone formation post condensation and ossification (Setiawati and Rahardjo, 2019). Concomitantly with the bone development, the formation of the joints occurs. In between the developing bones, the connective tissue of the joints starts to form on the sixth week of the embryonic development. On the eighth week, the articular capsule starts to form. The cells in the middle of the connective tissue induce apoptosis,

forming the joint cavity that is filled with synovial fluid secreted by the mesenchymal stem cells (Breeland *et al.*, 2021).

Joints are of multiple types and are classified by the type of tissue present (fibrous, cartilaginous, and synovial) (Fig. 1.1) and by the degree of movement permitted (synarthrosis, amphiarthrosis and diarthrosis).

```
                                    ┌─── Sutures
                        ┌─ Fibrous ─┼─── Gomphoses
                        │           └─── Syndesmoses
                        │
                        │                ┌─── Synchondroses
Joints ─────────────────┼─ Cartilaginous ┤
                        │                └─── Symphyses
                        │
                        │           ┌─── Hinge
                        │           ├─── Saddle
                        │           ├─── Plane
                        └─ Synovial ─┼─── Pivot
                                    ├─── Condyloid
                                    └─── Ball and Socket
```
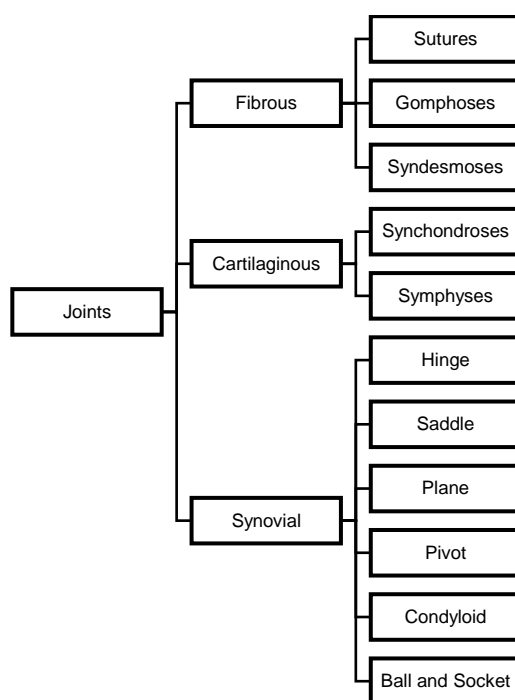
Figure 1. 1. Classification of joints based on the tissue

The most common type of joint is the synovial joint, and its general structure is defined by three main parts: articular capsule, articular cartilage, and the synovial fluid, as shown in Fig. 1. 2 (Tarafder and Lee, 2016). Articular capsule consists of a fibrous layer that holds together the articulating bones, and of a synovial layer that mediates the nutrient exchange between the blood vessels and the joint and secretes the synovial fluid. Synovial fluid is located in the joint capsule, and it helps with lubrication, shock absorption and nutrient, waste and dissolved gas distribution to and from the articular cartilage. The articular hyaline cartilage is avascular, aneural and alymphatic with lubricated surface and with key roles in friction-reduction, shock absorption and load bearing. It is constituted of a dense network of extracellular matrix (ECM)

containing chondrocytes distributed in spaces called lacunae. ECM is made of water, collagen fibres, proteoglycans, and other non-collagenous proteins such as fibronectin, cartilage oligomeric matrix protein (COMP) and link proteins (Hui *et al.*, 2012).

About two-thirds of the adult articular cartilage is made of collagen. The most predominant type is Collagen type II. Collagens III, VI, IX, X, XI, XII and XIV are also present, but in a much lower percentage (Dimicco *et al.*, 2002). Together with the proteoglycans, collagen forms the fibrillar networks characterised by collagen distribution in collagen fibrils (Becerra *et al.*, 2010). The orientation of these is crucial for the strength of the articular cartilage. In the mechanism of tissue injury, collagen breakdown is considered irreversible, without the possibility of repair.

Aggrecan, known also as cartilage-specific proteoglycan core protein is the most abundant proteoglycan in the ECM and critical for cartilage structure and the function of the joint. Structural, aggrecan consists of two globular domains (G1 and G2) at the N-terminal end and one globular domain (G3) at the C-terminal end, separated by a large extended domain (CS) that is heavily modified by glycosaminoglycans (GAGs) (Kiani *et al.*, 2002). Aggrecan interacts with hyaluronic acid and link proteins, inducing aggregation and modulation of chondrocytes in the ECM. Together with type-II collagen, aggrecan forms the majority of articular cartilage, this link being critical for the tissue homeostasis (Kiani *et al.*, 2002).
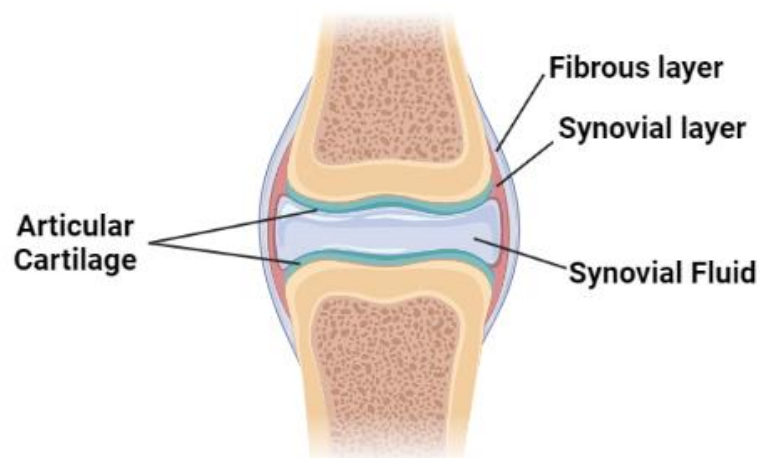
Figure 1. 2. Schematic representation of the synovial joint

In terms of innervation, synovial joints hold a dense network of articular nerves, mainly in the articular capsule, which transmit both, proprioceptive and nociceptive signals. The articular arteries that ensure the blood supply of the joint are located in the joint capsule, no further away than synovial fluid. They are accompanied by the articular veins in the synovial membrane (Sperry *et al.*, 2017).

1.2.   Osteoarthritis

1.2.1. Disease pathology

The most common joint pathology is osteoarthritis. According to The State of Musculoskeletal Health 2021 of Versus Arthritis, in UK over 8.5 million people suffer from osteoarthritis. It is considered a condition of musculoskeletal pain and it affects mainly the limb joints and the spine (The State of Musculoskeletal health 2021 Arthritis and other musculoskeletal conditions in numbers, 2021). It mainly occurs in the older population and the main risk factors are considered the age, sex, obesity, previous joint injury as well as genetic factors. According to the data presented in the Versus Arthritis report, women are more prone to develop degenerative osteoarthritis and the most common affected joint are in arms, hands, hips, legs and feet. Osteoarthritis leading symptom is the chronic pain, which can lead to physical inactivity and overall decrease of quality of life.

The second most common joint condition is rheumatoid arthritis. In 2021, in the UK only, over 430,000 adults suffer from this condition. It is considered an inflammatory condition and in comparison, with osteoarthritis it can affect any age, it has a rapid onset and can affect any part of the body, including the internal organs. It is treated by suppressing the immune system. Genetic factors, sex, smoking and obesity are the main risk factors in this order.

In UK, the healthcare cost of the osteoarthritis and rheumatoid arthritis is estimated to be over £10 billion each year. It is projected that this amount will increase in the next years.

Joints are designed to be used over and over again and to be resistant to daily activities without occurrence of injury.

Osteoarthritis arises when articular cartilage presents injury, and the repair process cannot sustain it. Unfortunately, the main cause of degenerative osteoarthritis remains still an unclear at this moment in time. Although, there have been established the risk factors that can make joints susceptible to osteoarthritis. Joint deformity, malalignment, and previous injury to the protective structures of the joint represent some of the central risk factors. Together with those, vulnerabilities such as age, gender, genetic susceptibility, or nutritional factors can contribute to the onset or the progression of osteoarthritis (Martel-Pelletier *et al.*, 2016).

Osteoarthritis is a disease that occurs mainly later in age. However, elderly individuals do not always develop osteoarthritis, suggesting that it is not a universal characteristic of aging. Moreover, osteoarthritis has a higher prevalence in women than men. Before the age of 50, men are more likely to develop osteoarthritis, while after the age of 50 women are more prone to it. It is thought that this gender difference is related to the hormone deficiency that progresses in women around the age of 50 (Zhang and Jordan, 2010). In contrast, rheumatoid arthritis affects women more and the onset of the disease can appear at any age. Less than 30% of people affected by rheumatoid arthritis in UK are men, while over 70% of those suffering of this condition are women, according to Versus Arthritis 'The State of Musculoskeletal Health 2021' report.

The prevalence of the osteoarthritis is different across the joints. It seems to affect specific joints while sparing the others. The most affected joints appear to be the hip, the knee, the cervical and lumbosacral spine, and metatarsophalangeal joint. The affected joints are mainly located in the lower limbs and implicated in the load bearing support. On the other hand, the joints such as the wrist, the elbow are less affected by osteoarthritis on-set with time. The most obvious explanation for this could be the load bearing stress that the lower limbs joints are exposed to. Researchers such as Richard *et al.*, brought up to light the hypothesis that osteoarthritis might arise as an evolutionary problem. Before the evolution to biped occurred, the human body weight was distributed across all four limbs for movement. At the current evolutionary scale, the human body relies only on lower limbs for movements and on the spine for holding the body erect. All of these come in addition to the hypothesis that osteoarthritis might have wear and tear causes.

At the same time, there are joints that are subjected to the same amount of load but are affected differently by this degenerative disease. Research in this topic revealed that the inflammatory component of osteoarthritis has the potential to worsen the degeneration more in the knee than in the ankle joint, throughout the cytokine-mediated injury response (Eger *et al.*, 2002).

The first indication of osteoarthritis disease is the loss of hyaline articular cartilage in the joint. Consequently, the joint as a whole becomes less effective in lubrification and shock absorption when normal movements are executed. Repeated friction results in degeneration. Symptoms associated with it are discomfort, stiffness, and chronic pain. This condition mainly affects the joints that are responsible of the full body weight support, such as hip and knee joints. The damage at the articular cartilage level is central for the on-set of osteoarthritis, but not the only part of the joint that is involved in the pathophysiology. In the early stages, the mechanism of the disease tends to be dynamic, where the damaged cartilage attempts to repair itself through increased extracellular matrix synthetises. This process is controlled by the growth factors and cytokines secreted by the cells located in the synovial layer (Goldring and Marcu, 2009).

In normal adult cartilage, chondrocytes are relatively idle cells. In osteoarthritis, the normal resting state of chondrocytes is disrupted, and these types of cells start to proliferate, form clusters, and increase the production of matrix proteins and enzymes (Goldring and Marcu, 2009). These are activated as part of the injury response. When mechanical injury occurs results in an inflammatory response, resulting in chondrocytes being activated through NF-kB and MAPK pathways (Choi *et al.*, 2019).

Aggrecan, is the most abundant macromolecule found in healthy cartilage, which is mainly responsible of the mechanical properties of the cartilage. Aggrecan consists of small negatively charged GAG chains. This property makes GAGs to be in close proximity of each other and when intertwined with Collagen type II induces electrostatic repulsion. Electrostatic repulsion of aggrecan is what creates the stiffness of the cartilage (Sophia Fox, Bedi and Rodeo, 2009).

Apart from aggrecan, the matrix of healthy cartilage includes Collagen type II. It becomes organised in collagen fibrils under the influence of aggrecan, forming the support network that maintains the ECM's integrity (Han, Grodzinsky and Ortiz, 2011).

In osteoarthritis, the viability of ECM is altered by a series of events. First of all, the synthesis of aggrecan is decreased. These changes in the ECM composition affects the stiffness of the tissue making it more prone to mechanical fault. Secondly, collagen type II's synthesis is decreased while collagen type I's synthesis is increased (Maldonado and Nam, 2013). Collagen type I is specific to bone, and it has a lower content of hydroxy-lysine, glucosyl and galactosyl residues, comparative with Collagen type II. These residues are essential in the interactions with aggrecan in collagen fibril formation (Gelse, Pöschl and Aigner, 2003). The collagen type I fibrils are shorter than Collagen type II fibrils. This aspect affects the elasticity of the matrix. The cartilage affected by osteoarthritis is less elastic making it predisposed to fissure formation and fibrillation (Silver, Bradica and Tria, 2002).

Moreover, the disruption in the aggrecan-collagen ratio increases the presence of negative charges in the ECM and attracts more water, causing swelling of the tissue.

Factors across all three structure, synovium, cartilage, and bone are involved in the osteoarthritis onset and progression. These are illustrated in Fig. 1.3.
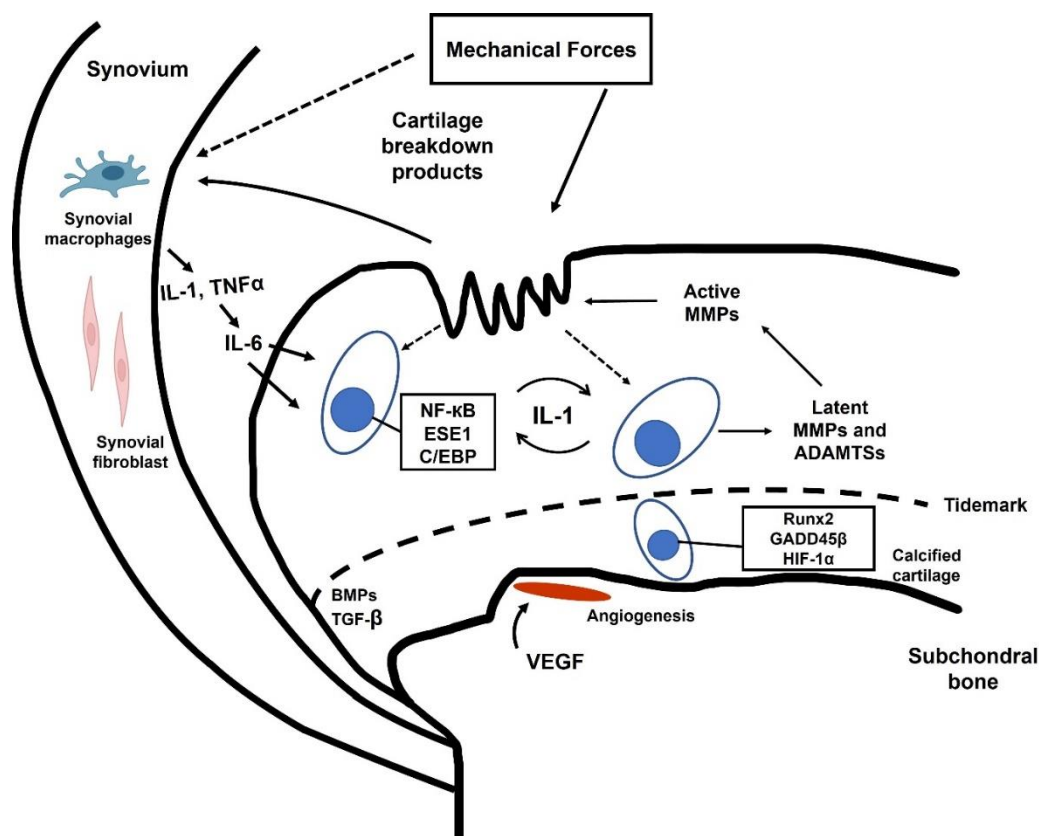
Figure 1. 3. Factors involved in the osteoarthritis process in the synovium, cartilage and bone (adapted from Goldring and Marcu, 2009).
This diagram depicts the cartilage being destroyed as a result of mechanical stress and biological processes. Stress-induced intracellular signals, catabolic cytokines such as interleukin-1 (IL-1) and tumour necrosis factor alpha (TNF-α), chemokines, and other pro-inflammatory mediators produced by synovial cells and chondrocytes result in the upregulation of cartilage-degrading enzymes of the matrix metalloproteinase (MMP) and ADAMTS families. Matrix degradation products have the potential to act as a feedback regulator of these cellular activities. Additionally, anabolic molecules such as bone morphogenetic proteins (BMPs) and transforming growth factor beta (TGF-β) may be increased and contribute to osteophyte production. Along with matrix loss, early changes such as chondrocyte proliferation and hypertrophy, increased cartilage calcification with tidemark advancement, and microfractures with angiogenesis from the subchondral bone, possibly mediated by vascular endothelial growth factor (VEGF), can be observed in late osteoarthritis samples obtained from patients after total joint replacement.

Furthermore, Wnt/ β-catenin signalling pathway may also be implicated in the cartilage damage in osteoarthritis. When activated through the Frizzled receptors of chondrocytes (FRP1, FRP2, FRZB/FRP3, FRP4 and FRP5), increased β-catenin activity has the potential to promote matrix destruction (Luyten, Tylzanowski and Lories, 2009; Blom *et al*., 2009). Studies where Wnt signalling pathway was inhibited

in patient with hip osteoarthritis showed a reduction in the progression of the disease (Lane *et al.*, 2007). Overall, the implication of Wnt signalling pathway, while well defined in the process of osteo-chondro differentiation, remains still largely unknown in osteoarthritis.

In the event of cartilage tissue damage due to injury, an immune response is generally initiated. It is mainly characterised by the secretion of degradative enzymes. This response's main aim is to maintain tissue homeostasis while ECM is re-constructed in the right proportions.

In cartilage tissue presenting osteoarthritis characteristics, the immune response can be triggered by increase of ECM synthesis following chondrocyte proliferation. A prolonged inflammatory response can lead to formation of autoantibodies which can severely impair the tissue repair. An uncontrolled ECM formation can lead to over-production of unnecessary non-viable tissue in the joint. As the joint is a mobile structure, any additional tissue inhibits natural motions, resulting in tissue friction, that finally will lead to the structural damage.

This complex process affects not only the articular cartilage but also the rest of the structures in the joint, making osteoarthritis a whole joint disease with a strong inflammatory component.

The erosion can extend from the cartilage to the subchondral bone. This can lead to bone growth into the cartilage area (Oegema *et al.*, 1997). This type of growth is called chondro-osteophytes. The mechanism of action is still unclear. It seems to appear in parallel with the rapid bone remodelling responsible of dense bone tissue. Some investigators suggest that a combination of cell migration and impaired differentiation are responsible of this occurrence (Lu *et al.*, 2014; Ding *et al.*, 2012; Catheline *et al.*, 2019) As a result of chondro-osteophytes growth, the friction in the joint increases, and can lead to discomfort and movement impairment. Extensive bony remodelling can also result in denser bone by ossification of the endochondral bone, with obliteration of the intertrabecular spaces (Hauge *et al.*, 2001; Pan *et al.*, 2012). This makes the bone less able to attenuate shock.

1.2.2. Diagnosis

Clinically, osteoarthritis is generally diagnosed based on the joint pain and discomfort along with radiographic indications of the disease (the presence of osteophytes in the cartilage and/or dense bone in the vicinity of the joint, reduced cartilage layer, possible increased bone density and sometimes the presence of bone cysts) (Braun and Gold, 2012). Osteoarthritis is not a single type of joint degenerative disease. It appears to have a complex pathophysiology that manifests differently in different patients (Glyn-Jones *et al.*, 2015). Many people that have been diagnosed with structural osteoarthritis experience mild to non-existent pain. They usually get diagnosed through radiographic evidence (Wang, Yuan and Xie, 2018). While other patients with early-onset osteoarthritis experience episodes of chronic pain with no structural changes observed in their radiographic investigation. This indicates that structural changes occur relatively late in the disease course. By then, many irreversible pathologic changes have taken place in the joint (Taruc-Uy and Lynch, 2013). In addition, tests can be carried out in order to rule out other causes of the joint chronic pain, such as rheumatoid arthritis (Maloley *et al.*, 2021). Furthermore, testing of the synovial fluid can determine the status of inflammation in the affected joint, helping clinicians taking more precise decision regarding the stage of the disease (Becker, Daily and Pohlgeers, 2016).

1.2.3. Therapies

Osteoarthritis causes chronic pain and can severely impair daily activities leading to disability and an overall low quality of life. All these aspects make osteoarthritis a significant burden to the worldwide healthcare systems (Hunter, Schofield and Callander, 2014).

Upon diagnosis, the initial treatment approaches focus on the relieving of the symptoms. Pain is the primarily symptom and the medication offered to relieve it includes topical pain medication and oral analgesics. For the osteoarthritis chronic pain, nonsteroidal anti-inflammatory medications (NSAIDs) are used (van de Laar *et al.*, 2012). For the treatment of discomfort and stiffness, physical therapy is introduced in the treatment scheme of the patients with moderate osteoarthritis where pain is

manageable. Occupational therapy support can help patients to develop different approaches that reduce the stress on the affected joints when carrying out everyday tasks (Dorsey and Bradshaw, 2017). Cortisone injections or electrical nerve stimulation are between therapies used in the osteoarthritic analgesia, by numbing the affected joint. Unfortunately, they provide only short-term pain relief and can worsen the condition of the affected joint over time. The above-mentioned treatment approaches for the pain management tend to work for patients with early-stage osteoarthritis. Unfortunately, they will not stop the progression of the disease (Cheng and Abdi, 2007). In an attempt to re-establish the lubrication of the joint, hyaluronic acid injections are used to create a cushion like effect between the structures of the joint. Unfortunately, it only provides temporary results, and it does not provide analgesic improvement (Migliore and Procopio, 2015).

Furthermore, therapies where growth factors and nutrients are injected in the affected joints have been developed in an attempt to promote the repair process and re-establish the joint homeostasis. Platelet-Rich Plasma (PRP) isolated from the patient's own blood is injected in the synovial area of the affected joint. It is predominantly used in knee osteoarthritis, and it has shown reduction in treated patients comparative with placebo (Xie, Zhang and Tuan, 2014). However, side effects have also been described such as infection and swelling in some patients. This therapeutic approach is poorly understood and despite its initial promising results in pain relief, it is not recommended by the experts due to lack of standardization in the preparation and administration method and as well as poor understanding over the mechanism of action. At this moment in time, it is unclear if PRP injections reduce the progression of osteoarthritis (Filardo *et al.*, 2021).

The ultimate solution is the surgical approach, where the damaged joint surfaces or the whole joint in some cases is replaced with artificial joints. Recovery time can take up to 12 weeks and the average lifespan of the artificial joint is around 10-15 years as they can wear out over time or become loose. Arthroplastic interventions do not provide a permanent solution (Michael, Schlüter-Brust and Eysel, 2010).

1.3. Stem Cells

Stem Cells are defined as unspecialised cells that have the ability to self-renew and differentiate into specialised types of cells. They have been described as the body's "raw material". The self-renewal capacity of stem cells is maintained by telomerase, an enzyme highly expressed in stem cells. Telomerase maintains the length of telomeres during division, preventing cell senescence (Hiyama and Hiyama, 2007). Based on their abilities, stem cells have become the foundation of regenerative medicine.

Stem cells can be distinguished in two types based on their origin, embryonic stem cells (ESCs) and adult stem cells (ASCs). ESCs are cells derived from the undifferentiated inner mass cells of the embryo at the blastocyst stage (3-5 days old). They are pluripotent, which it means they have the ability to differentiate into all derivates of the germ layers. The second type of stem cells are the adult stem cells. They are found in the adult tissue, and they make up a small part of tissues when compared with more specialised differentiated cells. Based on their differentiation capacity they are described as multipotent. ASCs can differentiate into more than one cell type, but by comparison with the embryonic stem cells, adult stem cells have a limited capacity of differentiation. In adult tissue, stem cells are found in a specific microenvironment called the stem cell niche. ASCs maintain their undifferentiated state because of the stem cell niche. This is generally composed of stem cells themselves, their progeny, stromal or mesenchymal cells, osteoblast, osteoclast, pericytes, long range component represented by endothelial cells or neurons, basement membrane, extracellular matrix, cytokines, and maintenance proteins (Rezza, Sennett and Rendl, 2014). All these factors provide and environment that balances the division and the differentiation, conserving cells in an undifferentiated stem cell state. In the event of local injury, the stem cell niche is summoned through morphogenic factors released by the injured tissue. Once the intrinsic signal reaches the stem cells, proliferative and differentiation events are triggered leading to the production of more mature cellular derivates to replace the damaged tissue. The division during injury response is asymmetrical for the maintenance of the local stem cell pool, meaning that one stem cell and a more mature cell type are produced (Yang, Plikus and Komarova, 2015).

Stem cells research has significantly increased in the last decade with the focus of developing cell-based therapies for degenerative conditions, such as osteoarthritis, with varying degrees of success. The therapies that aim to utilise the regenerative properties of stem cells can be split into two paths; the direct utilisation of stem and progenitor cells for treatment by transplantation or modulation of the already present in the tissue stem and progenitors cell populations.

Stem cells research has also contributed to the understanding of embryonic development, the pathophysiology of disease, as well as the tissue regeneration.

Ethical considerations limit the potential use and application of ESCs. This however does not apply to ASCs, which have been investigated for the application of cell-based therapies

The usage of stem cells in cell-based therapies began with Dameshek's observations in 1957. He transplanted bone marrow from healthy mice into irradiated mice. As a result of the transplantation, the bone marrow haematopoietic component was re-established.

However, while ASCs can differentiate into more than one cell type, their specialisation capacities are still limited when compared with ESCs. In order to enhance their differentiation capacity, terminal differentiated somatic cells were altered, using genetic reprograming. In 2006, Takahashi and Yamanaka obtained induced Pluripotent Stem Cells (iPSCs) by transducing mouse fibroblasts with the genes of Oct-3/4, SOX2, c-MYC and KLF4. By genetically reprogramming somatic cells with these transcription factors, they obtained cells in ESC-like state, called induced pluripotent stem cells (iPSCs) This discovery gave rise to a powerful tool that allows the usage of allogenic cells, eliminating the issues of rejection that is encountered in autologous ASCs-based therapies, where the patient's cells cannot be used due to age (Wolff, 2002). As well as accessing pluripotency without the ethical controversary around embryo destruction. However, iPSCs are not used in clinical practice at this moment in time due to the safety concerns of their genetical instability that can lead to oncogenic potential of the genetically altered cells, as well as the unpredictability of the viral vectors that are used in genetic alteration of somatic cells in order to obtain iPSCs. The alternative, non-viral vectors bring the issue of unstable transfection (Attwood and Edel, 2019). Overall, more research with the focus on genetic stability is

necessary in iPSCs technology. However, iPSCs remain a powerful tool for research by providing the opportunity to create disease models. The study of iPSCs based models, especially for degenerative disorders, has contributed to the understanding of disease mechanism as well as the ability to test and improve cell-based therapies and to study new pharmacological agents (Ebert, Liang and Wu, 2012).

Currently, stem cell-based therapies have involved ASCs and Foetal Stem Cells (sourced from umbilical cord or Wharton's jelly). Clinical studies have provided promising results for the usage of stem cells in the treatment of illnesses such as myeloid leukaemia, pulmonary fibrosis, diabetes mellitus, heart failure, Crohn's disease, spinal injury repair and neurodegenerative disorders such as Parkinson (Jaber *et al.*, 2021); Dolstra *et al.*, 2017; Li *et al.*, 2021; Kong *et al.*, 2019); Curtis *et al.*, 2018; Lindsay *et al.*, 2017; (Eichler *et al.*, 2017). Moreover, stem cells were also proven to be a potential treatment for the COVID-19 induced pneumonia (Zhang *et al.*, 2020).

The main concern in stem cell therapies is the post-transplantation rejection with severe immune response as well as unregulated cell proliferation that can induce tumorigeneses (Bongso and Fong, 2013; Musiał-Wysocka, Kot and Majka, 2019)).

1.3.1. Mesenchymal Stem Cells

In mammalian organisms, mesenchymal cells are adult stem cells in stromal compartments that persist throughout life and realise the function of repair and replacement of cells within different tissues (e.g., chondral, osteo or adipose tissue) in response to traumatic events and natural cell turnover (Ullah, Subbarao and Rho, 2015).

Mesenchymal Stem Cells (MSCs) are a mixed population of fibroblast-like plastic adherent cells. First described in 1970 by Friedenstein *et al.* as "clonal, plastic adherent cells", mesenchymal stromal cells have been initially distinguished from the other types of cells, based on their plastic adherence properties and their ability to form colony-forming unit fibroblasts (CFU-Fs), indicating progenitor cell properties. MSCs were separated from the non-adherent cells from the bone marrow when cultured in plastic dishes long enough.

The term MSCs was introduced by Arnold I. Caplan in 1991 (Caplan, 1991), referring to adult bone marrow (BM) progenitors with similar properties as described by Friedenstein. Due to their ability to differentiate into specialized cells which are mesoderm derived, this type of cells received the term "mesenchymal" (Ullah, Subbarao and Rho, 2015).

Currently, the term mesenchymal stem cells (MSCs) refers to a population of adult progenitor cells with the ability to produce progeny that differentiate into cells of specific lineages. *In vivo*, MSCs have at least five primary roles: progenitor cells for bone transformation during bone remodelling, cartilage formation, vascular support, haematopoietic support and progenitors for adipocytes.(Danisovc *et al.*, 2016).

MSCs participate in the formation of a niche environment that supports haematopoiesis by secreting growth factors and cell to cell interactions with Hematopoietic Stem Cells (HSCs), directly impacting on the proliferation and the differentiation of them (Mendelson and Frenette, 2014). Additionally, MSCs are multipotent, having the capacity to differentiate into a range of mature cell types such as osteocytes, chondrocytes, adipocytes, smooth muscle cells ((Pittenger *et al.*, 1999) Dezawa *et al.*, 2005). MSCs populations showing all or many of the above characteristics have been successfully isolated from many different tissue (e.g., trabecular compartment at the ends of long bones, the bone marrow, adipose tissue, dental pulp, liver, skeletal muscle, embryonic tissue such as umbilical cord or amniotic fluid and even peripheral blood) suggesting that MSCs are diversely distributed *in vivo*. (Álvarez-Viejo, 2015a). However, the differential potential is dependent on the source tissue.

The unique biological characteristics of MSCs such as, plasticity, long-term self-renewal, secretion of various bioactive molecules (e.g., trophic factors, cytokines and neuroregulatory peptides), which play a role in tissue repair and regulate inflammatory and immune responses (Wehling *et al.*, 2017) and ability to actively migrate to diseased tissues, make them an unique tool for regenerative medicine. (Nicodemou and Danisovic, 2016). MSCs have received an increased interest due to their substantial therapeutic potential. Different methods of isolation and expansion as well as characterisation have been employed to describe an MSCs population in many research studies ((Secunda *et al.*, 2015) (Soleimani and Nadri, 2009). For example,

the isolation of MSCs from tissues through methods such as the enzymatic method (the digestion of the tissue with enzyme such as Collagenase for the release of MSCs) or, the explant method (the culture the whole tissue in MSC like media allowing the cells to migrate into the new environment) are used, as well as cell sorting based on the immuno-profile of the cells. These are considered efficient isolation methods accepted in primary MSCs research. However, the poor description of MScs phenotype allowed irregularities in the isolation and identification of MSC. A reliable comparison of the research outcomes that were claiming as being MSCs based studies became difficult. For this reason, in 2006, the Tissue Stem Cell Committee of the International Society of Cellular Therapy proposed a set of minimum criteria to define human MSC population (Dominici *et al.*, 2006).

1. Adherence to plastic when cultured in standard culture conditions. MSCs highly express Integrin α5β1, a surface protein that is known to mediate attachment, migration, and proliferation of this specific cell population.

2. Positive expression of cellular markers: CD29, CD44, CD90, CD49a-f, CD51, CD73, CD105, CD106, CD166, Stro-1 (only a minimum of 3 positive cellular markers are required for MSC confirmation).
   And negative expression of the cellular markers which are specific to the tissue source, CD45, CD34, CD14 or CD11b, CD79a or CD19, HLA-DR.

3. Tri-Lineage differentiation confirmed by structural staining. Alcian Blue staining for chondrocytes, Alizarin Red staining for osteocytes and Olio Red staining for adipocytes. To induce tri-lineage differentiation MSCs are cultured in medium supplemented with specific supplements (TGF-β for inducing chondrogenesis, dexamethasone, ascorbic acid and β-glycerol phosphate for inducing osteogenesis and isobutyl methylxanthine for inducing adipogenesis).

In bone, MSCs rest in the perivascular niche. They play a crucial role in injury response. When this occurs, MSCs migrate to the site of injury and re-establish tissue homeostasis by producing bioactive molecules such as growth factors, cytokines, pro-angiogenic and antioxidant agents that stimulate cell proliferation and vascularization. Having the capacity to differentiate in other cell types, MSCs can help with re-building the affected tissue. Moreover, MSCs modulate inflammatory and immune responses that follow immediately after tissue damage.

Furthermore, even if the majority of MSCs rest in the perivascular niche of the bone, they have the potential to migrate to the joint and restore the damaged cartilage, when injury occurs and to re-establish the tissue homeostasis by stimulating chondrocytes proliferation and secretion of antiapoptotic and anti-scarring mediators.

Articular cartilage itself is avascular, aneural and alymphatic. Chondrocytes are the only type of cells present in the articular cartilage. They are low metabolically active cells, mainly modulated by the aggrecan protein resting in ECM lacunae. When injured or diseased, articular cartilage is considered unable to initiate endogenous repair (Hu *et al.*, 2021). Mainly due to the low and inactive cellular component, comprised of idle chondrocytes located in the lacunae, that in the event of injury initiate poor cellular signalling. In addition, injury-associated products such as ECM fragments, cell lysates, high-mobility group box 1, HMGB1 as well as stromal cell derived factor-1 SDF-1 have the capacity to activate the ASCs that are resting in stem cell niches of the skeletal tissue with the aim to induce tissue repair by migration to the site of injury (Riegger, Palm and Brenner, 2018; Zhang *et al.*, 2016).

MSCs from the perivascular niche of the bone have the potential to migrate to the articular cartilage when activated by injury-associated molecules and differentiate into adult chondro-progenitors, in order to replace the compromised chondrocytes.

Moreover, through their secretion of cytokines, growth factors, hormones and chemokines, MSCs have the potential to modulate the immune response at the site of injury, by suppressing it (Wang, Yuan and Xie, 2018). Indoleamine 2,3-Dioxygenase (IDO), TNF-Stimulated Gene 6 (TSG6), NO, IL-10, CC-Chemokine Ligand 2 (CCL2) and prostaglandin E2 (PGE2) are several of the immunosuppressors secreted by MSCs, when activated by IFN-γ, IL-1α, IL-1β and TNF-α that are secreted by T cells and antigen-presenting cells (Németh *et al.*, 2009; Tang *et al.*, 2008).

More recent studies have shown that synovial fluid from the joints also contains MSCs (Dai *et al.*, 2006; Jones *et al.*, 2004) that have the ability to repair damaged articular cartilage, not only by replacing the compromised chondrocytes but also to secrete growth factors that can modulate the rebuilt of ECM stiffness and lubrication.

1.3.1.1.   MSCs: Jack of all Trades in Regenerative Medicine

Since their discovery in the late 70's, MSCs have received a great interest from research groups around the world.

They have been showed to be present in almost all tissues and can be easily isolated. MSC's key quality, in addition to their accessibility, is their extensive differentiation potential. They can differentiate into an array of end-stage lineage cell, including osteocytes, chondrocytes, adipocytes, muscle cells and even neuronal lineages (Jahan *et al.*, 2017; Pittenger *et al.*, 1999; Dezawa *et al.*, 2005). Anti-inflammatory, immunoregulatory and immunosuppressive characteristics add to their potential as immune tolerant agents.

All these excellent properties make MSCs the ideal cell source for tissue regeneration with feasible clinical applications. Optimizations in extraction, culture and differentiation procedures have brought MSCs closer to clinical applications for disease therapy and tissue rebuilding in recent years.

To date, MSCs have been extensively investigated and used in regenerative medicine (Wagers, 2012). They have been utilised for a variety of applications: bone regeneration (Giannotti *et al.*, 2013), cartilage repair (De Windt et al., 2016, regeneration of musculoskeletal tissues (Orozco *et al.*, 2011), central nervous rebuilding (Wang *et al.*, 2013), peripheral nervous system rebuilding (Matthes *et al.*, 2013), myocardium restoration (Nagaya *et al.*, 2005), liver regeneration (Valfrè Di Bonzo *et al.*, 2008), corneal reconstruction (Ma *et al.*, 2006), tracheal reconstruction (Elliott *et al.*, 2012), skin regeneration (Yang *et al.*, 2013), kidney repair (Jiang *et al.*, 2015), lung disease treatment (Dai *et al.*, 2018), bladder regeneration (Zhou *et al.*, 2018), even blood thinning (Kolesky *et al.*, 2016).

Despite a significant number of preclinical and clinical research, the safety of MSC-related therapies remains the most serious concern for clinical use. The main concerns when it comes to MSC-based therapies are the tumorigenicity, proinflammation and fibrosis that can be induced when MSCs are transplanted.

MSCs have been declared to be isolated with a higher yield from a variety of tissues, including adipose tissue and synovium, as well as human umbilical cord blood. With

all of these, bone marrow remains one of the most important sources of MSCs. The great majority of research studies that explore the potential of primary MSCs, have utilised bone marrow as the cell source. Most of the criteria used nowadays to describe MSCs, rely on the *in vitro* culture-expanded cells. However, these cells are believed to exhibit different behaviour *in situ*, which contradicts the *in vitro* data. To begin with, the name employed to characterise this cell type is riddled by inconsistency and controversary. Many scientists disagree with the use of the term MSC, firstly introduced by Caplan in 1991. Lack of consistency in sourcing and the medium of culture are two of the main factors. Terms such as multipotent MSCs, cultured mesenchymal stromal cells or cultured stromal cells, multipotent stromal cells and many other were proposed to describe plastic adherent fibroblast-like cells that have the potential to differentiate into adipocytes, chondrocytes, and osteocytes and express CD73, CD90 and CD105 on their surface while being negative for cellular markers specific for their tissue source. Many specialists in the discipline, however, believe that these criteria are insufficient. When the aforementioned parameters are utilised, a heterogenous cell population is obtained. Moreover, because cultured stromal cells differ from their *in vivo* progenitors (Yang *et al.*, 2018), it is crucial to determine the phenotype of primary MSCs before studying them further. The identification of a pan mesenchymal cellular marker is important to maintain homogeneity in MSC focused research and for better yield in clinical applications. Several surface markers have been reported to be effective for enriching MSC populations sourced from bone marrow in recent years. Starting with the criteria established by ISCT, different cellular markers have been examined in primary isolated MSCs, particularly from bone marrow, in attempt to establish a unique marker that is distinctive for a homogenous population of MSCs.

In 2002, Quirici *et al.*, reported that CD271 is specific for a population of multipotent bone marrow cells and recommended that this marker be used to select MSCs from bone marrow. In the same year, Jones *et al.*, published a study where they discovered that not only the D7-FIB positive fraction include all of the CFU-F activity, but it also contained a distinct population of CD45^{low}/LNGFR^{+} cells. Following cell sorting and routine expansion, these cells were adherent, proliferative, and showed multipotency in their differentiation. Based on observations from the above-mentioned research groups, the immunophenotype CD45^{low}/LNGF^{+}/D7FIB was proposed as identification

method for MSCs. Up until 2006, confirmation through CFU-F assays was the main criteria for MSCs identification. The Kuçi *et al.*, study demonstrated that CFU-F activity was exclusively present in CD271+ cells, while no CFU-F was found in the CD271-population. However, when further investigated, CD271+ MSCs isolated from bone marrow and synovium, co-expressed CD34, which is a hematopoietic stem and progenitor cells specific marker (Kim *et al.*, 2009). As for this reason, CD271 cannot be considered a unique marker for the isolation of MSCs. Nevertheless, the use of CD271 in conjunction with other markers such as CD45$^{low/-}$ to identify primary MSCs has been proven in a number of studies, including the ones listed above. By putting all this information together, Mabuchi *et al.*, screened a large number of potential surface markers in order to find the ones that would be the most effective in the detection of a pure population of MSCs. They concluded that for the isolation of "true" MSCs (higher multipotency and genetic stability) from bone marrow, a combination of the CD271+ CD90+ and CD106+ markers is the most effective method.

All of these studies conclude that positive selection with CD271 resulted in the isolation of a homogenous population of multipotent MSCs, although considerations need to be made and negative controls need to be used to ensure high specificity.

CD271 is not only a cellular marker. It is also known as Low Affinity Nerve Growth Factor Receptor (LNGFR), or p75NTR (neurotrophin receptor) and it has been demonstrated to be involved in a range of processes, mainly in response to neurotrophins activation. Its various roles include morphogenesis, growth factors secretion and apoptosis. Nevertheless, the role of CD271 on MSCs still remains unclear.

Further advances in the study of CD271 role in MSCs is made difficult by its rapid downregulation when the cells are isolated and placed in culture. Upon isolation, primary MSCs from healthy bone marrow highly express CD271, but this is greatly downregulated when the cells were placed in culture (Calabrese *et al.*, 2015). This can be attributed to the disruption of the cells' microenvironment and activation of a series of processes for initiating the accommodation to the new conditions, which leads to downregulation of CD271. Therefore, CD271 might describe only a quiescent population of MSCs. The CD271+ MSCs that reside in the bone perivascular niche and are ready to act only when activated by tissue injury signalling. This suggests that

CD271 may be selective for real MSCs in bone marrow and may serve as the foundation for *in vivo* MSC identification, with applications in regenerative medicine.

Although CD271 has been shown in many studies to be a suitable marker for MSCs from bone marrow it appears to be insufficient for isolating MSCs from other tissues. Adipose tissue provides an abundant and easily accessible comparative with bone marrow, source of MSCs. When MSCs isolated from adipose tissue were screened for CD271, the obtained results were comparable to those seen in bone marrow MSCs. When the CD271+ adipose derived MSCs were further investigated, a correlation was confirmed between the age of donor and the number or viable MSCs. This was also observed in bone marrow originated MSCs, suggesting that for these two types of tissue at least the proportion of CD271+ MSCs decreases with age (Cuevas-Diaz Duran *et al.*, 2013). Despite all of this, adipose tissue remains the most preferred tissue source for the isolation of MSCs for tissue regeneration and stem cell therapy.

Umbilical cord has been shown to be a valuable source of stem cells. Comparative with the isolation of stem cells from adult tissues, umbilical cord possesses ethical advantages and does not require a clinical based intervention in order to be obtained. The umbilical cord, along with the placenta are considered biological waste and after delivery they are normally discarded. Attempts have been made to isolate MSCs from umbilical cord blood, Wharton's jelly, and placenta. Contrary to the expectations, MSCs are present with a low frequency in the structures of umbilical cord, which makes them inferior to bone marrow MSCs. These cells are morphologically and molecularly comparable to bone marrow derived MSCs, including the lack of hematopoietic surface antigens. Therefore, when recently described MSCs markers, such as CD271 have been used to isolate cells from the umbilical cord, the obtained yield was significantly inferior when compared with bone marrow and adipose tissue derived MSCs (Watson *et al.*, 2013).

Overall, evidence from literature suggests that CD271 should be used as a universal marker to identify MSCs, for bone marrow and adipose derived cells only (Watson *et al.*, 2013). In general, bone marrow and adipose tissue continue to be the main sources of MSCs for therapeutic purposes.

In order to determine a marker or markers for optimum selection and identification of MSCs, more study in this field is required. This has the potential to facilitate the generation of purer cultures than those obtained based on the current MSC criteria.

1.4. Low Affinity Nerve Growth Factor Receptor

Low Affinity Nerve Growth Factor Receptor also known as p75NTR or CD271, hereafter called p75NTR, is a cell surface receptor that has been identified in 1973 by Herrup and Shooter, 1973), initially as receptor for the neurotrophin, nerve growth factor. Later on, p75NTR has been shown to be a receptor for all neurotrophins, not only NGF (Rodriguez-Tebar, Dechant and Barde, 1990; Squinto *et al.*, 1991; Rodriguez-Tebar' *et al.*, 1992).

p75NTR is a type I transmembrane protein with a molecular weight of 75kDa. It is a member of Tumor Necrosis Factor receptor (TNFR) superfamily due to the highly conserved TNFR specific cysteine-rich repeats structure present in the binding site of the extracellular domain. P75NTR also contains a death domain in the intracellular region. Only a small number of TNFR family members have this trait. TNFRs are involved in a variety of biological responses, and depending on the type of cell and circumstances, they can induce cell death or survival. TNFRs are among the mains pharmaceutical targets due to their involvement in a variety of diseases, mainly in neurodegeneration (Vilar, 2017).

In terms of structure, the extracellular section of p75NTR has four 40 amino acids repeats with six cysteines at fixed positions, followed by a serine/threonine-rich region. P75NTR has a single transmembrane domain that contains Cys257, an important mediator of covalent dimers formation in the absence of neurotrophin bindings (Baldwin *et al.*, 1992). The cytoplasmic domain is made of 155 amino acids and contains 2 different regions, a flexible juxtamembrane domain and a highly folded death domain (Vilar *et al.*, 2009). The total length of p75NTR is 427 amino acids (Vilar, 2017).

The extracellular domain contains several sites of O-linked glycosylation and only one of N-linked glycosylation. The interaction with neurotrophins takes place through the

four cysteine domains and is done through homodimers formation (He and Garcia, 2004).

In cell death p75NTR mediated signalling, its extracellular domain is cleaved by proteins such as ADAM1 or TACE that reduce the receptor to an only 28kDa membrane bound C-terminal fragment (Bronfman, 2007). This is further processed by γ-secretase at the transmembrane level and as result, the p75NTR intracellular domain gets released (Gowrishankar, Zeidler and Vincenz, 2004). The intracellular region does not have any catalytic domains. As a substitute, it contains a death domain that is responsible for protein-protein interactions. Therefore, p75NTR signalling is dependent on protein-protein interactions (Underwood *et al.*, 2008).

p75NTR is prominently expressed during synaptogenesis and developmental cell death in the developing central and peripheral nervous systems. In adult tissue, p75NTR is down regulated but it becomes upregulated when injury occurs. Hence, it is the target for many treatments in neurodegenerative illnesses (Meeker and Williams, 2014). The p75NTR death signalling pathway has been linked to a number of diseases. Alzheimer's disease and motor neuron disease are two of the disorders where elevated levels of p75NTR have been found to be closely linked with the onset of neurodegeneration (Dechant and Barde, 2002). Experiments in animal models where the expression of p75NTR was inhibited, resulted in decreased cell loss, and improved function (Distefano *et al.*, 1993).

Besides the implications in the cell survival and death, p75NTR mediates the neurite outgrowth throughout Rho A. This process occurs after the activation of myelin proteins with Nogo66 as co-receptor (Barker, 2004,).

Given this receptor's potential to stimulate neurite outgrowth, differentiation, and signal survival, p75NTR as target might be useful in developing pharmacological strategies not only for neurodegeneration by its inhibition, but also for neurotrauma regeneration therapy by its promotion (Kelamangalath and Smith, 2013).

P75NTR does not mediate all of the above-mentioned processes only independently, but some of them through collaborations and interactions with other cell surface proteins, such as sortilin and Trk receptors, mainly Trk A, or through secondary messengers. A clear mechanism of how p75NTR interacts with these receptors has not been elucidated to date (Reichardt, 2006).

P75NTR binds all 4 human neurotrophins with similar low affinities (10^{-9} M), hence the name of Low Affinity Neurotrophin Receptor. Trk receptors are neurotrophins specific receptors and are known to be co-expressed with p75NTR. When their expression is p75NTR independent, Trk Receptors bind neurotrophins with the same affinity (10^{-9}M). however, when p75NTR is present, Trk receptors affinity for their favoured neurotrophins rises by about 100 times (10^{-11} M) (Bothwell, 1995; Jung *et al.*, 2003).

p75NTR is not only expressed by the cells of central and peripheral nervous systems. It has been reported that p75NTR expression defines a population of cells with great regenerative potential, MSCs, derived from bone marrow and/or adipose tissue. Moreover, p75NTR has been demonstrated to be a specific marker for identifying bone derived MSCs (Álvarez-Viejo, 2015b) and due to its high expression, p75NTR can be employed to isolate a homogenous population of MSCs with minor hematopoietic contamination. Knowing that in adult tissue, p75NTR is usually highly expressed following neuro trauma or neurodegenerative diseases, and due to its presence in bone derived MSCs, p75NTR has also been investigated in other degenerative conditions. Campbell *et al.* and Jones *et al.* have revealed that p75NTR from bone MSCs is likely to be linked with enhanced cartilage damage, bone sclerosis and an overall rapid progression of osteoarthritis. Moreover, elevated levels of NGF, one of the main p75NTR ligands, have been recorded in the synovium fluid of patients with osteoarthritis (Halliday *et al.*, 1998; Rocco *et al.*, 2018). Elevated levels of NGF have been associated with chronic pain in osteoarthritis affected joints (Sarchielli *et al.*, 2001).

The above observations suggest that p75NTR is involved in osteoarthritis in some way.

Overall, p75NTR together with NGF and possibly the rest of the Neurotrophic factors, may play an important role in the disease mechanism of inflammatory joint disease. However, the p75NTR mediated mechanism of action in this context is poorly understood. Based on the potential involvement of p75NTR and NGF in skeletal tissue degeneration and accompanying chronic pain (Deponti *et al.*, 2009) , p75NTR mediated signalling became the focus of pharmaceutical strategies in the treatment of the most common joint disease, osteoarthritis. As well as the modulation of tissue regeneration based on the observation of Jiang *et al*, which states that NGF together with the IL-1β activate cartilage stem-progenitor cells in osteoarthritis.

Monoclonal antibodies against NGF have been developed with the aim to treat the chronic pain induced by osteoarthritis. Tanezumab, Fasinumad and Fulranumab are several of the monoclonal antibodies-based chronic pain treatments of this type, which target all NGF molecules present in the synovial fluid of patients with knee osteoarthritis. Without NGF, its receptors, Trk A and p75NTR will not be able to induce the signalling involved in pain. A complete depletion of NGF was thought to also stop or reduce the progression of the bone tissue degeneration (Tomlinson *et al.*, 2017). With promising initial results in pain reduction, anti-NGF monoclonal antibodies, raises serious safety concerns. Despite reporting of significant pain numbing in patients with knee osteoarthritis, imaging evidence (MRI, X-ray) together with post-treatment induced mobility issues, revealed a serious side effect. A complete NGF depletion at the joint level improves analgesia in degenerative knee osteoarthritis, but it also causes rapid tissue degradation. The findings suggest that NGF, in conjunction with its receptors, is involved in not just chronic pain signalling, but also critical processes in skeletal tissue regeneration. Wang *et al.* supported this observation with their findings demonstrating that inhibiting p75NTR in the MSC population has a detrimental effect on bone formation in mice.

More studies where NGF related activity was investigated in *in vitro* MSC populations, showed a decrease in proliferative capacity, colony-forming efficiency, and down-regulation of stem cell phenotype markers as direct a result of p75NTR inhibition (Kolli *et al.*, 2019). When treated with NGF, primary isolated MSCs from rabbit bone marrow showed increased proliferation (Lu *et al.*, 2017). However, NGF has been demonstrated to not directly influence MSC colony-forming capacity (Gronthos and Simmons, 1995). MSC proliferation and colony-formation is rather positively influenced by NGF than directly induced by it. NGF is considered to increase the potency of other surrounding stimulatory factors on the proliferation and differentiation of MSCs and does not have any direct impact on the cells.

NGF has been shown to positively impact not only the proliferation and the colony forming capacities of MSCs, but also their differentiation potential (Kolios & Moodley, 2012; Lu *et al.*, 2017). According to more studies, NGF has been shown that may enhance MSC proliferation via increasing their sensitivity to external stimuli rather than directly promoting the proliferation (Gronthos and Simmons, 1995). NGF is mainly well

known for inducing neurite outgrowth and support of the growth and survival of central nervous system neurons.

Studies where MSCs were treated with differentiation media supplemented with NGF reported better yield in differentiation and improved therapeutic effect when transplanted to animal models. Mouse bone marrow derived MSCs exhibited enhanced chondrogenic differentiation after being treated with NGF. When NGF was present in chondrogenesis, Aggrecan, SOX9 and COL II, cartilage-specific genes were upregulated. This resulted in an increased secretion of GAG and Collagen type II (Lu *et al.*, 2017). Moreover, when compared with TGF-β1 in chondrogenic differentiation of bone derived MSCs, NGF appears to have an increased potential to activate proliferation and differentiation pathways, such Pi3K-Akt (Zhan *et al.*, 2019).

Furthermore, superior histological scores were achieved in *in vitro* studies. A study by Hermida-Gómez *et al.*, was the first to show that MSC implants can repair focal defects in human articular cartilage. Articular cartilage in which p75NTR+ MSCs were transplanted showed a better filling of the chondral defect and an overall greater integration of the regenerated tissue with the healthy tissue when compared with p75NTR- MSCs treated cartilage samples. The post-implantation histological and immunostaining results imply that p75NTR+ MSCs may be more effective in promoting articular cartilage repair (Hermida-Gómez *et al.*, 2011).

In summary MSCs, NGF and p75NTR are potentially important players in the pathophysiology of degenerative joint diseases such as osteoarthritis and could prove to be the key in the effort to better describe and effectively treat this disease.

1.5. Neurotrophins

Neurotrophins or neurotrophic factors are a family of closely related proteins that are known to control many aspects of neuron survival, development, and function in both the peripheral and central nervous systems. Neurotrophins have been discovered as neuronal survival promoters, but it is now recognised that they govern many aspects of neuronal growth and function, including synapse formation and synaptic plasticity (Huang and Reichardt, 2001a).

The first discovered neurotrophin was Nerve Growth Factor. Levi-Montalcini observed that the development of the chick embryo nervous system is stimulated when a mouse originated tumour was implanted anywhere on the embryo. The stimulated development was observed particularly in the sensory and sympathetic nerves. Given the fact that the tumour explant did not need direct contact with the chick embryo in order to induce nerve outgrowth towards it, Levi-Montalcini determined that a growth factor was secreted by the tumour and recognised by particular types of nerves. Stanley Cohen was later able to purify the protein that seems to serve a critical function in the development of the nervous system based on these first observations.

The second neurotrophin, Brain-Derived Neurotrophic Factor (BDNF) was isolated from pig brain when searching for a survival factor specific to neuronal populations unresponsive to NGF (Barde, Edgar and Thoenen, 1982).

The characterisation of NGF and BDNF structures made possible the identification of Neurotrophin 3 (NT-3) and Neurotrophin 4 (NT4). In total, neurotrophin family has a total of 4 members (Maisonpierre *et al.*, 1990); Berkemeier *et al.*, 1991).

Neurotrophins are particularly important for developmental neurobiology. The research that led to their discovery showed the critical significance of cellular interactions in cell survival and differentiation in early development, by the secretion of trophic factors (Jacobson and Weil, 1997).

Studies on the structure of the four neurotrophins revealed that they all share a highly homologous structure, a tertiary fold and cysteine knot, that is present in several other growth factors such as Transforming Growth Factor-β (TGF-β) and platelet derived growth factor (PDGF) (Sherbet, 2011).

Neurotrophins interact with two types of receptors in order to activate a variety of signalling pathways that are responsible for numerous biological processes.

The first neurotrophins receptor to be discovered was p75NTR. Initially it was identified as low affinity for NGF, but it was later shown to bind each of the neurotrophins with similar affinity (Rodriguez-Tebar, Dechant and Barde, 1990; Frade and Barde, 1998). p75NTR has a wide range of functions that sometimes are contradictory. In response to neurotrophins, p75NTR may exert pro-survival as well as pro-apoptotic effects, depending on the cellular environment in which it is expressed. Moreover, it promotes

neurite outgrowth, mediates differentiation, and enhances proliferation. Additionally, it is possible that p75NTR plays a significant role in the synthesis of myelin (Roux and Barker, 2002).

All four neurotrophins are synthesized as precursor proteins (proNGF, proBDNF, proNT-3 and proNT4). This precursor form undergoes proteolytic cleavage and mature neurotrophins are generated (NGF, BDNF, NT-3 and NT4). The precursor form of the neurotrophins is relatively unstable compared with the mature form and has the capacity to bind the neurotrophin receptors. Moreover, proNGF binds to p75NTR with higher affinity than NGF. *In vivo* it has been shown that the activation of p75NTR by the proNGF induces cell death (Beattie *et al.*, 2002). It has also been suggested that proNGF is released as a pathologic death-inducing ligand after adult central nervous system injury (Harrington *et al.*, 2004). This observation is particularly important as it offers a promising therapeutic strategy for the treatment of neurodegenerative diseases characterised by neuronal loss, via interfering with the binding of proNGF to p75NTR. A significant breakthrough in the study of neurotrophin activated p75NTR mediated signalling has been the discovery of sortilin. Sortilin is a member of VSP10p-domain receptor family that binds to proNGF and co-operates with p75NTR to trigger apoptosis (Teng *et al.*, 2005). The apoptotic effect of p75NTR-sortilin co-expression is not limited to only proNGF binding; proBDNF has been found to induce the same effects *in vitro* when both receptors are expressed (Teng *et al.*, 2005).

The binding of mature neurotrophins to p75NTR may also induce apoptosis. The p75NTR apoptosis signalling pathway can be triggered not only by pro-neurotrophins, but also by mature neurotrophins. When activated by mature neurotrophins, p75NTR induced apoptosis is dependant of the interactions with other intra-cellular proteins, such as TNF receptor-associated factor 6 (TRAF6), Np95/ICBP90-like RING finger protein (NRIF), Neurotrophin Receptor Interacting MAGE protein (NRAGE), NH(3)-dependent NAD(+) synthetase (NADE) and SPARC-like 1 (SC-1). The outcome of neurotrophin-induced p75NTR activation is determined by the cellular context (Volosin *et al.*, 2008). As described previously, due to the lack of catalytic activity in the intracellular domain, the signalling of the p75NTR is carried out by protein-protein interactions. The signal is carried out in the same way when triggered by neurotrophin binding.

p75NTR when activated by neurotrophins does not initiate cell apoptosis only. The NF-κB pathway, an important pro-survival signalling pathway, is selectively activated through p75NTR when activated by NGF, but not by BDNF or N-T3 (Carter *et al.*, 1996). TRAF6, p62, interleukin-1 receptor-associated kinase (IRAK), and receptor-interacting protein-2 (RIP2) are all necessary for the Nuclear Factor kappa B (NF-κB) activation due to protein-protein interactions in the p75NTR mode of action ("Kuruvilla et al., 2000," 2000; Khursigara, Orlinick and Chao, 1999; Khursigara *et al.*, 2001; Mamidipudi, Li and Wooten, 2002; Yeiser *et al.*, 2004). In this process NF-κB translocates to the nucleus and increases the production of Hes1/5 during dendritic formation in neurons, when p75NTR is activated in response to neurotrophins. Hes1/5 plays a vital role in numerous physiological processes, including cellular differentiation, cell cycle arrest and apoptosis in neurons as well as the capacity to self-renew (Salama-Cohen *et al.*, 2005).

In addition, p75NTR may also control the axonal development of neurons, through p75NTR-RhoA signalling pathway. Guanosine triphosphatase Ras homolog (GTPase RhoA), a member of the Rho family, is known to regulate the actin cytoskeleton structure in many cell types (Jaffe and Hall, 2005). Its activity has an inhibitory effect on the axonal growth. Rho A remains activate through the interaction with p75NTR. Neurotrophins can promote the axonal growth by inhibiting the activity of Rho A. When Neurotrophins bind p75NTR, it causes the dissociation of Rho A from the receptor. As a result, Rho A becomes inactive and no longer has the ability to impede axonal development.

In summary, the binding of mature neurotrophins and pro-neurotrophins to p75NTR activates key signalling pathways that affect survival, death, axonal development, and the cell cycle of neurons from central and peripheral nervous system.

The second type of receptors that neurotrophins bind to, are the Tyrosine kinase (Trk) receptors. Trk receptors are three receptor tyrosine kinases (Trk A, Trk B and Trk C) that contain an extracellular domain characterised by three leucine-rich motifs surrounded by two cysteine clusters, two immunoglobulin-like C2 type domains (Ig-C2), a single transmembrane domain and an intracellular region with a kinase domain. Neurotrophins bind to Trk receptors primarily via the Ig-C2 domain. This region is responsible of monomeric form stabilization of the receptor. It prevents spontaneous

dimerization in the absence of the neurotrophins. This feature makes this type of receptor more stable in comparison with p75NTR. As described above, Trk receptor are known as high affinity neurotrophins receptors. The formation of high-affinity binding sites on Trk receptors is modulated by p75NTR and requires an even distribution of both types of neurotrophins receptors on the cell membrane.

When neurotrophins bind to Trk receptors, they form dimers. The receptors phosphorylate in trans, recruit other various adaptors and enzymes, leading to the activation of important signalling pathways involved in cell survival, cell differentiation, cell plasticity, synapse formation, axonal and dendritic development. The Ras-MAPK, Rap-MAPK, PI3K-Akt, and PLCγ-protein kinase C (PKC) pathways are among the signalling pathways activated by Trk receptors in response to neurotrophins.

The following description of signalling pathways activated by neurotrophins binding to the Trk receptors is being mainly described for neuronal cells where the receptors have been studied in great detail.

MAPK:

When activated by neurotrophins, Trk can trigger the SHC-RAS-MAPK downstream. This has been linked with neuronal survival and neuro-differentiation. The activity of MAPK can be further sustained by the internalisation of the phosphorylated Trk receptors. This process results in the activation of CrkII/CrkL-GEF-C3G-GTPase and Rap1-B-Raf downstream. An active MAPK pathway downstream can further activate the cyclic adenosine monophosphate response element-binding protein (CREB) with important roles in gene expression for neuronal survival and differentiation. The activation of CREB generates a sustained response, without the need of neurotrophin-Trk signalling (Deak *et al.*, 1998; Ginty,'t Axad Bonni & Greenberg', 1994; Xing et al., 1996.).

PI3K-Akt:

Neurotrophins exert their role in the cell survival mainly through activation of PI3K and Akt signalling pathway. This signalling pathway, that promotes cell survival neurotrophin activated Trk receptors interact with Shc, which is associated with Grb2 and Gab1 to activate PI3K and later Akt. The neurotrophins effects on the cell survival are dependent on the several downstream effectors from the Akt signalling pathway.

BAD and FKHRL1 are some of the pro-apoptotic transcription factors, that are additionally phosphorylated in order to prevent their effect on the cell survival (Datta *et al.*, 1997; Zheng *et al.*, 2002). PI3K-Akt neurotrophin activated signalling pathway has been reported to mediate not only cell survival, but also axonal development. PI3K-Akt inactivates GSK-3β, which allows the assembly of microtubules that have the capacity to promote axonal growth (Zhou *et al.*, 2004).

PLCγ-PKC:

The activation of PLCγ in response to neurotrophins has also been linked with cell differentiation and survival. When compared with other signalling pathways, Trk receptors have been reported to be direct mediators of PLCγ downstream (Vetter *et al.*, 1991).

The phosphorylation of Trk receptors in response to neurotrophin binding leads to direct recruitment and activation of PLCγ. Inositol trio-phosphate (IP3) and diacylglycerol (DAG) are generated through hydrolysis of PtdIns (4,5) P2. DAG and IP3 induce the activation of PKC that subsequently activates the Erk1 signalling pathway via Raf (Corbit et al., 1999). PLCγ is also important for synaptic plasticity. Trk B is essential in the regulation of synaptic functions and long-term potentiation of brain synapses. Trk B activates PLCγ-PKC signalling pathway in response to BDNF in the hippocampal neurons and studies suggest that BDNF/ Trk B may be involved in cognitive and behavioural functions (Lu *et al.*, 2011).

1.5.1 Neurotrophins in Skeletal Tissue

Neurotrophins functions have mostly been investigated within the CNS and PNS, and their properties have been explored in this context. Neurotrophins have been found not just in the CNS and PNS, but also in cancer, and joint degeneration in recent scientific investigations.

NGF is the most widely investigated neurotrophin. As mentioned previously, it has been identified in a variety of developmental processes, cellular differentiation, and survival as well as in trauma and degenerative disorders, The discovery of the NGF-Trk A binding structure revealed crucial details about how neurotrophins and their receptors function. Other neurotrophins have been studied using this paradigm.

Together with their receptors, p75NTR and Trk, neurotrophins may play crucial roles in many more physiological and pathological processes, not currently described. In-depth neurotrophins focused research may pave the way for a variety of treatment options.

There is growing evidence suggesting that neurotrophins and their receptors have important functions in bone physiology and regeneration.

Neurotrophins, mainly NGF has been found in osteoprogenitor cells, marrow stromal cells, osteoblasts, certain chondrocytes, endothelial cells, the periosteal matrix of the fracture callus, and skeletal muscle, indicating that NGF could be involved in the maintenance of skeletal tissue homeostasis, repair mechanisms and re-innervation (Grills and Schuijers, 1998). Furthermore, after injury in an animal model, BDNF and NT-3 were found in the bone forming region, together with their Trk receptors (Asaumi *et al.*, 2000).

Studies have shown that neurotrophic factors may also play a key role in the injury-induced or inflammatory pain of skeletal tissue. However, the mechanism of action of neurotrophins and their receptors in bone-injury-induced pain remains relatively unclear. Many studies suggest that post-injury inflammation triggers a cascade of proinflammatory cytokine upregulation, which increases the synthesis of NGF in macrophages, chondrocytes, fibroblasts, and osteoblasts at the site of injury. The released NGF may act on sensory neurons either directly or indirectly, resulting in the sensation of pain (Fig. 1.4).
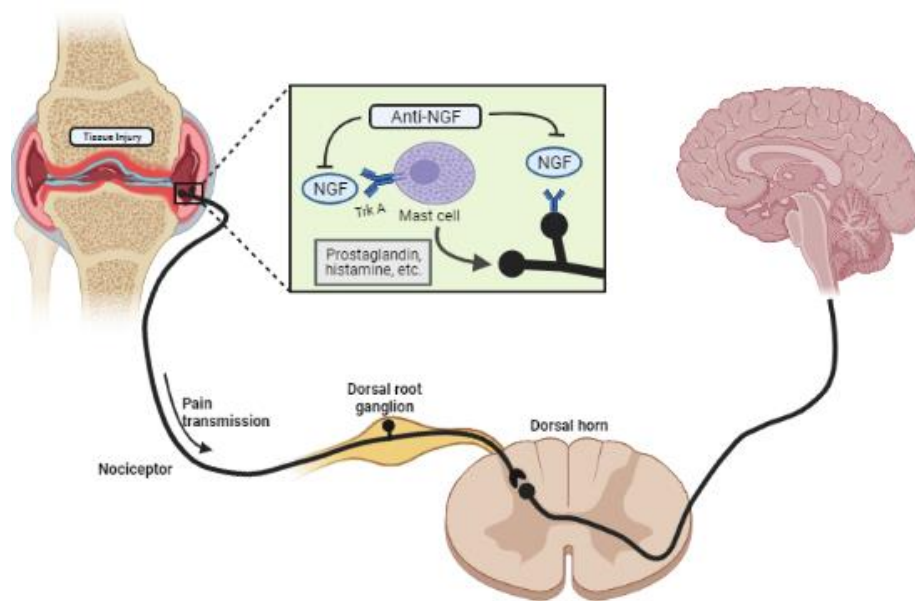
Figure 1. 4. *NGF mediated mechanism of action in post-injury pain (adapted from Lane and Corr, 2017).*
At the site of injury, inflammatory and/or bone healing cells upregulate NGF, which can act directly or indirectly act on sensory neurons, resulting in pain. NGF directly induces pain by activation of Trk A in sensory neurons, which stimulates the development of pronociceptive substances such as BDNF and neuropeptide, which mediate nociception through peripheral and central mechanisms. Alternatively, it may generate pain indirectly by activating the Trk A receptor on mast cells, which then secrete a variety of nociceptive activators on sympathetic neurons.

These observations raised the prospect of neurotrophin inhibitor-based treatments that could represent an alternative to the non-selective anti-inflammatory drugs (NSAIDs), without impairing bone healing and remodelling.

Although NGF is the most studied of all four neurotrophins in humans, NT-3 seems to have comparable roles in various cellular mechanisms. NT-3 has been shown to induce rapid phosphorylation of Erk1/2 and Akt in Trk C positive bone marrow stromal cells. Etk1/2 is also known to be essential in osteoblastic differentiation (Su *et al.*, 2016). During *in vitro* studies looking at the implications of neurotrophins in differentiation and proliferation of mouse calvaria osteoblast, NT-3 and NGF increased mRNA expression has been described (Nakanishi *et al.*, 1994). These observations may indicate that, NGF and NT-3 could play important roles in the proliferation and differentiation of progenitors from bone tissue. Moreover, specific neurotrophin receptors have also been linked with osteoblast differentiation. In actively dividing canine osteoblasts, Trk A signalling was thought to have anti-apoptotic effects, maintaining cell proliferation (Fan *et al.*, 2008).

Neurotrophins' potential involvement in growth plate cartilage were also explored. BDNF and Trk B were reported present in the growth plate cartilage in young rats. These two appeared highly expressed in the proliferation zone, moderate expressed in the hypertrophic zone and low expressed in the mineralised cartilage (Yamashiro *et al.*, 2001). Furthermore i*n vitro* studies revealed that BDNF inhibits IGF-I-dependant chondrogenic proliferation and stimulates chondro-differentiation by inhibiting the ERK-MAPK signalling pathway (Hutchison, 2012).

NGF together with its receptors have been found present in the chondrocytes from the knee articular cartilage, meniscal tissue, and epiglottis cartilage. The presence of NGF was hypothesised to have a role in controlling chondrocyte metabolism as well as cell survival (Gigante *et al.*, 2002). Moreover, while evidence supports the effect of NGF on cell proliferation and differentiation, *in vitro* studies showed no effect when cartilage progenitor cells were treated with NGF (Hutchison, Bassett and White, 2010).

Since neurotrophins and their receptors have been found present at the site of injury in the bone and cartilage level, researchers further investigated their roles in bone and cartilage repair. NT-3 and its receptor, Trk C, showed the highest expression level in the rat tibial growth plate and bone, post-injury (Su *et al.*, 2016).

In the same study, the effect of NT-3 on tissue regeneration has been investigated in the bone and cartilage injury animal model. The immunoneutralization of endogenous NT-3 resulted in severe bone and cartilage repair impairment, while treatment with recombinant NT-3 had the opposite effect. Elevated levels of mRNA for osteogenic markers in the site of injury in tibial bone was shown together with angiogenic markers at the tibial growth plate. When NT-3 effects on bone and cartilage repair were further investigated *in vitro*, it was shown that NT-3 induce Erk1/2 and Akt phosphorylation and enhance the expression of BMPs and VEGF in the differentiated cells (Su *et al.*, 2016). These results imply that NT-3 might be a promising target for enhancing bone fracture repair in regenerative medicine.

1.6. Aims and objectives:

The aim of our study was to investigate the role of neurotrophic factors in the repair process of the bone and cartilage tissue as well as to identify possible markers of the joint degenerative disease.

Elevated levels of neurotrophins have been detected in patients with diagnosed advanced osteoarthritis, indicating that they might play a crucial role in the pathophysiology of the disease. Among the four neurotrophins, NGF was reported to be present in the highest level. It is also known that NGF presence in the human joint is responsible for chronic pain and has become the focus of pharmacological strategies for analgesia. Recent exploratory studies have implicated changes in NGF as well as BDNF and NT-3 in the disruption of joint homeostasis. Moreover, they might play an important role in the tissue repair process.

We began our study by looking into the presence of the neurotrophin receptors in the joint of an osteoarthritic animal model. Strong presence could indicate a role for the neurotrophin signalling pathway in the pathophysiology of the disease. In addition, the affinity of neurotrophins for the Trk receptors was examined in order to identify one or more candidate molecules. This data was considered in conjunction with the animal model data for a prevalent receptor in the osteoarthritic joint. From then on, we decided to focus on the neurotrophins NGF and NT-3. According to the literature, these are the neurotrophins with the higher proliferation and differentiation potential.

We then continued our work on human joint derived cells and focused on a progenitor cell population derived from the osteoarthritic hip joint. Progenitor cells were isolated and the effect the selected neurotrophins, receptor binding and subsequent signalling was explored.

For our study we isolated bone and cartilage stroma cells from the trabecular bone of the femoral head. The tissue was obtained from the patients that underwent hip replacement surgery. Following surgery, the femoral head is considered biological waste, and it is discarded. Healthy bone marrow aspirates were used as a healthy control, as this was the closest available source of cells with similar physiology.

Stroma cells isolated from healthy bone marrow and diseased trabecular bone were expanded *in vitro* and were investigated for the expression of stem cells markers, the

detection of MSC surface markers, as well as their differentiation potential. All of these were carried out in order to confirm the progenitor nature of the isolated cells before further investigation.

The impact of NGF and NT-3 on cell proliferation, as well as osteogenic and chondrogenic differentiation was tested on diseased hip derived progenitors by and healthy progenitors from bone marrow. The neurotrophin treatment was tested at multiple concentrations as previous studies have shown that neurotrophins can be cytotoxic at high concentrations.

Moreover, we investigated the composition of the secretome for osteoarthritic joint trabecular bone and cartilage derived stroma cells. These were compared with the secretome of healthy bone marrow derived stroma cell. The aim of this was to identify potential osteoarthritis specific disease markers. To this end we examined the protein and small peptide content of extracellular vesicles derived from the stroma cells during the post-isolation *in vitro* expansion period.

Overall, we believe that this study provides interesting insights in the biology and cellular signalling of osteoarthritic bone and cartilage stroma cells. In addition, our work can provide an important insight into the molecular characteristics of osteoarthritis pathology, which could prove the starting point for novel treatment options.

Chapter 2: General Materials and Methods

The resources listed below were used to carry out the work presented in this thesis.

Table 2. 1. List of cells and cell culture reagents

Material	Product Code	Supplier	Further Information
PC12	299022401-1VL	Sigma-Aldrich UK	Cell line from Rat adrenal gland (phaeochromocytoma)
hMSCs			Isolated from the bone marrow of healthy donors and from the femoral head of patients with osteoarthritis.
MG-63	86051601	Sigma Aldrich UK	Human osteosarcoma
SW-1353		ATCC	Human chondrosarcoma
hCPCs			Isolated from the femoral head of patients with osteoarthritis.
Gibco™ DMEM, high glucose, GlutaMAX™ supplement, pyruvate	12077549	Fisher Scientific UK	
Gibco™ RPMI-1640 Medium	11530586	Fisher Scientific UK	
Gibco™ Fetal Bovine Serum	11573397	Fisher Scientific UK	FBS
Horse Serum			
Gibco™ L-Glutamine (200mM)	15410314	Fisher Scientific UK	
Gibco™ MEM Non-Essential Amino Acids Solution (100X)	11350912	Fisher Scientific UK	NEAA
Antibiotic-Antimycotic (100X)	15240096	Fisher Scientific UK	PSA
Gibco™ Trypsin-EDTA (0.25%), phenol red	11570626	Fisher Scientific UK	
Collagenase Type I (0.25%)	07902	Stem Cell Technologies	

Pronase from *Streptomyces griseus*	10165921001	Sigma-Aldrich UK	
Gibco™ ACK Lysis Buffer	11509876	Fisher Scientific UK	
Gibco™ PBS [-CaCl$_2$, -MgCl$_2$]	15374875	Fisher Scientific UK	[-CaCl$_2$, -MgCl$_2$]
Collagen type IV from human placenta	C5533	Sigma-Aldrich UK	
Fibronectin, huma plasma	F2006	Sigma-Aldrich UK	
Pierce™ Dimethyl sulfoxide (DMSO)	10127403	Fisher Scientific UK	
Gibco™ Trypan Blue solution, 0.4%	11538886	Fisher Scientific UK	
Resazurin Sodium Salt	11464687	Fisher Scientific UK	
L-ascorbic acid-2-phosphate	A8960	Sigma-Aldrich UK	
β-glycerol phosphate	50020	Sigma-Aldrich UK	
Dexamethasone	D4902	Sigma-Aldrich UK	
Gibco™ Insulin-Transferrin-Selenium (ITS-G) (100X)	12097549	Fisher Scientific UK	
Transforming Growth Factor-β1 human	T7039	Fisher Scientific UK	
Indomethacin	PHR1247	Sigma-Aldrich UK	
3-Isobutyl-1-Methylxanthine	I5879	Sigma-Aldrich UK	
Bovine pancreas derived Insulin	I6634	Sigma-Aldrich UK	
Animal-Free Recombinant Human β-NGF	AF-450-01	PeproTech	
Animal-Free Recombinant Human/Murine/Rat BDNF	AF-140-02	PeproTech	
Animal-Free Recombinant Human NT-3	AF-450-03	PeproTech	

Material	Product Code	Supplier	Further Information
Animal-Free Recombinant Human NT-4	AF-450-04	PeproTech	

Table 2. 2. List of antibodies and reagents used for immuno-staining and histology staining.

Material	Product Code	Supplier	Further Information
Anti-p75NTR unconjugated antibody	Ab8874	Abcam UK	1:2500
Anti-Trk A unconjugated antibody	MA5-15509		1:200
Anti-Trk B unconjugated antibody	Sc-377218	Santa Cruz Biotechnology	1:250
Anti-Trk C unconjugated antibody	Ab33656	Abcam UK	1:100
Donkey anti-rabbit Alexa Fluor 568	Ab175470	Abcam UK	1:200
Donkey anti-mouse IgG Alexa Fluor 647	Ab150111	Abcam UK	1:200
Goat anti-mouse IgM mu chain Alexa Fluor 647	Ab150123	Abcam UK	1:200
Donkey anti-goat IgG Cy5	Ab6566	Abcam UK	1:1000
Goat anti-mouse IgG HRP antibody	Ab6789		1/500
Goat anti-mouse IgM HRP antibody	Ab97230	Abcam UK	1:200
Rabbit anti-goat HRP antibody	Ab6741	Abcam UK	1:1000
Normal Rabbit IgG Control	AB-105-C	R&D Systems UK	
Normal Mouse IgG	Sc-2025	Santa Cruz Biotechnology	
Normal Mouse IgM	Sc-3881	Santa Cruz Biotechnology	
Normal Goat IgG	AB-108-C	R&D Systems UK	
DAPI stain	D9542	Sigma-Aldrich UK	
Paraformaldehyde	P6148	Sigma-Aldrich UK	
Triton X-100	11408706	Fisher Scientific UK	
Tween-20	11417160	Fisher Scientific UK	

Gibco™ PBS Tablets	11510546	Fisher Scientific UK	
HistoChoice® Clearing Agent	H2779	Sigma-Aldrich UK	
10x Citrate Buffer pH 6.0	Ab64214	Abcam UK	
Goat Serum	Ab7481	Abcam UK	
Bovine Serum Albumin	11413164	Fisher Scientific UK	
Haematoxylin	H3136	Sigma-Aldrich UK	
Acid Alcohol	56694	Sigma-Aldrich UK	
Ammonium Chloride	11437227	Fisher Scientific UK	
DPX Mountant	06522	Sigma Aldrich UK	
Mowiol® 4-88	81381	Sigma Aldrich UK	
Alcian Blue staining solution	TMS-010	Sigma-Aldrich UK	
OIl Red O staining solution	1024190250	Sigma-Aldrich UK	
Alizarin Red S sodium salt	11319707	Fisher Scientific UK	

Table 2. 3. List of antibodies and reagents used for flow cytometry analysis

Material	Product Code	Supplier	Further Information
CD105 abtibody, anti-human, FITC, Clone 43A4E1	130-098-778	Miltenyi Biotec	1:100
CD90 (Thy1) antibody, anti-human, Alexa Fluor® 700, Clone 5E10	328120	BioLegend	1:100
CD146 antibody, anti-human APC/Fire™ 750, Clone P1H12	361028	BioLegend	1:100
CD271 antibody, anti-human, FITC, Clone 43A41	130-117-696	Miltenyi Biotec	1:100
CD9 antibody, anti-human, FITC, Clone REA1071	130-118-806	Miltenyi Biotec	1:100

CD63 antibody, anti-human, APC-Vio® 770 Clone H5C6	130-100-171	Miltenyi Biotec	1:100
CD81 antibody, anti-human, APC, clone REA513	130-119-787	Miltenyi Biotec	1:100
CytoFLEX Daily QC Fluorospheres	B53230	Beckman Coulter USA	
VersaComp Antibody Capture Bead Kit	B22804	Beckman Coulter USA	

Table 2. 4. List of kits

Material	Product Code	Supplier	Further Information
Cell Counting Kit 8 (WST-8/CCK8)	Ab228554	Abcam UK	
EnVision Detection Systems Peroxidase/DAB, Rabbit/Mouse, HRP Visualisation Kit	K5007	Agilent UK	
QuantiNova SYBR RT-PCR Kit	208352	QIAGEN UK	

Table 2. 5. List of other reagents and materials.

Material	Product Code	Supplier	Further Information
Sodium Dodecyl Sulfate (SDS)	1540685	Fisher Scientific UK	
Glycerol	10021083	Fisher Scientific UK	
Tris HCl	11420203	Fisher Scientific UK	
EDTA	10011123	Fisher Scientific UK	
DTT	15846582	Fisher Scientific UK	
Bromophenol Blue	10497573	Fisher Scientific UK	
12% Mini-PROTEAN® TGX Stain-Free Protein Gels	4568033	Bio-Rad Laboratories UK	
EZ-Ru™ Prestained Protein Ladder	10638393	Fisher Scientific UK	

Bio-Safe™ Coomassie Blue Stain	1610786	Bio-Rad Laboratories UK	
Methanol	11367996	Fisher Scientific UK	
Acetic Acid	10005910	Fisher Scientific UK	
Polyethylene glycol 6,000 (PEG 6,000)	11448177	Fisher Scientific UK	
Invitrogen™ TRIzol™ Reagent	12034947	Fisher Scientific UK	
Isopropanol	11388461	Fisher Scientific UK	
Ethanol	15552393	Fisher Scientific UK	
Chloroform	11332878	Fisher Scientific UK	
Ammonium Hydroxide	15522233	Fisher Scientific UK	
Glutaraldehyde	10366890	Fisher Scientific UK	
Halt™ Protease Inhibitor Cocktail (100X)	10516495	Fisher Scientific UK	
30% Acrylamide	EC-890	National Diagnostics	
Ammonium Persulfate	10081503	Fisher Scientific UK	
N,N,N',N'-Tetramethylethylenediamine (TEMED)	T9281	Fisher Scientific UK	
Glycine	10467963	Fisher Scientific UK	
Ammonium Bicarbonate	10532775	Fisher Scientific UK	
Acetonitrile	10207120	Fisher Scientific UK	
2-Chloroacetamide	10071660	Fisher Scientific UK	
Formic Acid	10736834	Fisher Scientific UK	
Trifluoracetic Acid	13464279	Fisher Scientific UK	
Pierce™ Trypsin Protease, MS grade	13464189	Fisher Scientific UK	
Pierce™ C 18 Spin Tips	11814141	Fisher Scientific UK	

2.1. Cell Culture

2.1.1. Semi-adherent cell culture: Rat adrenal phaeochromocytoma (PC12)

Commercially acquired PC12 cells were cultured in RPMI-1640 supplemented with 10% (v/v) Horse Serum, 2 mM L-Glutamine, 1% (v/v) Penicillin-Streptomycin. For the subculture routine, cells were fed three times a week and split 1:3 to 1:6 with a seeding density of 2 - 4 x 10^4 cells/cm^2.

The total number of cells was determined through haematocytometer counting, as described below in the cell viability section.

For monolayer culture of PC12 cells, the culture dishes were treated with 10 µg/cm^2 of sterile collagen type IV solution prior to seeding. The culture surface was evenly covered with Collagen type IV solution and incubated for 2 hours at 37°C for or overnight at 4°C. The collagen solution was removed, and the culture dishes were rinsed once with sterile tissue culture grade water before introducing the cells and the media.

2.1.2. Adherent cell culture: Human Primary MSCs and CPCs.

Human MSCs were isolated from two different sources: Bone Marrow Aspirates of two healthy donors and fragments from the femoral head of five patients with osteoarthritis.

2.1.2.1. Fibronectin coating of tissue culture flasks

Prior to seeding, the surface of the tissue culture flasks was covered with 10 ng/ml sterile Fibronectin solution for 1 hour at 37°C. The excess solution was removed, and the freshly isolated cells were seeded in the Fibronectin coated dishes.

2.1.2.2. Isolation of human MSCs from bone marrow

hMSCs were isolated from commercially available human bone marrow aspirates (purchased from Lonza) using the plastic adherence selective method. The whole

bone marrow, extracted from the iliac bone of two healthy donors, was seeded at a density of 1 x 10^5 mononuclear cells/cm^2 on fibronectin coated tissue culture flasks in DMEM-GlutaMAX media supplemented with 10% FBS/5% PRP, 1% NEAA, 1% Penicillin-Streptomycin.

2.1.2.3. Isolation of human MSCs from bone tissue

 hMSCs were isolated from the bone compartment of the femoral heads from the patients that underwent hip replacement surgery.   Consent was obtained prior to the intervention. The human tissue collection was ethically approved following the REC submission, Reference: 18/LO/1015, IRAS project ID: 230993 (available in the Appendix section).

The freshly removed femoral head was cut in approximative 1 cm^2 fragments and transported n tissue culture grade 1X PBS [-Ca, -Mg] supplemented with 1X Penicillin-Streptomycin in sterile collection containers. The cells from the bone fragments were mechanically disrupted in 1x PBS [-Ca, -Mg] – 1% Penicillin-Streptomycin with a sterile set of pestle and mortar. The obtained cell suspension was filtered through 40 μm cell strainers and collected in 50 ml collection tubes. The bone fragments were crushed until the saline solution appeared clear. The cell suspension was digested with 0.25% Collagenase type I for 45 minutes at 37°C with regular vortexing at every 10 -15 minutes. The digested cell suspension was filtered through 40 μm cell strainers in a collection tube. The cell suspension was centrifuged at 1,200 rpm for 5 minutes and the supernatant was discarded. The cells were washed once with 1x PBS – 0.5% FBS. The cell suspension was cleared from erythrocytes by incubation (1:1) with 10 ml of Gibco™ ACK Lysis buffer for 5 minutes. The cell suspension was washed twice with 1x PBS – 0.5% FBS and resuspended in appropriate volume of cell culture media. The cells were counted using a haematocytometer as mentioned above in the semi-adherent cell culture section. Haematocytometer method is described in detail below in the cell viability section of this chapter.

Approximately 2 x 10^4 cells/cm^2 were seeded in 75 cm^2 fibronectin coated tissue culture flasks in DMEM-GlutaMAX media supplemented with 10% FBS, 1% NEAA, 1% Penicillin-Streptomycin.

The cells were maintained at 37$°C$, 5% CO_2 and 21% oxygen.

2.1.2.4. Isolation of human CPCs from articular cartilage

Articular cartilage from the surface of the femoral heads collected from the osteoarthritic patients was surfaced shaved in approximative 1 cm long sections, with a sterile scalpel without damaging the tidemark. The tissue was further shredded and transferred in 15 ml centrifuge tubes. The cartilage fragments were digested by incubation in 2% Pronase in DMEM non-supplemented media for 1 hour, followed by 3 hours incubation in 0.075% Collagenase type 2 in DMEM non-supplemented media. The tissue digest was sieved through a 40 µm cell strainer in a 50 ml collection tube. The cell suspension was centrifuged at 1,200 rpm for 5 min. The supernatant was discarded, and the cell pellet was washed twice in sterile PBS, reconstituted in a low volume of DMEM media and counted with a haematocytometer. The cell pellet was reconstituted in Gibco™ DMEM-GlutaMAX supplemented with 5% PRP, 1% NEAA and 1% PSA and seeded in Fibronectin coated tissue culture flasks at a 2 x 10^3 cells/cm^2 density.

2.1.2.5. Primary human MSCs and CPCs expansion:

After the isolation and seeding in Fibronectin coated plates, primary human MSCs and CPCs were allowed to attach for a total of 14 days, where media was 50% refreshed at day 7 post-isolation and 100% refreshed at day 14 post-isolation. The media at these time points was collected and stored at -20$°C$ for the isolation of extra-cellular vesicles (EVs).

Seeded cells from all sources (diseased hip joints and healthy bone marrow) were maintained in culture for two weeks in a humidified atmosphere at 37$°C$, 5% CO_2, 21% O_2. On day 7 post-isolation, 50% of the culture media was collected and replaced with similar volume of fresh media. On day 14 post-isolation, the whole media was collected and replaced with fresh media. After two weeks expansion, the number of attached cells was assessed and the isolated human MSCs and CPCs were either seeded for experiments in microplates (if sufficient cell number was obtained), cryopreserved (if high number of cells was obtained), or maintained in culture (if low number of cells was obtained).

2.1.3. Cell Expansion

The cells (hMSCs and hCPCs) were passaged when 80% confluency was reached, by enzymatic cell dissociation with Trypsin-EDTA. The culture medium was discarded, the cells were washed three time with cell culture grade Gibco™ PBS (-$CaCl_2^-$, -$MgCl_2$). A volume of 3 ml, for cells in 75cm2 flasks, and 1 ml, for the cells in 25 cm2 flasks, of 0.25% Trypsin-EDTA was added with the cells and incubated at $37^{\circ}C$ for 5 minutes. Once the cells were detached, the enzyme was inactivated by pipetting an equal volume of culture medium containing FBS. The detached cells were split 1:2 to 1:4 in fresh tissue culture flasks. Extra culture medium: Gibco™ DMEM GlutaMAX supplemented with 10% (v/v) FBS, 1% (v/v) PSA and 1% (v/v) NEAA. The cells were incubated in a humidified atmosphere at $37^{\circ}C$, 5% CO_2, 21% O_2.

2.1.4. Cell cryopreservation

For both, adherent and semi-adherent cells included in this study, stocks were cryopreserved for future use.

For the cryopreservation of PC12, confluent cells cultured in 75cm2 flasks were harvested in 15 ml sterile centrifuge tubes and centrifugated for 5 minutes at 1,200 rpm. The supernatant was discarded carefully without disturbing the cell pellet. This was reconstituted in 1 ml of cryopreservation media (90% Horse Serum and 10% sterile DMSO). The Horse Serum-DMSO-cell suspension was transferred into a 1.5 – 2 ml tissue culture grade cryovial and placed in Mr. Frosty™ Freezing Container at -$80^{\circ}C$. After a minimum of 24 hours of slow-freezing in the -$80^{\circ}C$ freezer, the cryovials containing the cell stocks were transferred into liquid nitrogen.

For the cryopreservation of hMSCs and hCPCs, media of confluent monolayer cell populations in 75cm2 flasks was aspirated and the cells were washed 3 times with PBS [-$CaCl_2$, -$MgCl_2$]. The cells treated with 3 – 5 ml of 0.25% Trypsin – EDTA and incubated at $37^{\circ}C$ for no longer than 5 minutes. Once the cells dissociated from the tissue culture flasks, equal volume of culture media was added to the trypsin-cell

suspension, to neutralise the trypsin. The media-cell-trypsin suspension was transferred to 15 ml sterile centrifuge tubes and centrifugated for 5 minutes at 1,200 rpm. The supernatant was carefully discarded without disturbing the cell pellet. The cells were reconstituted in 1 ml of cryopreservation media (90% FBS, 10% sterile DMSO). The cells in cryopreservation media were transferred in 1.5 – 2 ml tissue culture grade sterile cryovials. The cells were slow-frozen using Mr. Frosty™ freezing container in the -80℃ freezer. After a minimum of 24 hours, the cryovials containing the cells were transferred to liquid nitrogen.

2.2. Multipotency and characterisation of progenitor cells: hMSCs and hCPCs *in vitro* tri-lineage differentiation

2.2.1. Osteo-differentiation

For osteogenic differentiation, hMSCs and hCPCs isolated from the healthy bone marrow aspirates and osteoarthritic femoral heads were seeded in 6 well plates at a density of 4×10^3 cells/cm^2 and cultured for 21 days in osteogenic medium (DMEM supplemented with 10% FBS, 1% PSA, 0.2 mM L-ascorbic acid-2-phosphate, 20mM β-glycerol phosphate and 100 nM dexamethasone. Medium was refreshed every 3 – 4 days. At day 21, the medium was aspirated, and the cells were fixed and stained for the detection of calcified matrix with Alizarin Red.

2.2.2 Chondro-differentiation

For chondrogenic differentiation, hMSCs and hCPCs from the healthy bone marrow aspirates and osteoarthritic femoral heads were seeded in 6 well plates by micro-drop technique: 5 drops (25 – 50 µl) containing 4×10^3 cells in each drop were pipetted per well. The plate was carefully transferred to the incubator (37℃, 5% CO_2, 21% O_2) without disturbing the cell suspension drops and the cells were allowed to attach for 30 minutes. The cells were treated with chondrogenic media (DMEM supplemented with 1% PSA, 1% insulin-transferrinselenous acid, 0.2 mM ascorbic acis-2-phosphate, 100nM dexamethasone and 10 ng/ml transforming growth factor-β1. Medium was

refreshed every 3 days. At day 21, the chondrogenic media was aspirated, cells were fixed and the distribution of glycosaminoglycans (GAGs) was confirmed with Alcian blue staining.

2.2.3. Adipo-differentiation

For adipogenic differentiation, hMSCs and hCPCs isolated from healthy bone marrow and osteoarthritic hip joints were seeded in 6 well plates at a density of 8×10^3 cells/cm^2. The cells were cultured in culture media until attached and treated for 21 days with adipogenic media (DMEM supplemented with 10% FBS, 1% PSA, 0.01 mM indomethacin, 83 mM isobutyl methylxanthine and 1.72 µM bovine pancreas-derived insulin. The medium was refreshed every 3 days. At day 21, adipogenic media was aspirated and the samples were fixed and stained for intracellular lipid vesicles with Oil Red O.

2.3. Cell viability

2.3.1. Haematocytometer cell counting

For the assessment of PC12 cell number, the cells were mechanically dissociated from the surface of the tissue culture flasks by media flushing and transferred to 15 ml centrifuge tubes. The cells were separated from the media by centrifugation at 1,200 rpm for 5 minutes. The media was discarded, and the cell pellet was reconstituted in known volume of media (3 – 5 ml, cell density dependant).

For the assessment of hMSCs and hCPCs cell number, the media was aspirated, and the cells were washed three times with sterile PBS [-CaCl$_2$, -MgCl$_2$]. The cells were treated with 3 – 5 ml of 0.25% Trypsin – EDTA at 37ºC. Once the cells were dissociated from the tissue culture flasks, 3 – 5 ml culture media was used to neutralise the effect of trypsin.

Once the cells (both adherent and semi-adherent cells) were in low volume suspension, 20 µl of each sample was collected in a 1.5 ml microcentrifuge tube and

mixed (1:1) with 20 µl of 0.4% (w/v) Trypan Blue solution. 10 µl of the stained cell suspension was transferred on the grid section of a haematocytometer and covered with a glass coverslip. The viable (purple to white) cells were counted by visualisation with an inverted microscope. The total number of cells was determined using the formula below:

Cells/ml = (Total cells counted x Dilution Factor x 10, 000 cells/ml)/ Number of 1mm^2 squares counted

2.3.2. Alamar blue assay: NGF and NT-3 effect on the proliferation of PC12

5×10^4 PC12 cells were seeded in clear flat bottom 96 well plates in RPMI-1640 media supplemented with 2% Horse Serum, 2mM L-Glutamine and 1% Penicillin-Streptomycin. On day 1, the media was replaced with 150 µl of cell culture media containing serial dilutions of human NGF and NT-3 recombinant proteins (12.5 ng/ml, 25 ng/ml and 50 ng/ml). In parallel to the neurotrophin treatment, control wells (untreated cells, media only and PBS solution) were included in the same plate. The cells were incubated in a humidified atmosphere at $37^{\circ C}$, 5% CO_2 and 21% O_2. Each treatment was carried out in 3 technical replicates. 50 µl of the treatment media was applied every two days. On day 7, 30 µl of 1.6 mM (w/v) Alamar Blue sterile solution was pipetted in each of the wells and the experimental plates were incubated in a humidified atmosphere at $37^{\circ C}$, 5% CO_2 and 21% O_2, for 6 hours. The mitochondrial activity of the cell population will reduce the Alamar Blue reagent, known as Resazurin into a highly fluorescent substance, called Resorufin. The fluorescence of this in each of the conditions was recorded at 544 nm with BMG LabTech FLUOstar microplate reader.

2.3.3 Cellular viability of hMSCs and hCPCs under NGF and NT-3 treatment: CCK8 cell counting assay

For the assessment of cellular viability of hMSCs and hCPCs, the CCK8 Cell Counting Kit was used.

5×10^3 cells were seeded in black 96 well plates with flat clear bottom and incubated in DMEM supplemented with 10% FBS, 2mM L-Glutamine, 1% PSA, 1% NEAA at 37°C, 5% CO_2, 21% O_2 until full attachment to the microplate was reached across all samples.

On day 1, the media was replaced with DMEM supplemented with 5% FBS, 2mM L-Glutamine, 1% PSA, 1% NEAA and a range of concentrations for recombinant NGF, NT-3 or both at different concentrations: 12.5 ng/ml, 25 ng/ml and 50 ng/ml. A set of negative control wells (culture media without recombinant neurotrophins) were included in parallel. The cells were incubated at 37℃, 5% CO_2, 21% O_2. The media was aspirated and replaced with fresh media at day 4, day 8, day 12, day 16 and day 20 to maintain the effects of the neurotrophin treatment.

At day 0 day7, day 14 and day 21, the cellular viability of the cells under NGF and NT-3 treatment was examined with the CCK8 cell counting kit. The mechanism of action for the non-cytotoxic detection of cellular viability provided by this kit, is described in the methodology section of the Research Chapter No.2 (Chapter 4). 10 µl of WST-8 solution was added to each well and the plates were incubated for 6 hours at 37℃, 5% CO_2,21% O_2. The incubation time was determined following a set of optimisation experiments carried out previously. After 6 hours, the absorbance at 460 nm was measured with the BMG FLUOStar microplate reader and MARS data Analysis Software.

2.4. Gene expression analysis

2.4.1. Total RNA extraction

RNA was extracted from cell lysates following trypsinisation of the cells, centrifugation of the cell suspension and incubation of the cell pellet with 1 ml of Trizol reagent. The pellet was dispersed in Trizol reagent by mechanical separation and allowed to incubate at room temperature for 5 minutes. If precipitation of RNA was not immediately carried out, the cell pellets in Trizol reagent were stored at -80°C until further processing. 200µl of 100% chloroform was added to the cells-Trizol suspension and the solution was vigorously shaken for 15 – 30 seconds per reaction. The cells-Trizol-chloroform solution was incubated at room temperature for 5 minutes and

centrifugated at 12,000 x g for 15 minutes at 2 – 8°C. Following centrifugation, the tubes containing the cells-Trizol-chloroform solution showed 3-layer phase separation (red, white, and clear). The clear aqueous solution containing the RNA was collected in fresh 1.5 ml microcentrifuge tubes. The RNA was precipitated with 500 μl of 100% isopropanol per sample.   The samples were allowed to incubate at room temperature for 10 minutes and then centrifuged at 12,000 x g for 10 minutes at 2 – 8°C. After centrifugation the RNA precipitate formed a gel-like pellet at the bottom of the tube. The liquid supernatant was carefully discarded without disturbing the RNA precipitate. The RNA was washed with 1 ml of 75% Ethanol and centrifugated at 7,500 x g for 5 minutes at 2 – 8°C. The supernatant was discarded, and the RNA precipitate was allowed to air-dry for 15 minutes at room temperature. The dry RNA precipitate was dissolved in 20 – 40 μl of nuclease-free water (depending on the size of the pellet) and stored at -80°C until further processed.

2.4.2. RNA quantification

The extracted RNA was quantified using the DeNovix DS11 Quantification system that measures absorbance at the 260/280 nm ratio. Triplicate absorbance measurements were acquired per sample. The mean concentration value per sample was used to calculate the amount of RNA used in each of RT-PCR reactions for gene expression analysis.

2.4.3. Real-Time Reverse Transcriptase Polymerase Chain Reaction (RT-PCR)

The QuantiNova SYBR Green RT-PCR kit was used for gene expression analysis according to the manufacturer guidelines.

10 μl of 2x QuantiNova Probe RT-PCR Master Mix, containing QuantiNova DNA Polymerase composed of: Taq DNA Polymerase, QuantiNova Antibody, QuantiNova Guard, QuantiNova Probe RT-PCR Buffer (Tris-HCl, KCl, NH4Cl, MgCl2), and dNTP mix (dATP, dCTP, dGTP, dTTP) and 0.2 μl of 100x QuantiNova RT Mix, containing: HotStaRT-Script Reverse Transcriptase, RNase Inhibitor, DNase were mixed with the

Forward and Reverse primers for each gene. The final reaction was adjusted with RNase-Free Water to a final reaction volume of 20 µl, including the RNA template.

Customised primer sets were designed using human genes data from the Ensembl genome Browser and the NCBI Gene Database. The alignment specificity of the designed primers was assessed with NCBI Primer-BLAST.

Table 2. 6. Table of Primers sequence and their specificity details

Gene		Sequence	Annealing Temperature (°C)	Amplicon Size (bp)
GAPDH	F	CTCCTGTTCGACAGTCAGCC	60	120
	R	TGACCAGGCGCCCAATAC		
PCNA	F	GGTTACTGAGGGCGAGAAGC	60	117
	R	TTCAGGAGCCTCAGAGCGA		
BCL2	F	TGCAGGTATTGGTGAGTCGG	60	100
	R	ACAAAAGTATCCCAGCCGCC		
Cas3	F	GCATTGAGACAGACAGTGGTG	60	151
	R	GCACAAAGCGACTGGATGAAC		

Reaction set up

The Real-time RT-PCR was carried out on the Bio-Rad CFX Connect Real-Time PCR System as follows: cDNA Synthesis at 50°C for 10 minutes, denaturation at 95°C for 2 minutes and then 40 cycles that consist of denaturation at 95°C for 5 seconds, annealing and amplification at 60°C for 10 seconds followed by fluorescence reading of the plate after each cycle. The data was collected, and the relative gene expression was calculated using the comparative CT method. The data for each gene was normalised against the GAPDH CT mean values and the fold change was determined by comparison with the data collected from control samples.

2.5. Histological staining

2.5.1. Alizarin Red S staining

The media from the osteo-differentiated and the control cells was removed, and the cells were fixed with 70% ethanol at room temperature for 10 minutes. The fixing solution was removed, and the cells were washed with distilled H_2O for 5 minutes. Distilled H_2O was then aspirated, and the cells were evenly covered with 40mM Alizarin Red S solution of pH 4.1 – 4.3 and incubated at room temperature with movement for 45 to 60 minutes. Following incubation, the stain was removed, and the cells were washed with distilled H_2O five times. Once the water became clear, the liquid was removed, and the cells were allowed to dry at room temperature before imaging. The stained calcium deposits were visualised using Leica BMi1 inverted microscope and the data was collected with the already integrated camera system.

2.5.1.1. Semi-quantification of Alizarin red staining

For the semi-quantification of calcium deposits that resulted from the osteo-differentiation process, approximately 84 µl/cm^2 of 10% (v/v) acetic acid was added on dry Alizarin red stained cells and incubated at room temperature for 30 minutes with movement. The cells were scraped using a plastic cell scraper and transferred to 1.5 ml microcentrifuge tubes. The tubes with the collected cells in 10% acetic acid were vortexed for at least 30 seconds to disperse the stain in solution. The collected samples were heated at 85℃ for 10 minutes. To avoid evaporation of the sample, the tubes were sealed with parafilm prior to heat treatment. Following the heat treatment, the samples were immediately placed on ice for 5 minutes. The samples were the centrifuged at 20, 000 x g for 15 minutes. Depending on sample size 500 or 200 µl of the supernatant was transferred to a fresh 1.5 ml microcentrifuge tube. The acidity of the sample was neutralised with 200 µl (for the 500 µl samples) or 75 µl (for the 200 µl samples) of 10% ammonium hydroxide (v/v). 150 µl/ 50 µl per well, based on sample size, was transferred in a flat clear bottom 96-well plate in 3 replicates per collected sample. The absorbance at 405 nm was recorded with the BMG LabTech FLUOstar Omega microplate reader.

2.5.2. Alcian Blue staining

The cells treated with chondrogenic media for 21 days. Together with the untreated controls the cells were fixed with 70% (v/v) Ethanol for 10 minutes at room temperature on plastic culture dishes. The cells were rinsed with 1x PBS for 5 minutes, covered with 1% (w/v) Alcian Blue solution in acetic acid at pH 2.5 and placed on the rocking platform at room temperature overnight. The next day, the staining solution was removed, and the cells were rinsed with distilled H_2O until the liquid became clear. The cells were allowed to dry at room temperature and were imaged with the Leica BMi1 inverted microscope.

2.5.3. Oil Red O staining

The media was removed, and the cells were treated with adipogenic media for 21 days. Together with the untreated controls the cells were fixed with 70% (v/v) Ethanol for 10 minutes at room temperature on plastic culture dishes, were rinsed with 1x PBS for 5 minutes and stored at 4^oC until staining. Prior to staining with Oil Red O solution, the 1x PBS solution was removed and the cells were briefly treated with 60% (v/v) isopropanol for fixation. The alcohol-based solution was removed, and the cells were allowed to fully dry before staining. Dried cells were evenly covered with Oil Red O working solution (1 part Oil Red staining solution in 2 parts 100% isopropanol) and incubated at room temperature with movement for 15 minutes. The staining solution was removed, and the cells were rinsed with distilled H_2O at least five times to remove the excess stain. The cells were allowed to dry at room temperature prior to imaging. The stained lipids were visualised with EVOS M5000 Imaging System, and the data presented was collected using the microscope's integrated camera system.

2.6. Immunostaining

2.6.1. Immunohistochemistry (IHC)

Rat knee tissue preparation for paraffin embedding was undertaken by Levicept Ltd following their optimised in-house protocol. The tissue was cut at 4 µm thickness and placed on glass slides. For immunohistochemistry (IHC) staining, the slides were

placed overnight at 60$^{\circ C}$ and de-waxed twice in HistoClear for 20 mins. After all the paraffin was removed, the tissue was re-hydrated by being placed 10 minutes in decreasing concentrations of Isopropanol (100%, 95%, 90%, 80% and 70%). The tissue was rinsed and washed for 5 min twice with H_2O. For antigen retrieval, the tissue was incubated with heated 1x citrate buffer for 90 minutes. The tissue was rinsed and washed twice (for 5 min each time) with 1x PBS. Before being treated for endogenous peroxidase expression, excess water was removed with filter paper. The tissue slides were incubated with 150 µl of peroxidase block solution per slide in the dark for 20 minutes. The slides were rinsed and washed twice (for 5 minutes each time) with PBS. For the blocking of non-specific binding, the slides were incubated with 10% (v/v) goat serum in PBS for 15 minutes. Treatment with blocking buffer was not followed by washing. The tissue slides were incubated overnight with the primary antibody (Table 2.2) at 4$^{\circ C}$. The negative controls were incubated with the isotype of the primary antibody. The slides were washed three times (for 5 min each time) with PBS and incubated with the HRP-conjugated secondary antibody, for 1 hour at room temperature in the dark. The slides were washed 3 times (for 5 min each time) in PBS. The slides were then incubated with 200-300 µl (depending on tissue size) of DAB Substrate Buffer solution from Dako Kit for 10 minutes at room temperature in the dark. The slides were washed three times (for 5 min each time) with PBS. For counterstaining, the slides were places in Haematoxylin solution for 30 seconds, immediately rinsed in distilled H_2O and placed in 100% acid alcohol for 3 seconds. The slides were then washed twice (for 5 min each time) with distilled H_2O. The stained tissue samples were de-hydrated by being treated with increasing concentrations of Isopropanol (35%, 50%, 70%, 80%, 90%, 95% and 100%). The tissue samples were cleared with HistoClear for 5 minutes and again with fresh HistoClear for another 10 minutes. The tissue samples were finally mounted with 1-3 drops of DPX Mountant and covered with glass coverslips. The mounted slides were allowed to fully dry overnight in the fume cupboard, before being stored and analysed.

The intensity of the receptors staining was analysed and scored using light microscopy.

2.6.1. Immunocytochemistry (IF-IC)

Cells attached to either plates or glass coverslips were fixed with 4% paraformaldehyde, at pH 7.4 for 20 minutes at room temperature. The cells were rinsed 3 times in PBS for 5 min each time. The cells were permeabilised with PBS – 0.25% Triton X-100 for 10 minutes at room temperature. The cells were then washed three times in PBS for 5 minutes each time. In order to avoid autofluorescence, the cells were treated with 0.4 % NH_4Cl in PBS for 10 minutes at room temperature. The cells were then rinsed with PBS for three times (5 minutes each time). In order to prevent unspecific binding, the cells were incubated in blocking buffer (2% BSA in PBS – 0.2% Tween-20) for 1 hour. The cells were then incubated with unconjugated primary antibodies against p75NTR, Trk A and Trk C, which was diluted in PBS. Antibody incubation was carried out overnight at 4℃. The negative controls were incubated with specific isotypes corresponding to the chosen antibodies. The next day, the cells were washed 3 times with PBS (for 5 min each time).. The cells were then incubated with the secondary antibody (fluorescent tagged, isotype and host species - specific to the already applied primary antibodies) diluted in PBS for 1 hour at room temperature in the dark. The cells were then rinsed for three times with PBS (for 5 minutes each time). Finally, the cells were counterstained with DAPI solution (1/1000) for 5 minutes in the dark at room temperature. The counterstaining solution was rinsed three times with PBS (for 5 minutes each time). The cells were washed with distilled H_2O for 5 minutes. The immuno-stained cells were mounted with glass coverslips with 5-10 µl of 10% Mowiol® 4-88 mounting medium. The coverslips were sealed with clear nail varnish.

2.7. Flow Cytometry

In order to profile the cells by flow cytometry, a minimum of 1 x 10^5 cells were included per staining condition. The cells were collected by trypsinisation from the culture flasks and washed twice with PBS – 0.5% FBS. The cells were incubated with the fluorochrome conjugated antibodies (1/100 in PBS - 0.5% FBS) against CD105, CD90, CD146, CD45, and CD271, either single stain or multistain. for 30 min at 4℃ in dark conditions. Upon incubation, the cells were washed twice with PBS – 0.5% FBS, reconstituted in 300 µl of the same buffer and analysed with the   Beckman Coulter CytoFlex System using the CytExpert software Version 2.4. A minimum of 10,000 events were recorded per sample.

The data was analysed with the Kaluza Analysis Software Version 2.1. The recorded events were first visualised in an FSC-A/SSC-A plot and all events were gated, excluding cell debris based on event size (FSC-A) and internal complexity (SSC-A). In addition, an FSC-Width/FSC-A plot was used to exclude doublets before proceeding to marker specific analysis.

For the characterisation of the flow cytometry data, the recorded events were analysed using the following gating strategy: all events excluding debris were selecting from the FSC-A/SSC-A dot plots. From the "all gated events" single events were further gated on FSC-Width/FSC-A plots.

The gating strategy was applied on unstained and single stained controls in order to draw the boundaries of the gates used to determine antibody-stained cells recoded as positive events for the different fluorochromes.

Unstained cell samples in PBS – 0.5% FBS were used to exclude autofluorescence events and position the gates accordingly for the detection of antibody labelled cells.

Single stained cell samples and compensation beads for each of the fluorochrome conjugated antibodies. were used to calculate the degree of compensation between fluorochromes with overlapping emission spectra. Compensation was calculated with the CytExpert software Version 2.4 and confirmed with the Kaluza Analysis software Version 2.1.

The degree of fluorophore spill over and autofluorescence were taken into consideration for the final analysis of the recorded events, through compensation.

2.8. Extracellular Vesicles (EVs) isolation – PEG precipitation method

For the isolation of bone and cartilage cells derived EVs, media from day 7 and day 14 post isolation was collected from a total of 7 osteoarthritis patients and two healthy bone marrow donors

The media was cleaned of any cellular debris by centrifugation at 2,000 rpm for a minimum of 5 mins. For the precipitation of EVs, the supernatant was collected and incubated 1:1 with 16% PEG 6000 sterile solution for 18 hours at 4°C. Afterwards, the

solution was centrifugated at maximum speed (3,240 x g) for 1 h. The supernatant was discarded, the EVs pellet was reconstituted in 50-100 µl sterile PBS and stored at -80℃ until further processed.

2.9. EVs staining for SEM visualisation

10 µl of the EVs sample diluted in PBS was incubated 1:1 with 10 µl 2% (v/v) glutaraldehyde for 30 minutes at room temperature. 5 – 7 µl of the stained EVs solution was loaded on 200 mesh carbon-coated with formvar film copper grids. The samples on the grids were incubated for another 10 minutes at room temperature, prior to visualisation. The topology of the collected EVs recovered the secretome of bone and cartilage stroma cells were examined with the Hitachi SU8030 Scanning Electron Microscope and the accompanying software. Access to the equipment was granted through collaboration with University of Greenwich, Medway Campus. The manipulation of the equipment and image acquisition was completed with the help of Dr. Andy Hurt.

2.10. SDS-PAGE – Protein analysis

The EVs samples were collected as mentioned above by PEG enrichment, the obtained pellets were reconstituted in sterile PBS and stored at -80℃ until they were further processed.

The protein concentration of the collected samples was determined with the Denovix DS11 Quantification System.

2.10.1. Sample preparation

5 µg of protein diluted in 20µl PBS containing 1X Halt™ Protease Inhibitor was added to an equal volume of 2x sample buffer (4% SDS, 20% Glycerol, 10mM Tris-HCl pH 6.8, 2mM EDTA, 200mM DTT and 0.1% (w/v) bromophenol blue). The samples were reduced and denatured by heat treatment at 95ºC for 5 minutes.

2.10.2. Gel casting

The acrylamide gel was prepared with Bio-Rad Gel Casting instruments. For a total 8 ml 12 % resolving gel, 2.6 ml distilled H_2O, 3.2 ml 30% acrylamide, 2 ml of 1.5 M Tris pH 8.8, 80 µl of 10% (w/v) SDS, 80 µl of 10% (w/v) ammonium persulfate and 8 µl TEMED were mixed in a glass beaker in above mentioned order.

The liquid resolving gel was pipetted 2/3 between 2 pre-set casting plates secured on a stand. The resolving gel was layered with 100% isopropanol and allowed to set at room temperature for 20 minutes. Before applying the stacking gel, the isopropanol was removed with filter paper and the resolving gel was washed with distilled H_2O. For the preparation of a single 4% stacking gel, 3 ml distilled H_2O, 670 µl 30% acrylamide, 1.25 ml Tri pH 6.8, 10% (w/v) SDS, 10% (w/v) ammonium persulfate and 5 µl TEMED were mixed in a glass beaker. The stacking gel solution was pipetted on top of the resolving gel and the comb was placed carefully. The stacking gel was allowed to set for 10 minutes at room temperature.

2.10.3. Sample run

The comb was removed and the gel together with the casting plates was placed in the gel tank. The tank was filled with 1x TGX running buffer t pH 8.3 (25 mM Tris, 192 mM glycine and 0.1% (w/v) SDS). 40µl of the denatured sample were loaded per well. The gel was run at 50 V for 10 – 15 minutes and then at 120 V until the dye front reached the bottom of the gel.

2.10.4. Gel staining and visualisation

The gel was carefully separated from the casting plates, placed in a staining dish and covered with 50 – 100 ml of Coomassie staining solution. The gel was incubated at room temperature with gentle agitation for 1 hour followed by de-staining in de-Staining solution (40% (v/v) methanol, 10% (v/v) acetic acid) several times until the bands were visible and the background turned clear. The gel was visualised with Bio-Rad ChemiDoc Imaging System.

2.11. In-gel digestion – Mass Spec sample preparation

2.11.1. Sample preparation

Protein concentration of the EV samples was measured with the Denovix DS11 Quantification System. 10µg of protein was diluted 1:1 in 2x sample buffer (4% SDS, 20% glycerol, 10mM Tris-HCl pH 6.8, 2mM EDTA, 200mM DTT and 0.1% (w/v) bromophenol blue) and denatured at 95ºC for a minimum of 5 min.

2.11.2. Running the gel

The samples were loaded in alternate wells of 4-20% Mini-PROTEAN TGX Precast Protein Gel and run at 50 V in 1xTGX Buffer until the dye front reached 1 cm distance in the resolving gel.

2.11.3. Coomassie gel Staining

 Each gel was placed in a plastic plate pre-washed with methanol plastic plate and stained in 50-100 ml of Bio-Safe™ Coomassie stain for at least 1 hour. The gels were destained in a 50% (v/v) methanol/10% (v/v) acetic acid solution for 30 min.

2.11.4. Bands excision

The bands were excised and cut in smaller pieces (~ 2 x 1 mm), transferred in 1.5ml microcentrifuge tubes and kept in 100 µl distilled water at 4ºC until further processing.

2.11.5. Sample reduction and alkylation

The gel pieces were washed in 150 μl of 50 mM NH_4HCO_3: acetonitrile (1:1) for 15 min and span down 1 min at 5,000 rpm The supernatant was discarded, and the gel pieces were allowed to shrink in 150 µl fresh acetonitrile for 15 min. The gel samples were span down for 1 min at 5,000 rpm, the acetonitrile was discarded, and the shrunk pieces were incubated in 100 µl of 10 mM DTT in 50 mM NH_4HCO_3, at 56ºC for 30 min. The samples were then span at 5,000 rpm for 1 minute and the liquid was

removed. The gel pieces were treated briefly with acetonitrile (~100 µl) for 1 minute. The liquid was removed, and the samples were incubated in 100 µl of 55 mM chloroacetamide in 50 mM NH_4HCO_3 for 20 minutes at room temperature in the dark. The gel pieces were span down at 5,000 rpm for 1 min, the chloroacetamide solution was removed, and the gel pieces were washed with 150 µl of 50 mM NH_4HCO_3: acetonitrile (1:1) for 15 min. The samples were span down at 5,000 rpm for 1 min and all the liquid was removed. The gel pieces were washed again with 150 µl of 50 mM NH_4HCO_3 for 15 min. Another 100 µl of acetonitrile was added and the gel pieces were left to incubate for another 5 minutes. Post incubation, the gel pieces were separated by centrifugation at 5,000 rpm for 1 min and the liquid was discarded. Gel pieces were again left to shrink in 200 µl fresh acetonitrile for 15 min.

2.11.6. Sample digestion

For the in-gel protein digestion, the acetonitrile was separated from the gel pieces by centrifugation (5,000 rpm for 1 min) and discarded. The gel pieces were incubated overnight at room temperature in 50 µl digestion buffer (12.5 mM NH_4HCO_3, 10% acetonitrile) containing 5 ng/µl of trypsin.

For the extraction of peptides, 15 µl of acetonitrile was added to the digested samples. The samples were then sonicated in an ultrasound bath for 15 mins. The samples were centrifugated at 5,000 rpm for 1 min and the supernatant was collected in 0.5 ml microcentrifuge tubes pre-cleaned with methanol. For the full extraction of peptides, the gel pieces were sonicated again for 15 min with 30 µl 50% acetonitrile, 5% formic acid solution per sample. The samples were centrifugated, the supernatant was collected and combined with the supernatant collected in the first peptide extraction step described above. The gel pieces were retained until the samples were analysed with mass spectrometry.

2.11.7. Nano LC-MS/MS sample run

For proteomics analysis with the nano-LC-MS/MS, the freshly prepared samples were vacuum dried and resuspended in 20 µL of 5% acetonitrile, 0.1% TFA.

In order to achieve increased purity, the samples were cleaned with Pierce C18 Spin Tips according to the manufacturer specifications.

The samples were grouped based on experimental time points and tissue origin (Bone – Day 7, Bone – Day 14, Cartilage – Day 7 and Cartilage – Day 14).

The nano-LC-MS/MS bases proteomic analysis was carried out by Dr. Kevin Howland, University of Kent.

The proteomic data obtained by mass spectrometry was analysed using the Progenesis Software and the peptide sequences obtained where identified against the UniProt protein database. The amount of each peptide detected per sample was recorded and further analysed with OriginPro 2021b (Learning Edition) and QIAGEN Ingenuity Pathway Analysis Software.

2.12. Statistical analysis

The statistical analysis of the quantitative data presented in this thesis was carried out using the MiniTab™ software Version 17. The significance of the data sets is represented by p values, which are indicated by the symbol "* "and signify the following: * for p <=0.05, ** for p-value<=0.01, and *** for p-value<=0.001. The statistical test used to determine the significance for each data set is described in the equivalent graph legend. Before proceeding with the statistical tests, the normal distribution of the data was assessed for every set of data with Anderson-Darling normality test. For normally distributed data, a multi-way ANOVA or T-test were used for data sets comparison.

Chapter 3: Neurotrophins and osteoarthritis: exploring their contribution in disease pathophysiology

3.1. Introduction:

3.1.1. Neurotrophins and their receptors

Neurotrophins are growth factors with a significant role in the survival of the Central and Peripheral Nervous System (CNS and PNS). The human neurotrophin family consists of four closely related members. Nerve Growth Factor (NGF) was the first one to be identified in 1956 by Rita Levi-Montalcini and Stanley Cohent. They were awarded the 1986 Nobel Prize in Medicine for this discovery. Since this pioneering moment in neurobiology, three more neurotrophins were identified by other research groups: Brain Derived Neurotrophic Factor (BDNF), Neurotrophin 3 (NT-3) and Neurotrophin 4 (NT-4), all of them primarily identified as important players in the physiology of CNS and PNS (Barde *et al.*, 1982; Berkemeier *et al.*, 1991, Mainsopierre *et al.*, 1990). Neurotrophins are known to promote the survival and the differentiation of vertebrate neurons. They exert these processes through the activation of Tyrosine Kinase Receptors (Trk receptors). In terms of binding affinity, each of the neurotrophins present different affinities towards each of the Trk receptors. NGF binds with high affinity to Trk A, while BDNF and NT-3 bind to Trk B and Trk C respectively. Finally, NT-4 was found to prefer Trk B. (Fig. 3.1). The specificity of Trk receptors for neurotrophins has been attributed to the presence or absence of specific short amino acids sequences in the binding sites of the receptors (Clary *et al.*, 1994).
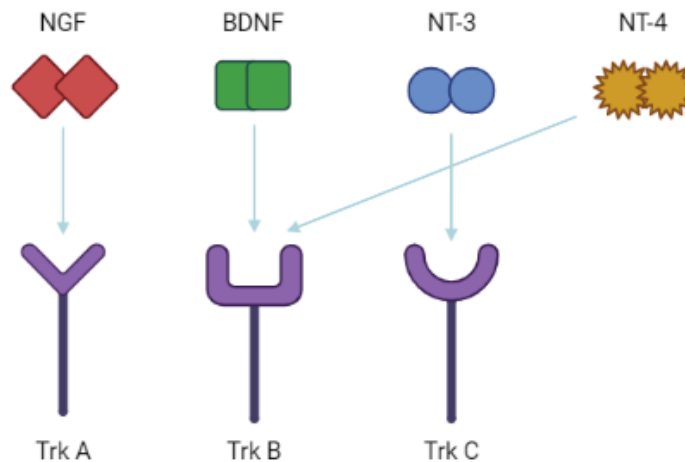
***Figure 3. 1.* Schematic representation of neurotrophins specificity for Trk receptors.**
All Trk receptors can be activated by all neurotrophins, with some differences. Because of structural variations, neurotrophins bind certain Trk receptors with a greater affinity than others. NGF has Trk A as preferred receptor, BDNF and NT4 favour Trk B over Trk A and Trk C, while NT-3 specifically activates Trk C.

Following neurotrophin characterisation, research studies focussed on the trophic effects of NGF, revealed its multiple functions in the proliferation and survival of neurons, synapse formation, neuronal functionality and plasticity, axonal and dendritic growth and reconstruction and cytoskeleton assembly and remodelling (Huang and Reichardt, 2003). However, the mechanism of action behind all these processes remained unclear until the discovery of Tropomyosin kinase receptors (Trk receptors). This had a revolutionary impact on the understanding of the molecular basis for the above-mentioned actions and more, since it supplied key instruments for the tracking of the signal pathways induced by neurotrophins.

3.1.2. Trk receptors

By comparison with other growth factor receptor tyrosine kinases, Trk receptors can be mainly distinguished due to their structural organisation of their extracellular domain. This is constituted of an array of 3 leucine-rich 24 residue motifs, surrounded by 2 cysteine-rich clusters and followed by 2 C2-type IgG-like domains (Fig. 3.2).
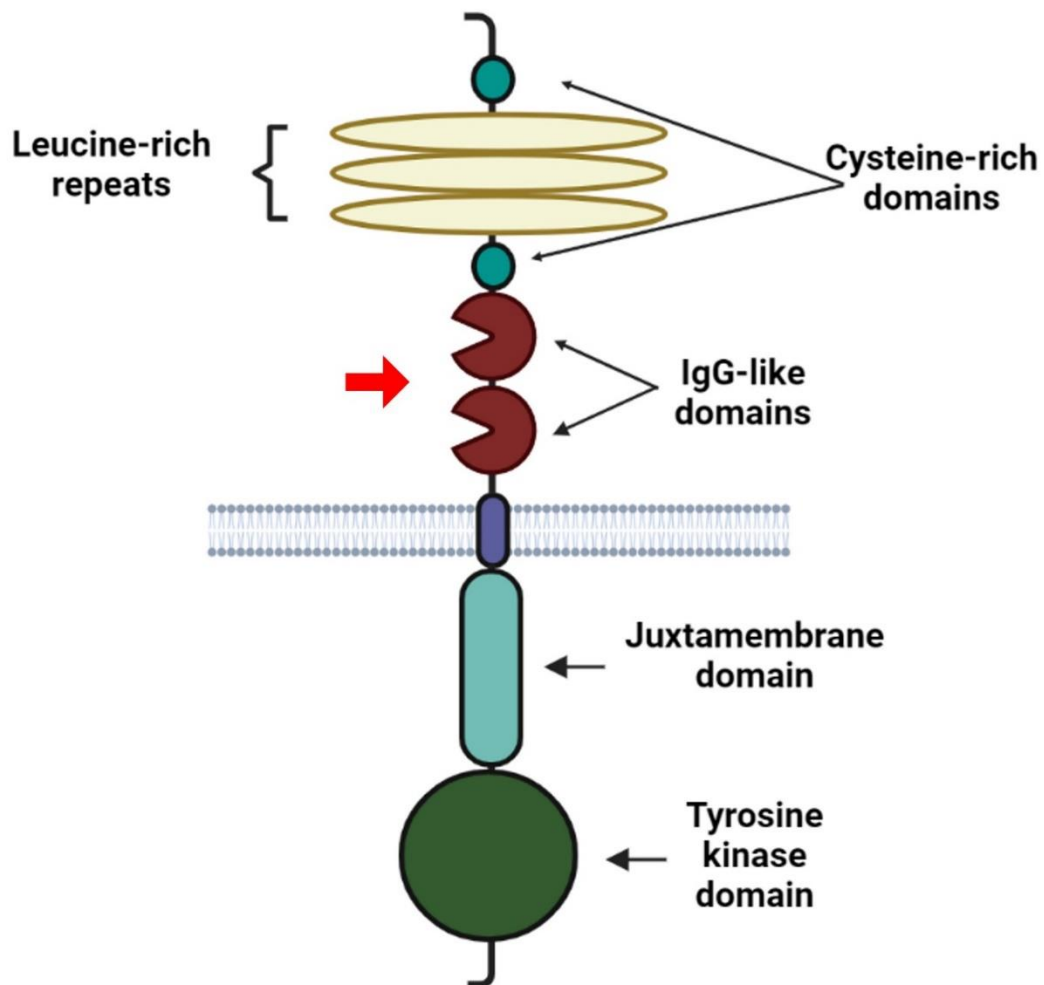
Figure 3. 2. Schematic representation of the Tropomyosin receptor kinase (Trk) structure.
The current figure shows a general representation of Trk receptors. The extracellular domain contains 2 IgG-like domains and 2 cysteine-rich domains with 3 leucine-rich repeats in between the later. The intracellular domain of the receptors has a juxtamembrane region and a Tyrosine Kinase like domain. Trk receptors distinguish themselves through different short chains of amino acids in the binding sites (red arrow). This characteristic is responsible of their different affinities towards ligands.

When first identified, NGF-high affinity receptor, Trk A, was named Tropomyosin-related Kinase because its gene sequence contains 7 out of 8 total exons encoded likewise in the non-muscular tropomyosin (Huang and Reichardt, 2003). When NGF binds to Trk A this leads to receptor dimerization that induce autophosphorylation of the intracellular tyrosine kinase domain. This leads to the activation of the, the Ras/MAPK and PI3K/Akt pathways, leading to modulations of cell survival by impairing pro-apoptotic transcriptional factors (Reichardt, 2006).

Trk B activation by BDNF and NT4 initiates intracellular signalling cascades with important roles in the function and survival of the neurons in the CNS. Although both BDNF and NT-4 have high specificity for Trk B, they trigger different intracellular processes, which makes them non-interchangeable.

For example, Fan *et al* in their *in vivo* experiments have shown that the outcome of the Trk B mediated signalling is dependent on which neurotrophin activates the receptor. In the intra-uterine development, Trk B signalling is involved in the formation of hippocampal neurons. In their experiments, they have shown that activation of the Trk B receptor by BDNF has a different outcome compared with the activation of Trk B by NT-4. Synapse formation and sensory neuron support have been demonstrated to have a higher yield in Trk B$^+$ hippocampus neurons in the presence of NT4 compared to BDNF only. When NT4 was depleted and replaced with high levels of BDNF this resulted in impairment of neuronal viability (Fan *et al.*, 2000).

Trk C is mainly expressed in the PNS by proprioceptive sensory neurons and binds NT-3 with high specificity. Although NT-3 can bind with low affinities to the other two Trk receptors, Trk C tends to have aversity for the other neurotrophic factors.

Trk C and NT-3 mediated signalling pathway plays important roles in the development of neurons, axon growth, development of synapses and overall plasticity in the nervous system. Both, Trk C and NT-3 are expressed in the embryonic as well as the adult brain (Maisonpierre *et al.*, 1990). In the hippocampal neurons, NT-3 mediated Trk C activity has been shown to be vital for synaptic organization (Ammendrup-Johnsen *et al.*, 2015).

Despite the fact that the presence of Trk receptors in the CNS and PNS facilitates critical neurophysiological processes, their expression has also been linked to the development of cancer, inflammatory arthritis, Alzheimer's disease, and Parkinson's disease, as well as mental health disorders such as bipolar disorder and schizophrenia. (Soontornniyomkij *et al.*, 2011).

Overall, Trk receptors have become the focus of many therapeutical strategies for the treatment of neurodegenerative, psychiatric, and proliferative conditions (Gupta *et al.*, 2013).

3.1.3. Low Affinity Neurotrophin Receptor

Alongside Trk receptors, all neurotrophins bind and activate another receptor, known as p75 Neurotrophin Receptor (p75NTR) or Low-Affinity Nerve Growth Receptor. p75NTR is a member of Tumor Necrosis Factor (TNF) receptor superfamily. It is mainly expressed during early neuronal development with major implications in the formation of neurons. In the adult body, its high expression has been linked with various pathological conditions such as neurodegeneration, epilepsy, axotomy and recent studies also indicate implications in the amyloid accumulation which can lead to Alzheimer's disease (Dechant and Barde, 2002).
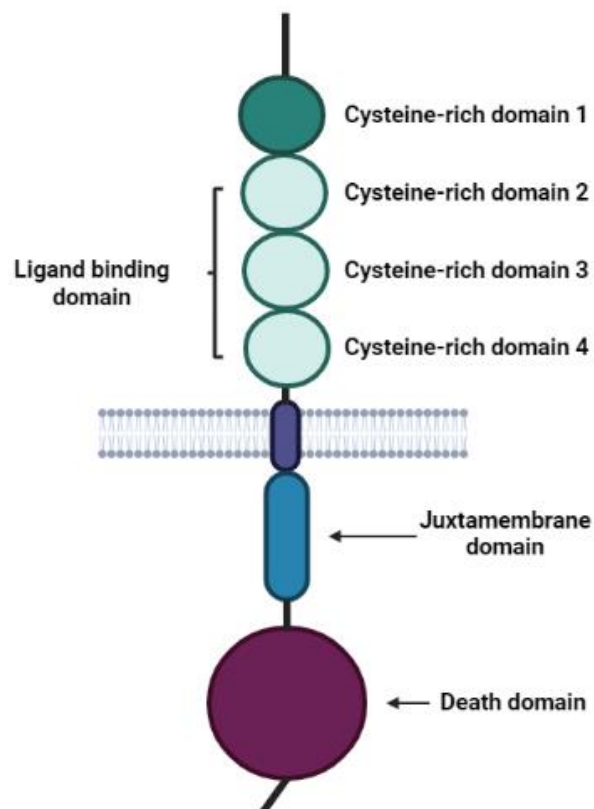
Figure 3. 3. Schematic representation of the low affinity nerve growth factor receptor, p75NTR, structure.
This figure shows relevant structures that are included in the intra-cellular and the extra-cellular domains of p75NTR. The extracellular domain contains 4 successively placed cysteine-rich regions, that distinguishes p75NTR from the other members of the Tumor Necrosis Factor Receptor Superfamily (TNFRSF) that contain just one. Three of those constitute the ligand binding region. In the intracellular region, p75NTR has a juxtamembrane region followed by the death domain.

All neurotrophins present a low affinity for the p75NTR. Through this receptor, whose structure is shown in Fig. 3.3, neurotrophins can promote the similar processes as binding to Trks. Additionally, through p75NTR, neurotrophins can induce cell death, making p75NTR a key player in the death and survival of neurons. Both types of neurotrophin receptors, Trks and p75NTR can be co-expressed. This observation raises many questions towards the neurotrophin signalling pathway, especially on the initiation of apoptosis. Is there an interaction between Trks and p75NTR? Or is p75NTR initiating cell death on its own through spontaneous signalling caused by receptor multimerization? Research in this field has provided some insight on the p75NTR paradox. The term paradox is mainly attributed to this receptor based on its inconsistency and unpredictability in term of the signalling outcome. It is well known to induce cell death but at the same time it has been shown to trigger differentiation and be involved in a direct and indirect manner in cell survival (Defreitas, Mcquillen and Shatz, 2001).

Considering the interaction of neurotrophins and their receptors, it has been shown that p75NTR plays an important role. In the absence of p75NTR expression, Trks and neurotrophin binding affinity is reduced, compared with when p75NTR is present (Hempstead, 2002). Moreover, p75NTR was shown to play key roles in the migration of the Schwann cells that are required for the survival and the repair of sensory neurons (Woldeyesus *et al.*, 1999). It has been demonstrated that p75NTR has an apoptotic function, but it may also play a critical role in the proliferation and survival of neurons in an indirect manner (Bamji *et al.*, 1998; Becker *et al.*, 2018).

The intracellular domain of p75NTR lacks a catalytic domain. p75NTR triggers intracellular signalling pathway initiation via protein-protein interactions. It relies on the intracellular present proteins for the transduction of the signal. The paradox around p75NTR appears to be based more on the cellular context and the recruitment of different cytoplasmic factors rather than the receptor on its own.

3.1.4. The implication of neurotrophins and their receptors in musculo-skeletal chronic pain.

In the last decade, neurotrophins together with their receptors have also been shown to be essential not just in CNS and PNS, but also in the skeletal joints' homeostasis and pathology. Elevated levels of NGF have been detected in the synovial fluid of patients with osteoarthritis while searching for biomarkers (Halliday *et al.*, 1998; Jones *et al.*, 2004). Later, neurotrophin, particularly NGF, mediated signalling pathway was shown to have implications in the chronic pain that is associated with this condition. (Lewin', Rueff and Mendell, 1994). This is initiated and maintained throughout the sensitization of nociceptors by the over-expression of NGF (Eskander *et al.*, 2015).

In addition, studies aiming to characterise human Mesenchymal Stem Cells (hMSCs) and investigate their potential have shown that the low affinity neurotrophin receptor, p75NTR is specific to bone marrow and adipose tissue hMSC populations (Flores-Torales *et al.*, 2010). This type of cell is highly involved in multiple processes, including tissue repair and immune modulation of the post-injury immune response. In these cells, p75NTR is not merely a cellular marker. On the contrary, it has been shown that the receptor is involved in enhancing the differentiation potential of hMSC. For example, p75NTR has been shown to induce the upregulation of α1 Integrin, resulting in osteogenic differentiation (Li *et al.*, 2020).

From these findings, NGF on its own and in cooperation with p75NTR has become the target for a number of pharmacological treatments to treat osteoarthritic chronic pain, with promising outcomes. Studies where the endogenous NGF was inhibited, resulted in a reduction of the chronic pain experienced by the patients with degenerative joint disease (Enomoto *et al.*, 2019). Unfortunately, when analysing the effect of NGF inhibition in tissue damage, it was reported that it did not help with the regression of the disease. Contrary, total depletion of NGF resulted in a more rapid progression of the disease comparative with the placebo subjects (Wise, Seidel and Lane, 2021).

With the aim to improve anti-NGF based treatment for osteoarthritic chronic pain without inducing rapid regression of the disease, the UK based bio-technology company Levicept Limited developed a p75NTR-IgG1 Fc engineered molecule that aims to be a safer alternative to the already available antibody-based anti-NGF therapies. They believe that increased neurotrophins levels are a response to damage.

The elevated levels are necessary for repair. Unfortunately, over-expressed neurotrophins also induce sensitisation of the pain receptors. Levicept Ltd. developed a p75NTR Fc protein that aims to selectively reduce the levels of neurotrophins, with specificity for NGF, causing a reduction in pain with minimal disruption of the cartilage repair process.
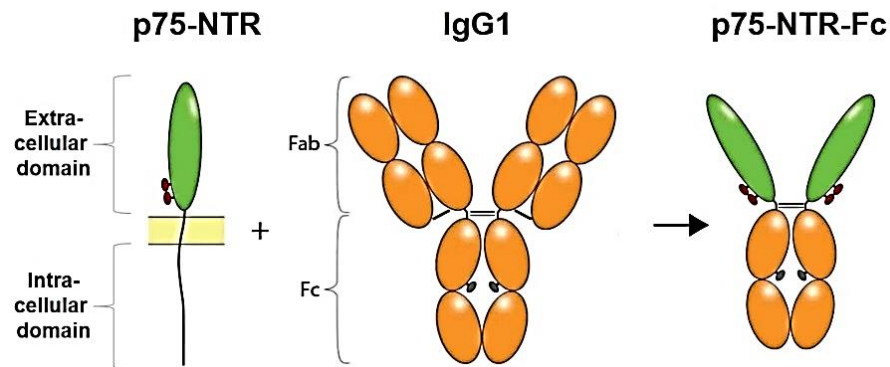
Figure 3. 4. Schematic representation of the p75NTR-Fc developed by Levicept Ltd. p75NTR-Fc molecule incorporates the binding domain of the p75NTR for capturing the neurotrophins and the Fc region of IgG1.

Initial *in vitro* and *in vivo* tests of the molecule have shown safe usage, pain reduction, as well as cartilage repair comparative with the control (osteoarthritis without treatment). When compared with the previous developed anti-NGF monoclonal antibody treatments, the p75NTR-IgG1 Fc engineered molecule aims to block only the excess NGF in patients with osteoarthritis and works in re-establishing the NGF concentration to the homeostatic level and keep it under control, instead of a complete depletion. As mentioned previously, NGF appears to be essential for the cartilage tissue repair and maintenance of the overall joint homeostasis. It is hypothesised that by bringing the level of NGF closer to homeostatic levels, it would not only alleviate chronic pain caused by NGF nociceptors sensitization but will also promote an unimpaired tissue healing process.

For this project, we collaborated with Levicept Ltd. to investigate the implications of neurotrophins and neurotrophin mediated signalling pathways in the homeostasis and the pathology of human skeletal joints, focussing on the femoral joint.

In this chapter we aim to explore the interactions between neurotrophins and their receptors within the context of osteoarthritis pathology. We focussed mainly on NGF and NT-3 due to their differentiation, and proliferation potentials, which together makes them potential candidates for bone and cartilage repair and regeneration.

3.2. Methodology:

3.2.1. Neurotrophin affinity for Trk receptors.

For the assessment of neurotrophins ligand affinities for Trk receptors, commercially available Discover X assays were carried out. This is an enzyme fragment complementation assay which is based on the chemiluminescence detection of phosphorylation through restoration of attached B-galactosidase fragments. In this assay, the osteosarcoma cell line U2OS cell line was modified to expresses Trk receptors with a small β-galactosidase fragment attached and partner proteins that contain SH2 domains and a larger fragment of β-galactosidase. When the ligand activates the receptor, it caused dimerization which results in cross-phosphorylation. The partner proteins bind to phosphorylated receptors, which brings in contact the attached β-galactosidase fragments, resulting in the restoration of the enzyme that becomes active. Activated β-galactosidase is detected by the added chemiluminescent substrate and is directly proportional to the rate of Trk phosphorylation (Fig. 3.5).
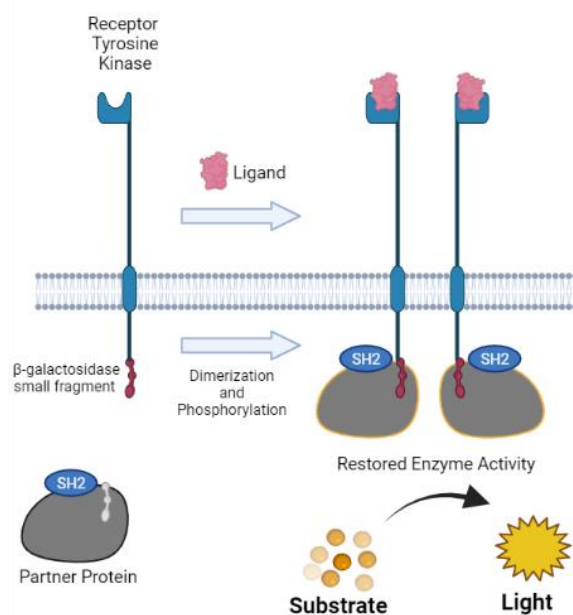
Figure 3. 5. Schematic diagram of the mechanism for the Discover X assay: enzyme fragment complementation.
The activation of the receptors by ligands results in their dimerization and phosphorylation. The activated receptor is quantified indirectly by detecting the chemiluminescence induced by the restoration of the β-galactosidase enzyme activity.

According to the kit manufacturer guidelines, the provided PathHunter eExpress Receptor Kinase cell line should be thawed and plated at least 18 hours before the assay is run. The cells were reconstituted in a total of 12 mL of provided Cell Plate reagent. 100µl of cell solution, which represents approximately 1 x 10^4 cells were seeded in each well of a 96 well tissue culture plate. The cells were placed in a 37°C, 5% CO$_2$ aseptic atmosphere, for a total of 24 hours before testing.

A stock solution for each of the recombinant neurotrophins (NGF, BDNF, NT-3 and NT-4) was prepared in PBS + 0.1% BSA at a concentration of 100µg/ml. From that, serial dilutions of 1 µg/ml, 100 ng/ml, 10 ng/ml, 1 ng/ml, 0.1 ng/ml, 0.01 ng/ml and 0.001 ng/ml were prepared in Cell Plate reagent at 11x of the final screening concentration. 10µl of each of serial dilutions was added to the corresponding wells in the 96 wells microplate prepared. The cells were incubated at room temperature for 3 hours. Following incubation with the neurotrophin treatment, 55µl of Working Detection Reagent solution, containing 19 parts of Cell Assay Buffer, 5 parts of Substrate Reagent 1 and 1 part Substrate Reagent 2, were added to each of the wells. The plate was incubated for an additional 60 minutes at room temperature in the dark, prior to

chemiluminescence signal detection. The luminescence was recorded with LUMIstar Omega BMG Labtech microplate reader and the data has been analysed with MARS Data Analysis Software.
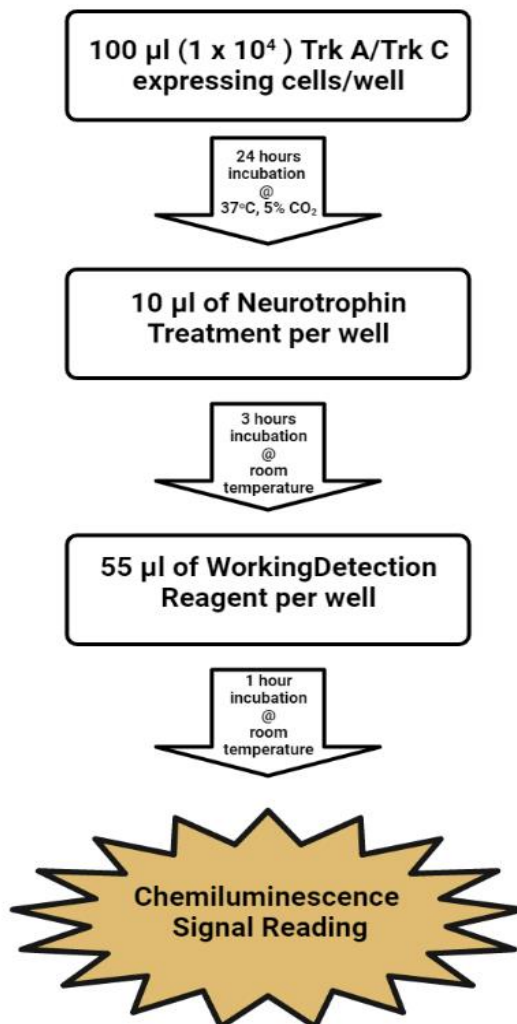
Figure 3. 6. Schematic diagram of Discover X assay workflow for the detection of neurotrophin affinity in bioengineered U2OS Trk expressing cells.

3.2.2. Cell Viability

For assessing the effects of neurotrophins (NT-3 and NGF) in *in vitro* differentiation and proliferation, the PC12 cell line was used as model. Due to their semi-adherent characteristic, PC12 cells require attachment aid. This proved to be one of the main challenges in the effort to optimise assays conditions. We tried polymers such as poly-L-Lysine and poly-D-Lysine with little success, and collagen (Type I and Type IV), that provided better results. Unfortunately, even with the pre-treatment of plates with attachment enhancement agents, cell attachment remained suboptimal during the neurotrophin treatment of PC12.

PC12 cells were seeded at 5 x 10^4 cells/cm^2 in Collagen type IV coated clear flat bottom 96-well plates and allowed to attach for a minimum of 24 hours. Once the cell attachment reached an approximate 80% rate (light microscopy assessed), the cells were treated with media (150µl/well) supplemented with human recombinant NGF and NT-3 (50 ng/ml, 25 ng/ml and 12.5 ng/ml; individual and combined) for a total of 7 days with media being refreshed (50 µl) at day 2, day 4 and day 6, resulting in a total of 300µl media/ well.

At day 7, morphological changes were assessed and recorded through light microscopy. At the same time point, the number of cells was assessed with Alamar Blue assay. 30 µl of 1.6 mM sterile Resazurin Sodium Salt in PBS Solution was added to each well. The Resazurin detection solution was incubated for a total of 6 hours. The fluorescent signal of Resorufin resulted from the reduction of Resazurin by the metabolic activity of the present cells was recorded with FLUOstar BMG microplate reader at 544nm, every 60 minutes until maximization of the signal was reached across the plate, except in the negative control wells which did not include cells and no colour change was expected. The obtained data was analysed with MARS Data Analysis Software. The final number of cells in each well, following fluorescent signal detection, was calculated based on standard curve calculations (please refer to the Appendix section).

Figure 3. 7. Schematic representation of the enzymatic reduction of resazurin to resorufin.
Resazurin is a dark blue to purple non-cytotoxic dye, sensitive to enzymatic activity. In assays measuring cell viability, it is reduced by the metabolic activity to resorufin, a bright pink solution, highly fluorescent. By measuring the fluorescence of resorufin, cell line metabolic activity can be quantified and provide a measurement of] the cell viability in comparison with controls.

3.2.3. Immunostaining

Immunohistochemistry (IHC) was utilised to examine p75NTR and Trk receptors in tissue and cells, as well as morphological alterations as a consequence of treatments.

3.2.3.1. Immunocytochemistry

The presence of high specificity neurotrophin receptors on the surface of PC12 was evaluated using fluorescence microscopy. Cells were attached to glass coverslips, fixed, permeabilised and stained with anti-Trk A, B and C, and anti-p75NTR fluorescent tagged antibodies (antibody details are available in Chapter 2). Upon antibody incubations, cells were washed thoroughly and mounted on the glass slides. The presence of the receptors was qualitatively assessed with Olympus iX83 Fluorescent Microscope. Full method available in the Materials and Methods chapter.

3.2.3.2. Immunohistochemistry

The presence of neurotrophin receptors in osteoarthritic knees was examined in a rat osteoarthritis OA-induced diseased model (referred to as OA from now on). The rat knee sections were donated by the industrial collaborating partner Levicept Ltd.

For analysing the histopathology of the OA, a series of changes (biochemical, histological, and behavioural) that resemble human OA have been induced in rats through injections with MIA. MIA disrupts cellular glycolysis by specifically inhibiting glyceraldehyde-3-phosphatase and eventually resulting in cell death (Sabri and Ochs, 1971).

The diseased model work was carried out externally by RxCelerate Ltd in Cambridge in accordance with the guidelines of the Home Office Procedures Act of 1986.

The rats were injected with MIA in just one knee, cartilage degradation was allowed to occur for a total of 21 days. At the end of the study the animals were sacrificed, knees were dissected, decalcified, fixed, and preserved in paraffin blocks.

For the assessment of neurotrophins receptors in the knee joint of the osteoarthritic rat model and heathy animals the tissue was cut at 4 μm thickness and immuno-stained with HRP tagged anti-Trk A, B and C, and anti-p75NTR antibodies. The presence of receptors has been done semi-quantitatively through light microscopy, using the below intensity scoring scale by having the positive and negative controls as a reference.

Table 3. 1. Intensity score utilised for the semi-quantitative assessment of receptors immunostaining in rat knee tissue sections.

Signal Intensity	Score
Strong (+++)	3
Moderate (++)	2
Weak (+)	1
No staining (-)	0

3.2.4. Anti-NGF monoclonal antibody treatment on an animal model for osteoarthritis.

For the assessment of NGF antagonist (Tanezumab vs. p75NTR-Fc molecule) antibody treatment, rats were injected with MIA in one knee to induce OA-like damage.

The damage was allowed to develop for a total of 21 days. When this was completed, rats were organised in 6 groups and treated. 3 groups were treated with different concentrations of p75NTR-Fc molecule (0.3mg/kg, 1mg/kg, 3mg/kg). One group was treated with 3mg/kg Tanezumab for comparison purposes. And the other 2 groups served as positive and negative controls. The treatment was re-applied every 7 days for a total of 21 days. At day 21, the rats form all groups, were sacrificed, dissected and the knees where the experiment was performed were histologically assessed. The rat knees were decalcified, fixed, and prepared in paraffin. The preserved tissue was cut in 4µm thick slides pre-stained processed, and Safranin O stained for the assessment of cartilage surface. The slides were quality assessed under an inverted light microscope and the representative slides were sent externally for x-ray scanning, where the thickness of the cartilage was measured.

The animal study was carried out by RxCelerate Ltd and the access to this data was acquired through collaboration with Levicept Ltd.

3.3. Results:

3.3.1. Neurotrophin affinities for Trk receptors

The affinities of neurotrophins for the Trk A, Trk B and Trk C were tested *in vitro* for each receptor and summarised in the graphs below.

3.3.1.1. Trk A affinity for human recombinant neurotrophins

The data summarised in the graph shown in Fig. 3.8 indicates a high affinity of Trk A for NGF, similar affinity for NT-3 and NT-4 and low to no affinity for BDNF. The latter appears to activate Trk A only in high concentration, 1000 ng/ml, but with a low rate.
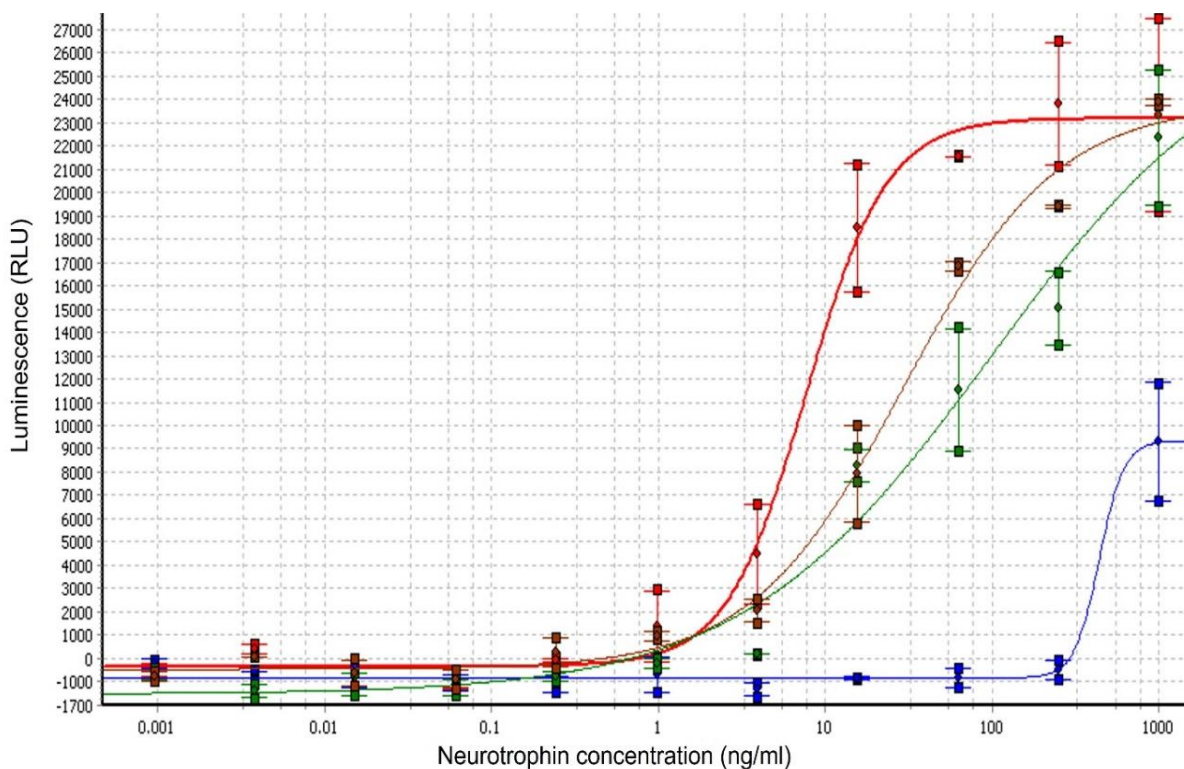
Figure 3. 8. *Trk A agonist curve on serial dilutions of neurotrophins: NGF=Red, BDNF=Blue, NT-3=Green, NT-4=Brown.*
This graph shows the luminescence signal (RLU) recorded (+/- SD) after 3 hours under the influence of neurotrophins treatment. The signal is directly proportional to the phosphorylation of Trk A receptor overexpressed in U2OS cells. The data was collected from 3 technical replicates and summarised in the present figure using MARS Data Analysis Software from BMG LabTech. It is observed that Trk A receptor has different affinities for each of the neurotrophins, the higher one being NGF.

3.3.1.2. Trk B affinities for human recombinant neurotrophins

The data collected and summarised in the Fig. 3.9 indicates that Trk B receptor is activated by all 4 human neurotrophins. Contrary to the expectations, Trk B displayed the highest affinity to NT-3 and NT-4 and the lowest affinity to BDNF, as shown below. A minimum amount of at least 1 ng/ml of neurotrophins is necessary for the dimerization and phosphorylation of Trk B.
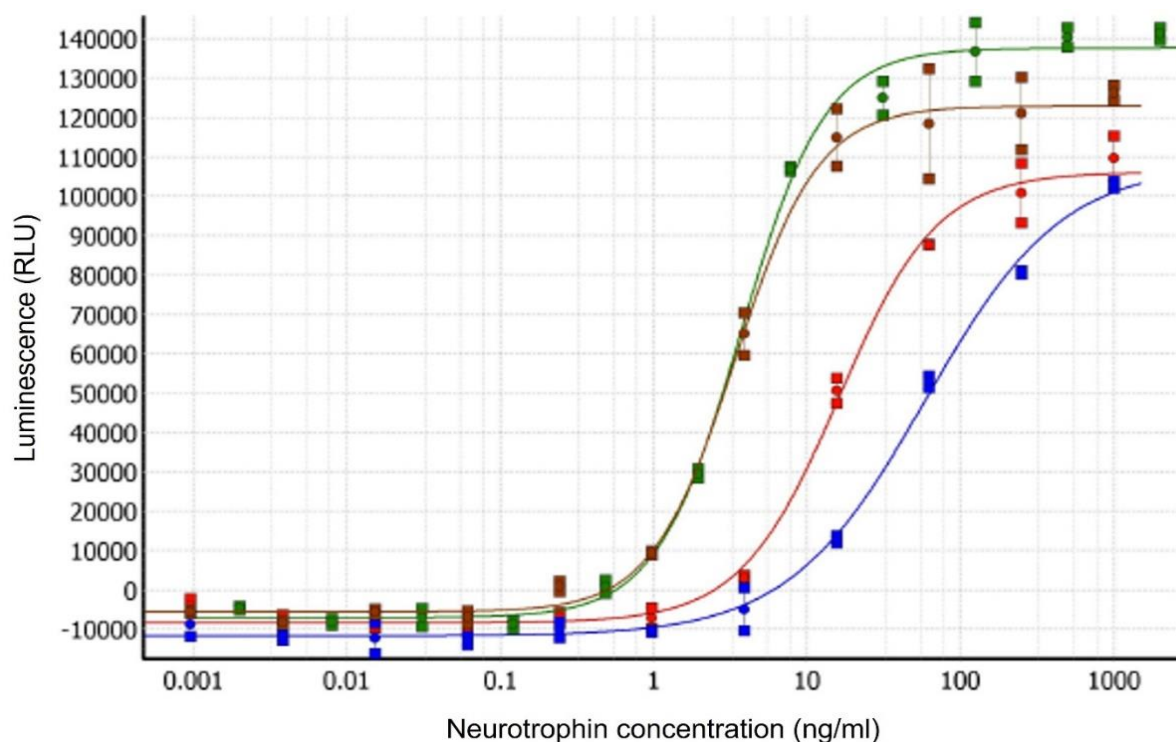
Figure 3. 9. Trk B agonist curve on serial dilutions of neurotrophins: NGF=Red, BDNF=Blue, NT-3=Green, NT-4=Brown.
This graph shows the luminescence signal (RLU) recorded (+/- SD) after 3 hours under the influence of neurotrophins treatment. The signal is direct proportional with the phosphorylation of Trk B receptor overexpressed in U2OS cells. The data was gathered from 3 technical replicates and summarised in the present figure using MARS Data Analysis Software from BMG LabTech. It is observed that Trk B receptor has different affinities for each of the neurotrophins, the higher ones being for NT-3 and NT-4.

3.3.1.3. Trk C affinity for human recombinant neurotrophins

When affinity for all human neurotrophins was tested on Trk C expressing cells, only NT-3 and BDNF caused receptor activation. The data summarised in the graph below indicates a high affinity for NT-3 and moderate affinity to BDNF in Trk C⁺ cells. No phosphorylation of the receptor was detected upon NGF and NT4 treatment, in any of the concentrations.
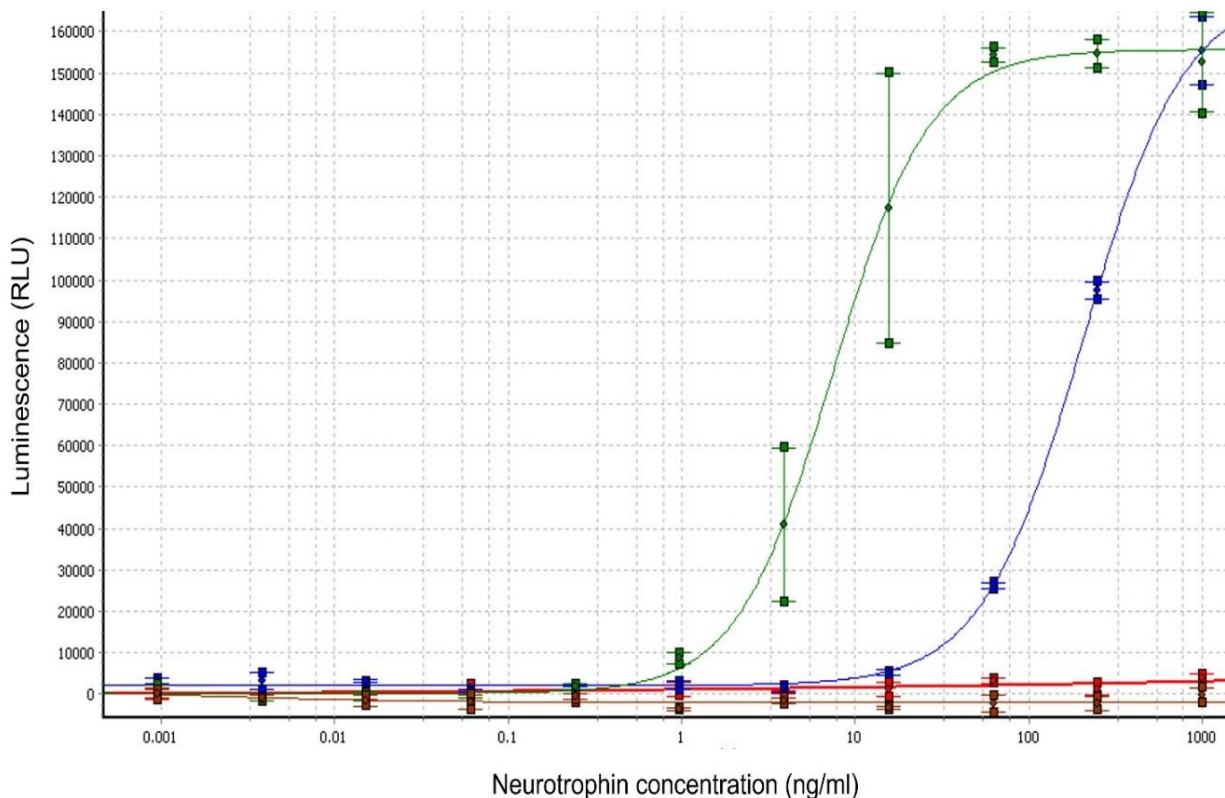
Figure 3. 10. Trk C agonist curve on serial dilutions of neurotrophins: NGF=Red, BDNF=Blue, NT-3=Green, NT-4=Brown.
This graph shows the luminescence signal (RLU) recorded (+/- SD) after 3 hours under the influence of neurotrophins treatment. The signal is directly proportional with the phosphorylation of Trk C receptor overexpressed in U2OS cells. The data was gathered from 3 technical replicates and summarised in the present figure using MARS Data Analysis Software from BMG LabTech. A major difference is observed between the uptake of NT-3 and the rest of the neurotrophins. This shows the high affinity of Trk C receptor for NT-3.

3.3.2. Neurotrophin receptor localisation in PC12 cells

The expression of neurotrophin receptors was verified in the *in vitro* model, PC12.

According to the observations made following the immuno-staining and summarised below in Fig. 3.11, the PC12 rat pheochromocytoma of the adrenal medulla cell line positively expresses all neurotrophin receptors, p75NTR, Trk A, Trk B and Trk C. The PC12 cell line is a well-known *in vitro* model for the study of neurodegeneration and neurodevelopment. It has been widely used in the study of NGF and p75NTR.

No colocalization was conducted due to the limitations in antibody choices at the moment the experiment was conducted.
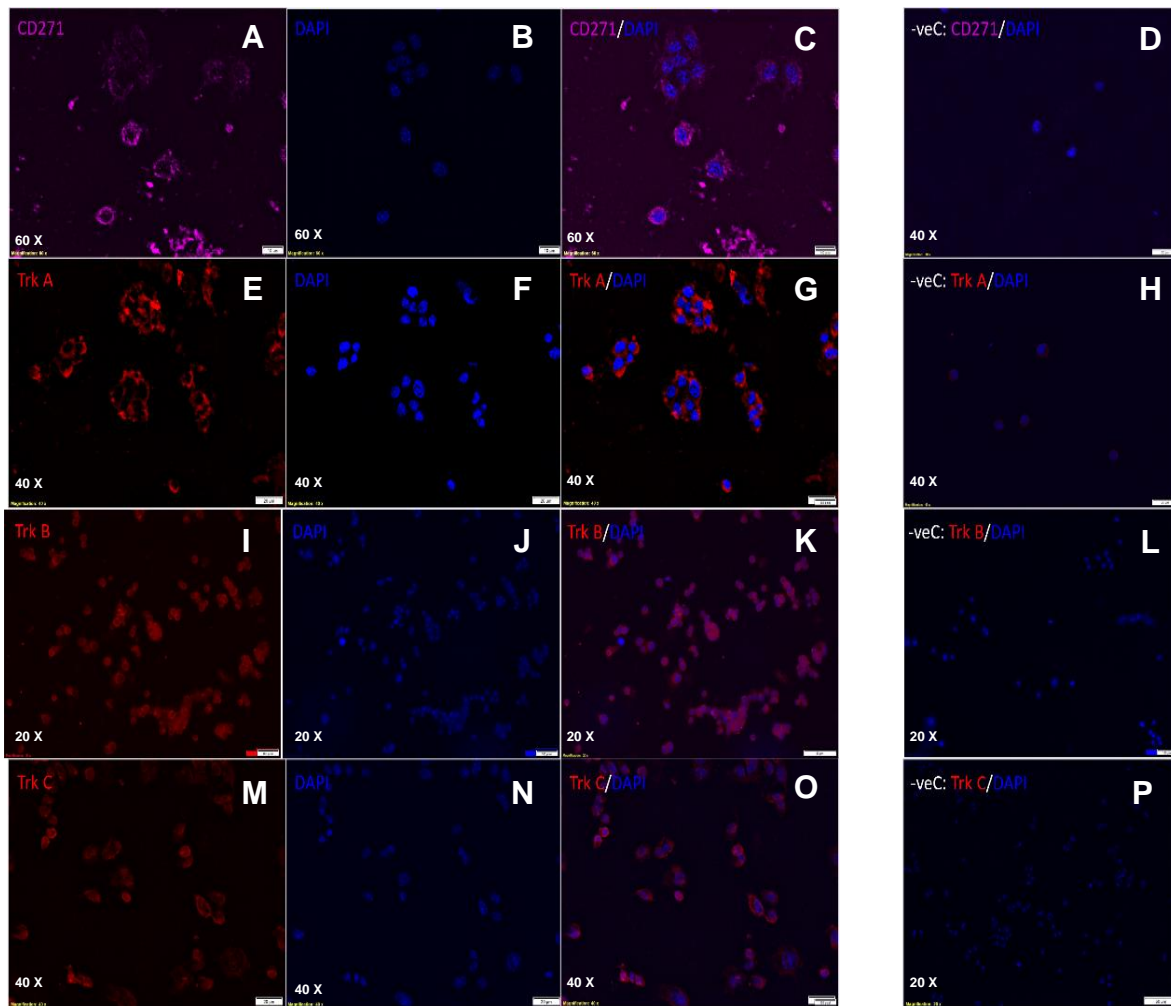
Figure 3. 11. Immunofluorescence staining of neurotrophins receptors on the PC12 cell line.
The presence of p75NTR, Trk A, Trk B and Trk C on the PC12 cells has been qualitatively assessed through Immunofluorescence (IF) staining. Attached cells were fixed on glass coverslips and stained with fluorescent tagged antibody for the detection of (A). p75NTR in TexasRed channe (purple)l; (E). Trk A protein in Cy5 channel (red); (I). Trk B protein in Cy5 channel (red); Trk C protein in Cy5 channel (red); (B;F;J;N). DNA counterstained with 4',6-diamidino-2-phenylindole (DAPI) (blue); and (C;G;K;O) merge; (D;H;L;P). Negative controls (cells stained with the IgG isotype specific to the primary antibody host species) were used together with the primary antibody staining to consider the level of background staining and avoid false detection. DAPI was used for counterstaining.

The presence of neurotrophin receptors, especially p75NTR and Trk C receptor, together with the capacity to differentiate into neurites when treated with NGF, make this cell line a viable model for the initial assessment of NGF and NT-3 effects on differentiation and cell proliferation.

Since Trk receptors were confirmed to be present on PC12 cells, we proceeded to investigate their involvement in the proliferation and differentiation of these cells. To this end we looked into whether NT-3 induces the proliferation of PC12 cells, as well as the combined effects of NGF and NT-3 in both the differentiation and proliferation of the cells. Considering findings in the field of neurotrophin activity we expect that a combined treatment of NGF and NT-3 can induce rapid cell differentiation of increased cell numbers.

3.3.3. The effect of NGF and NT-3 treatment on PC12 viability.

PC12 cells were seeded at 5 x 10^4 cells/cm^2 in collagen type IV coated clear flat bottom 96-well plates and treated with cultured with media supplemented with human recombinant NGF and NT-3 (12.5 ng/ml, 25 ng/ml, 50 ng/ml; individual and combined) for a total of 7 days with media being refreshed at day 2,4 and 6.

After 7 days under neurotrophin treatment, neurites outgrowth was observed in most wells treated with NGF (combined and individual) and no differentiation was observed in the NT-3 treated wells. Differentiated cells showed signs of senesce and no visible proliferation.

NT-3 only, seems to induce an increase in the cellular proliferation of PC12 cells. This was quantified with Alamar Blue based cell viability assay (graph below).
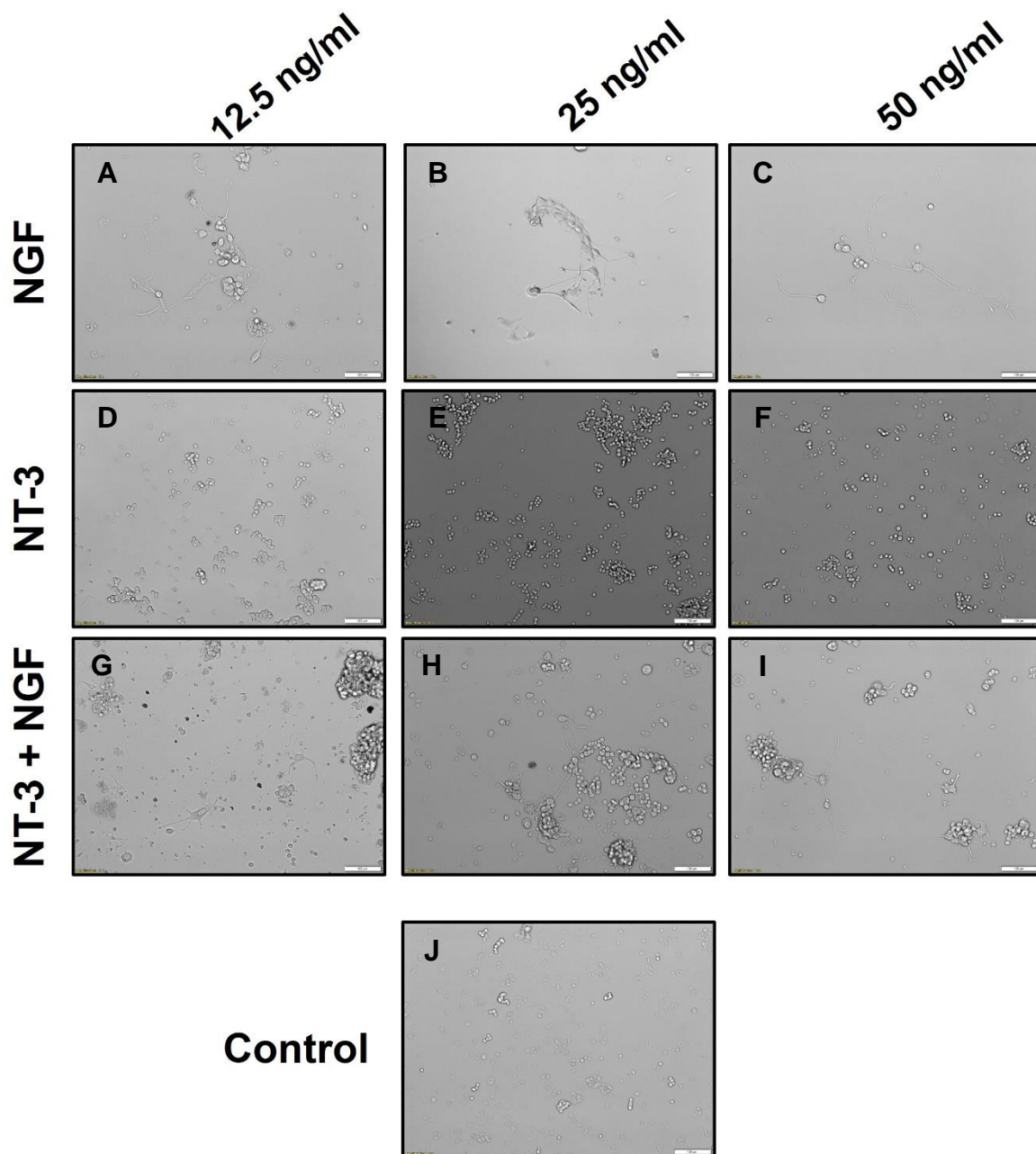
Figure 3. 12. The effects of neurotrophins on the proliferation and differentiation of PC12 cells.

This figure summarises representative light microscopy images of the differentiation and proliferation induced by NGF and NT-3 treatment on the PC12 cell line after 7 days; PC-12 were cultured in Collagen type IV coated plates and treated for 7 days with (A). 12.5 ng/ml NGF, (B). 25 ng/ml NGF, (C). 50 ng/ml NGF, (D). 12.5 ng/ml NT-3, (E.). 25 ng/ml NT-3, (F). 50 ng/ml, (G). 12.5 ng/ml NGF + NT-3, (H). 25 ng/ml NGF + NT-3, (I). 50 ng/ml NGF + NT-3 and (J). no neurotrophin treatment. Magnification x10; 100 µm scalebar.

P75NTR[+]/Trk A[+]/Trk C^{+} PC12 cells showed increased proliferation when NT-3 was present. The treatment with NGF, on the other hand, had a detrimental impact on the proliferation of the cells. The decrease of cell viability in NGF conditions suggests either the activation of cell differentiation, which it can impact the cell proliferation, or a possible cytotoxic effect of NGF.

The combined treatment of both, NGF and NT-3, showed positive effects on proliferation when both neurotrophins were present at no more than 12.5ng/ml and negative effects when in 25 and 50 ng/ml.
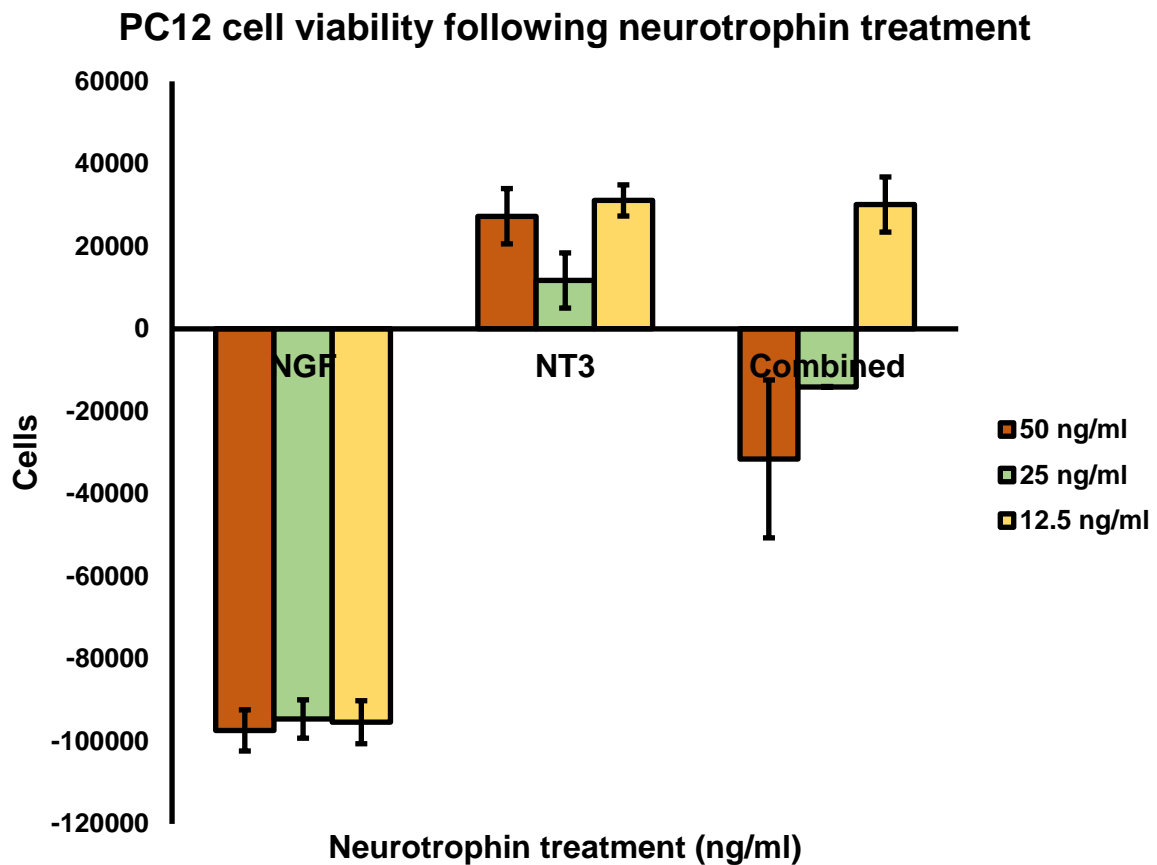
Figure 3. 13. The effects of neurotrophins (NGF and NT-3) on the proliferation of PC12 cells.
This graph shows the increase and the decrease (+/- SD) in number of cells, by comparison with the control (0=no neurotrophin supplemented media), when treated with different concentrations of NGF and NT-3 (individual and combined). The data was collected from 4 technical replicates and summarised in the graph.

3.3.4. Regenerative effects of the p75NTR-Fc molecule in an animal osteoarthritis model

As a result of the partnership with Levicept Ltd., a series of *in vivo* studies, looking at the effects of the p75-NTR-Fc bioengineered molecule on an osteoarthritic animal model compared with the existent monoclonal antibody treatment for OA, was conducted externally.

Rats with MIA-induced OA were treated for a total of 21 days with different doses of anti-NGF monoclonal antibody. For the assessment of the articular cartilage surface, the rats were sacrificed, the treated knees were dissected, fixed and sections of the tissue were stained with Safranin O (cartilage stain).

Histology staining of the rat knees with Safranin O showed a stimulation of cartilage repair induced by the treatment with p75NTR-Fc molecule in comparison with the negative control (non-treated).
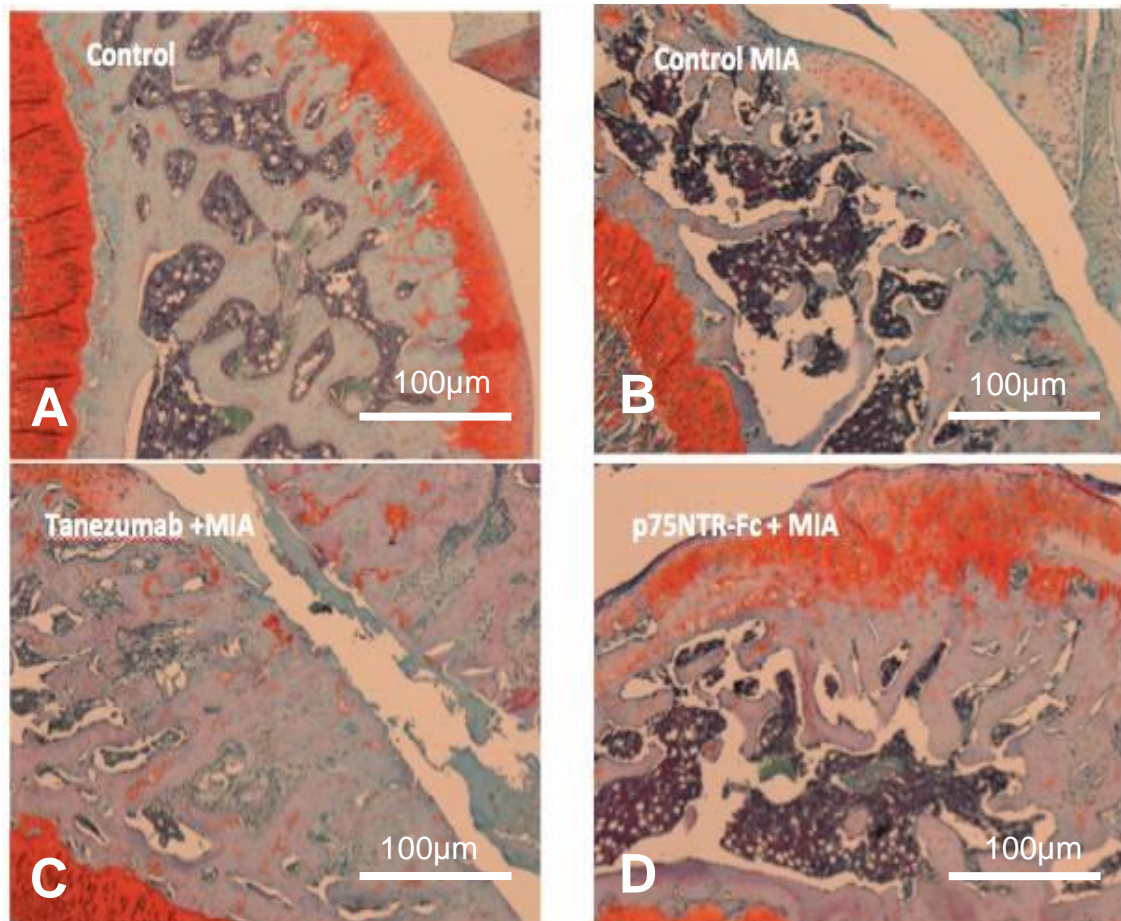
Figure 3. 14. Safranin O staining of the osteoarthritic rat knees after 21 days of treatment with Tanezumab vs. p75NTR-Fc molecule (Scale bar = 100µm) (A). Positive Control Group – Healthy rats; (B). Negative Control Group – Rats with MIA induced OA; (C). Tanezumab treated group – rats with MIA induced OA treated with Tanezumab; (C). p75NTR-Fc treated group – rat with MIA induced OA treated with p75NTR-Fc; Safranin O (red) for cartilage staining and counterstaining (blue) with Haematoxylin Eosin. 100µm scalebar.

Rat knee tissue from 4 different conditions (Negative Control, Positive Control – MIA induced osteoarthritis, rats with MIA-induced osteoarthritis treated with NGF-inhibitor drug, Tanezumab and rats with MIA-induced osteoarthritis treated with p75NTR-Fc molecule). The images selected show representative results following a total of 21 days of treatment.

The Safranin O-stained cartilage from the rat knee sections was analysed with an x-ray scanner to determine the differences in the cartilage area induced by the applied treatments.

Measurements of the knee cartilage area of animals treated with different doses of the p75NTR-Fc molecule showed growth stimulation of the cartilage, especially for the 1 mg and 3 mg/kg treatments with the p75NTR-Fc molecule.

The effect of different anti-NGF treatments on the knee cartilage area of rats with MIA-induced OA
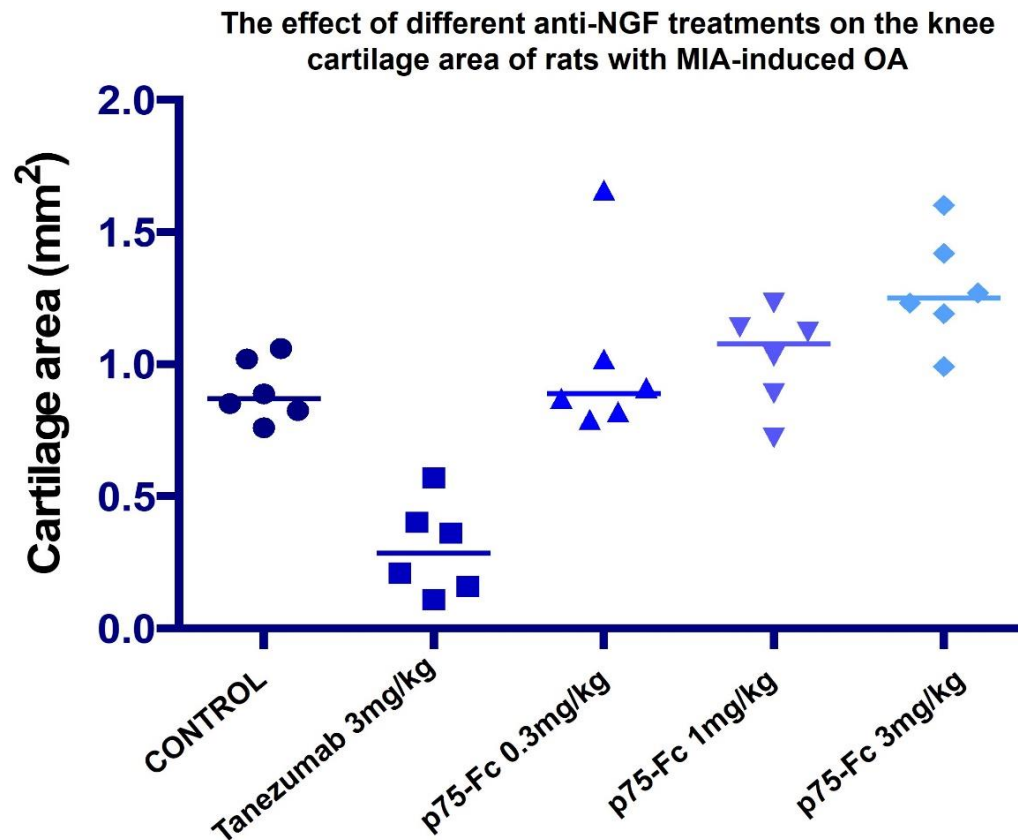
Figure 3. 15. The effect of different anti-NGF antibody-based treatments on rat knee cartilage in an osteoarthritic animal model.
The effects on the cartilage area of the osteoarthritic knee joints were assessed in rats treated with two different anti-NGF antibody-based treatments (Tanezumab and p75-NTR-Fc). The data summarised in this graph presents the results collected from a total of 12 rats, 3 rats per treatment.

3.3.5. Localisation of neurotrophin receptors in the knee joint

In order to investigate   the presence of neurotrophin receptors in the knee joint (healthy and diseased (OA)), a series of IHC experiments were conducted. Tissue sections of healthy and MIA-induced osteoarthritic rat knees were immuno-stained with antibodies against neurotrophin receptors.

Both types of neurotrophin receptor, p75NTR and Trk receptors, were identified in all structures of the knee joint, in both healthy and diseased (induced OA) animals. The intensity of all Trk receptors staining appeared stronger in the healthy tissue compared with the diseased tissue. This can indicate a decrease in the expression of the neurotrophins receptors in the pathology of osteoarthritis. On the other hand, it can suggest that the receptors were already activated, by bound ligands, as a response to osteoarthritis pathology, making them unavailable for this type of detection.

3.3.5.1. p75NTR in rat knee sections

Overall, the staining for p75NTR showed strong expression for the receptor in both, the healthy and disease rat knee joints. However, when it comes to cartilaginous components like the growth plate (Fig. 3.16, C and H) and the cellular component of the articular cartilage (Fig. 3.16, A and F), p75NTR seems to have a greater signal in healthy tissue than in OA-model samples. In the assessed bone tissue, the p75NTR intensity appears similar in both, healthy and diseased tissue.

p75^NTR IHC staining
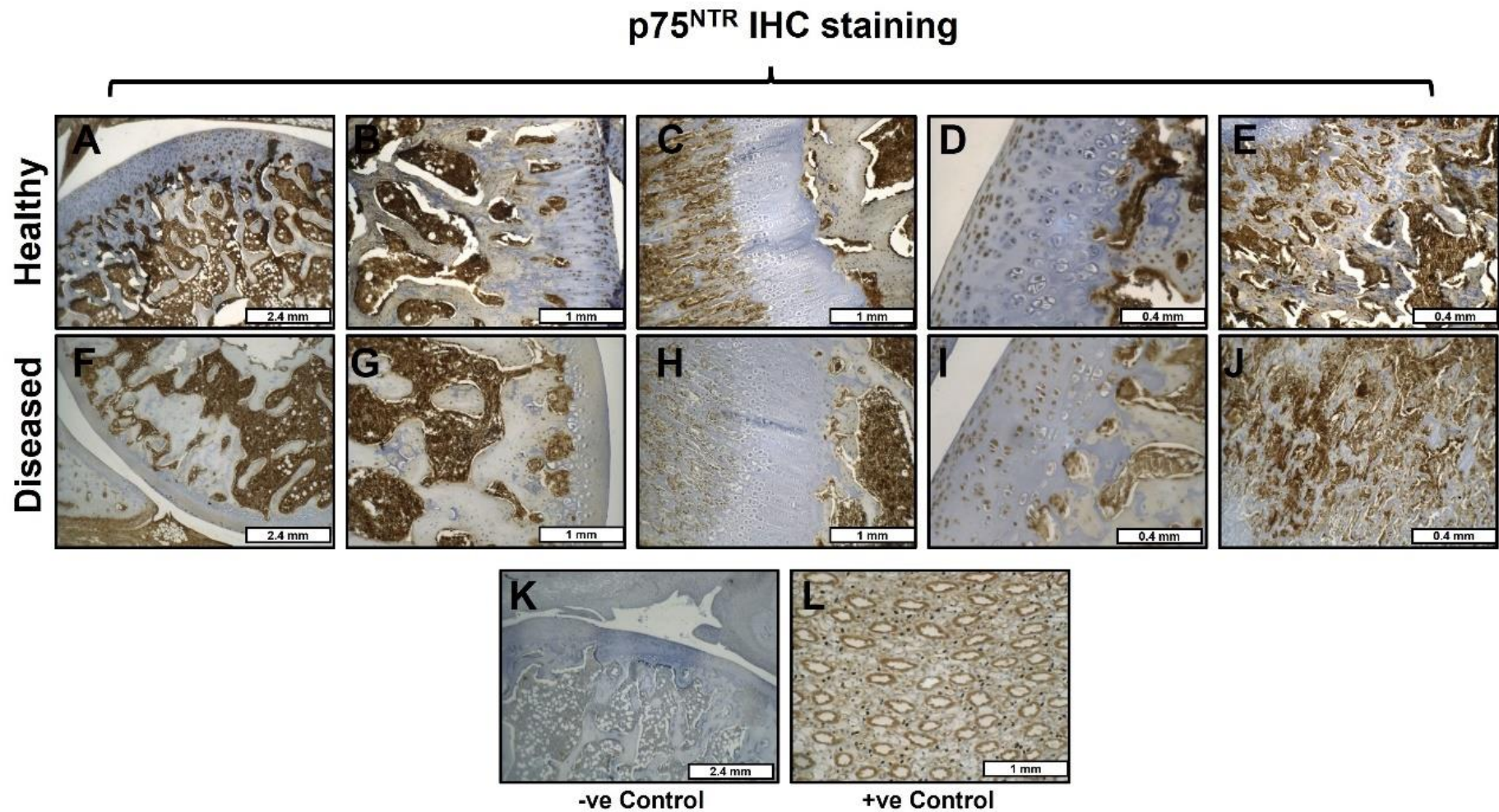
Figure 3. 16. p75NTR in rat knee tissue

Tissues were stained with p75NTR antibody and developed with 3,3 0-diaminobenzidine (DAB) for protein detection (BROWN) and counterstained with Haematoxylin for the detection of cell nuclei (BLUE).

This figure shows representative images from different knee sections (A and F. Cartilage and subchondral bone; B and G. Subchondral bone; C and H. Growth plate; D and I. Chondrocytes; E and J. Spongy bone) acquired while investigating the presence of p75^NTR in the osteoarthritis animal model. The analysis is primarily qualitative, and the intensity of antigen signal was scored as stated in Table. Rat brain tissue was used for positive control staining.

3.3.5.2. Trk A in rat knee sections

When the tissue has been stained for Trk A, a reduction in signal was recorded in diseased samples in comparison with the healthy samples. Even the thickness of the cartilage (Fig. 3.17. A compared with F) appears to be reduced in diseased (OA) rats. In comparison to healthy rats, the diseased rat knees show a reduced intensity of Trk A in the spongy bone of the rat knees (Fig. 3.17. B and G)
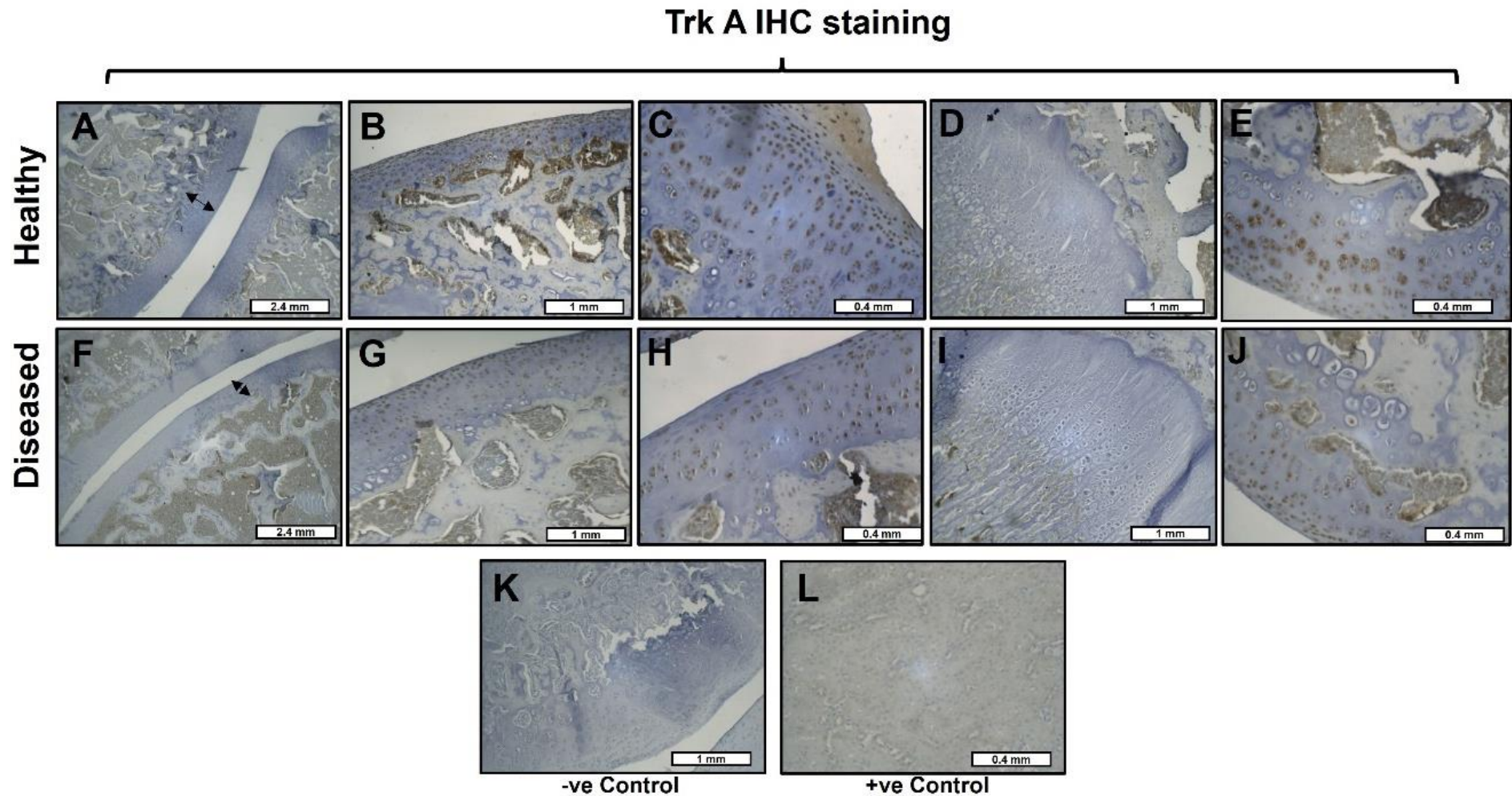
Figure 3. 17. Trk A in rat knee tissue.
Tissues were stained with Trk A antibody and developed with 3,3 0-diaminobenzidine (DAB) for protein detection (BROWN) and counter-stained with Haematoxylin for the detection of cell nuclei (BLUE).This figure shows representative images from different knee sections (A and F. Cartilage and subchondral bone; B and G. Spongy bone; C and H. Chondrocytes; D and I. Growth plate; E and J. Subchondral bone) acquired while investigating the presence of Trk A in the osteoarthritis animal model. The analysis is primarily qualitative, and the intensity of antigen signal was scored as stated in Table 3.1. Rat kidney tissue was used for positive control staining.

3.3.5.3. Trk B in rat knee sections

Trk B-stained slides indicate the presence of this receptor in both diseased and healthy rat knees but with different intensities across the structure of the knee. The spongy bone (Fig. 3.18 E and J) and the growth plate (Fig. 3.18 C and H) show weak detection signal for Trk B in both diseased and healthy animals. When looking at the chondrocytes from the lacunae of the articular cartilage (Fig. 3.18 B and G) and the subchondral bone (Fig. 3.18 E and J), Trk B staining shows a stronger signal in healthy rats compared with the diseased ones.

Trk B IHC staining
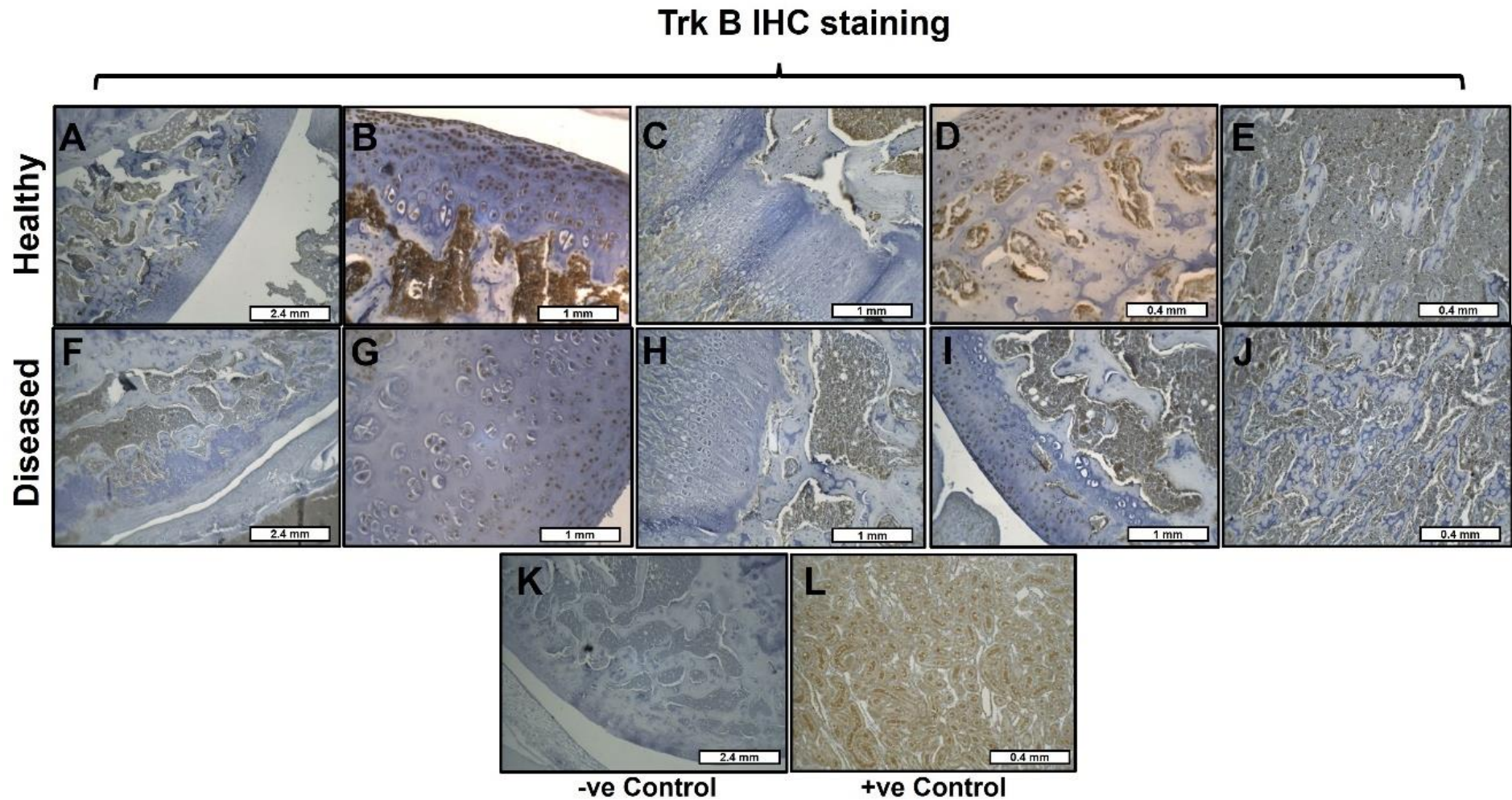
Figure 3. 18 Trk B in rat knee tissue
Tissues were stained with Trk B antibody and developed with 3,3 0-diaminobenzidine (DAB) for protein detection (BROWN) and counter-stained with Haematoxylin for the detection of cell nuclei (BLUE).
This figure shows representatives images from different knee structures (A and F. Knee joint; B and G. Chondrocytes; C and H. Growth plate; D and I. Subchondral bone; E and J. Spongy bone) acquired while investigating the presence of Trk B in the osteoarthritis animal model. The analysis is primarily qualitative, and the intensity of antigen signal was scored as stated in Table 3.1. Rad kidney was used for positive control staining.

3.3.5.4. Trk C in rat knee sections

The staining of Trk C of healthy and OA-induced rat knees indicates an overall weak presence of Trk C with even weaker signal in diseased knee tissue when compared with the healthy knee tissue. Out of all the structures of the stained knees, the subchondral bone (Fig. 3.19 E and J; B and G) and the growth plate (Fig. 3.19 C and H) showed increased Trk C signal in healthy tissue compared with the diseased tissue.
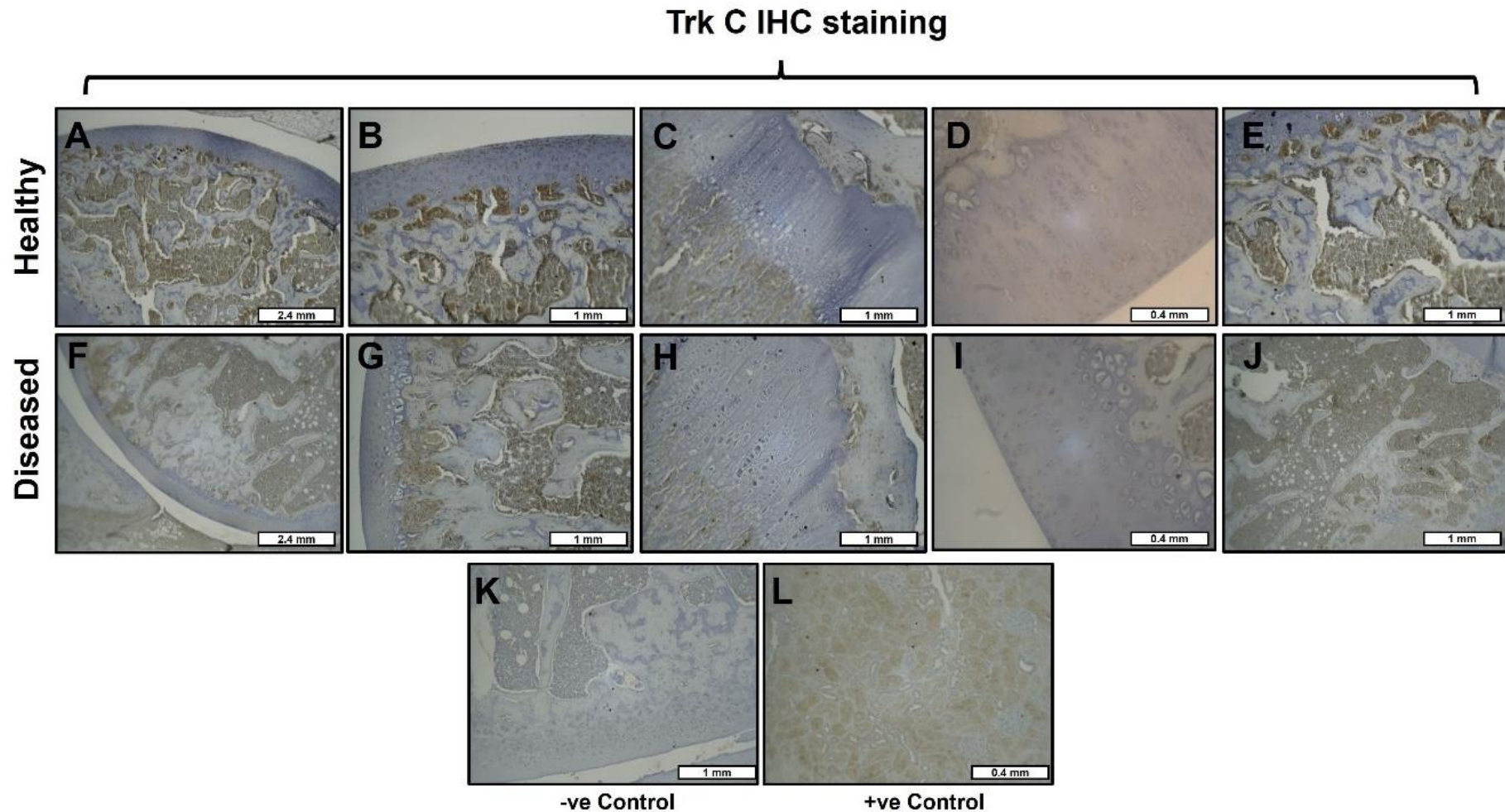
Figure 3.19. Trk C in rat knee tissue
Tissues were stained with Trk C antibody and developed with 3,3 0-diaminobenzidine (DAB) for protein detection (BROWN) and counter-stained with Haematoxylin for the detection of cell nuclei (BLUE).
This figure shows representative images from different knee structure (A and F. Knee joint; B and G. Subchondral bone; A and H. Growth plate; D and I. Chondrocytes; E and J. Subchondral bone) acquired while investigating the presence of Trk C in the osteoarthritis animal model. The analysis is primarily qualitative, and the intensity of antigen signal was scored as stated in Table 3.1. Rat kidney was used for positive control staining.

3.3.6. The presence of Neurotrophin receptors in rat knee sections

The signal intensity across all assessed slides was scored according to the scoring system presented in Table 3.1, and the results were plotted in the graph below. An overall decrease of all neurotrophins' receptors was observed in the knee of MIA induced OA animal model. This observation can either indicate a down-regulation of neurotrophin receptors in pathology or the fact that receptors were already activated by the endogenous neurotrophins in damaged tissue, limiting the capacity of detection with the IHC assay. By comparison, p75NTR appears to have a higher expression in the knee tissue of the rats, comparative with Trk receptors. Trk receptors are present with similar intensity levels, according to the IHC detection. A decrease of Trk C is observed in diseased tissue, by comparison with other Trk receptors in same type of tissue. This can indicate either the presence of endogenous NT-3 that has blocked the binding site of the receptor and a possible internalisation of receptors, down-regulation of this receptor in degenerative joint disease or loss of TrkC +ve cells
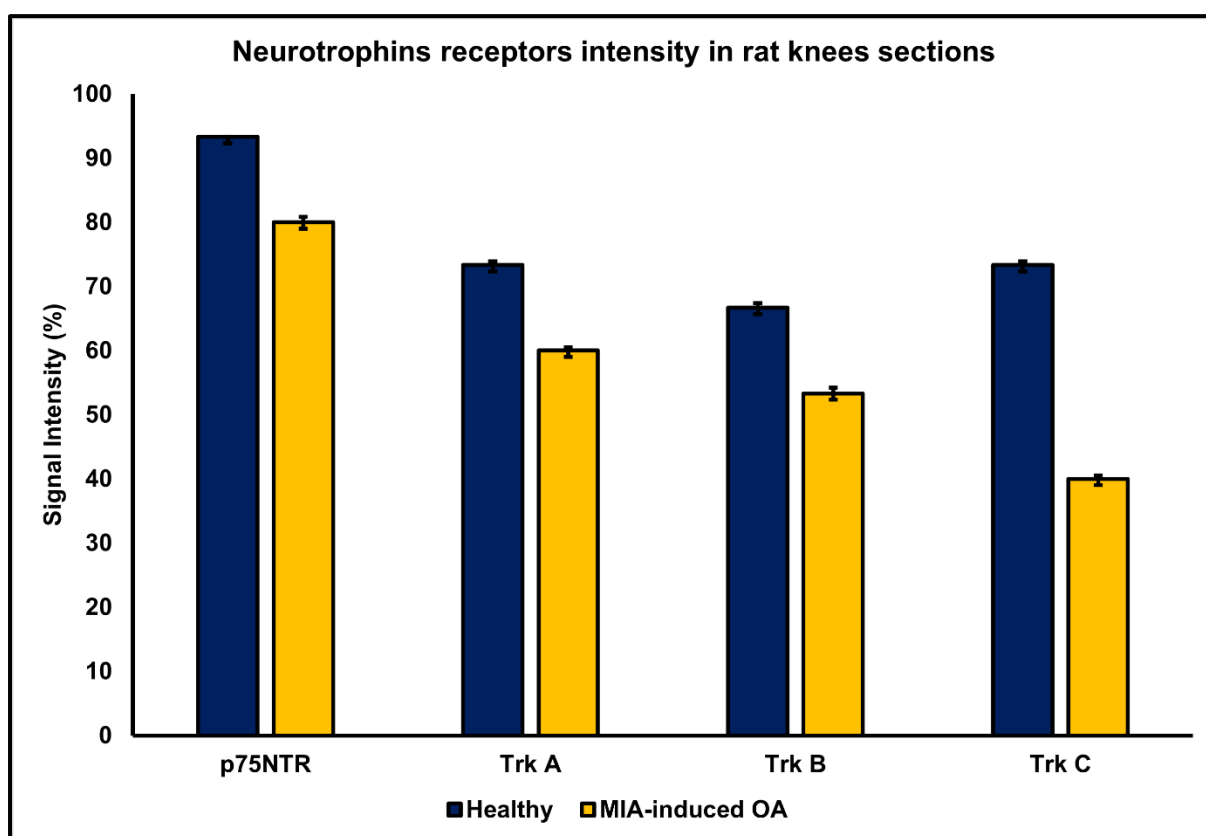
Figure 3. 18. Intensities of neurotrophin receptors in an animal disease model.
This graph summarises the intensity of the signal detected (+/-SD) in the immuno-stained slides used for the IHC analysis of neurotrophin receptors in rat knees. The data was collected from 3 biological technical replicates and summarised in the present graph using Microsoft Excel.

3.4. Discussion:

Neurotrophins are considered essential for the proliferation, differentiation, and overall survival of neuronal, as well as non-neuronal cells. They exert their actions through their receptors (p75NTR and Trk receptors). Neurotrophins can also play important roles in regenerative medicine, since they were shown to promote regeneration of injured nerves (Houlton *et al.*, 2019). As their presence has been reported in other types of tissue, especially following damage, it can indicate a general implication of neurotrophins in the tissue repair process.

Elevated levels of NGF have been detected in the synovial fluid of patients suffering of joint degenerative disease and linked with sensitization of nociceptors from the synovial membrane, leading to induced chronic pain. To help with patient analgesia, selective inhibitory drugs having NGF as target have been developed. Tanezumab is an antibody-based treatments developed for the osteoarthritis analgesia. The mechanism of action behind this molecule implicates a complete tracking and capturing of all the expressed NGF. The studies of this type of drugs provided important information for the tissue repair process that happens in the synovial joints. Data collected from animal testing and clinical trials indicates that NGF is indeed responsible of skeletal joint chronic pain, but also it has important roles in tissue repair. Total depletion of NGF resulted in a chronic pain reduction of patients suffering of osteoarthritis, but also rapid progression of the disease was observed, which ultimatum can lead to disability. This implies that endogenous NGF is involved in both tissue homeostasis and healing, most likely through supporting cell survival.

In the broad spectrum of neurotrophins, not only NGF possesses regenerative capacity. NT-3 is well-known for promoting nerve regeneration and angiogenesis (Shen *et al.*, 2013; Wu *et al.*, 2018; Idrisova *et al.*, 2022). Its involvement in tissue repair and healing should be given more consideration.

In this project, through a series of experiments we analysed the effects of not only NGF, but also NT-3 on cell proliferation and differentiation, with indications to possible regenerative applications.

The affinity of all neurotrophins for Trk A, Trk B and Trk C was analysed with the Discover X assay. Trk A displayed high affinity not only for NGF, but also NT-3 and

NT-4 (Fig. 3.8). In the presence of BDNF, Trk A was phosphorylated only when high concentrations of the neurotrophin were present (1000ng/ml).

Trk B phosphorylation was induced by all four neurotrophins. NT-3 and NT-4 with similar high affinity, NGF with moderate affinity and BDNF with low affinity, according to the data presented in Fig. 3.9.

Trk C was phosphorylated by NT-3 starting from concentrations low as 1ng/ml. 10ng/ml has been shown to be enough for the phosphorylation of total population of Trk C on the cell membrane of the bioengineered U2OS cell line. Phosphorylation of Trk C has been induced by BDNF binding as well, but only in high concentrations (100ng/ml, 1000ng/ml). These findings corroborate neurotrophins capacity to activate all Trk receptors, although at varying doses, while Trk receptors bind neurotrophins with different degrees of affinity. As we already know that p75NTR is activated by all neurotrophins with similar low affinities from literature, this was not investigated further.

To test the effects of NGF and NT-3 on proliferation and differentiation, the rat pheochromocytoma of the adrenal medulla PC12 cell line was used for exploratory studies. PC12 is a well-established *in vitro* model for neuronal investigations, and it relies on the p75NTR positive expression that activates the neurite outgrowth when treated with NGF (Wiatrak *et al.*, 2020). PC12 was chosen for the initial investigations of NGF and NT-3 effects, due to the positive expression of p75NTR (confirmed as shown in Fig. 3.10). Trk A and Trk C have also been found localised on the cell membrane of PC12 cells. The immunofluorescence profile of this type of cell line encountered some difficulties as PC12 are semi-adherent cells that adhere poorly to plastic and tend to aggregate in clusters. First of all, due to the semi-adherent nature of this cell line, the initial recommended attachment agents for neuronal cell culture (Gordon, Amini and White, 2013), such as Poly-L-Lysine and Poly-D-Lysine failed in providing a sufficient cell attachment of PC12 to the coverslips in order to resist the staining procedure. Collagen coating has been attempted as well. Collagen type IV showed the best results for our applications. Another challenge around cell culture of PC12, is constituted by their tendency to aggregate in clusters, making it difficult to apply a constant treatment across the cell population. This was avoided when mechanical separation of the cells was applied prior to seeding. After all the aspects

around PC12 cell culture were optimised, the effects of NGF and NT-3 were assessed in a 7-day *in vitro* study, where 1×10^5 cells/ well were seeded in 96-well culture plates and treated with serial dilutions of individual and combined NGF and NT-3.

The morphological changes summarised in Fig. 3.12 show that all NGF treated wells, except in low NGF concentration (12.5ng/ml) in combination with low NT-3 concentration (12.5ng/ml) treatment, displayed neurite outgrowth. No well treated with NT-3 showed, except those in combination with NGF, morphological indications of differentiation. Interestingly higher density of cells was observed, when compared with the negative control (non-treated cells). Based on these observations, Alamar Blue assay was carried out for the quantification of cell viability after 7 days of NGF and NT-3 treatment. The data summarised in Fig. 3.13 indicated that NT-3 induces cell proliferation in both, high (50ng/ml) and low (12.5 ng/ml) concentrations. Moreover, when applied together with NGF, only in low concentrations can NT-3 have a positive effect on cell proliferation. By analysing the degree of differentiation resulted from combined treatments by comparison with NGF only treatments, it can be assumed that NT-3 does not impair the differentiation process. Contrary, it seems that NT-3 promotes it through preserving the vitality of differentiated cells. When cells are stimulated to differentiate, they tend to cease division. Based on the data summarised in the Fig. 3.12, even during differentiation, the cell proliferation can be maintained with small concentrations of NT-3 (12.5ng/ml). The findings observed in differentiated PC12 cells are consistent with previously reported effects of NT-3 on cell proliferation. NT-3 has previously been shown to promote neural stem cell differentiation and proliferation. The chemical mechanism through which NT-3 promotes cell differentiation and proliferation has been speculated to be via the Notch signalling (Yan *et al.*, 2016). Due to its positive influence on the cell differentiation and proliferation, and the fact that it is not harmful to cells in comparison to NGF that can induce pain, NT-3 has been examined in systems other than the CNS and PNS. When investigated in the cardio-vascular system, NT-3 has been shown to be responsible of cell proliferation of interstitial cells and collagen production in the human aortic valve (Yao *et al.*, 2017), with possible implications in aortic valve sclerosis. Animal studies investigating the effects of NT-3 on tissue repair upon skeletal injury showed significant improvement in fracture healing. In comparison to the control groups, rats treated with NT-3 had increased BMP-2, TGF-β, and VEGF levels, as well as improved bone mineral density

(Li *et al*., 2018). The data collected from our *in vitro* experiments comes in support to the proliferative properties of NT-3, already reported in the literature. Based on the positive expression of p75NTR, Trk A and Trk C on the surface of PC12 cells determined by immunofluorescent antibody staining, the NT-3 activated signalling pathway that induces cell proliferation seems to be triggered by the activation of any of these receptors. By considering the rapid phosphorylation of Trk C by NT-3 recorded in the bio-engineered *in vitro* model (Fig. 3.10), and the confirmed localisation of Trk C receptor on the surface of the cells, we can conclude that the increase in PC12 cell proliferation after the treatment with NT-3 is Trk C mediated and most probably induced the further activation of PI3K/Akt pathway.

Throughout the collaboration with Levicept Ltd, access to novel data in tissue repair has been granted. In order to determine drug safety of the p75NTR-Fc designed molecule, studies on animals were carried out. Improved cartilage area was observed when the knees of the OA rat model were treated. The data obtained indicates that treatment with p75NTR-Fc not only reduces osteoarthritis symptoms, like chronic pain, but also stimulates the tissue repair process. Comparative with the previously NGF inhibitory pharmacological strategies, p75NTR-Fc, selectively tracks and captures only the excess NGF molecules, while maintaining a better NGF balance in the knee joint. It is believed that endogenous NGF is present in homeostatic stages of the tissue, with trophic roles. Previously designed NGF inhibitory drugs (e.g. Tanezumab) were completely depleting the entire population of NGF molecules present in the joint, leading to rapid regeneration of the disease.

Looking at the data presented in this chapter, especially the unexpected positive effect on the articular cartilage surface of a treatment that was primarily targeted at safe release from chronic pain, we decided to explore the role of p75NTR and the cooperating Trk receptors in bone and cartilage regeneration. Due to the proliferative effect of the Trk C and NT-3 cooperation of PC12 cells we selected this receptor for further studies. Moreover, we looked to explore the regenerative properties of NT-3 in comparison with the better described NGF with the focus on joint specific tissue repair (bone and cartilage).

The localisation of neurotrophin receptors was assessed in the knee joint of healthy and MIA-induced osteoarthritis rats. All 4 neurotrophins' receptor were found positively expressed in all structures of the knee joint, in both, diseased and healthy states.

The presence of neurotrophin receptors in healthy knee tissue indicates that the signalling cascade produced by neurotrophins could play a critical role in tissue homeostasis.

Decreased signal was observed across all diseased samples when compared with the receptor intensity of the healthy samples. This can indicate a possible disease mechanism of action that inhibits the neurotrophin receptors and impact on cell survival. On the other hand, the decreased detection of receptors in diseased knee sections compared to healthy knee sections may imply that the receptors have previously been subjected to ligand binding, influencing detection through immunohistochemistry. This observation might indicate that neurotrophins activate and potentially induce internalisation of the receptors in attempt to initiate internal signalling pathways for the support of tissue repair.

The data presented in this chapter indicate that NGF, could be involved in the disease mechanism of osteoarthritis that leads to joint tissue degeneration. In addition, the *in vitro* studies assessing the effects of neurotrophins on proliferation and differentiation suggest that NT-3 on its own and in collaboration with NGF has the capability to induce cell proliferation and contribute to enhanced neurite outgrowth by maintaining cell proliferation during differentiation. The mechanism underpinning this function could be applicable to the other tissues and progenitor cell types where the neurotrophin receptors are present. In addition, the mesenchymal stem and progenitor cell specific marker p75NTR, was shown to have an effect on the pathophysiology of tissue regeneration in an osteoarthritis animal model. As described previously, p75NTR cooperates with Trk receptors and is involved in the regulatory mechanism of functions essential for cell maintenance and viability.

In conclusion, our data suggests that p75NTR and the Trk C/NT-3 interaction could be involved in joint tissue maintenance and regeneration, and we have explored this hypothesis further.

Chapter 4: The effects of NT-3 and NGF on hip joint derived bone and cartilage progenitor cells proliferation and differentiation

4.1. Introduction

4.1.1. The biology of bone tissue

Bones provide structural support for the body, protect the internal organs, serve as the site for haematopoiesis and provide a reservoir for minerals and growth factors as well as an avenue for the deposition of toxins away from the bloodstream.

Contrary to the general belief that bone is inert and static, this is a dynamic organ that undergoes a significant degree of turnover. By looking at the ability to repair itself, rapidly mobilise mineral deposits and adapt its mass and morphology on the metabolic and functional demands, the bone tissue should in fact be considered a more "versatile material" and an example of "form follows function" in biological systems (Sommerfeldt and Rubin, 2001). A number of significant advances in the cell biology of the bone have demonstrated the complexity of intercellular signalling that regulates and adjusts bone cells during remodelling and growth.

Bone tissue is composed of three distinctly different cell types, osteoblasts, osteoclasts, and osteocytes. Out of the total bone cellular component, only 10% is composed of osteoclasts and osteoblasts, and the rest of 90% is comprised of osteocytes. Osteoblasts and osteocytes are derived from the mesenchymal stem cell lineage while the osteoclasts are of hematopoietic origin. Osteoclasts are formed by the fusion of monocyte/macrophage progenitors (Teitelbaum, 2000). In healthy bone, osteoclasts are responsible of bone resorption while osteoblasts are responsible of generating new tissue. The balance between these two processes is important for the maintenance of bone homeostasis.

Bone tissue can form through the differentiation of mesenchymal stem cell directly into osteoblasts, which then proceed to form bone, or through endo-chondral ossification,

which involves the formation of bone from chondrocytes that emerge though the differentiation of mesenchymal stem cells and form cartilaginous templates that then undergo mineralization.
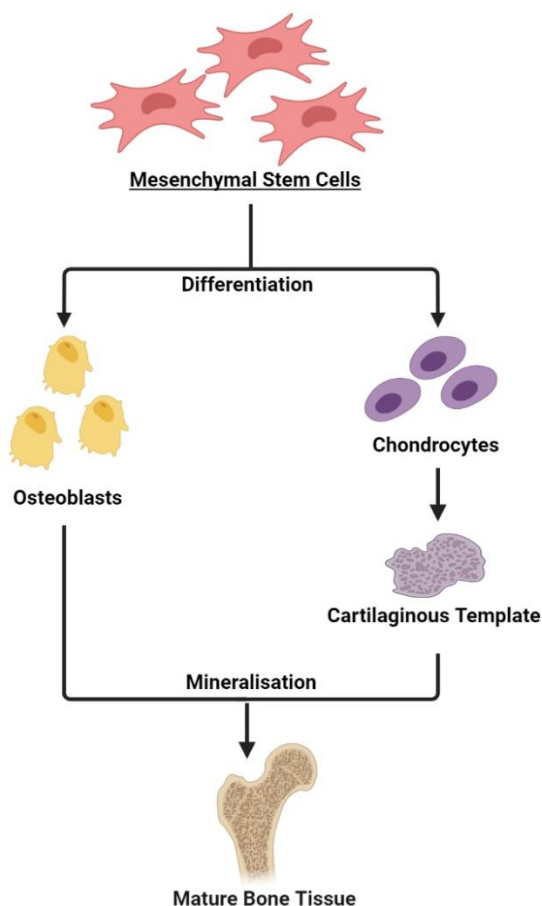
Figure 4. 1. Schematic representation of the mature bone tissue formation process

Mature bone consists of approximately 25% organic matrix (cells constitute 2-5% of this), 5% water and 70% of inorganic mineral. Bone mineral is in general referred to as hydroxyapatite [$Ca_{10}(PO_4)_6(OH)_2$]. The mineralization process is believed to start when extracellular vesicles that contain calcium ions, phospholipids, and phosphates, are secreted by hypertrophic chondrocytes or osteoblasts. Mineral crystallization begins when the vesicles reach saturation, and their content is exposed to the matrix. From then on, the process of mineralization proceeds in a self-perpetuating manner (Christoffersen and Landis, 1991). Just before the mineralization, at the osteoid stage, bone tissue consists predominantly of collagen, approximately 94%. Bone morphogenic proteins, adhesion molecules, growth factors and cytokines are

embedded too in the extracellular matrix. They are implicated in important signalling functions and proteins such as osteopontin and osteonectin have been shown to play an important role during the mineralization process. In this process the role of collagen is to determine the organization and orientation of the mineral crystals in the bone. Mineralization is also controlled by glycoproteins. They are regulators of the excess mineralization through mediation of calcium dependant phosphatase and ATPase activities in hypertrophic chondrocytes. (De Bernard, 1982; Yagami *et al.*, 1999). However, multiple elements of the process of bone mineralization have so far remained elusive.

4.1.2. MSC: osteo- and chondro- differentiation

Stroma derived mesenchymal stem and progenitor cells (MSCs) are adult stem cells with fibroblast-like morphology and the capacity to differentiate in osteocytes, chondrocytes, and adipocytes. According to the International Society of Cellular Therapies they are characterised by the following phenotypic features: ≥ 95% of the total cell population expresses the CD105, CD73 and CD90 surface markers and ≤ 2% of total cell population is positive for the markers CD45, CD34, CD14 or CD11b, CD19, CD79α and HLA-DR. The testing for negative markers should be done in order to avoid contamination with cells of haematopoietic lineages. In recent years, many studies have described other markers such as CD271, STRO-1, CD146, SSEA-4, CD49f as MSCs specific markers. This can create some controversy regarding the ideal set of markers for MSCs. In addition, variations of cellular marker expression can be influenced by the cell source or expansion protocol *in vitro* (Ullah *et al.*, 2015).

Since 2006, MSCs received a lot of attention for clinical applications and based on their plasticity they became a valuable tool in regenerative medicine. MSCs paracrine and immunomodulatory effects are mainly responsible for the positive results in cell therapies that utilise these cells (Caplan, 2017). Also, their potential to proliferate, differentiate and repopulate the target organ, makes them good candidates for the reconstructions of damaged tissue (Bacakova *et al.*, 2018).

The main characteristic that has made MSCs the focus of many therapeutic strategies is their differentiation potential. The mechanism of cell differentiation is complex and despite current advances in the effort to describe this process, the molecular events

taking place during the differentiation of MSCs towards the osteogenic, chondrogenic or adipogenic lineages are yet not fully understood.

4.1.3. Osteoarthritis

Osteoarthritis (OA) is defined as a multi-factorial degenerative disorder of the synovial joints, and it is often related to ageing and/or trauma. While OA is described as the most common musculoskeletal disease worldwide, its causes have not been clearly defined yet. Current therapeutic approaches are focused on analgesia and re-establishment of the mobility by artificially replacing the whole affected joint. This method will eventually lead to improvement of quality of life and pain relief for patients with OA. But this comes with disadvantages such as long recovery period and a 15-year maximum usage of the prosthetic (Martel-Pelletier *et al.*, 2016).

 OA is relatively known as a slow progressive joint disease. Despite this, no therapies have been able to stop or delay the progression of it. Referring to progression, not sufficient diagnosis tools are available to detect OA at the early stages. The diagnosis of OA is established at the advanced stage and is done predominantly through the use of imaging modalities. Usually, this diagnosis is followed by treatment for pain management and the joint replacement, as there is the ultimate option to reduce pain and re-establish mobility for the patient (Hunter, March and Chew, 2020).

The complexity of the OA makes it very difficult to identify at early stages and describe the cause. However, even without an exact aetiology, certain factors, such as joint overloading, mal-alignment, genetic disorders, metabolic syndromes, could play a role in the onset and progression of OA (Kraus *et al.*, 2015).

Current advances on understanding OA pathology, focus on the process of degradation and inflammation with regards to all three joint tissue components, the cartilage, the synovium, and the bone. It is crucial that any changes in either tissue degradation or the onset of inflammation to be detected early on, before major structural and functional alterations of the tissue are taking place. This is essential as the efficacy of utilised therapies will be reduced or will be less successful, when these are employed later on in disease progression. On top of that, the heterogeneity of the

OA makes the development of one universal therapeutic option very difficult (Man and Mologhianu G, 2014).

A number of studies have examined the content of synovial fluid in OA patients in search for biomarkers that could be beneficial for the detection of early OA. By analysing the synovium, researchers have been able to develop novel therapeutic approaches, such as anabolic drugs, anti-nerve growth factor strategies, opioid treatment of the peripheral receptors, cell cycle inhibitors, targeting of metabolic factors. Nevertheless, considering the complexity of the OA, data collected from only the synovium might miss important mechanisms of disease progression that take place in the cartilage and the subchondral bone (Grässel and Muschter, 2020).

4.1.4. Neurotrophin signalling pathway in OA chronic pain

Pain is generally defined as 'an unpleasant sensory and emotional experience associated with actual or potential; tissue damage or described in term of such damage (Merskey and Watson, 1979).

Pain is the primary symptom of OA.

NGF, initially described as crucial for neuronal growth and survival, has also been shown to act as the key pain mediator. Elevated levels of NGF have been reported during injury, inflammation, and chronic pain. Research and clinical studies have provided important evidence that support the role of NGF in pain sensation in the event of acute and chronic pain (Hefti *et al.*, 2006). In this study increased level of NGF have been detected for conditions such as cystitis, prostatitis, chronic headaches, and arthritis. In animal studies, NGF has been found to increase greatly in skin and muscle after the surgical incisions. Increase of NGF has also been observed in response to inflammation produced by a variety of factors. Moreover, high levels of NGF have been found to correlate with chronic pain in patients with OA. In an osteoarthritic joint, increased levels of NGF activate p75NTR and Trk receptors, which modulate the expression of peripheral and central pain-related substances (calcitonin, substance P, histamine, serotonin, 5-hydroxytryptamine), and induces sensitization of nociceptive neurons as response to inflammation (Shang, Wang and Tao, 2017). This newly discovered implications of NGF in OA chronic pain have led to the development of a

novel class of analgesics that act as antagonists of signalling triggered by NGF. These are monoclonal antibodies designed to track and trap NGF molecules. Without NGF, nociceptor sensitization will cease to occur. The current developed anti-NGF therapeutic options can induce a moderate reduction in chronic pain. Unfortunately, the need for joint replacement increased in comparison with the control (Gruen, Myers and Lascelles, 2021). Overall, blocking the effect of NGF in the osteoarthritic joint can cause a reduction in pain but at the same time induce a rapid progression of the disease, leading to severe mobility impairment. Therefore, there is still the need for novel therapeutic approaches for OA to target chronic pain.

The neurotrophin signalling pathway is well known to promote cell survival, plasticity, differentiation, synapse formation and axonal outgrowth. It is also reported to be activated via p75NTR and can induce cell cycle arrest and even apoptosis.

In this chapter we are investigating the effect of NT-3 on the proliferation and differentiation of human joint derived stroma cells and compare this with the effect of NGF. Our findings can contribute to the development of new treatment approaches for hip joint degenerative osteoarthritis.

4.2. Methodology

In this study, a total of 7 human samples have been included, 5 from patients with osteoarthritis and 2 healthy subjects. The diseased samples were obtained through collaboration with the Oxleas NHS Foundation Trust. The healthy bone marrow aspirates were purchased from Lonza.
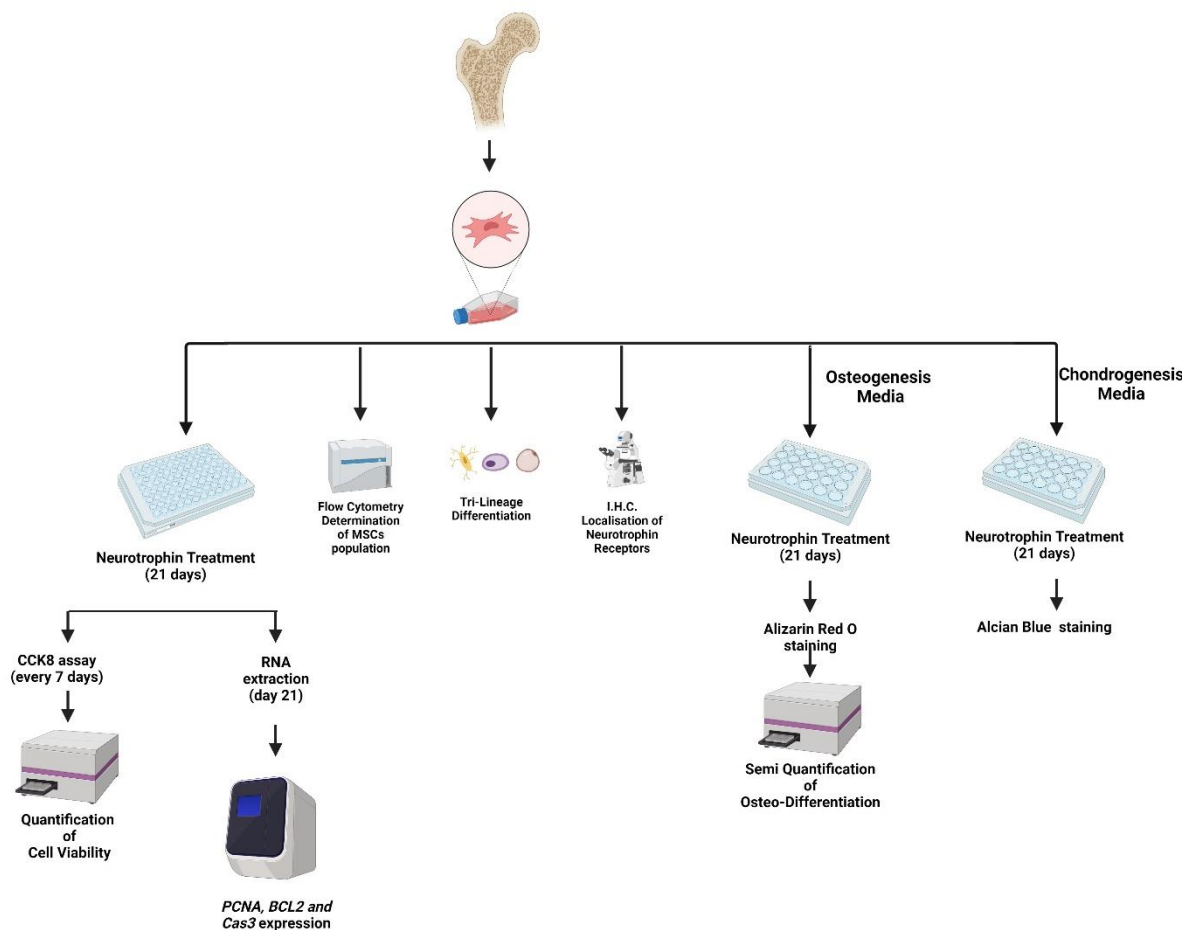
Figure 4. 2. Schematic diagram of the experimental workflow described in this chapter. *A series of techniques such as flow cytometry, histological staining and immune-cyto-fluorescence were carried out for the characterisation of the isolated cells. A series of in vitro assays including the semi-quantification of histological staining were conducted for the assessment of neurotrophin effects on mesenchymal stroma cells proliferation and differentiation (diagram generated in Biorender).*

Flow cytometry analysis and tri-lineage differentiation were carried out in order to validate the MSC phenotype of the human tissue isolated cells. The effects of human

NT-3 and NGF recombinant proteins on the proliferation and differentiation of hMSCs from the hip joint and bone marrow, as well as of the chondroprogenitors (hCPCs) from diseased human articular cartilage, were assessed through a series of *in vitro* assays. The cellular viability was monitored with CCK8 assays and the possible enhancement or impairment of osteogenic and chondrogenic differentiation induced by NGF or NT-3 was assessed by semi-quantification of the Alizarin Red staining. The effects of NGF and NT-3 on chondro-differentiation of hCPCs was assessed by staining with Alcian Blue.

4.2.1. Isolation of bone and cartilage stroma cells
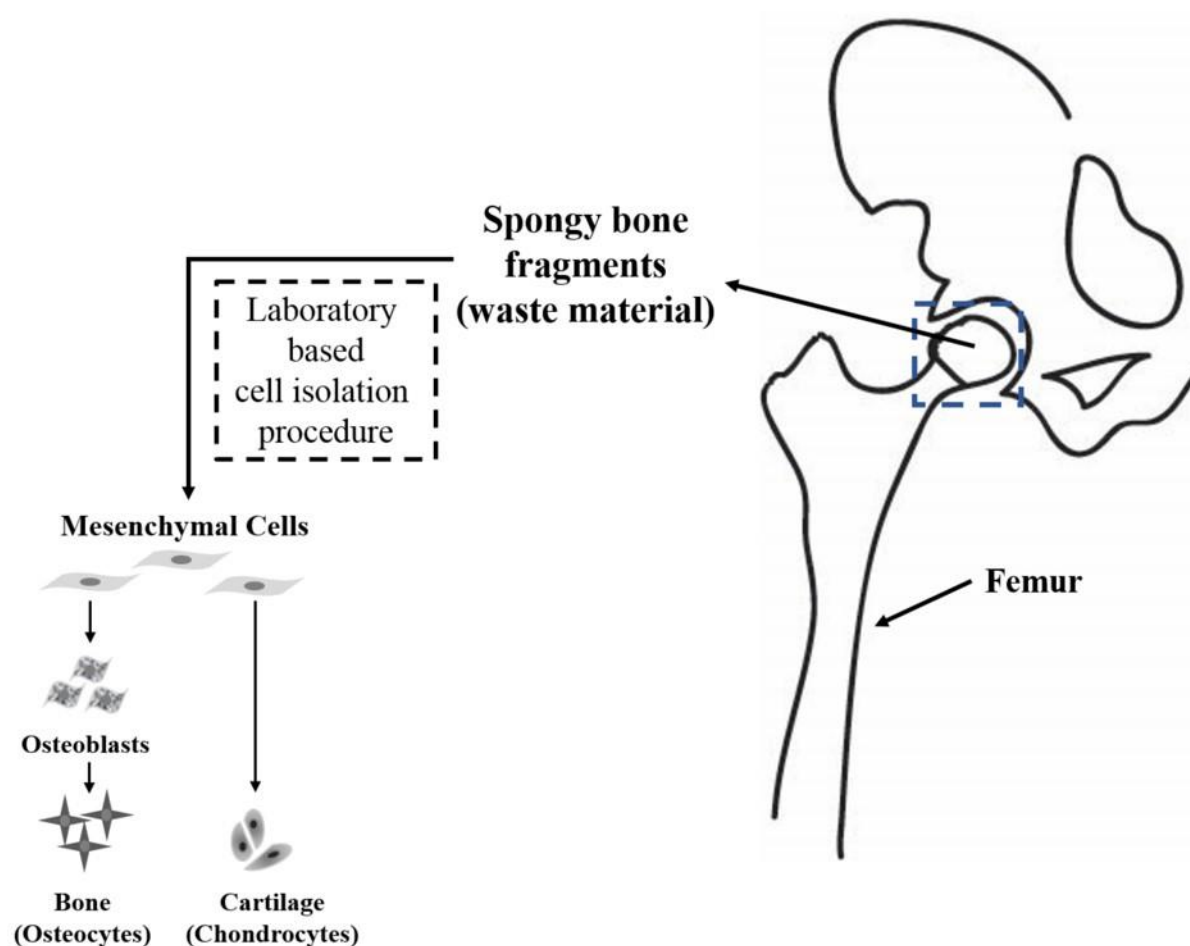
Figure 4. 3. Schematic representation of e hMSCs isolation from the hip joint
hMSCs were isolated from the femoral head obtained following a hip arthroscopy surgical procedure. The femoral head is waste biological material. A detailed description of the series of steps for cell isolation has been provided in Chapter 2.

Primary bone and cartilage stroma cells were isolated from the femoral head of 5 different patients that underwent total hip replacement surgery. In this type of surgery,

the affected femoral head is removed and is replaced with an artificial smooth like ball joint that is attached to a short, angled metal stem that is fixed with cement in the hollow of the femur.

Through collaboration with Mr. Saif Ahmed, orthopaedic surgeon at Oxleas NHS Foundation Trust, access to diseased tissue has been obtained. The patients willing to donate their discarded tissue, signed a consent form prior to the surgery. After removal, femoral heads were placed in 1x Mg⁻, Ca⁻ PBS – 1% PSA solution. The tissue was transported to the laboratory where it was processed for the isolation of stroma cells. Available cartilage was sectioned and digested over-night before being placed in culture. The bone was drilled and dissected in 1 cm^3 fragments. The cells from the bone fragments were mechanically dispersed in suspension with a sterile set of mortar and pestle. Full procedure is described in Chapter 2.

Since MSCs are known to express Integrin α5β1, a high-affinity fibronectin receptor, the culture dishes pre-set for the expansion of the isolated cells were pre-coated with fibronectin. Through this method, newly isolated cells were assisted in attaching to the culture dish, and the yield of cell isolation increased compared with the use of non-fibronectin coated plates. Cells were allowed to adapt and expand for a total period of 14 days post-isolation, where media has been refreshed (50% media change) on day 7 and totally replaced (passage 1), on day 14.

hMSCs were also isolated from commercially available bone marrow aspirates from Lonza. Two healthy MSCs sources were included in this study. For the isolation of hMSCs from healthy subjects, 500ul of HIV and Hep. B negative raw bone marrow was seeded in fibronectin coated culture flasks and cultured and allowed to expand for a total of 14 days before carrying out any assays.

4.2.2. Flow Cytometry

For the characterisation of isolated cells in accordance with the characteristics of the MSC phenotype, bone and bone marrow isolated and culture expanded cells were analysed though flow cytometry. 1 x 10^5 cells were stained with 1/100 fluorescent antibodies against CD271, CD45, CD90, CD105, and CD146 in 1x PBS – 0.5% (v/v) FBS and incubated for 30 minutes in the dark at 4ºC. The cells were washed 3 times

and analysed with the Beckman Coulter CytoFlex Flow Cytometry System. Unstained controls were run in parallel. For antibody compensation, the VersaComp™ kit was used according to the manufacturer guidelines. For full method description and the parameters used for data analysis please refer to Chapter 2.

4.2.2.1. Flow cytometry data analysis

For the analysis of recorded events, these were analysed using dot plots. The final gates shown in the results section were drawn on dot plots containing only single recorded events, free of debris (identified through size exclusion) and compared against unstained cells and compensation dot plots in order to exclude the recording of false positive events for each of the antibodies used.

The analysis of the collected flow cytometry data for all samples was carried out according to the following steps. A detailed example of the flow cytometry data analysis strategy is available in the Appendix.

1. For the unstained cells control, single stained cells control and all stained samples an initial gate was drawn on FSC/A vs SSC/A dot plots to size exclude debris and from the analysis. The gate was labelled as "all events".

2. FSC/A vs FSC-Width dot plots were used to exclude doublet events from "all gated events". On these plots a secondary gate was drawn to include single cells only.

3. The unstained cells control was used to draw the positive antigen gates on dot plots with fluorochromes selected for the x and y axes. These antigen positive events specific gates were set up to include exclude any false positive events. In order to ensure this the gate position and shape was adjusted to capture events cells with the appropriate fluorescent intensity and scatter properties. Please note that at the start of the flow cytometry data analysis fluorochrome spill overcompensation has been applied for all analysed samples.

4.2.3. Tri-Lineage Differentiation:

To assess the differentiation potential of the isolated cells, hMSCs were seeded in tissue culture multi-well plates and treated with adipogenic, chondrogenic and osteogenic media for a total of 21 days. The cells were fixed and stained with Oil Red O, Alcian Blue S and Alizarin Red solutions to visualise the differentiated adipocytes, chondrocytes and osteocytes respectively. A full method description can be found in Chapter 2.

4.2.4. Neurotrophin receptor localisation

To determine the presence of neurotrophin receptors on the membrane of the human joint derived progenitors, hMSCs were seeded on plastic coverslips, allowed to attach, fixed and stained with fluorescent tagged antibodies against p75NTR, Trk A, Trk B and Trk C. The localisation of the receptors was analysed with the Olympus IX83 Inverted Fluorescent Microscope and the Cell Sens Software.

4.2.5. The effect of NGF and NT-3 on the proliferation of hMSCs and hCPCs.

In order to assess cell proliferation under neurotrophin treatment, 5×10^3 cells/cm^2 of either hMSCs or hCPCs were seeded in clear flat bottom with dark walls 96-well culture plates in DMEM supplemented with 5% FBS, 1% NEAA, 1% PSA and 2mM L-Glutamine. The cells were allowed to fully adhere to the culture surface and on day 0 of the experiment, the media was replaced with low serum media supplemented with the neurotrophin treatment. The media was refreshed every 3 days. For the assessment of cell proliferation, a commercially available cell viability kit (CCC8 Cell Viability Kit) was used. This type of assay uses WST-8 tetrazolium salt (NADH+ binder), a non-toxic reagent that is reduced by mitochondrial activity of cellular dehydrogenases to orange formazan. The amount of orange formazan is easily detected through the measurement of absorbance at 460nm and is directly proportional with the number of living cells. Due to the fact that cells were obtained from a variety of patients, they exhibited a range of variabilities. For this reason, they presented different time points for maximization of the cell viability detection reagent.

As consequence, multiple readings over a total of 24 hours were performed with the aim to collect the most relevant data for each patient sample. When compared with other methods for monitoring cell viability (for example MTT or Alamar Blue), CCK8 is a non-cytotoxic assay and provides the option for continuous monitoring over prolonged periods in culture.

4.2.6. Analysis of neurotrophin effect on osteogenic and chondrogenic differentiation

To determine the effect of NGF and NT-3 in the osteogenic and chondrogenic differentiation of joint derived progenitors, bone marrow derived healthy, and bone derived diseased cells were seeded at the density of 4×10^3 cells/cm^2 in clear flat bottom 48 well plates. The cells were treated with osteogenic media supplemented with 12ng/ml, 25 ng/ml and 50ng/ml of NGF/NT-3/NGF+NT-3 for a total of 21 days. The treatment was refreshed every 3 days. At the end of the treatment, the cells were fixed and stained with Alizarin Red staining solution for the analysis of osteogenic differentiation. The intensity of the staining was semi-quantified though acetic acid dilution of the uphold stain. The absorbance of the samples was recorded at 405nm wavelength with BMG LabTech FLUOstar microplate reader and analysed with MARS Software.

A full method description can be found in Chapter 2.

In addition, the effect of NGF and NT-3 treatment was tested on the chondrogenic differentiation of diseased joint derived cartilage isolated cells. However, the differentiation potential was evaluated only qualitatively. The neurotrophin treatment was applied as described above using the same cell density and at the same concentrations in chondrogenic supplemented media.

A full method description can be found in Chapter 2. 4.3. Results

4.3.1. The benefits of using Fibronectin in the isolation of Bone Stroma Cells

Selective hMSCs isolation has been optimised using fibronectin for the pre-treatment of culture dishes. Representative light microscopy evidence is shown in Fig. 4.3.

Previous attempts of hMSCs isolation without fibronectin pre-coating of the culture dishes, resulted in poor cell adhesion and the need for a longer than 14 days post-isolation acclimatisation period. Culturing hMSCs from both, healthy and diseased, individuals, in fibronectin coated culture dishes, resulted in a better retainment of the progenitor population and an overall healthier cellular appearance (confirmed through light microscopy). All cell isolates used for the collection of the data presented in this chapter have been isolated and expanded in fibronectin coated culture dishes.
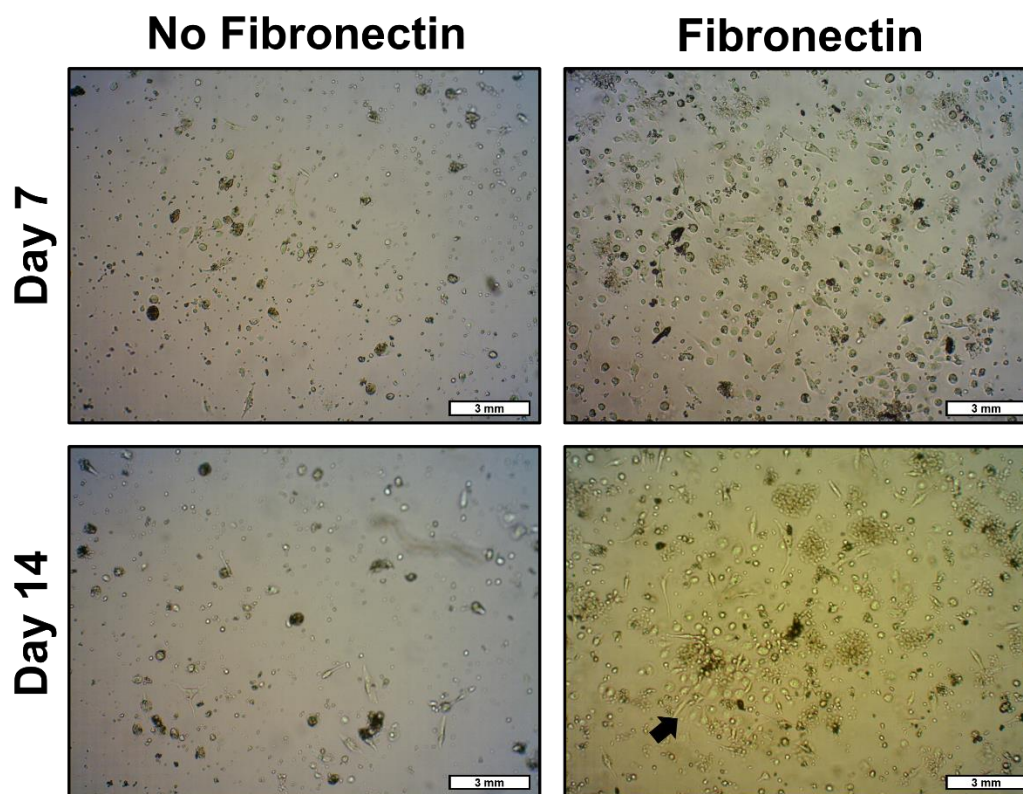
Figure 4. 4. Isolated CFU-like stroma cells showing plastic adherence.
The images show the retained cellular density obtained at day 7 (A;C) and day 14 (B;D) post-isolation in non-coated culture dishes (left) and in fibronectin coated culture dishes (right). Fibronectin coated flasks not only selectively isolated the progenitor cell population, but also provided a better environment for the MSC specific, colony forming units (indicated by the arrow in D); 3mm scalebar.

4.3.2. Flow cytometry analysis

Representative isolated cells for the healthy bone (BM2-hMSC), diseased bone (OA5-hMSC) and diseased cartilage (OA5-hCPCs) have been analysed for the immunophenotype specific for MSCs by flow cytometry.

The collected data summarised in the figure below (Fig. 4.5) indicates that the analysed cell populations contain subpopulations with an MSC phenotype. Cell populations that were positive for the MSC markers CD105, CD90 and CD146, were identified within the cultured stroma cells isolated from healthy and disease donors. However, a difference between the size of those cell populations was also observed. This was not unexpected since a reduction in the population of MSCs in ageing has been previously described (Rebolj et al., 2018). This has been recorded even within the richest source of MSCs, the bone marrow, where these cells were found to be present in low frequencies. . In addition, it is important to consider that the analysed cell populations presented in Figure 4.5 were subjected to mechanical disruption and enzymatic treatment, to isolate single cells, which could have negatively impacted the frequency of viable of MSCs.

Sample	CD105	CD90	CD146	CD271
BM2-hMSC	4.66%	3.69%	2.38%	5%
OA5-hMSC	2.37%	1.2%	0.72%	1.25%
OA5-hCPC	0.64%	0.8%	0.94%	1.61%
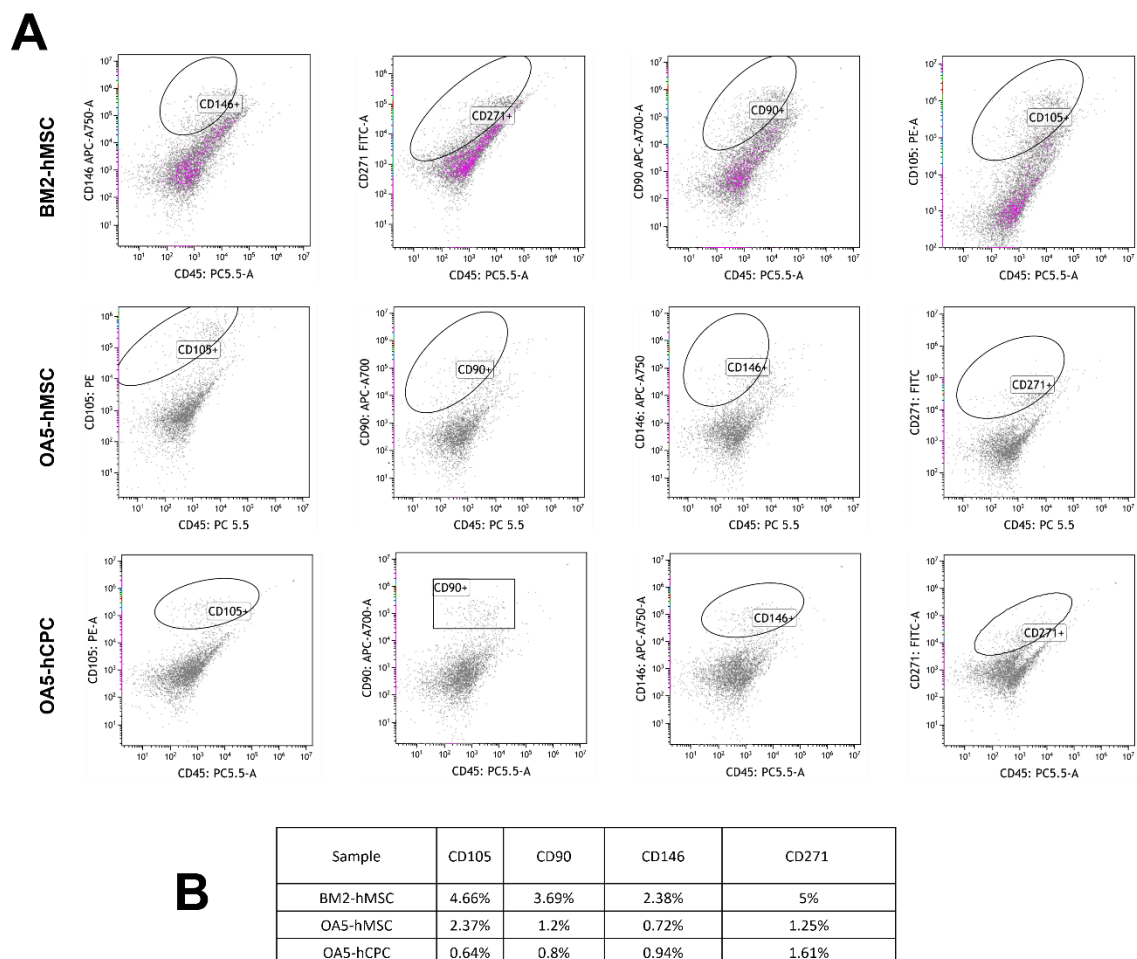
Figure 4. 5. Flow cytometry analysis of bone and bone marrow stroma cells.
Representatives dot plots (A) showing the surface MSC markers expression of early passage stromal cells derived from healthy bone marrow (BM2-hMSC), diseases bone (OA5-hMSC) and diseased cartilage (OA5-hMSC). One representative source per biological groups (Table

4.1) is presented. The percentage of positive cells for CD105, CD90, CD146 and CD271, of all single cell recorded events, are summarised in the B section of the figure.

4.3.3. Tri-Lineage differentiation

To confirm that the isolated cells from human bone marrow and the human femoral head have MSC like characteristics, induced differentiation into adipocytes, chondrocytes, and osteoblasts was carried out on representative isolates for healthy bone, osteoarthritic bone, and osteoarthritic cartilage. The findings summarised in Fig. 4.6 suggest that the isolated progenitor cells, using the fibronectin method, have the capacity to support adipogenesis, osteogenesis and chondrogenesis. According to the standard established by the ISCT, tri-lineage differentiation is one indication of the MSC cellular phenotype.

Tri-lineage differentiation of the healthy bone marrow stroma cells (Fig. 4.6) resulted in successful osteo-differentiation demonstrated by the positive staining with Alizarin Red of the Calcium deposits in cells treated with osteogenic media, compared with the day 0. BM-hMSCs responded positively to treatment with chondrogenic media; condensation of the cells is marked by increased intensity of the Alcian Blue staining. Cells treated with adipogenic media also displayed signs of adipo-differentiation, when compared with control wells; cellular condensation and adipo-vacuole structures stained by Oil Red O staining solution.

BM2-hMSC

| Osteo-differentiation | Chondro-differentiation | Adipo-differentiation |
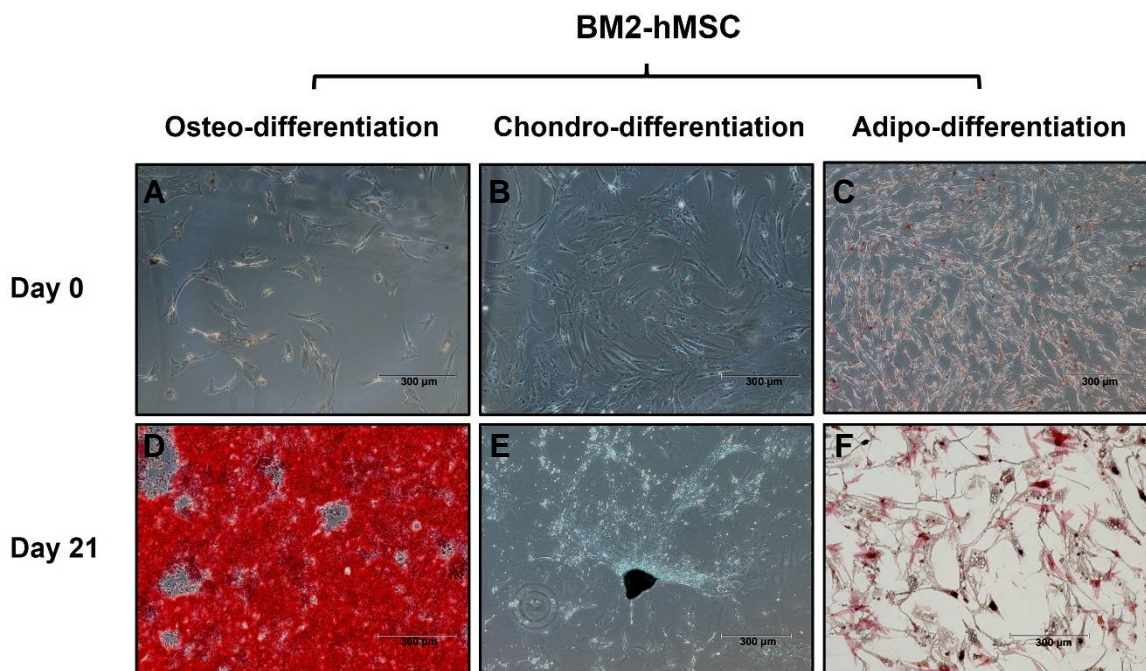
***Figure 4. 6*. Trilineage Differentiation of BM2-hMSCs.**
The multipotent differentiation potential of isolated cells was tested by culturing different seeding densities of BM2-hMSCs in osteogenic, chondrogenic and adipogenic media for 21 days. The tri-lineage differentiation potential of the cells was validated by histological staining and presented in this figure; (A; D). Alizarin Red staining to validate the formation of calcium deposits as result of osteo-differentiation; (B;E). Alcian Blue staining to validate the GAGs synthesis as result of chondro-differentiation; (C;F). Oil Red O staining to validate the formation of lipid vacuoles as result of adipo-differentiation; 300 μm scalebar.

Tri-lineage differentiation of isolates obtained from the bone compartment of osteoarthritic hip joints (femoral head) (Fig. 4.7), resulted in successful osteo-differentiation shown by positive Alizarin red staining of the calcium deposits. The chondrogenic treatment resulted in positive Alcian Blue staining of the ECM secreted by the hMSCs after 21 days. The Oil red staining of the OA5-hMSCs cultured in adipogenic media showed positive staining for the lipid vacuoles.

OA5-hMSC

| Osteo-differentiation | Chondro-differentiation | Adipo-differentiation |

Day 0 — A, B, C

Day 21 — D, E, F

300 µm
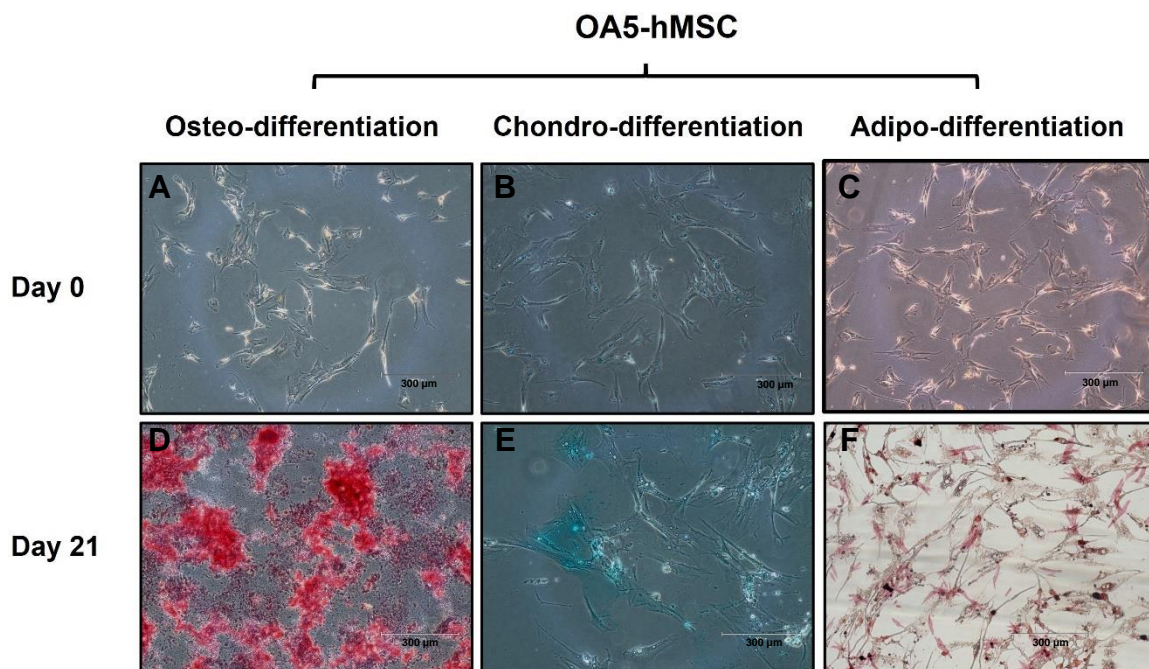
Figure 4. 7. Trilineage differentiation of OA5-hMSCs.
The multipotent differentiation potential of isolated cells was tested by culturing different seeding densities of OA5-hMSCs in osteogenic, chondrogenic and adipogenic media for 21 days. The tri-lineage differentiation potential of the cells was validated by histological staining and presented in this figure; (A; D). Alizarin Red staining to validate the formation of calcium deposits as result of osteo-differentiation; (B;E). Alcian Blue staining to validate the GAGs synthesis as result of chondro-differentiation; (C;F). Oil Red O staining to validate the formation of lipid vacuoles as result of adipo-differentiation; 300 µm scalebar.

Tri-lineage differentiation treatment on the chondro-progenitors isolated from the articular cartilage of diseased hip joint (Fig. 4.8), resulted in successful osteo-differentiation (calcium deposits positively stained by Alizarin Red staining solution), chondro-differentiation (cellular condensation and collagen detected by Alcian Blue staining) and adipo-differentiation (Oil red staining of the lipid vacuoles).

OA5-hCPC

Osteo-differentiation   Chondro-differentiation   Adipo-differentiation
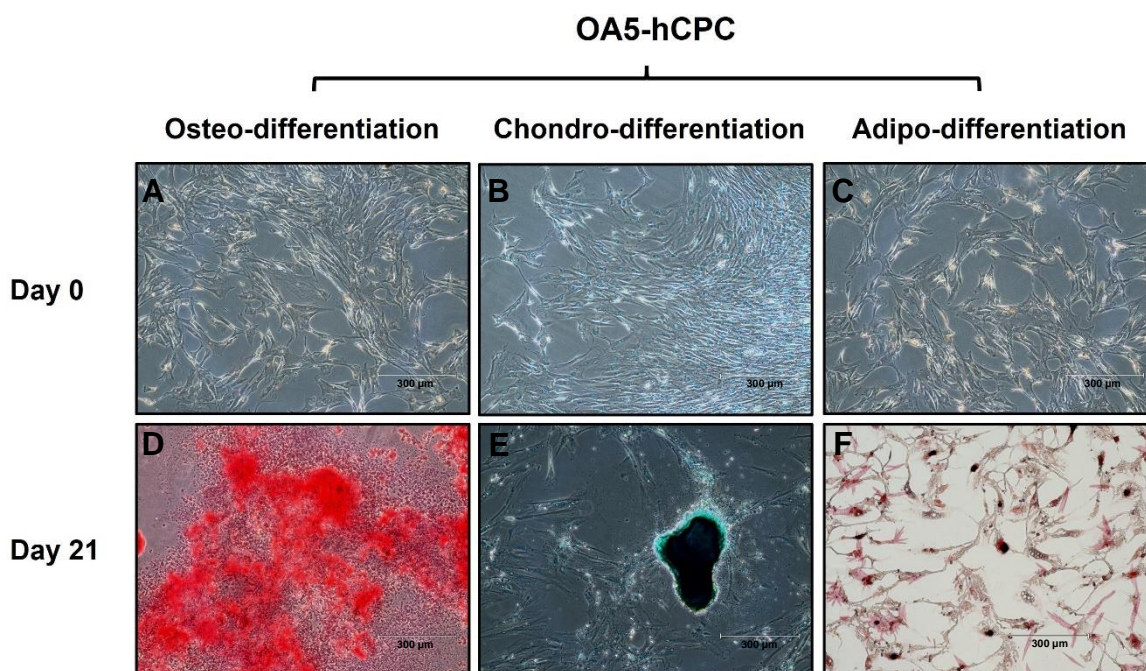
Figure 4. 8. Trilineage Differentiation of OA5-hCPCs.
The multipotent differentiation potential of isolated cells was tested by culturing different seeding densities of OA5-hCPCs in osteogenic, chondrogenic and adipogenic media for 21 days. The tri-lineage differentiation potential of the cells was validated by histological staining and presented in this figure; (A; D). Alizarin Red staining to validate the formation of calcium deposits as result of osteo-differentiation; (B;E). Alcian Blue staining to validate the GAGs synthesis as result of chondro-differentiation; (C;F). Oil Red O staining to validate the formation of lipid vacuoles as result of adipo-differentiation; 300 µm scalebar.

4.3.4. IF-IHC localization of p75NTR and Trk C on representative

Immuno-localisation of the neurotrophin receptors, p75NTR and Trk C was analysed in representative isolates for the healthy bone, diseased bone, and diseased cartilage. All 3 analysed cell isolates were found positive for p75NTR.

According to the data presented in the Fig. 4.9 and Fig. 4.10, healthy bone marrow stroma cells (BM2-hMSC), osteoarthritic bone derived stroma cells (OA5-hMSC) as well as osteoarthritic cartilage derived stroma cells (OA5-hCPC) positively stained for p75NTR.
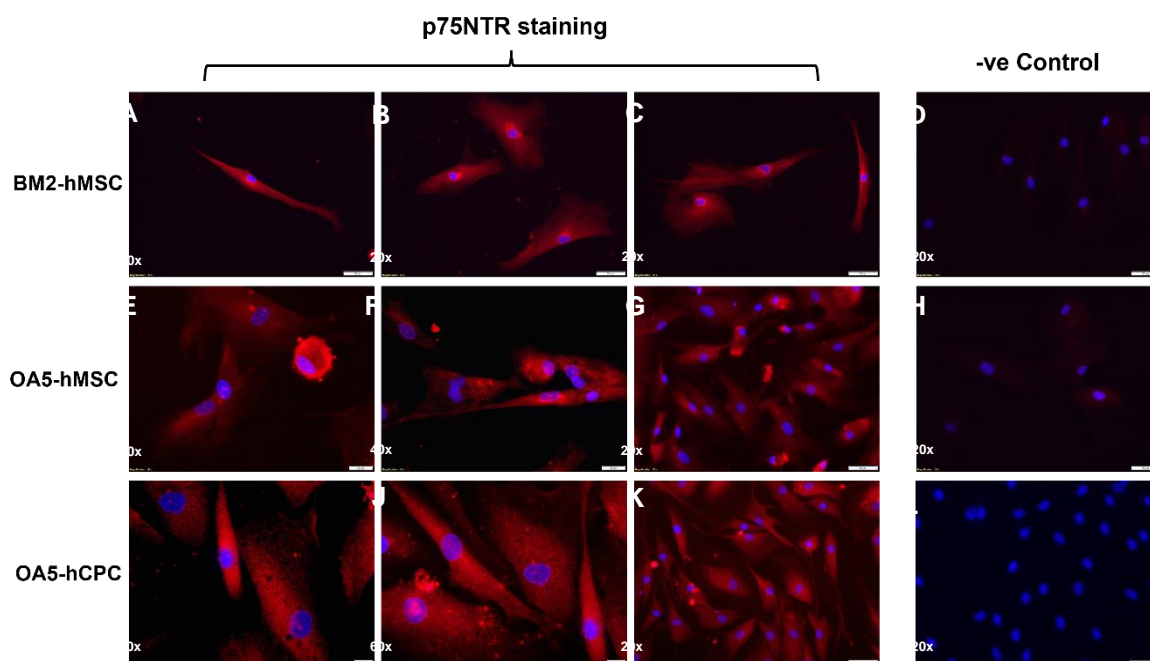
Figure 4. 9. IF-IHC detection of p75NTR on the healthy bone marrow derived MSCs BM2-hMSCs, diseased OA5-hMSC and OA5-hCPC.
p75NTR protein was detected by immuno-staining with fluorescent tagged antibody, visible in Cy5 channel (red), in representatives cellular populations *isolated from healthy bone marrow (A;B;C), diseased bone (E;F;G) and diseased cartilage (I;J;K). Cell nuclei stained with DAPI (blue). For negative controls (D;H;L), cells were incubated with IgG controls and used for the assessment of background staining.*

Trk C receptor has been localised in on the cellular membrane of diseased OA5-hCPC, diseased OA5-hMSC (low detection). The cell isolates from healthy bone marrow (BM2-hMSC) were found negative for Trk C receptor staining.
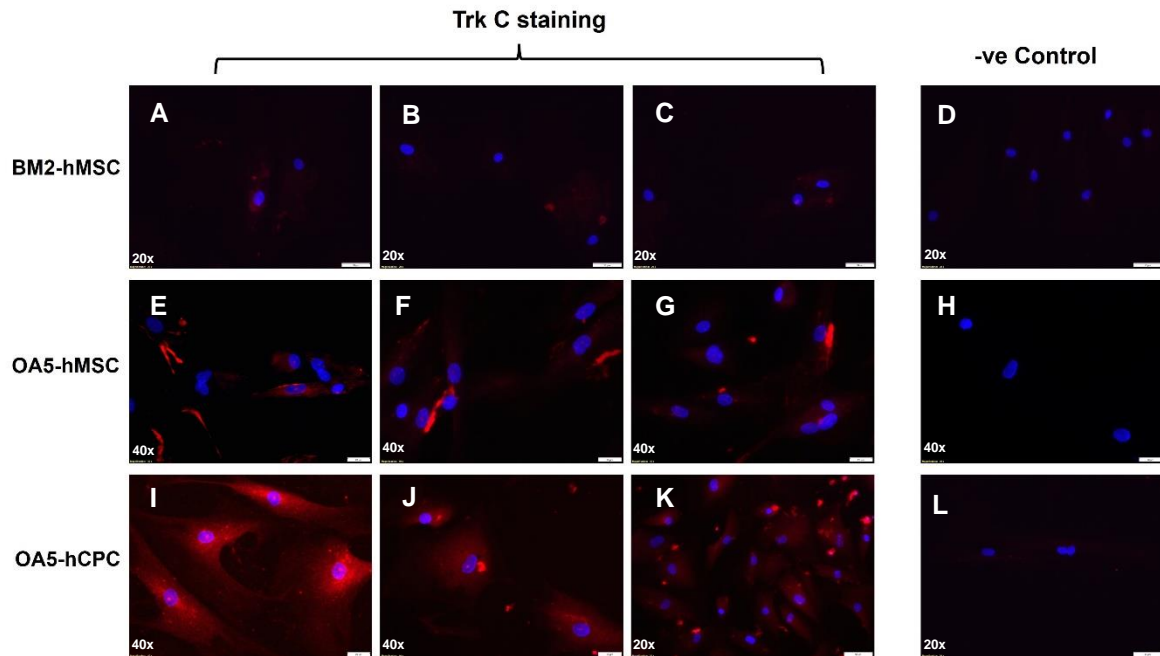
Figure 4. 10. IF-IHC detection of Trk C on the healthy BM2-hMSC, diseased OA5-hMSC and OA5-hCPC.

The localisation of Trk C protein was assessed in representative cellular population isolated from healthy bone (A;B;C), diseased bone (E;F;G) and diseased cartilage (I;J;K) by immuno-staining with antigen specific fluorescent tagged antibody visible in Cy5 (red). Cell nuclei stained with DAPI (blue). For negative controls (D;H;L), cells were incubated with IgG controls and used for the assessment of background staining.

4.3.5. The effect of NT-3 and NGF on the cellular viability of osteosarcoma and chondrosarcoma cell lines.

The effect of the neurotrophins NT-3 and NGF was initially tested on two cell lines with bone and cartilage characteristics, the MG-63 human osteosarcoma and the SW-1353 human Chondrosarcoma cell lines.

Cells were treated with neurotrophins for 21 days and the cell viability was investigated at 7-day intervals.

The data summarised in Fig. 4.11. shows that the effect of NT-3 is minimal after 7 days of treatment and when the cells are exposed for longer to NT-3 they display a decrease in cellular viability. A significant negative effect for the NT-3 treatment was observed at 25 ng/ml in comparison with the control (no neurotrophin treatment). This was recorded on day 14.

The MG-63 cells treated with NGF showed an increase in proliferation on day 7 and only for the 25 ng/ml NGF condition. On day 14 and day 21, the NGF treated cells showed decreased cellular viability in comparison with the control (no NGF).

The combined NT-3 and NGF treatment on MG-63 cells, resulted in minimal proliferation only at 50 ng/ml concentration for both neurotrophins on day 7 and day 21. Finally, a significant decrease in MG-63 viability was observed on day 14 when the cells were treated with 12.5 ng/ml of NT-3 and NGF.
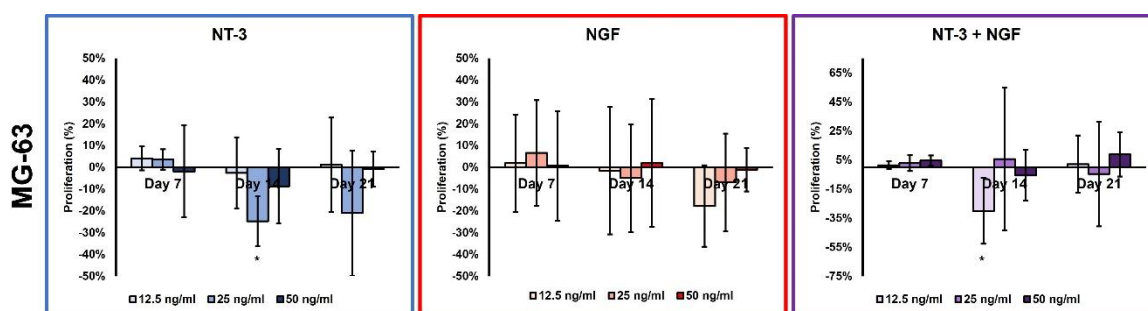
Figure 4. 11. The effects of NGF and NT-3 treatment on the viability of MG-63 (human osteosarcoma cell line)

*The graphs show the mean precentage +/- SD, of stimulation (+) and inhibitioan (-) of MG-63 cellular viability during 21 days of NT-3 and NGF treatment. The data has been analysed relative to the control (0 days-no treatment) for a clearer data representation. Statistical analysis of the presented data was done in Minitab Software, where significant data is marked by * (significant, p-value<=0.05), ** (very significant, p-value<=0.01), *** (highly significant, p-value<=0.001).*

This initial experiment carried out on the MG-63 cell line failed to provide an indication of the optimal NT-3 treatment conditions for cells with bone characteristics, as mixed results were observed.

The data summarised in Fig. 4.12 shows that cartilage like cells from a chondrosarcoma cell line respond positively to NT-3 by inducing proliferation, when low concentrations are used (12.5 and 25 ng/ml). Higher concentrations of NT-3, more than 25 ng/ml, appear to have a cytotoxic effect. The NGF treatment induced an increase in the viability of the SW-1353 cell line after 7 days of treatment. However, similarly to the NT-3 treatment, concentrations higher than 25 ng/ml appear to be toxic for the cells. The combined (NT-3 + NGF) treatment has a similar effect as the treatment with individual NT-3 and NGF. A small increase in proliferation at day 7 was observed only in low concentration treatments. When compared with the individual NT-3 and NGF treatments, the combined treatment led to an increase in cell numbers at the concentration of 12.5 ng/ml up to 21 days of treatment. A similar effect was detected in the 12.5 ng/ml NT-3 treatment, while treatment with 12.5 ng/ml of NGF, led to significant decrease in SW-1353 cell viability. This observation indicates a collaborative relationship between the two neurotrophins, with opposite effects when used individually.
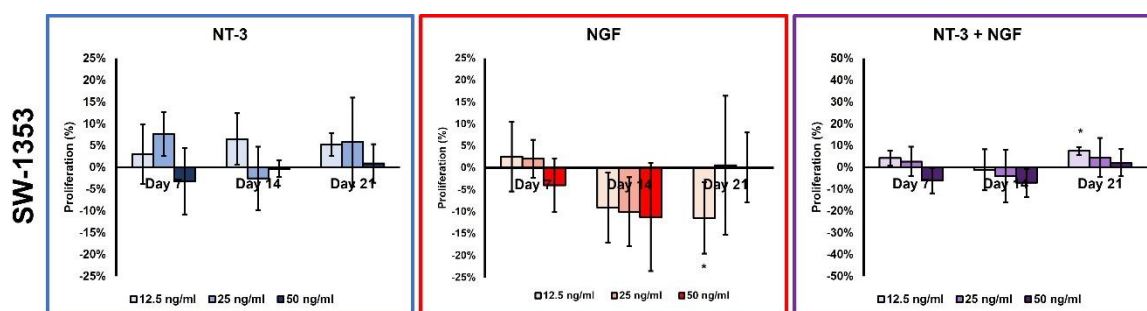
Figure 4. 12. The effects of NGF and NT-3 treatment on the viability of SW-1353 (human chondrosarcoma cell line).
*The graphs show the mean precentage +/- SD, of stimulation (+) and inhibitioan (-) of SW-1353 cellular viability during 21 days of NT-3 and NGF treatemnt . The data has been analysed relative to the control (0 days-no treatment) for a clearer data representation. Statistical analysis of the presented data was done in Minitab Software, where significant data is marked by * (significant, p-value<=0.05), ** (very significant, p-value<=0.01), *** (highly significant, p-value<=0.001).*

The data summarised in Fig. 4.11 and Fig. 4.12 indicate that cartilage and bone like cells exhibit an increase in viability in response to NT-3 or NGF treatment after 7 days;

however, the prolonged exposure induces cytotoxicity that is in some cases followed up by a recovery of the cellular viability.

4.3.6. The effect of NT-3 and NGF on the proliferation of hMSCs and hCPCs

5×10^3 cells isolated from healthy and diseased joint tissue were seeded per well in 96-well microplates with 4 technical replicates for each treatment per sample. The cells were allowed to acclimatise for 7 days as from previous observations, primary cells for joint tissue are characterised by different attachment times. After the acclimatisation time, an absorbance reading at 460nm in the presence of the WST-8 reagent was carried out at day 0 with no treatment to create a baseline for each of the samples. Cells were treated with different neurotrophin concentrations for a total of 21 days; media (with or without treatment) was refreshed every 3 days to avoid growth factor degradation. At time points 7, 14 and 21 days, absorbance readings at 460nm in the presence of the WST-8 reagent were carried out to monitor cell viability.

The table below summarises the samples studied in this experiment.

Table 4. 1. List of bone marrow and joint bone and cartilage derived cell populations that were treated with NT-3 and NGF.

Cell source	Cell sample ID
Healthy Bone	BM1-hMSC and BM2-hMSC
Diseased Bone	OA1-hMSC, OA2-hMSC, OA3-hMSC, OA4-hMSC and OA5-hMSC
Diseased Cartilage	OA1-hCPC, OA2-hCPC, OA3-hCPC, OA4-hCPC and OA5-hCPC

The graphs below summarise the data obtained from the whole experiment where the effects of neurotrophin on cell maintenance were assessed.

Overall, NT-3 treatment appears to have a positive impact on the cellular viability of healthy bone marrow stroma cells (Fig. 4.13 top graph) only when treated with small concentrations (12.5ng/ml) and when the cells are exposed to the treatment for less than 21 days. Higher concentrations of NT-3 were shown to reduce the viability of the healthy bone marrow stroma cells, when compared with the control (no neurotrophin). The cell viability data collected across the full 21 days of treatment indicate a significant (***) effect of NT-3 on the viability of this cell type.

Quantification of cell viability collected from the healthy bone marrow stroma cells treated with NGF treatment (Fig. 4.13 middle graph) for 21 days indicate a positive effect of the neurotrophin (25 ng/ml) after 7 days under treatment. 12.5 ng/ml NGF treatment has the same effect but recorded at day 14. However, the statistical analysis of the data indicates no significant effect of NGF on the cellular viability of this type of primary cells.

When the cells were treated with a combination of both, NGF and NT-3 (Fig. 4.13 bottom graph), only at day 14 a significant effect on cellular viability compared with the control was observed. According to the data statistical analysis, a treatment of 50 ng/ml NGF + NT-3 maintain the cell viability, when compared with the control.
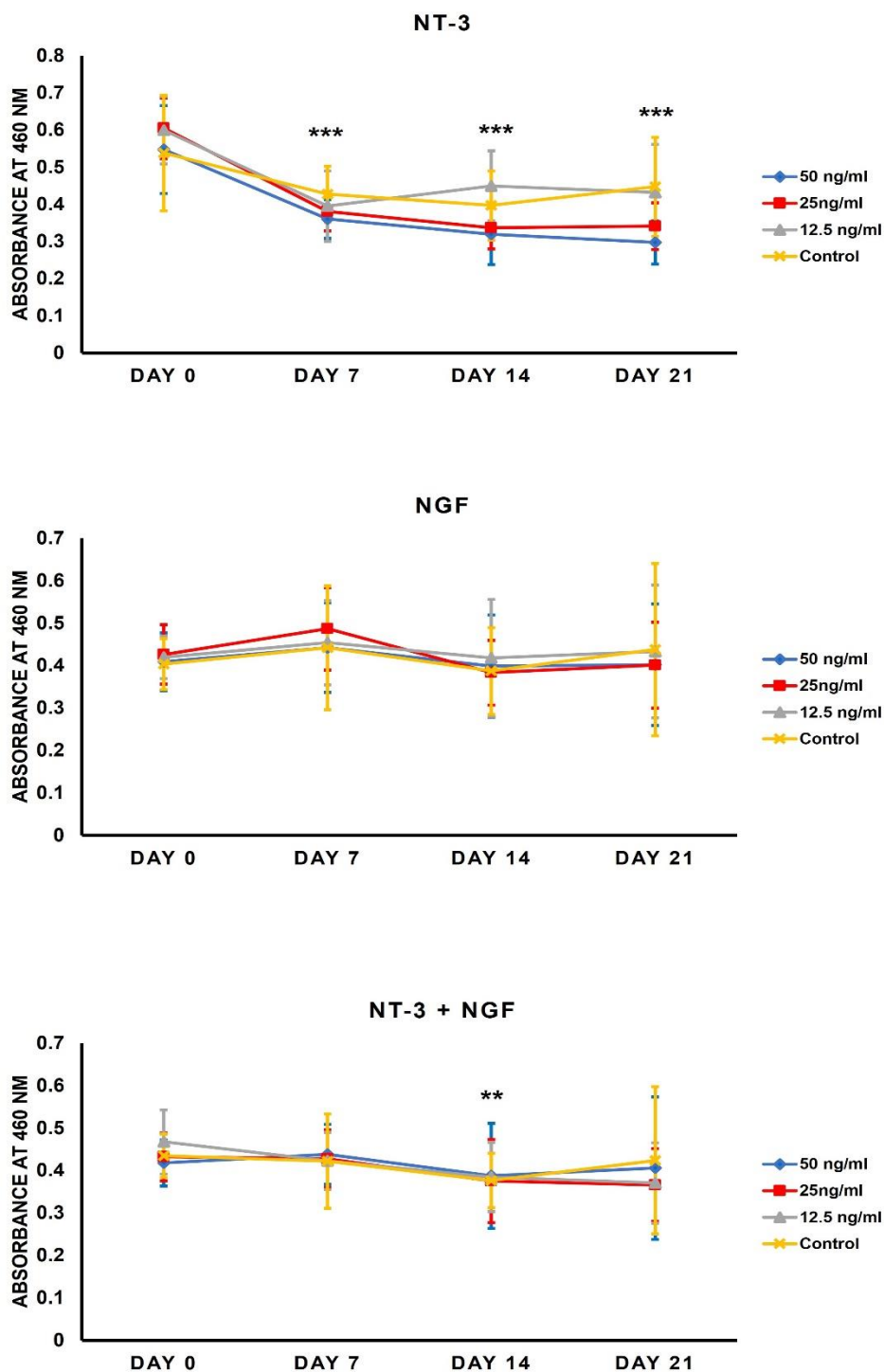
Figure 4. 13. The effect of neurotrophin treatment on the viability of healthy bone marrow stroma cells
The graph above shows the collective data from absorbance readings in the presence of the WST-8 reagent, across the healthy bone marrow stroma cells that were treated with different concentrations of NGF and NT-3. The graphs show the mean +/- SD where n=4 for each condition.

According to the data presented in the top graph of the Fig 4.14 NT-3 seems to have a significant negative impact on the cellular viability of diseased bone stroma cells, when compared with the untreated control (no neurotrophin). The cells present reduced viability after 7 days across all NT-3 concentrations. Reduced cellular viability compared with the untreated control is recorded across all 21 days of the experiment for the 25 ng/ml and 50 ng/ml of NT-3 treatment.

NGF treatment appears to have similar effects with NT-3 on the cellular viability of diseased bone stroma cells. On day 7, the treatment had a substantial detrimental effect on the cell samples across all NGF doses.

The combined treatment of NGF and NT-3 on the diseased bone stroma cells was also seen to have a negative impact on cell viability according to the data summarised in the bottom graph of the Fig. 4.14. This could be due to the initiation of cell apoptosis.
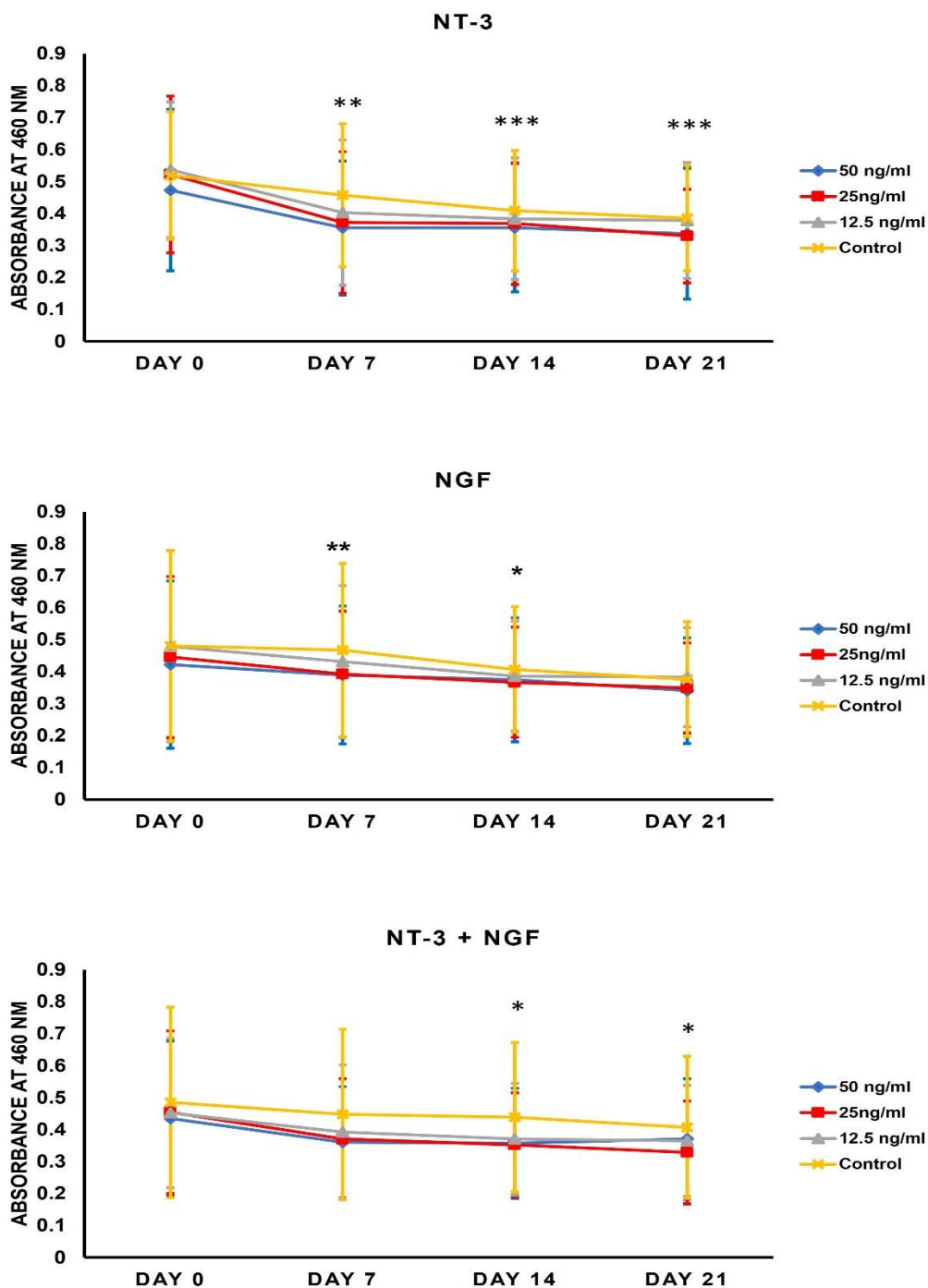
Figure 4. 14. The effect of neurotrophin treatment on the viability of diseased bone stroma cells
The graph above shows the collective data from absorbance readings in the presence of the WST-8 reagent, across the diseased bone marrow stroma cells that were treated with different concentrations of NGF and NT-3. The graphs show the mean +/- SD where n=4 for each condition.

Cells isolated form the articular cartilage of osteoarthritic patients (OA-CPCs) were treated with NGF and NT-3 to observe possible effects on proliferation (Fig. 4.15.

In comparison with the control, OA-CPCs stopped proliferating when treated with NT-3, across all concentrations. Statistical analysis of the data also indicates a significant (* p-value <= 0.05) effect of the treatment on the assessed cell isolates.

The viability of the control also recorded a decrease from day 14 to day 21. The decreased signal of cellular viability seen on untreated samples at day 21 can be attributed to cell senescence, which occurs when cells are cultured for an extended period of time.

When treated with NGF, OA-CPCs proliferation is negatively impacted due to the effect of the neurotrophin (Day 7 in the middle graph of the Fig. 4.15). All doses of NGF treatment induced cell arrest after 7 days, when compared with the untreated cells.

The combined treatment of NGF and NT-3 appears to induce no proliferation across the OA-CPCs cells isolated from the patients. The decrease in cellular viability of the control at day 7 might be attributed to the different recovery time across the cell isolates.
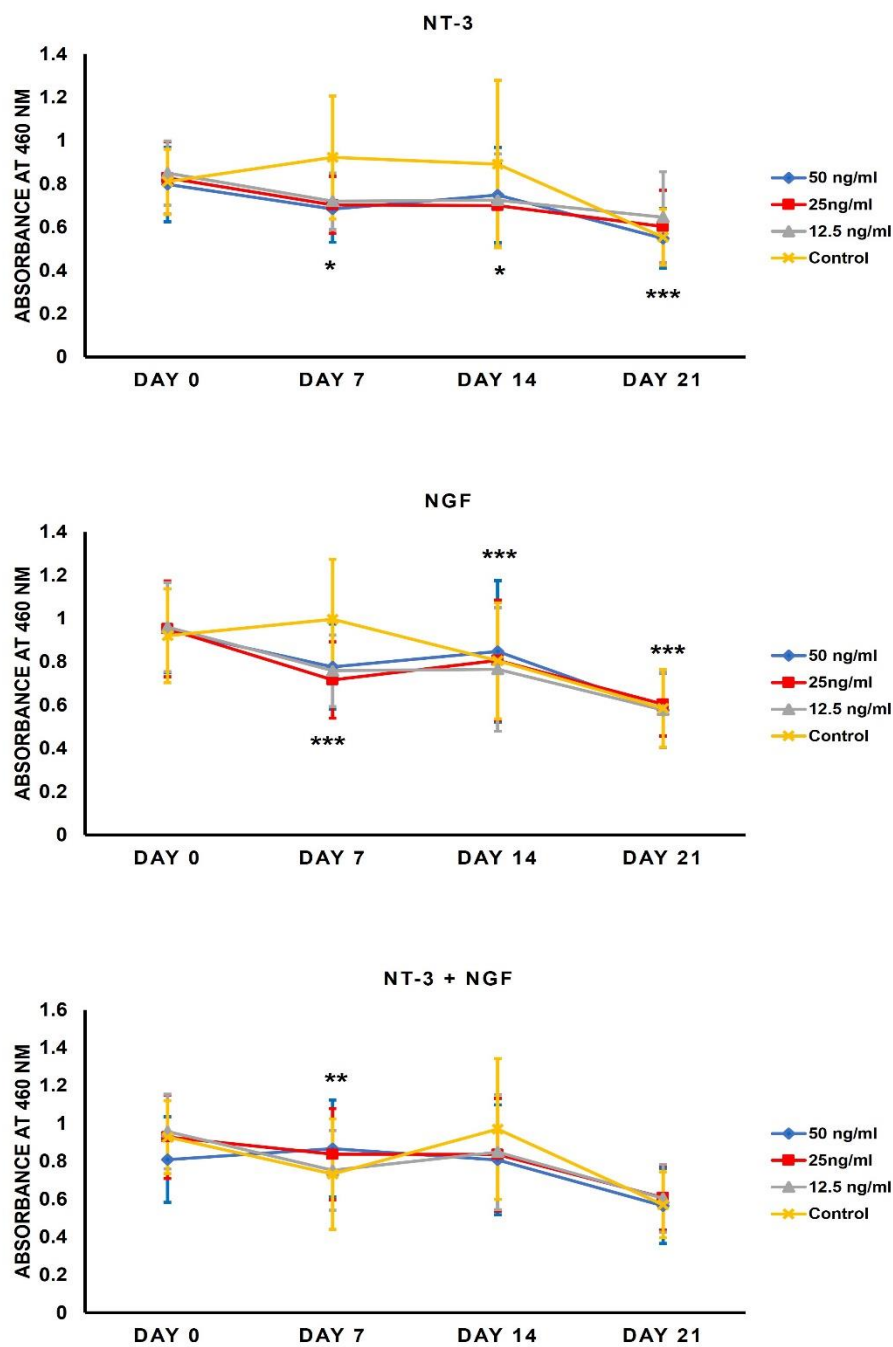
Figure 4. 15. The effect of neurotrophin treatment on the viability of diseased cartilage progenitor cells
The graph above shows the collective data from absorbance readings in the presence of the WST-8 reagent, across the diseased cartilage progenitor cells that were treated with different concentrations of NGF and NT-3. The graphs show the mean +/- SD where n=4 for each condition.

Interpretation of the analysed data summarised above poses limitations for an in-depth analysis The use of mean values for the detected absorbance as a measurement of cell viability of the samples summarised in Table 4.1 poses the caveat of masking the effect of neurotrophin treatment on cell viability due to the variability of each unique sample response. Cells used in this experiment were primary cells isolated from individual patients and may respond uniquely to the neurotrophin treatment.

Therefore, we proceeded to separate the cell viability absorbance data for each unique sample and re-analysed the quantification of cell viability. This is presented in the graphs shown below.

In cells isolated from healthy individuals, the response to neurotrophin treatment appears to be sample specific.

For BMA1 cells (top graphs in Fig. 4.16), day 14 appears to be the time point were positive effects of the neurotrophins treatment are observed. NT-3 treatment at 12.5 ng/ml induced a 3 - 5 % increase in cell proliferation after 14 days of treatment, while the 25 and 50 ng/ml concentrations appear to negatively affect cell viability. The negative effects are maintained in day 21 as well. The different concentrations of NGF had a similar effect; 12.5 ng/ml of NGF treatment recorded an increase in cellular viability comparative with the control at day 14 only. When treated with both neurotrophins combined, BMA1 cells showed above 5% increase in proliferation at 50 ng/ml treatment and under 5% increase at 25 ng/ml. However, follow-up statistical analysis indicated that the above-mentioned findings were not statistically significant for the positive impact of the neurotrophins on cellular proliferation. However, the application of NT-3 (>= 25 ng/ml) on the healthy bone marrow stroma cells has had a significant negative effect on cell viability.

In the BMA2 cells, increased proliferation was recorded only in the presence of NGF. As shown in Fig. 4.16, 7 days after NGF treatment, an increase in cell viability was observed in all concentrations. Significant 5% and 10% increase in cell viability was recorded after 7 days of 25 ng/ml NT-3 treatment and 50 ng/ml of NT-3+NGF treatment. According to the summarised data in Fig. 4.16, NT-3 exerts an inhibitory effect on the viability of isolated healthy bone marrow stroma cells.
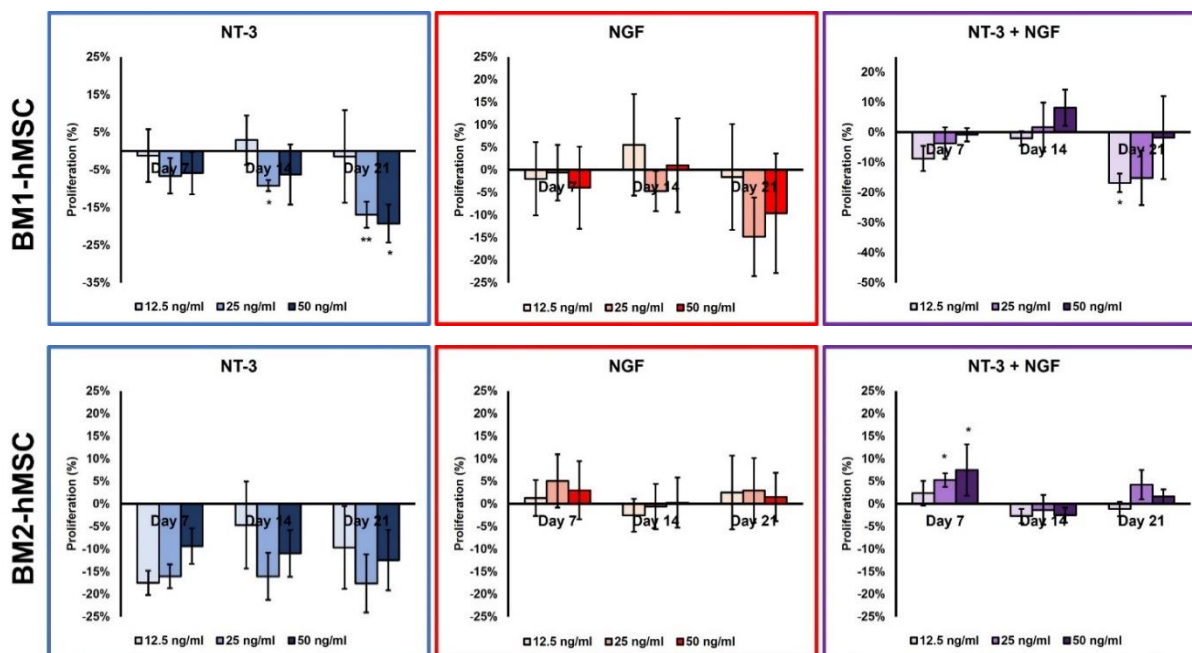
Figure 4. 16. The effect of neurotrophin treatment on healthy bone marrow stroma cells
The graphs show the mean percentage +/- SD, of stimulation (+) and inhibition (-) of proliferation in 2 primary bone marrow stroma cells populations isolated from 2 different healthy tissue sources. The data has been analysed and presented relative to the control (0 days-no treatment) for a clearer data representation. Statistical analysis of the presented data was done in Minitab Software, where significant data is marked by * (significant, p-value<=0.05), ** (very significant, p-value<=0.01), *** (highly significant, p-value<=0.001).

Looking at the data summarised in the graphs of Fig. 4.17, we can conclude that NT-3 could have a stimulating effect on the cell viability of isolates from osteoarthritis patient no.1. The effect is maintained for the whole duration of the treatment in the bone isolated cells. A similar observation was noted in the cartilage isolated cells; the increased proliferation was recorded starting at day 14. NGF (red graphs in Fig. 4.17) treatment not only had no positive effect on proliferation, but also appeared to significantly (*) inhibit the viability of the cells in both, the bone and cartilage originated cellular populations. A stimulation of cell viability was observed in the combined treatment of NGF and NT-3 but only at day 7 time point, primarily in the CPC population. According to the statistical analysis the positive effects mentioned above appear to be non-significant.

Figure 4. 17. The effects of NGF and NT-3 treatment on the viability of bone and cartilage stroma cells from osteoarthritic patient no.1
*The graphs show the mean precentage +/- SD, of stimulation (+) and inhibitioan (-) of cellular viability in the bone and cartilage originated cells from the diseased hip joint of the patient no.1. The data has been analysed relative to the control (0 days-no treatment) for a clearer data representation. Statistical analysis of the presented data was done in Minitab Software, where significant data is marked by * (significant, p-value<=0.05), ** (very significant, p-value<=0.01), *** (highly significant, p-value<=0.001).*

The cells isolated from the bone component of the diseased hip joint donated by patient no.2 appear to be stimulated to proliferate only by the highest concentration of NT-3 treatment (50 ng/ml) that was applied (top graphs in Fig. 4.18); however, when the data was statistically analysed, the recorded effect was found to be non-significant. In fact, both, NT-3 and NGF appear to induce significant inhibition of the cell viability in the patient no.2 bone stroma cells. The inhibitory effect of the NT-3 (day 7) is observed in the CPC population of the same patient (bottom blue graph in Fig. 4.18). A possible cell recovery is observed in day 21 of the treatment. The treatment with NGF (all concentrations in day 7 of the bottom red graph in Fig. 4.18) also appears to have a significant detrimental effect on the cell viability of cartilage originated progenitors; as in the NT-3 treatment, a cell recovery is observed at day 14. In contrast with the individual effects of NGF and NT-3 on the viability of OA-CPCs 2, when the two neurotrophins are combined they appear to stimulate the viability of the cells; however, the results were not statistically significant.

Figure 4. 18. The effects of NGF and NT-3 treatment on the viability of bone and cartilage stroma cells from osteoarthritic patient no. 2

The graphs show the mean precentage +/- SD, of cellular viability stimulation (+) and inhibitioan (-) in the bone and cartilage originated cells of the diseased hip joint of the patient no.2. The data has been analysed against the control (0) for a better representation. Statistical analysis of the presented data was done in Minitab Software, where significant data is marked by the * (significant, p-value<=0.05, ** (very significant, p-value<=0.01), *** (highly significant, p-value<=0.001).

The cells isolated from the bone and the cartilage component of the diseased hip joint donated by the patient no.3 appear to be negatively impacted by both the NGF and NT-3 treatments (data summarised in Fig. 4.19). Significant inhibition of the OA3-hCPCs viability was recorded in NT-3 treatment, NGF treatment, as well as NT-3 + NGF treatments. With all of these, very significant (**) stimulation of OA3-hMSCBSCs proliferation was observed after 21 days of treatment with 50 ng/ml NGF + NT-3 (top purple graph in Fig. 4.19). The viability of the OA3-hMSCs does not appear to be as significantly impacted by the individual treatments with NT-3 and NGF, when compared with OA3-hCPCs.
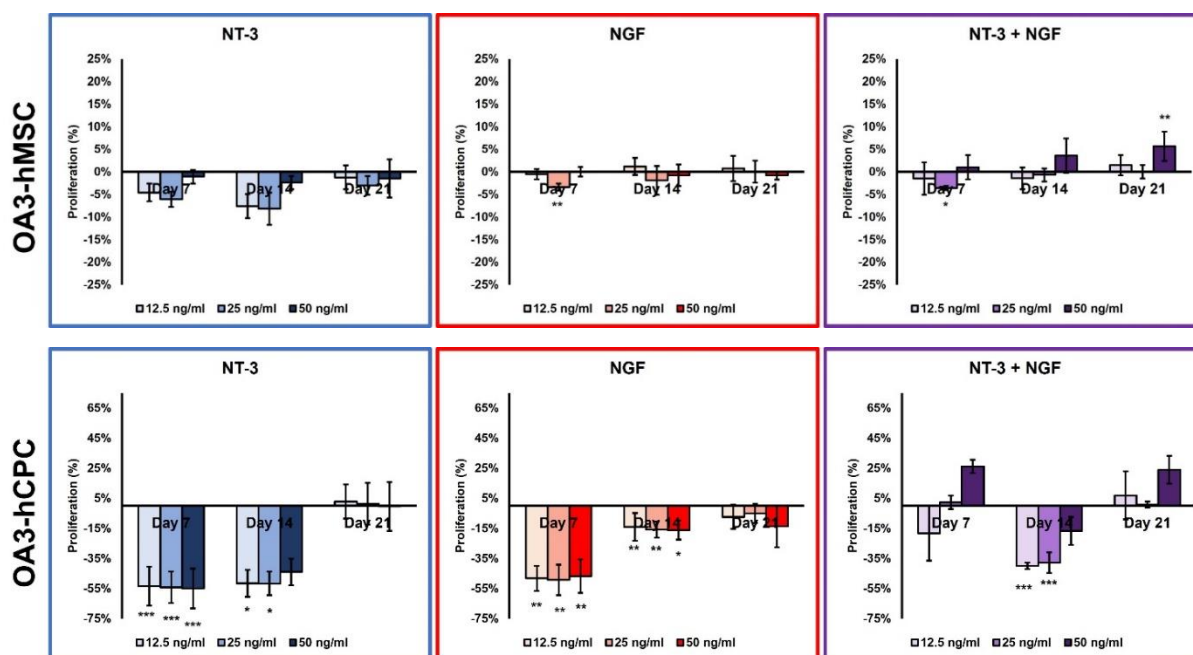
Figure 4. 19. The effects of NGF and NT-3 treatment on the viability of bone and cartilage stroma cells from osteoarthritic patient no. 3
The graphs show the mean precentage +/- SD, of cellular viability stimulation (+) and inhibitioan (-) in the bone and cartilage originated cells of the diseased hip joint of the patient no.3. The data has been analysed against the control (0) for a better representation. Statistical analysis of the presented data was done in Minitab Software, where significant data is marked by the * (significant, p-value<=0.05, ** (very significant, p-value<=0.01), *** (highly significant, p-value<=0.001).

Data collected from the investigation of cell viability of the diseased bone (OA4-hMSC) and cartilage (OA4-hCPCs) cells isolated from joint tissue donated by the patient no. 4 indicate that viability of the OA4-hMSC cells is inhibited by NT-3 treatment and possibly stimulated by the NGF treatment. When the OA4-MSCs are treated with both neurotrophins, the inhibitory effect of NT-3 on cell viability is maintained and not improved due to the presence of NGF. On the other hand, while OA4-hCPCs viability is significantly negatively impacted by individual treatments with NT-3 and NGF, the combination treatment of these two appears to have a significant stimulatory effect towards proliferation (bottom purple graph in Fig. 4.20).
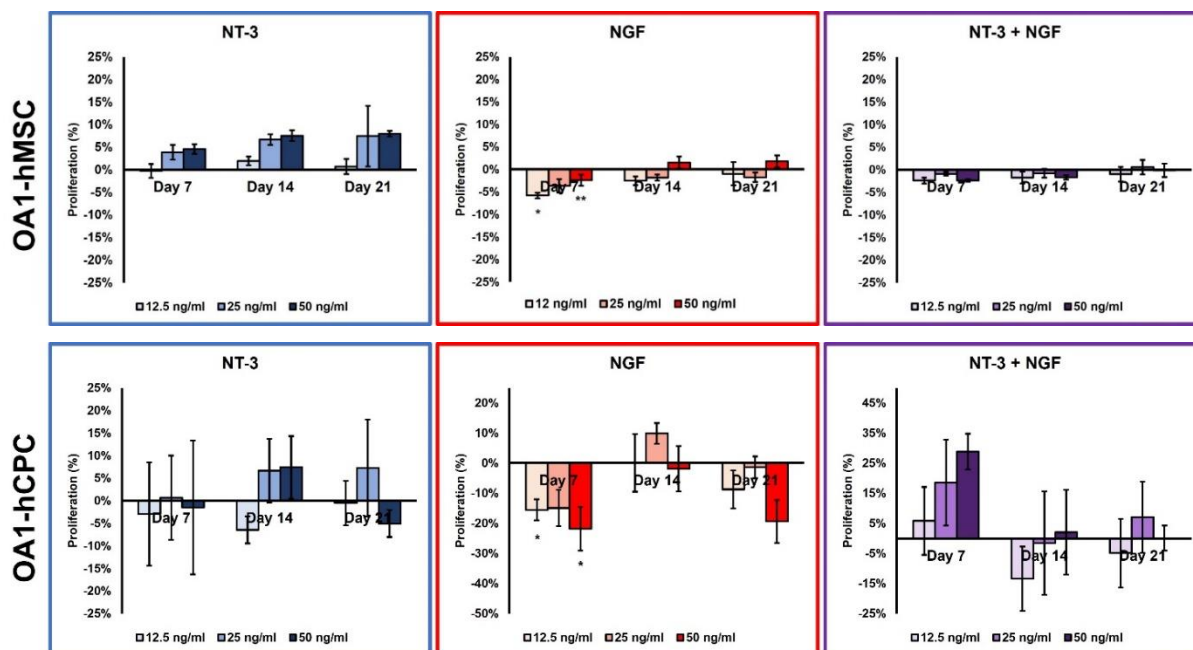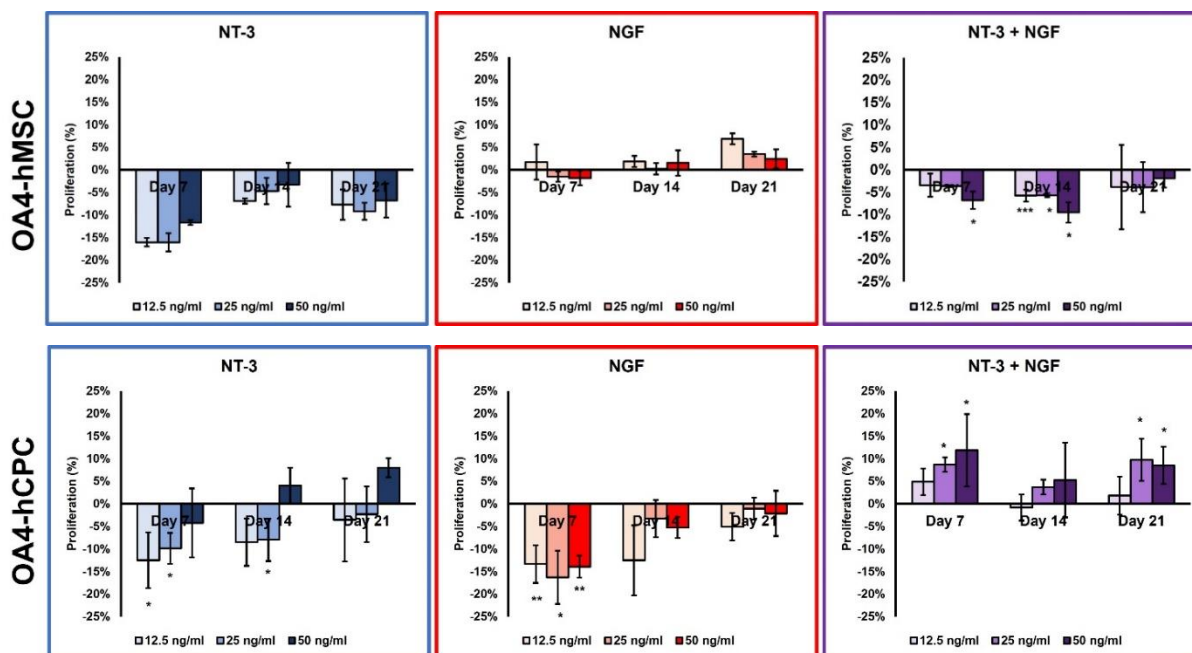
Figure 4. 20. The effects of NGF and NT-3 treatment on the viability of bone and cartilage stroma cells from osteoarthritic patient no. 4

The graphs show the mean precentage +/- SD, of cellular viability stimulation (+) and inhibitioan (-) in the bone and cartilage originated cells of the diseased hip joint of the patient no.4. The data has been analysed against the control (0) for a better representation. Statistical analysis of the presented data was done in Minitab Software, where significant data is marked by the * (significant, p-value<=0.05, ** (very significant, p-value<=0.01), *** (highly significant, p-value<=0.001).

Finally, the data summarised in the blue graphs of Fig. 4.21 indicate that NT-3 inhibits the cell viability of bone and cartilage osteoarthritic hip derived cells from patient 5, following 7 days of treatment. The negative effect on cell viability is maintained in day 14, but the effect appears to be non-significant. A recovery of OA5-hCPCs is observed after 14 days of NT-3 treatment with increased cell numbers relative to the control at day 21. The NGF treatments appear to be detrimental to the cell viability of both, bone and cartilage derived cells after 7 days of treatment, with significant negative impact on cell viability in the OA5-hCPC population. In OA5-hMSCs treated with NGF, a recovery is observed between day 7 and day 14, with increased proliferation relative to the control being recorded at day 14 (two concentrations) and day 21 (all concentrations). When the combine effect of NT-3 and NGF was assessed on the viability of bone and cartilage cells derived from the diseased femoral head of the patient no.5, only the high concentration treatment (50 ng/ml) appears to stimulate cell proliferation; at day 21 in BSCs5 and across all time

points in OA5-hCPCs. The effects have been found non-significant when the data was statistically analysed.
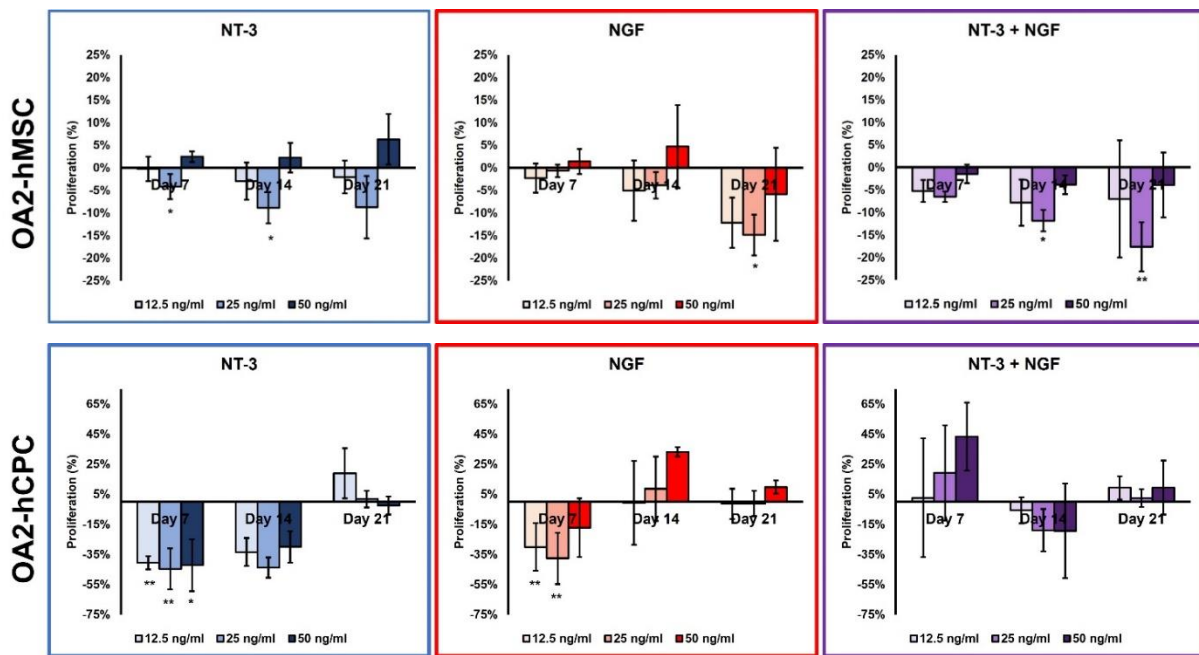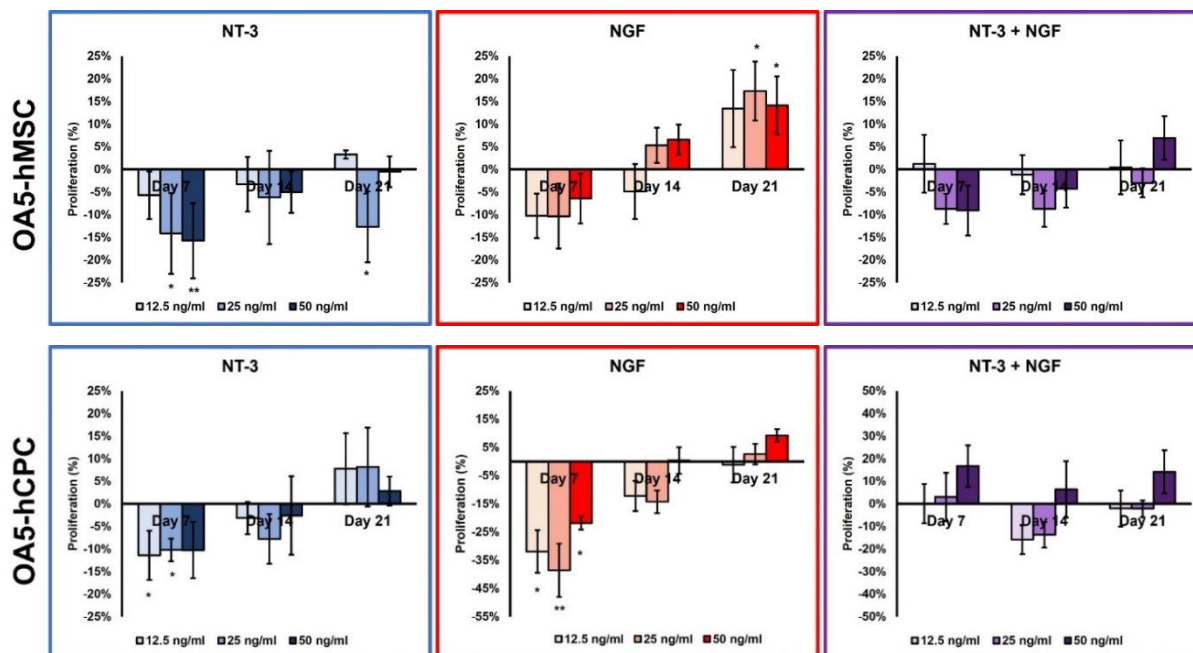

Figure 4. 21. The effects of NGF and NT-3 treatment on the viability of bone and cartilage stroma cells from osteoarthritic patient no. 5
The graphs show the mean precentage +/- SD, of cellular viability stimulation (+) and inhibitioan (-) in the bone and cartilage originated cells of the diseased hip joint of the patient no.5. The data has been analysed against the control (0) for a better representation. Statistical analysis of the presented data was done in Minitab Software, where significant data is marked by the * (significant, p-value<=0.05, ** (very significant, p-value<=0.01), *** (highly significant, p-value<=0.001).

In summary, NT-3 appears to exert an inhibitory effect on the proliferation of diseased hMSCs and hCPCs. Only hMSCs isolated from OA patient no.1 showed increased proliferation, following NT-3 treatment but with no statistical significance. For cells isolated from this particular patient, the positive effect of NT-3 was maintained across the experiment.

Considering the effect of NGF treatment on the viability of hip joint derived cells, the only significant increase in proliferation was observed in the OA5-hMSCs, following 21 days of treatment. Initially, NGF treatment induced a decrease in cellular viability of the diseased cells after 7 days, with an overall significant negative effect.

Analysing the effects of combined treatment (NT-3 + NGF), cellular proliferation has been recorded in the majority of OA patient derived CPCs. The cells isolated from the

articular cartilage of patient no. 4 showed the most positive effect in cellular viability after the treatment with NT-3 + NGF. The effect was maintained across 21 days of observations. In other isolates (OA1, OA2, OA3 and OA5) from OA articular cartilage, the proliferative effect of NT-3 + NGF treatment was recorder starting with day 7, mainly in 50 ng/ml concentration, but the results were mixed after this time point. Looking at the effects of combined treatment on diseased hMSCs, the overall cellular viability of this cellular population is inhibited.

In the healthy bone marrow derived hMSC, the combined treatment induced cellular proliferation only on BM2-hMSCs. This effect was recorded only at day 7. The rest of time points showed no significant increase in cellular viability.

4.3.7. Gene expression of proliferative and apoptotic markers following neurotrophin treatment of normal and joint derived stem/progenitor cells.

To establish a better understanding of the effects of NT-3 on the proliferation of bone and cartilage derived stem/progenitor cells, a gene expression analysis was carried out using RNA collected following neurotrophin treatment for 21 days, The expression of apoptotic regulators, *BCL2* and *CAS3,* and the proliferative marker *PCNA* was investigated.

The expression result was normalised against the housekeeping gene *GAPDH* and was expressed as a fold change of the control (0 ng/ml of NT-3).

PCNA was not detected across all samples (BM1-hMSCs, BM2-hMSCs, OA1-hMSCs, OA2-hMSCs, OA3-hMSCs, OA4-hMSCs, OA5-hMSCs, OA1-hCPCs, OA2-hCPCs, OA3-hCPCs, OA4-hCPCs and OA5-hCPCs) treated with 25 ng/ml. *PCNA* was also not detected in the 0 ng/ml NT-3, indicating in not detectable cell proliferation, possibly due to cell senescence in prolonged culture. This is not uncommon for primary cells and in this case the cells were collected for RNA harvesting and gene expression analysis after the day 21 timepoint of the cell viability experiment.

Increased levels of *BCL2* were detected mainly in the hMSCs treated with 25 ng/ml and in comparison, with the control (0 ng/ml NT-3). The highest fold change increase of *BCL* expression (Fig. 4.22), was detected in the OA2-hMSC sample, followed by the OA5-hMSC. Th lowest *BCL2* fold change was detected in the OA3-hMSC and OA4-hMSC samples.

CAS3 expression was not detected on hMSCs treated with NT-3, healthy or diseased. *CAS3* was detected only in the hCPCs cell isolates treated with NT-3 (Fig. 4.23). The highest *CAS3* expression was detected in the OA3-hCPCs treated with 25 ng/ml NT-3 relative to the control (0 ng/ml NT-3).
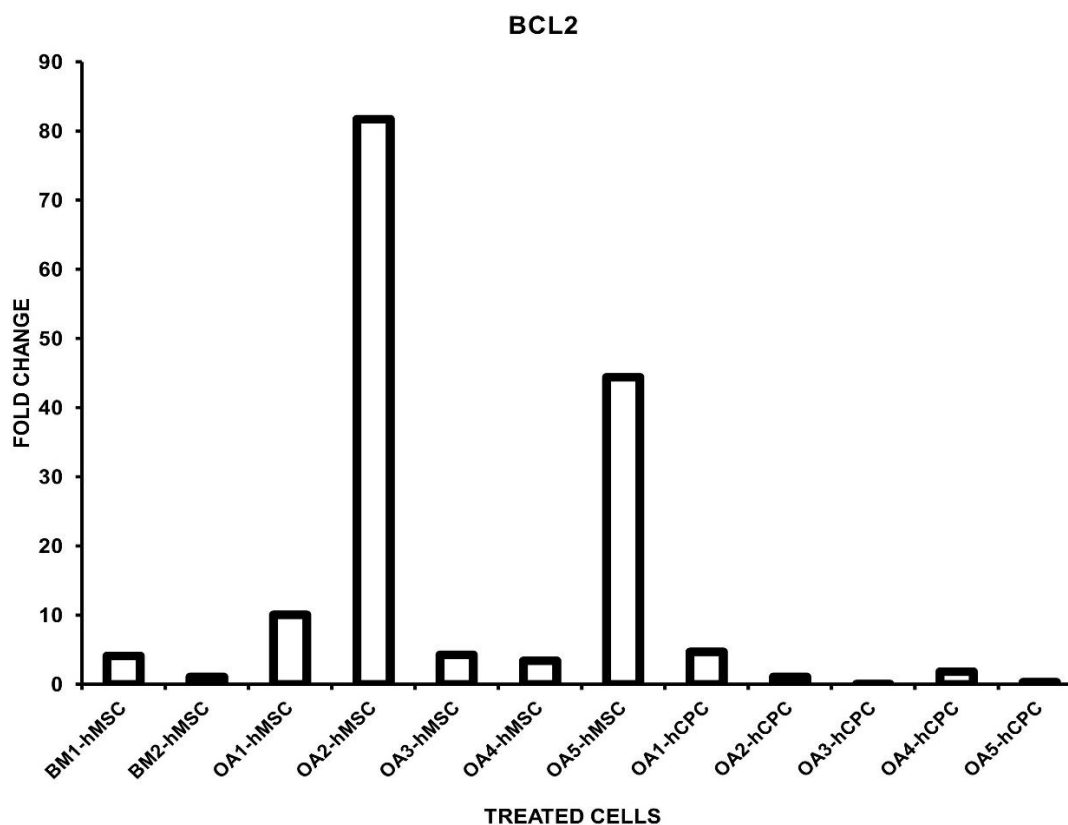
BCL2

Figure 4. 22. Real-Time PCR analysis of BCL2 expression in bone marrow and joint tissue derived stem/progenitor cells following treated with 25 ng/ml NT-3.
Primary hMSCs and hCPCs isolated from healthy and diseased tissue were treated for 21 days with 25 ng/ml NT-3. The expression of BCL2 was determined using real-Time PCR. The results are displayed as fold change in relative expression against the BCL2 expression level detected in non-treated cells (n=3).
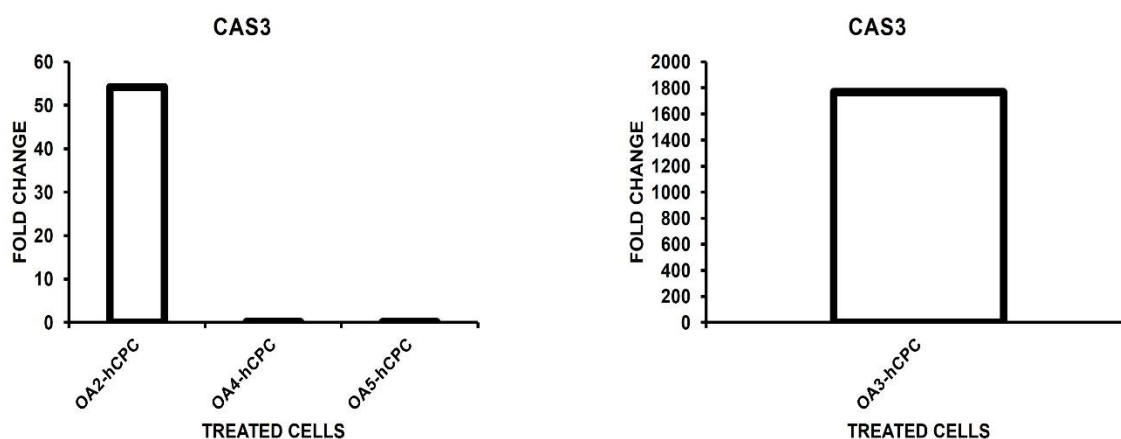
CAS3

CAS3

Figure 4. 23. qPCR analysis of CAS3 in samples treated with 25 ng/ml NT-3
Primary hCPCs isolated from the articular cartilage of osteoarthritic hip joint were treated for 21 days with 25 ng/ml NT-3. The expression of CAS3 was determined using qPCR. The results are displayed as fold change in relative expression against the CAS3 levels detected in non-treated samples (n=3).

4.3.8. The effect of NGF and NT-3 on the osteo-differentiation of hMSCs

In order to look into the possible effect of neurotrophins on the initiation of bone differentiation, 5×10^3 of bone derived stoma cells isolated from 6 different sources (1 healthy bone marrow and 4 diseased bone tissue from the hip joint) were seeded per well in 24-well plates. The cells were allowed to acclimatise and fully attach for a total of 7 days pre-treatment, due to their different attachment times. After the acclimatisation period, media was replaced with osteogenic media to induce osteo-differentiation. The media was supplemented with different concentrations of neurotrophins (NT-3 individual, NGF individual and NT-3+NGF) and refreshed every 3 days. Cells were allowed to differentiate for a total of 21 days, fixed, stained with Alizarin Red and the differences in osteo-differentiation were semi-quantified through Alizarin Red Quantification assay. Absorbance readings at 405 nm were carried out on 3 technical replicates per condition.
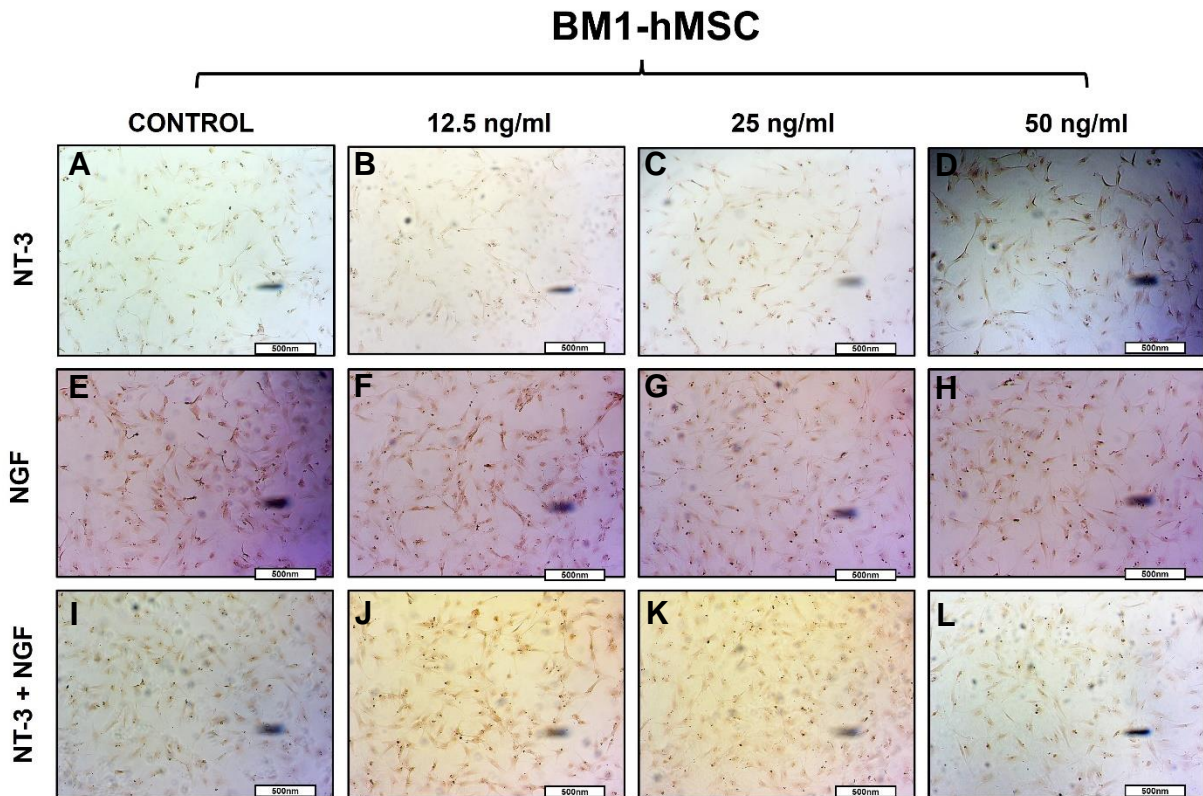
BM1-hMSC

Figure 4. 24. Osteo-differentiation of BM1-hMSCs following neurotrophin treatment

The effects of NGF and NT-3 on osteo-differentiation of stroma cells isolated from human healthy bone marrow (donor no.1) were tested by supplementation of osteogenic media with serial dilutions of NGF and NT-3 (0, 12.5, 25 and 50 ng/ml). The cells were cultured for 21 days in osteogenic media supplemented with human NT-3 (B;C;D), NGF (F;G;H) and NT-3 + NGF (J;K;L) recombinant neurotrophins; Negative controls (osteogenic media - no neurotrophin) were carried out in parallel (A;E;I). The osteo-differentiation was assessed through Alizarin Red S staining; 500nm scalebar.
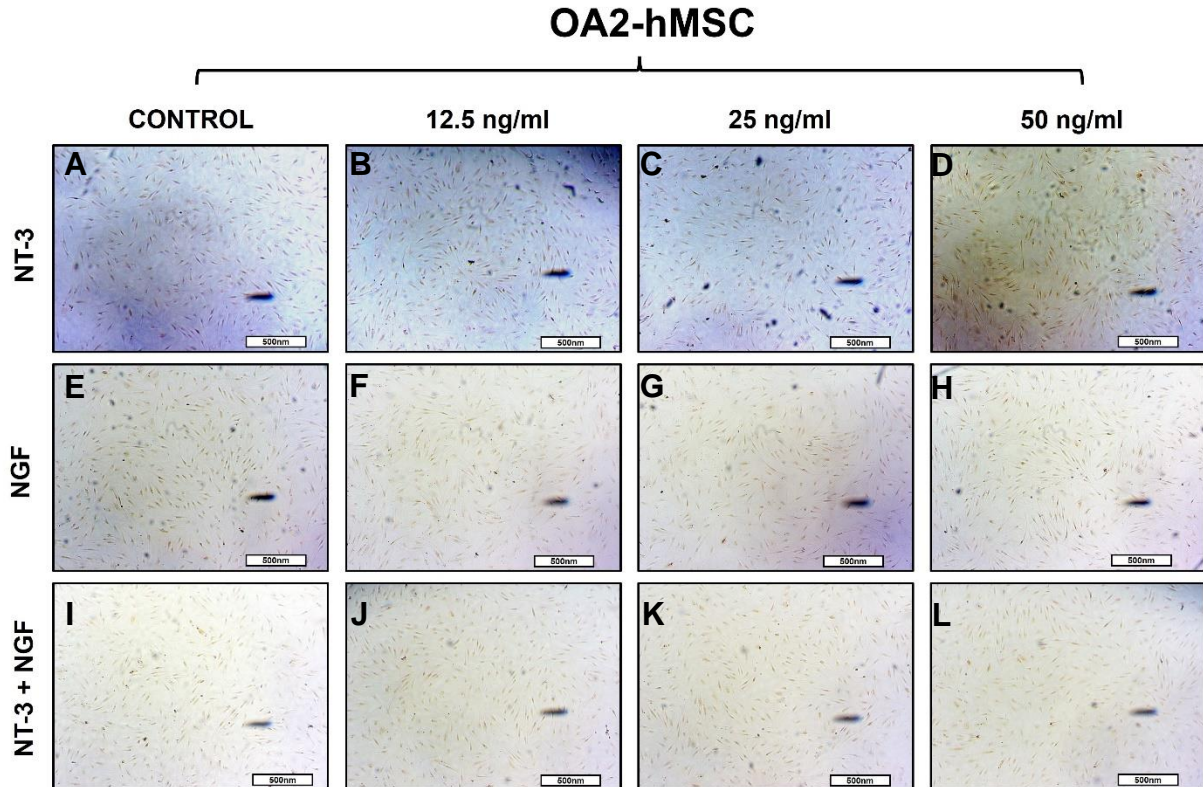
Figure 4. 25. Osteo-differentiation of OA2-hMSCs under Neurotrophin treatment
The effects of NGF and NT-3 on osteo-differentiation of stroma cells isolated from human osteoarthritic bone (patient no.2) were tested by supplementation of osteogenic media with serial dilutions of NGF and NT-3 (0, 12.5, 25 and 50 ng/ml). The cells were cultured for 21 days in osteogenic media supplemented with human NT-3 (B;C;D), NGF (F;G;H) and NT-3 + NGF (J;K;L) recombinant neurotrophins; Negative controls (osteogenic media - no neurotrophin) were carried out in parallel (A;E;I). The osteo-differentiation was assessed through Alizarin Red S staining; 500nm scalebar.
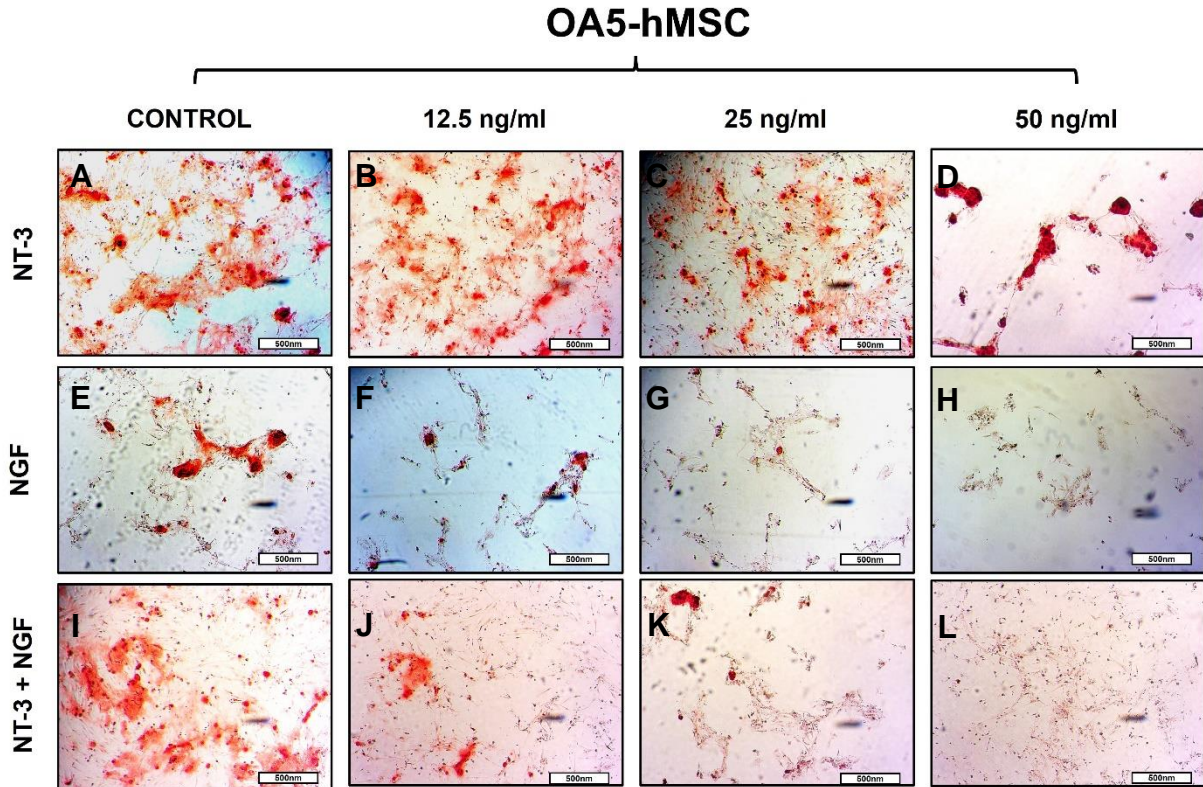
OA5-hMSC

Figure 4. 26. Osteo-differentiation of OA5-hMSCs under Neurotrophin treatment
The effects of NGF and NT-3 on osteo-differentiation of stroma cells isolated from human osteoarthritic bone (donor no.5) were tested by supplementation of osteogenic media with serial dilutions of NGF and NT-3 (0, 12.5, 25 and 50 ng/ml). The cells were cultured for 21 days in osteogenic media supplemented with human NT-3 (B;C;D), NGF (F;G;H) and NT-3 + NGF (J;K;L) recombinant neurotrophins; Negative controls (osteogenic media - no neurotrophin) were carried out in parallel (A;E;I). The osteo-differentiation was assessed through Alizarin Red S staining; 500nm scalebar.
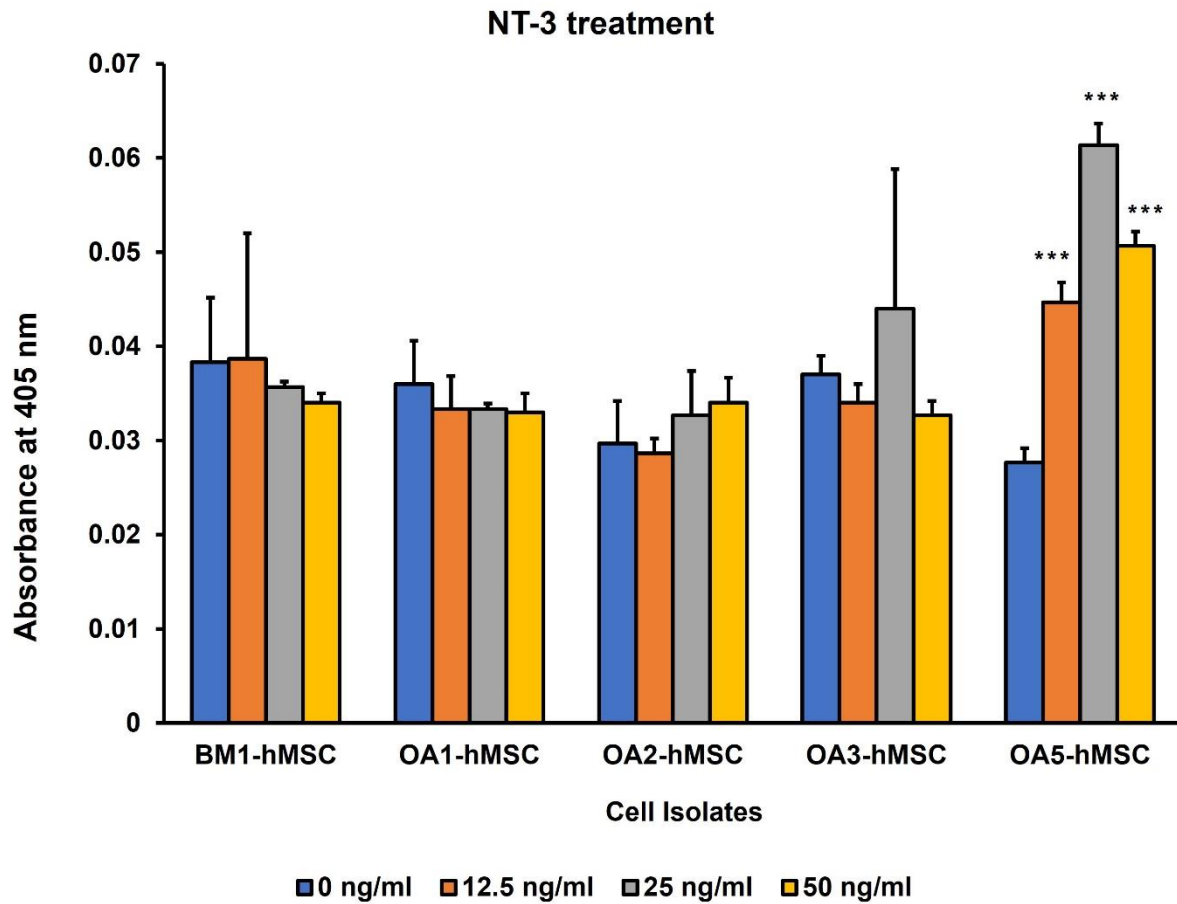
Figure 4. 27. The effects of NT-3 treatment on the osteo-differentiation of hMSCs
This figure shows the semi-quantification of calcium deposits stained with Alizarin Red S staining. hMSCs from were treated with osteogenic media supplemented with NT-3 for a total of 21 days. The graph shows the mean +/- SD, where n=3 for each condition.
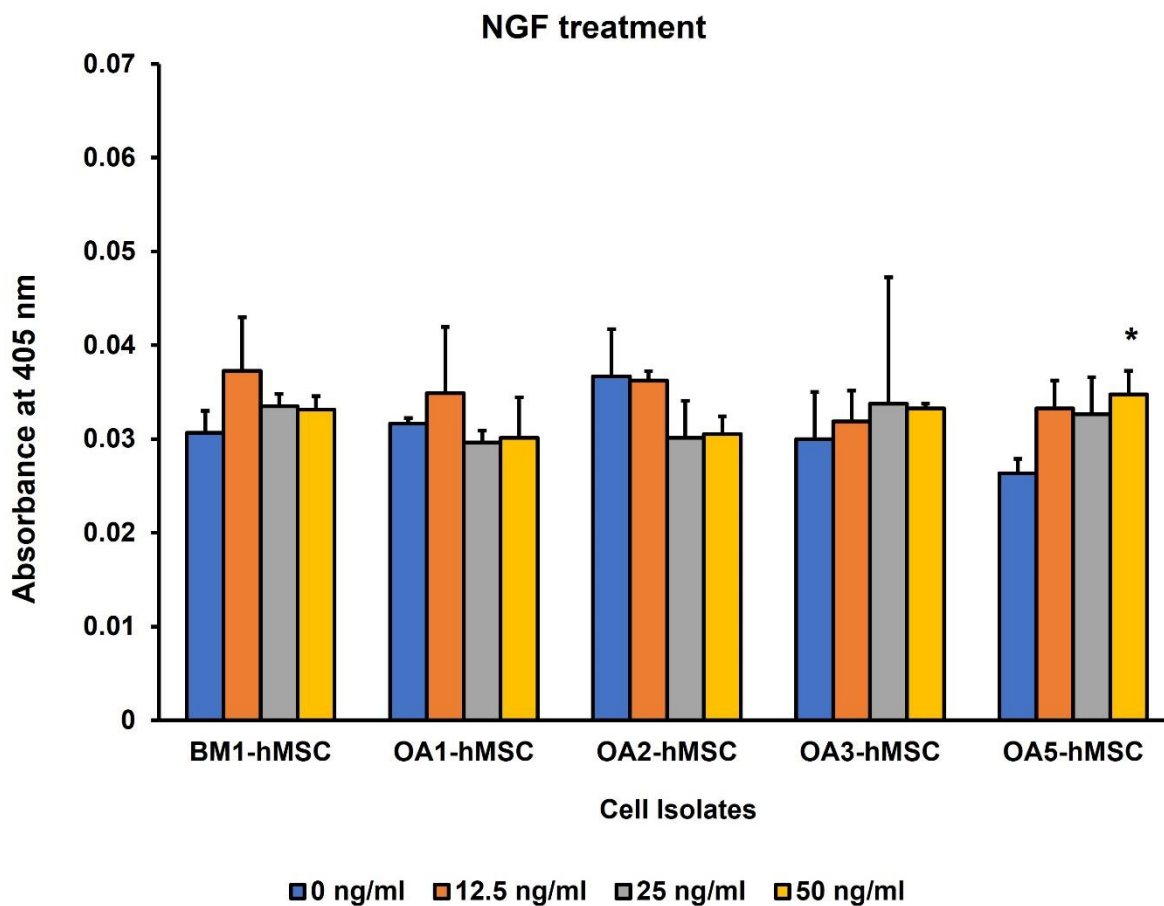
Figure 4. 28. The effects of NGF treatment on the osteo-differentiation of hMSCs
This figure represents the semi-quantification of Calcium deposits stained by Alizarin Red S staining. hMSCs from 4 different patients and from a healthy donor were treated with osteogenic media supplemented with human NGF recombinant protein for 21 days. The graph shows the mean +/- SD, where n=3 for each condition.
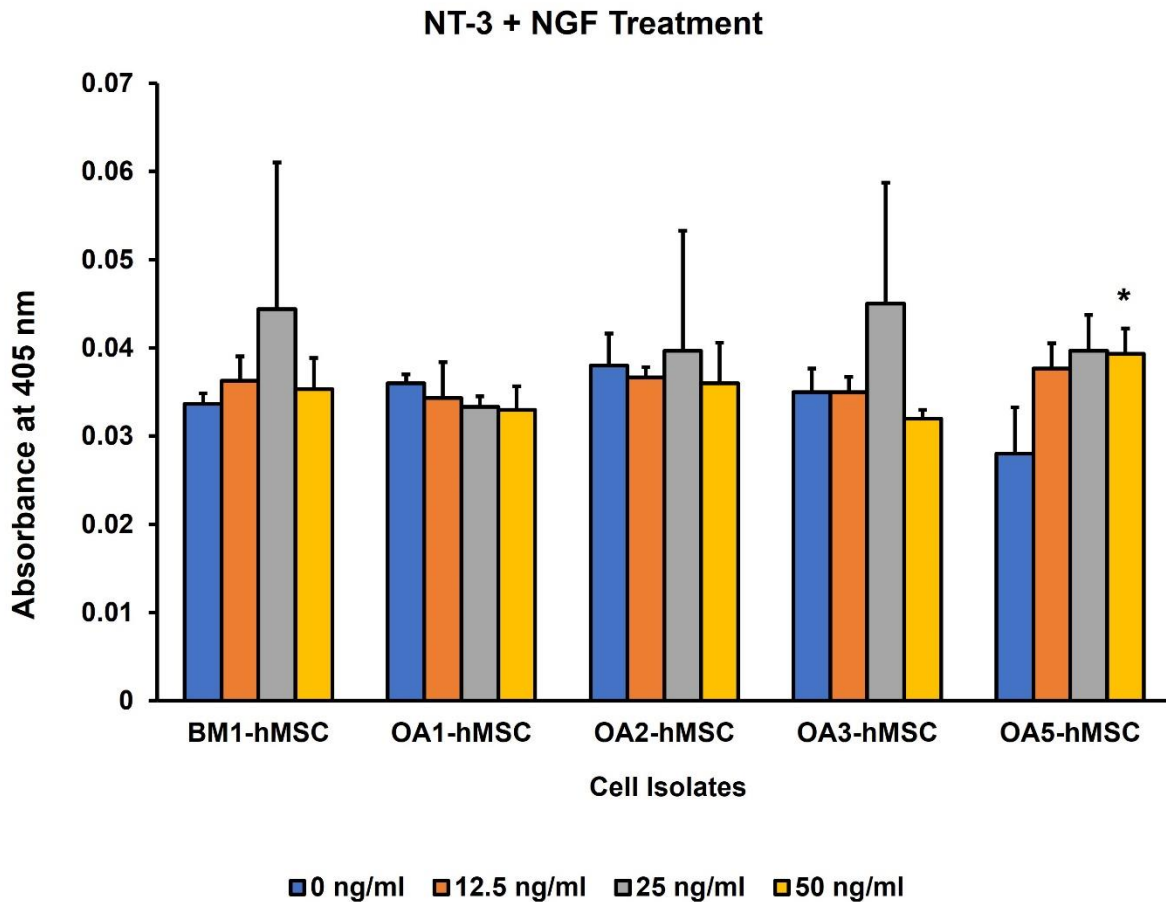
Figure 4. 29. The combined effects of NGF and NT-3 treatment on the osteo differentiation of hMSCs
This figure shows the semi-quantification of Calcium deposits formation in osteo-differentiation under the influence of combined NGF and NT-3 treatment. hMSCs isolated from 4 different patients and one healthy donor were treated for 21 days with osteogenic media supplemented with serial dilutions of NGF + NT-3. The graph shows the mean +/- SD, where n=3 for each condition.

The semi-quantification of osteo-differentiation under different concentrations of neurotrophins showed a response for some of the cell samples tested, but not all.

In terms of stimulation of differentiation in healthy bone stroma cells (BM1), NT-3 shows a decrease when compared with the control (0 ng/ml). However, where the cells were treated with NGF or in combination with NGF, the degree of differentiation presents an increase in comparison with the control.

The treatment seems to have a patient-specific result, since no generalized response, positive or negative, to neurotrophins supplemented osteogenic media was observed.

OA1-hMSCs and OA2-hMSCs showed little to no response to the NGF and NT-3 treatment, while OA3-hMSCs and OA5-hMSCs osteo-differentiation was enhanced by the osteogenic media supplemented with NT-3, or NGF, or NT-3+NGF. The most significant improvement of osteo-differentiation was recorded only in OA5-hMSC treated with NT-3 (across all treatment concentrations), NGF (50 ng/ml) and NT-3 + NGF (50 ng/ml).

4.3.9. The effect of NT-3 and NGF on the chondro-differentiation of hCPCs

The neurotrophin treatment was additionally carried out in chondro-differentiation of osteoarthritic hCPCs. Only the cartilage stroma cells from patient ref no. OA3 were assessed in 3 different replicates at an initial seeding density of 2,000 cells per well in 24-well plates. As in above-described osteogenic differentiation experiment, cells were allowed to acclimatise for 7 days and treatment was applied in chondrogenesis media for a total of 21 days, with the media refreshed every 3 days.

The initial light microscopy observations of the Alcian blue staining of the cells treated with chondrogenic medium supplemented with NGF and NT-3 showed no visible differences in the degree of chondro-differentiation (Fig. 4.30); neither enhancement nor inhibition by comparison with the control (only chondrogenic culture medium, no neurotrophin). In consequence, the semi-quantification of the staining was not carried out. In possible future work, this experiment could be repeated by analysing not only the intensity of chondro-specific staining, but also rely on gene expression analysis based on the investigation of cartilage differentiation markers and the differences in regulation in the samples treated with NGF and NT-3.

OA3-hCPC

| | CONTROL | 12.5 ng/ml | 25 ng/ml | 50 ng/ml |
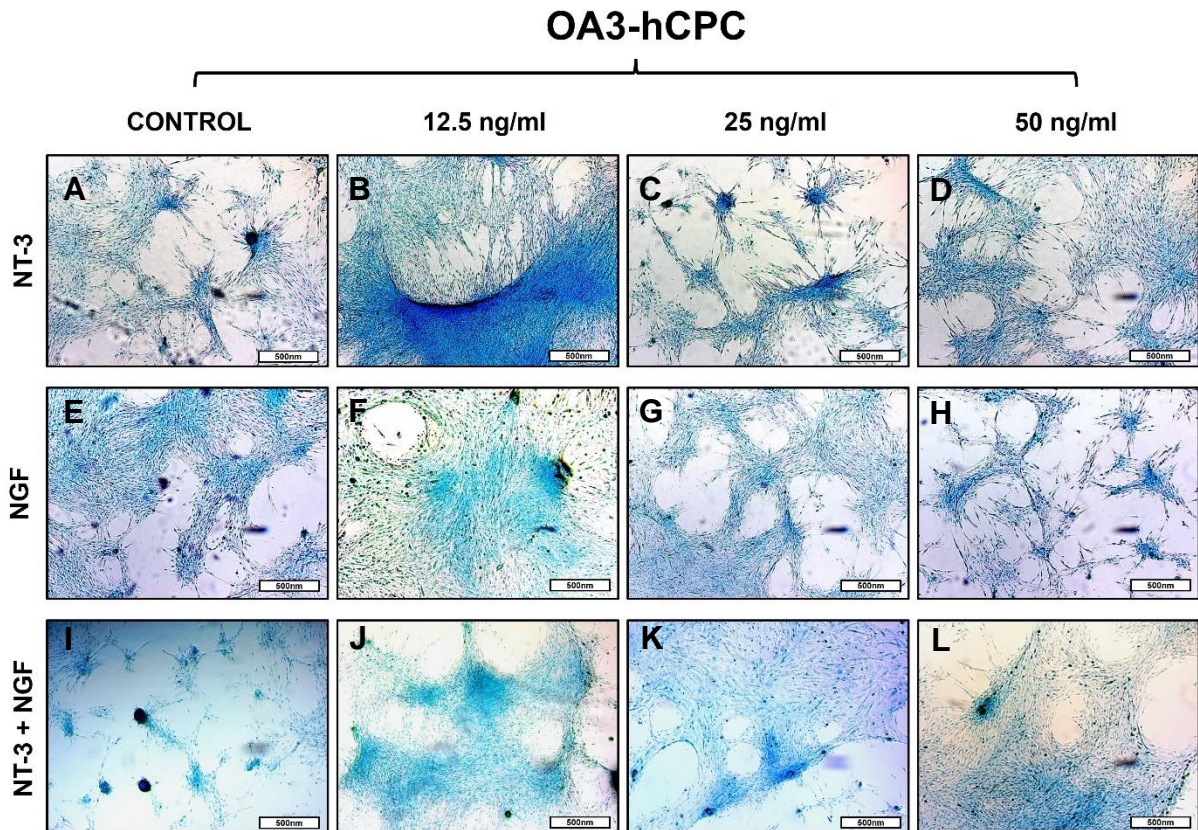
Figure 4. 30. *Chondro-differentiation of OA3-hCPCs under Neurotrophins treatment*
The individual and combined effects of NGF and NT-3 on chondro-differentiation of stroma cells isolated from human osteoarthritic cartilage (donor no.3) were tested by supplementation of chondrogenic media with serial dilutions of NGF and NT-3 (0, 12.5, 25 and 50 ng/ml). The cells were cultured for 21 days in chondrogenic media supplemented with human NT-3 (B;C;D), NGF (F;G;H) and NT-3 + NGF (J;K;L) recombinant neurotrophins; Negative controls (chondrogenic media - no neurotrophin) were carried out in parallel (A;E;I). The chondro-differentiation was assessed through Alcian Blue staining; 500nm scalebar.

4.4. Discussion

As their name implies, neurotrophins are neuron-specific growth factors that play critical roles in the proliferation, differentiation, and survival of the central and peripheral nervous systems. Their role in these processes has been the focus of investigation since the late 1950s', commencing with the study of NGF in neural development. Neurotrophins have been shown to play a critical role in intrauterine development and therefore their presence diminishes in the adult body, their expression is associated with nerve tissue homeostasis, based on their main trophic role in the central and peripheral nervous systems (Huang and Reichardt, 2001). Neurotrophin levels are elevated in post tissue injury and were subsequently validated by their role in tissue repair and rebuilding, most notably in nerve damage (Houlton *et al.*, 2019). Neurotrophins have a wider repertoire of activity than trophic functions. Disturbance in their normal levels, primarily characterised by a decrease, have been associated with neurodegenerative diseases such as Parkinson's disease, Alzheimer's disease, and Huntington's disease, as well as psychiatric disorders such as bipolar disorder, depression, and drug misuse (Mitre, Mariga and Chao, 2017). NGF, the most extensively researched neurotrophin, has also been associated with musculoskeletal chronic pain (Malfait, Miller and Block, 2020). We have set out to investigate the regenerative properties of neurotrophins in human joints affected by degenerative osteoarthritis, as well as their influence on the healthy bone marrow resident MSCs and look for a correlation between their already confirmed function in other adult tissues (e.g., neural tissue) and their potential role in these cells. We have focused our investigation of the neurotrophin NT-3 and the interaction with the associated receptors Trk C and p75-NTR and compared this with the function of the better described neurotrophin NGF.

NGF has been identified as the cause of chronic pain in patients with osteoarthritis. Elevated levels of this neurotrophin induce sensitization of nociceptor from the synovial membrane of the joint and create a continuous signalling, described in clinical investigation as chronic pain (Eitner, Hofmann and Schaible, 2017). NGF is abundantly secreted in joints after damage at the articular cartilage level, suggesting that its synthesis and release is involved in tissue regeneration, and that the chronic pain

induced by high levels of NGF is a side effect of this biological process (Shang, Wang and Tao, 2017).

As noted, before, NGF has become the target of many therapeutic treatments for osteoarthritic chronic pain. Over the past two decades researchers have been able to design more effective and safer pharmacological treatments for the primary symptom of degenerative osteoarthritis, chronic pain. In this current chapter, we focused on the involvement of NGF and NT-3 in the skeletal tissue repair in order to gain a better understanding of neurotrophin signalling in OA pathology, that can benefit therapies that rely less on surgical intervention.

NT-3 is generally known as the proliferative neurotrophic factor in the neural system (Yan *et al.*, 2016). Considering this important characteristic, we proceeded to investigate its proliferative as well as differentiation effect on hip joint derived stem/progenitor population and compare this with healthy bone marrow derived cells. In order to investigate this, we isolated stroma stem and progenitor cells from osteoarthritic human femoral heads (bone and cartilage compartments) with the aim to treat them with human recombinant NT-3 and NGF and observe the effect on cellular viability for these primary hip joint derived hMSCs. This was compared with the effect of NGF treatment as well as the combined effects of NT-3 and NGF.

For the selective isolation of stem and progenitor cells, we used the fibronectin adhesion method. The culture dishes where the cells were seeded, and expanded post isolation were pre-coated with fibronectin, in order to aid the attachment of mainly stem and progenitor cells that express Integrins on their surface. Integrin α5β1 has been found to be involved in the preservation of the progenitor state of adipose tissue derived MSCs (di Maggio *et al.*, 2017). In our study, the selective isolation of stem/progenitor cells resulted in increased yields in the cell density after 14 days of post-isolation culture on fibronectin coated dishes. CFUs specific to fibroblast cell populations (CFU-F) were observed in culture dishes coated with fibronectin, while the non-coated plates presented low cell density and a lack of CFUs.

Prior to the *in vitro* investigation of NT-3 and NGF effects in OA-hMSCs viability, we carried out an immuno-phenotype analysis by flow cytometry. As expected, the MSC phenotype, established by ISCT in 2006, was detected in a low percentage (Hernigou

et al., 2005). A difference is notable between the samples that originated from healthy bone marrow (BM2) compared to the disease bone (OA5) in Fig. 4.6. The reduction in stem/progenitor population by comparison with the healthy control can be attributed not only to the disease pathology of the tissue used for the isolation of OA5-hMSC but also to the age of the patient. Healthy bone marrow is sourced from 20-25 years old donors, while the OA5-hMSCs are isolated from the bone compartment of the femoral head donated by a patient of 70-75 years old (supplementary information on age ratio and sex of the donors and patients is available in Appendix section). It is well established that the bone marrow stem/progenitor cell populations decrease with age (Ganguly *et al.*, 2017). The cells isolated from the cartilage compartment of the hip joint showed little to no MSC immuno-phenotype when analysed by flow cytometry. A panel of antibodies specific for cartilage progenitor cells would have been more appropriate for identifying and classifying this cell population. Dicks *et al.*, described a $CD146^+/CD166^+/PDGFR\beta^+/CD45^-$ chondroprogenitor cell population that exhibited high chondrogenic potential. This panel of cellular markers should be considered in future studies, for the identification of chondroprogenitor cells.

It is important to note here that on assessment of the MSC immunophenotype for the cell populations derived from healthy human bone marrow, a low frequency of cells with an MSC phenotype was seen following flow cytometry analysis, in comparison with similar studies,. The source of non-diseased stroma cells in this study was bone marrow obtained from iliac crest aspirates from healthy young donors without any underlying conditions. Therefore, a higher frequency of cells with an MSC phenotype was expected. However,, recent studies suggest that the isolation yield of MSCs, even from the richest of sources, can be influenced by factors such as: the choice of anticoagulant, the method of isolation , any prior thawing, the choice of culture medium, the size of cell culture dishes used for expansion of isolated populations (Li et al, 2011; Walter et al., 2020). Considering that the bone marrow aspirates included in this study were obtained from a commercial source, no specific information regarding the specific harvesting protocol and the post-harvesting treatment of the aspirates was provided. Moreover, as the bone marrow aspirates originated in the U.S.A. prior to shipment, any alternation in the preservation steps such as low temperature storage could have a negative impact on the survival rate of MSCs.

The survival rate for these cells could also be influences by the expansion procedure for the isolated cellular population, including the choice of cell culture media and serums. which could have resulted in a reduced frequency of MSCs when stroma cells were further expanded. In addition, considering a new culturing environment post shipment, bone marrow stroma MSCs could have undergone enhanced differentiation, at the early stages of *in vitro* expansion, leading to a low detection of MSC frequencies with flow cytometry.

It is known that MSCs constitute a rare cell population of cells within the bone marrow comprising only a small percentage of the total nucleated cells present. These cells are heavily reliant on their specific and unique microenvironment for their maintenance, with any changes in this negatively impacting MSC survival rates. Typically, the percentage of MSCs in the human bone marrow ranges from 0.001 to 0.01% of the total nucleated cells (Heringou et al., 2005).

The tri-lineage differentiation potential of the isolated cells was assessed by culture in adipogenic, osteogenic and chondrogenic media for 21 days. The data presented in Fig. 4.7, Fig. 4.8 and Fig. 4.9 confirms that the isolated cells from healthy bone barrow, diseased bone and diseased cartilage have multi-lineage differentiation properties. Confirming this property of the isolated cells, in addition to their capacity to adhere to plastic and the expression of the MSC phenotype as shown by flow cytometry analysis, enables us to use the terms MSC and CPC to refer to the cell populations included in this work. However, we must note that the cell populations used in this study are heterogenous. Ideally, cell sorting should be used for the isolation and expansion of more homogenous cell populations CD105+/CD90+/CD146+/CD45- for bone tissue derived hMSCs derived from bone tissue and CD146+/CD166+/PDGFRβ+/CD45− for cartilage tissue derived chondroprogenitors.

Nevertheless, any neurotrophin specific effect on osteoarthritic joint tissue, either due to physiological changes or external treatment would apply to bone and cartilage heterogeneous cells populations. Therefore, it is important to consider the effect of neurotrophin exposure to the more heterogeneous cell populations that altogether make up the joint tissues.

Flow cytometry analysis confirmed the presence of the MSC specific marker, CD271, proposed by Quirici *et al* and Jones *et al*. From the total cell population isolated from

healthy bone marrow, 5% of stroma cells were found positive for CD271. The percentage of CD271+ cells decreased in cell populations isolated from diseased tissue (osteoarthritic cartilage and bone) to <2%. The difference in the presence of CD271 in healthy hMSC vs. diseased hMSCs can be attributed to various factors. As mentioned above, the healthy tissue was donated by a donor of 20-25 years old while the diseased samples were collected from patients with an age range of 50 to 80 years old. Age may affect the synthesis of CD271 in MSCs or the size of the CD271 positive cell population. On the other hand, downregulation of CD271, which is likewise a pan-neurotrophin receptor, may be associated with the pathophysiology of osteoarthritis.

Qualitative assessment of CD271 localisation found it as present in stroma cells isolated form all three sources (healthy bone marrow, diseased bone, and diseased cartilage) (Fig. 4.10). Together with the quantitative data provided by flow cytometry analysis, we can say that our heterogenous isolated cells contain a CD271 positive sub-population.

Not only CD271 (Fig. 4.10), was localised on the surface of the isolated cells. Additionally, Trk C, the NT-3 specific receptor, was localised on the surface of the isolated cells. Before proceeding with the investigation of NT-3 and NGF effects on cellular viability, the presence of the NT-3 specific receptor, Trk C, was investigated on the surface of the isolated stroma cells from healthy and diseased tissue. With IF-IHC staining as seen in Fig. 4.11, a difference in the presence of Trk C was detected for stem/progenitors derived from the bone marrow (healthy) or the bone compartment (disease) vs those isolated from the articular cartilage (in disease). Trk C detection was weaker in hMSCs and more intense in hCPCs in our dataset. This finding may reveal not just a phenotypical variation between MSCs and CPCs, but also indicate potential differences in response to stimuli, as the cells may express different levels of Trk C. Following a literature search we have not found any similar work that demonstrates this novel finding. We believe that this has the potential for an in-depth study on the role of Trk C in cartilage physiology and associated diseases pathology.

The examination of NT-3 effects on cell viability using bone and cartilage specific *in vitro* models (osteosarcoma and chondrosarcoma cell lines respectively) found that NT-3 has a poor proliferative impact on these cells, but a substantial cytotoxic effect.

The evaluation of BM- and OA- hMSCs viability following NT-3 treatment revealed variable and interesting results, without a clear outcome on the overall effect of NT-3 treatment impact on the proliferation for this particular cell populations. As all the samples included in this study were primary cells, the variability in response to the neurotrophins treatment was anticipated and not surprising.

Previous work demonstrated that NT-3 has proliferative effects on the bone marrow derived stem cells populations (Yan *et al.*, 2016). And its proliferative as well as differentiation potential has been well published in neuronal stem cells.

Gene expression analysis (Fig. 4.23) demonstrated that cells which exhibited reduced viability after NT-3 treatment developed an internal survival signal. The increased expression of BCL2, an apoptosis inhibitor, shows that the cells activated a survival mechanism, which was most likely triggered by the presence of NT-3 in the culture medium. Our initial experiments using the in cartilage *in vitro* model, SW-1353, indicate that NT-3 could have a proliferative effect. However, in hCPCs isolated from patients with osteoarthritis, NT-3 had the opposite effect. It induced significant decrease in the cellular viability of OA-hCPCs. Follow-up gene expression analysis showed that *CAS3*, an apoptotic marker is upregulated in these cells. While *CAS3* was only detected in OA-hCPCs, signs of cell survival signalling, detected through increased *BCL2* expression, were found for OA-hCPCs and OA-hMSCs after 21 days of NT-3 treatment.

The cellular viability results following NGF treatment on the cells isolated from healthy bone marrow and osteoarthritic hip joint indicate that NGF has a negative effect on the proliferation of this type of cells. This effect was expected as NGF is known for inducing differentiation, not proliferation (Lee *et al.*, 2021).

The combined effect of NT-3 and NGF on the proliferation and overall viability of hCPCs and hMSCs can act as the basis for the development of treatment approaches in regenerative medicine. Data collected from our work did not provide a summary view of the effects of NT-3 and NGF on cellular proliferation, when the data was analysed in biological groups organised as mentioned in Table 4.1. However, when the data was individually analysed, per patient, a clear pattern emerged. High concentrations of NT-3 neurotrophin treatment of hMSCs and hCPCs (50 ng/ml) induce a slow proliferation, only when administrated in combination with NGF. NT-3

also induces cell senescence following exposure longer than 7 days, as demonstrated by the majority of the results obtained at day 14 in the cell viability monitorisation assay. Further observations at day 21, together with gene expression analysis unveiled that the potential initiation of a cellular pro-survival mechanism. While this data may indicate the initiation of apoptosis following NT-3 treatment, this hypothesis could not be confirmed with gene expression analysis as we did not detect Cas*3* upregulation in these conditions and in hMSC isolates, healthy nor disease. *Cas3* was only detected active in 4 out of 5 cartilage originated progenitor cell populations treated with 25 ng/ml NT-3. Again, the biological variability due to the nature of the cells (primary cells) was observed. OA4-hCPCs and OA5-hCPCs treated with 25 ng/ml NT-3 for 21 days showed no difference in the relative expression of *Cas3* comparative with the control (0 ng/ml NT-3). On the other hand, OA2-hCPCs and OA3-hCPCs treated with 25 ng/ml NT-3 showed an upregulation of *Cas3*, indicating a strong apoptotic signalling. These results suggest that NT-3 can induce apoptosis. More work where the apoptotic effects of NT-3 in cartilage stem/progenitor cells are in detail assessed with a more extensive gene panel for the canonical signalling pathways that can result in cellular apoptosis can be investigates with the genetic material obtained from similar *in vitro* studies as the one currently presented one.

From our work we can hypothesise that NT-3 promotes hMSC differentiation. Studies in mice (Zhang *et al.*, 2020) demonstrated that NT-3 promotes osteo-differentiation of bone marrow derived MSCs. They also indicate that activation of Akt by NT-3 is responsible of this effect. Information available in literature suggest that NT-3 has an indirect effect on osteo-differentiation by enhancing the expression of osteogenic markers such as *OCN* and *Runx2*, as well as chondrogenic markers such *Sox9*, rather than directly inducing osteo-differentiation.

When comparing the healthy tissue sourced stem/progenitors with diseased tissue sourced stem/progenitor cells after the treatment with 25 ng/ml NT-3, we observed that diseased cartilage stem/progenitor cells (OA-hCPCs) appear to induce apoptosis in response to the treatment, while the bone stem/progenitor cells (OA-hMSCs and BM-hMSC) develop a survival response following the treatment with 25 ng/ml NT-3. When the pro-survival response of hMSC following the 25 ng/ml NT-3 treatment is compared between the healthy and diseased stem/progenitor cells, according to the expression of BCL2, OA-hMSCs appear to develop a better pro-survival response than BM-

hMSCs. This observation can constitute the basis for a larger study, where more donors and patient samples could be included for the *in vitro* treatment with NT-3. The BCL2 linked pro-survival response can be in detail analysed by assessment of BAX and other genes implicates in the regulation of cell apoptosis.

In this study, we also investigated the effect of NT-3, as well NGF and NT-3+NGF, on the osteo- and chondro-differentiation of primary hMSCs and hCPCs respectively. Prior to that we already established that these cell populations possess the capacity to multi-differentiate when cultured with adipogenic, chondrogenic and osteogenic medium (Fig 4.7, 4.8 and 4.9). We then exposed the isolated cells to osteogenic and chondrogenic media supplemented with recombinant NT-3 and NGF in order to assess a possible enhancement or suppression of differentiation. Evidence collected through microscope imaging of the stained cells after treatment with neurotrophins for 21 days in osteogenic media indicate that NT-3 and NGF definitely have an effect on osteo-differentiation. This was semi-quantified by dilution of the Alizarin Red S from the calcium deposits and absorbance measurement. Our collected data indicates that the response to NT-3 is patient specific. The osteo-differentiation of BM2-hMSCs appears to be inhibited by NT-3 but enhanced by NGF. The differentiation effect of NGF is maintained when NT-3 is also present. The response to NT-3 in osteo-differentiation of the diseased bone derived hMSCs appears to be patient specific, as 2 out of 4 cell isolates showed enhancement of osteo-differentiation in the presence of NT-3. Initially we suspected a correlation with the age of the patients (please refer to the supplementary data in the appendixes section). As mentioned above, the number of stem/progenitor cells decreases with age in all adult tissue, not only bone marrow. According to our collected datasets, no correlation is present between the age of the patients and the effects of NT-3 on the enhancement of osteo-differentiation of stem/progenitor cells.

As shown in the previously mentioned study, Zhang *et al.*, changes in the endogenous NT-3 expression have an impact on the osteo-differentiation potential of bone marrow derived MSCs. Taking into consideration, the effects of NT-3 observed in our work, we can state that NT-3 supports and can induce an enhancement of osteo-

differentiation for hMSCs. This comes in agreement with the study published by Zhang *et al.*

In conclusion, the data presented in this chapter indicate that NT-3 has the potential to either be involved in the tissue degeneration process characteristic of osteoarthritic joins or support the tissue repair process in the joint mainly through involvement in the osteo-differentiation of the MSCs.

However, in the consideration of NT-3 as a therapeutic option the toxic effect of prolonged exposure to NT-3 should be considered. Our findings indicate that there are differences in the phenotype as well as the response to different stimuli for the stem/progenitor cells derived from cartilage tissue and bone tissue of the same patient joint structure. A follow-up study looking at the immuno profile of freshly isolated cells from different tissues and structural elements of the osteoarthritic joint can provide valuable data on the joint specific stem/progenitor cell content and lead to the emergence of correlations between tissue physiology and disease pathology.

Chapter 5: Proteomic analysis of stroma stem/progenitor cell derived extracellular vesicles from healthy bone marrow and osteoarthritic hip joint

5.1. Introduction:

Osteoarthritis (OA) is defined as a chronic degenerative joint disease characterised by articular cartilage degradation, inflammation of the synovial membrane, subchondral bone remodelling and osteophyte formation (di Nicola, 2020). The low-grade inflammation component of this pathology seriously interferes with the tissue repair physiology by downregulating the proliferation of chondrocytes and the accumulation of cartilage matrix. Studies show that the formation of autoantibodies against cartilage components such as mesothelin, osteopontin, ykl-39, collagen and proteoglycan could lay behind the immune-dysfunction in OA and these become part of the complex pathogenic mechanism that causes tissue damage and induces chronic pain (Mödinger *et al.*, 2019). In the early stages of OA, injured cartilage tissue releases molecules that are recognised by the macrophage toll-like receptors (TLR2 and TLR4). The activation of these receptors will induce the migration of macrophages to the injury site and will initiate an immune response, with the aim to protect against any pathological factors, such as bacterial infection or hypoxia induced necrosis. In normal conditions, this post-injury acute inflammatory response aims to protect the joint tissue through accumulation of macrophages. However, prolonged chronic inflammation can be harmful for the joint. For this reason, the immune response in the joint following injury is controlled by the resident MSC population. They secrete anti-inflammatory factors such as transforming growth factor β (TGF-β) and prostaglandin-E2 (PGE-2) and have surface receptor with immunosuppressive properties such as programmed cell death protein 1 (PD-1) and Fas receptor (Nicola *et al.*, 2002; Aggarwal and Pittenger, 2005; Augello *et al.*, 2005; Gu *et al.*, 2013). These characteristics allow MSC to modulate immune responses and even interact with the immune cells, mainly blocking their activity.

 In inflammatory diseases such as OA, resident MSCs are considered compromised, as they fail to regulate the immune response which leads to prolonged tissue damage (Huang and Kraus, 2016).

Considering the above in cell-based therapies for inflammatory and degenerative disease, MSCs transplantation represent the most promising option, due to their multi-lineage differentiation potential, immuno-modulatory functions and pro-angiogenic characteristics (Harrell *et al.,* 2019). These characteristics make MSCs a great tool for novel treatment options in regenerative medicine.

In addition to their immuno-modulatory potential, MSCs have the capacity to modulate the proliferation of the neuronal and immune system cells in tissue repair and for the maintenance of tissue homeostasis (Wang *et al.,* 2013). Furthermore, MSCs have the capacity to enhance angiogenesis by secretion of vascular endothelial growth factor (VEGF) (Zhu *et al.,* 2015). All of these features made MSCs the focus of various cell-based therapies in the treatment of a number of conditions in all affecting more systems in addition to the musculo-skeletal, with encouraging results. Studies in the field propose MSCs for the treatment of conditions such as neurological damage, liver disorder, cardiac ischemia, diabetes, and skin injury (Webber *et al.,* 2012; Götherström *et al.,* 2014; Karantalis *et al.,* 2014; Thakkar *et al.,* 2015; Vega *et al.,* 2015; Fernández *et al.,* 2018)

Since the release of International Society of Cellular Therapies standards for MSC in 2006, the number of Investigational New Drug (IND) Applications that propose MSC-based therapies has seen a 3-fold increase, according to data recorded in 2012 (the highest number of MSC based INDs submitted to the Food and Drug Administration (FDA) (Mendicino *et al.,* 2014).

Despite the promising outcome of MSCs in cell-based regeneration and immuno-modulation therapies, follow-up experiments and clinical studies have drawn attention to limitations and challenges. These mainly refer to the safety and efficiency of MSC use in clinical applications. In some patients, transplanted MSCs resulted in side effects such as unwanted differentiation and excessive suppression of the immune response, which led to ossification in heart treated with MSCs (Gazdic *et al.,* 2015), vision loss, detached retinas and intraocular bleeding after the treatment with adipose-derived MSCs in patients with macular degeneration (Kuriyan *et al.,* 2017), respiratory and gastrointestinal infections in patients with idiopathic pulmonary fibrosis and inflammatory bowel diseases (Glassberg *et al.,* 2017).

Reports have shown that upon transplantation, MSC populations tend to remain trapped in the lung, liver and spleen (Hassanzadeh *et al.*, 2021) and don't reach the aimed target, the site of injury. This can be attributed to the lack of standardisation in the administration method. MSC cell-based therapies limitations as described above, highlight the importance of the development of cell-free therapies that deliver MSC regulatory actions without the need of the cell component administration. It was at this point that the search for a way to take full advantage of MSC functions without transplanting them, caught the interest of research groups in the field.

MSCs perform a variety of regulatory activities via the release of several bioactive substances. Capturing and delivering just the precise molecules involved in MSC-like responses in various types of conditions can potentially enable a cell-free therapeutic method. Results obtained from increased array of experiments demonstrate that in fact treatment with MSC-derived secretome instead of MSC transplantation showed therapeutic benefits similar to those observed in post-transplantation reports (Gnecchi *et al.*, 2006; Aslam *et al.*, 2009; Rossi *et al.*, 2012; Goolaerts *et al.*, 2014). Moreover, the efficacy of the treatment was improved, and the occurrence of side effects was reduced.

The benefit of using MSC-derived secretome instead of MSC transplants are not limited to just the reduction in side effects such as un-wanted differentiation and unwanted potential activation of allogenic immune responses. Additionally, this approach is beneficial for clinical applications since it employs a cell-free treatment strategy. Regarding safety, the content of MSC-derived secretome, can be constantly evaluated prior to clinical applications.

The MSC secretome is characterized by bioactive factors such as soluble proteins (enzymes, signal transduction molecules, immunomodulatory proteins, and growth factors), nucleic acids (DNA, RNA fragments and miRNAs), lipids and extra-cellular vesicles (EVs).

EVs are characterised by a lipid bilayer membrane that envelopes entities such as apoptotic bodies, and exosomes (Veziroglu and Mias, 2020). EVs secreted into the extracellular space that measure 30-150nm in diameter are defined as exosomes (Toh *et al.*, 2018). Not all EVs with the diameter of 30-150nm are considered exosomes. Only those that express endosomal proteins such as TSG101 and Alix, and tetraspanin

proteins such as CD9, CD63 and CD81. They can also be distinguished by their rich and diverse RNA content.

Exosomes are considered important intercellular communication mediators via their contents (lipids, nucleic acids, and proteins). Recent studies in the field have confirmed their key role in cell communication.

The content of exosomes varies according to the physiological and pathological state of cells. Therefore, exosomes might serve as a measure for physiological status and disease progression.

Considering their high specificity, at this moment in time the content of the exosomes, nucleic acids, and proteins, are being extensively investigated for their potential as biomarkers in clinical diagnosis. The analysis of microRNAs expression is one of the most popular method of exosomes content investigation.

Their involvement in various diseases has also been documented, including osteoarthritis (Qi *et al.*, 2016). A close relationship between exosomes and bone homeostasis has been revealed in recent studies (Gao *et al.*, 2018). Bone resorption and bone formation are the two processes that are primarily involved in bone homeostasis. Different studies have shown that the cells from the bone microenvironment (osteoblasts, osteoclasts, osteocytes and MSCs) can secrete exosomes to regulate bone resorption and bone formation for the maintenance of bone homeostasis. Table 5.1 summarises the roles of bone derived exosomes.

Table 5. 1. Summary of studies showing the effects of exosomes secreted by bone specific cell types.

Origins of exosomes	Effects	Ref.
Osteoblasts	Osteogenesis potential (eukaryotic initiation factor-2 signalling pathway)	*Ge et al., 2015*
Mineralizing osteoblasts	Promotion of bone marrow stromal cells differentiation into osteoblasts	*Cui et al., 2016*
Osteoclasts	Inhibition of osteoblast functionality, osteogenic differentiation, and bone formation	*Sun et al., 2016*
MSCs	Bone homeostasis promotion Apoptosis prevention Regeneration of bone defects Promotion of angiogenesis and osteogenesis	*Kuang et al., 2019* *Ren et al., 2019* *Qi et al., 2016* *Zhang et al., 2018*

Therefore, exosomes represent key biological entities for the diagnosis and treatment of bone related diseases. For example, in patients with cancer, the plasma exosomes contain lower levels of tumour suppressor specific genes (miR-15a) and high levels of oncogenic proteins, cytokines and adhesion molecules by comparisons with the content of exosomes from healthy patients (Roccaro *et al.*, 2013).

Analysis of plasma from patients with osteoporosis, showed elevated levels of RNA-derived fragments (tRFs) such as tRF-25, tRF-38 and tRF-18 when compared with the healthy controls. This outcome suggests that tRFs may be used as diagnosis markers for osteoporosis (Zhang *et al.*, 2018).

5.1.1. Exosomes Derived from Bone as a Diagnostic Biomarkers

In OA pathology, the study of secreted exosomes can have diagnostic and therapeutic applications. For example, exosomes have been detected in human synovial fluid (Skriner *et al.*, 2006; Domenis *et al.*, 2017; Gao *et al.*, 2020). Additionally, it is proposed that pathologies of the musculoskeletal system such as OA, rheumatoid arthritis, and reactive arthritis, are characterised by a change in exosomes quantity and

composition. Moreover, the synovial exosomes miRNA content from patients with OA appears to be gender specific (Kolhe *et al.*, 2017).

OA diagnosis is currently not possible at the early/on-setting stages, OA detection cannot be confirmed until it reaches medium to advanced stages, and this is accomplished by radiographic and physiologic clinical examination. The molecular profiling of joint derived exosomes can contribute on our understanding of OA progression, leading to diagnosis at earlier stages. The discovery of disease-specific biomarkers, or variations in the quantities of certain molecules when compared to a health, can aid in the early detection of OA. Additionally, a more detailed description of disease pathology development can be achieved.

The study of exosomes in OA progression can prove a suitable approach to early diagnosis and monitorisation of risk factors.

The objective of the work presented in this chapter is to isolate EVs from the secretion of human cartilage and bone stem/progenitor cell populations from healthy and osteoarthritic tissue, and to investigate their content with the main focus on the proteomics, by mass spectrometry analysis.

5.2. Methodology:

In order to analyse the extracellular vesicles (EVs) secreted from osteoarthritic joint derived cells compared with EVs secreted from the healthy bone marrow stroma cells, cell culture media was collected during the post-isolation cellular expansion, from 7 healthy and disease donors. For the OA specific samples, femoral heads were obtained from hip arthroplasty procedures. For the healthy samples, unprocessed bone marrow, was purchased from Lonza.

At day 7 and day 14 post-isolation cell culture media containing the secreted EVs was collected and furthered processed for proteomics analysis of the vesicles' content.

Prior to the isolation of the EVs, the media was cleared of cellular debris through centrifugation and filtration with 0.45µm sterile filters. For EV harvesting, a polyethylene glycol enrichment method was used. Cell culture media collected from day 7 and day 14 post isolation, and cleaned up cellular debris, was incubated with

16% (w/v) PEG-6000 (1:1) at 4°C for at least 18 hours. For the separation of PEG enriched EVs from the media, the samples were centrifuged at 3250 x g for at least 1 hour. The EV containing pellets were reconstituted in PBS and stored at -80°C prior to analysis. Pure culture media was also treated similarly to the samples. These were used for exclusion analysis of identified peptides in mass spectrometry. Full methodology is available in Chapter 2.

In order to analyse the morphology, identity, and the content of the isolated EVs, we used flow cytometry, scanning electron microscopy (SEM) and mass spectrometry (MS).
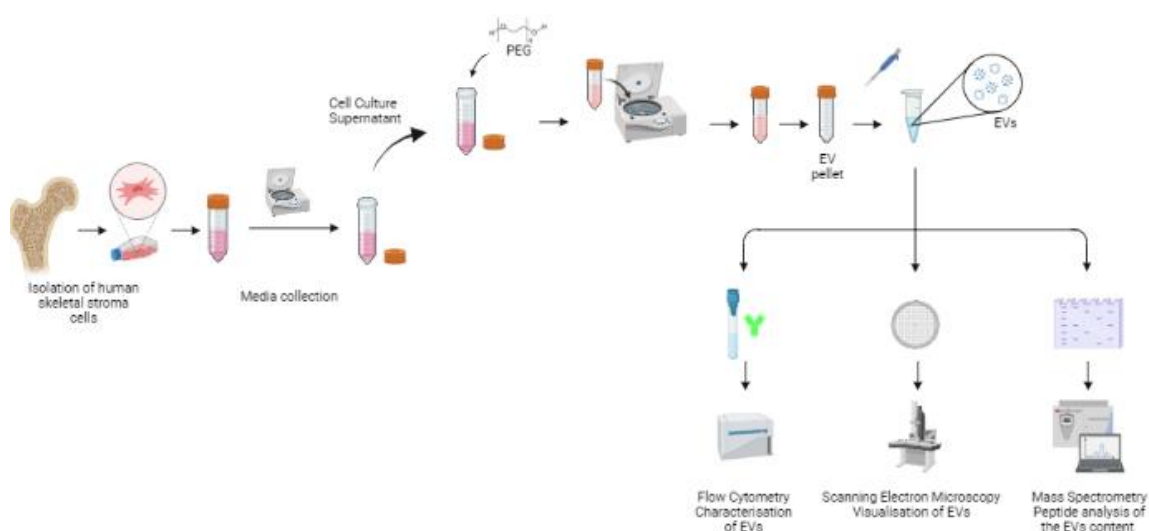
Figure 5. 1. Schematic representation of the techniques used for the isolation and characterisation of hip joint tissue derived EVs
The quality of isolated EVs through PEG enrichment was assessed with SEM and flow cytometry. The protein and peptide content of hip joint tissue derived EVs was determined with mass spectrometry, where the nano LC-MS/MS analysis was used (diagram generated in BioRender).

5.2.1. EVs characterisation by Flow Cytometry

In order to confirm the quality of the purified EVs flow cytometry was used to analyse representative samples from the healthy bone marrow, diseased bone and diseased cartilage. The EVs were immuno-stained with fluorescent tagged antibodies against CD9, CD63 and CD81 exosome markers, allowed to incubate for 30 minutes in the dark at 4°C.To reduce EV loss, due to their small size stained EVs required longer and

stronger centrifugation in the wash steps prior to analysis; 30 minutes centrifugation at 17, 000 rpm at 4°C. At least 10,000 events were recorded and analysed from each sample. The collected data was analysed with Kaluza Analysis Software Version 2.1.

5.2.2. Scanning Electron Microscopy (SEM)

For further qualitative analysis of the isolated EVs Scanning Electron Microscopy (SEM) was used and representative samples from diseased cartilage, diseased bone and healthy bone marrow were examined using SEM. The selected EV samples were fixed with 2% (v/v) glutaraldehyde for 30 minutes and placed on a 200-mesh carbon-coated with formvar film copper grids and further incubated for another 10 minutes prior to visualisation. Isolated EVs were visualised with the Hitachi SU8030 Scanning Electron Microscope, and their circumference was measured with the accompanying software.

5.2.3. Mass Spectrometry

For protein and peptide EV content analysis, nanoscale liquid chromatography coupled to tandem spectrometry (nano-LC-MS/MS) was used. This particular method was the most suitable for the samples included in this study, as it offers robust analysis of limited amounts of peptide mixture samples.

A total of 10 μg from each EV sample was in gel digested prior to nano-LC-MS/MS analysis. Samples were separated through electrophoresis in 12.5% SDS-PAGE for only approximately 1 cm in the resolving gel. The resulting bands were collected, and a series of steps were carried out for the reduction and alkylation of cysteines. The full method is described in chapter 2.

For the digestion of the samples, trypsin protease purified from porcine trypsin was used. Due to the high PEG content in the samples that can result in equipment congestion and increased background noise in the mass spectrometry, an extra cleaning step was carried out. The extracted peptides were cleaned with C18 Spin Tips.

Samples were arranged in 4 different groups (Table 5.2) based on the tissue origin and collection time points (day 7 and day 14). The samples together with the standards were processed by Dr. Kevin Howland in the Proteomics facility, School of Biosciences, University of Kent.

Table 5. 2. **The sample group organisation for the nano LC-MS/MS analysis**

Groups No.	Group 1	Group 2	Group 3	Group 4	Groups 5
Sample ID	OA1-hMSC-EVs Day 7	OA1-hMSC-EVs Day 14	OA2-hCPC-EVs Day 7	OA2-hCPC-EVs Day 14	FBS enriched media EVs
	OA2-hMSC-EVs Day 7	OA2-hMSC-EVs Day 14	OA3-hCPC-EVs Day 7	OA3-hCPC-EVs Day 14	
	OA3-hMSC-EVs Day 7	OA3-hMSC-EVs Day 14	OA4-hCPC-EVs Day 7	OA4-hCPC-EVs Day 14	
	OA4-hMSC-EVs Day 7	OA4-hMSC-EVs Day 14	OA5-hCPC-EVs Day 7	OA5-hCPC-EVs Day 14	
	OA5-hMSC-EVs Day 7	OA5-hMSC-EVs Day 14			
	BM1-hMSC-EVs Day 7	BM1-hMSC-EVs Day 14			
	BM2-hMSC-EVs Day 7	BM2-hMSC-EVs Day 14			

5.3. Results:

5.3.1. SEM visualisation of EV morphology and size

The morphology and size of bone marrow and diseased joint tissue secreted EVs, detected with SEM can be seen in Fig. 5.2.

The visualised EVs are characterised by hollow-like surrounding circles which can be attributed to the PEG enrichment method used.

EVs of various sizes were detected across the representative samples analysed, with their diameter varying from 20 to 500 nm.
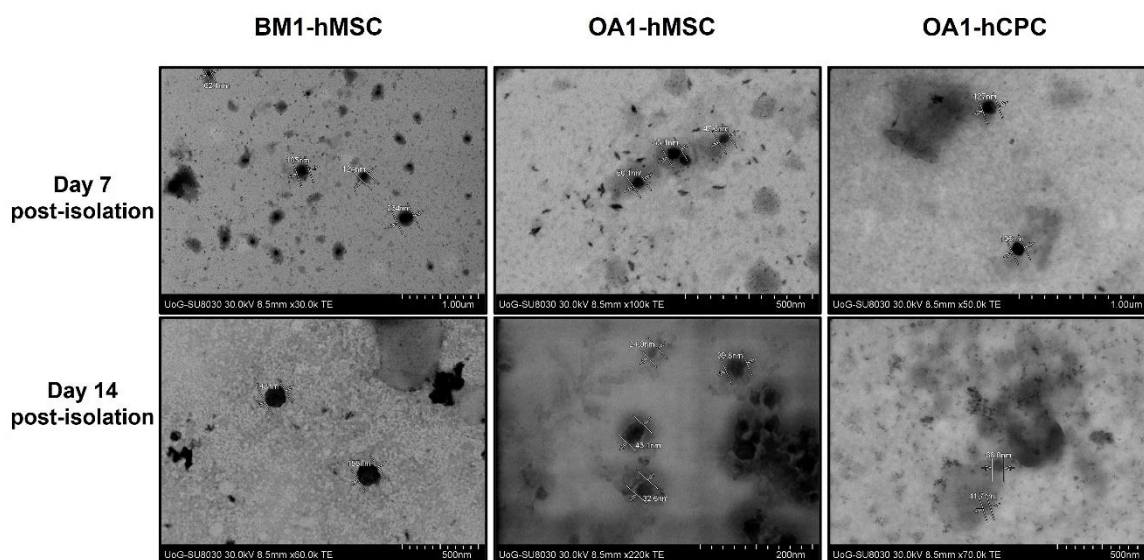
Figure 5. 2. SEM visualisation of healthy bone marrow and diseased joint tissue derived EVs isolated by PEG enrichment
Examples of EVs detected by SEM in the representative samples assigned for the healthy bone marrow (BM1-hMSC), diseased joint (OA1-MSCs) and diseased cartilage (OA1-hCPCs) isolates groups, at day 7 and day 14 post isolation.

Fresh cell culture media containing Foetal Bovine Serum (FBS) serum was also analysed for the presence of EVs by SEM. Representative EVs from the fresh media are shown in the Fig. 5.3. This analysis was carried out in to identify exclusion criteria for EVs originating from the media specific serum used compared with the bone marrow and joint tissue secreted EVs, looking at the samples presented in Fig. 5.2, FBS originating EVs appear larger in size and are characterised by lower intensity staining.

MSC culture media EVs **CPC culture media EVs**
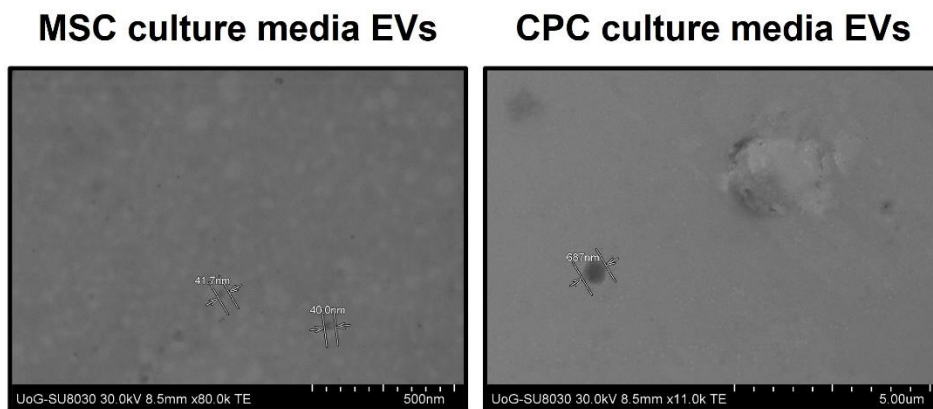
Figure 5. 3. Morphology of FBS EVs visualised by SEM.
This figure shows representative images for the vesicles isolated from FBS supplemented media. Both, small size (approx..40nm) and big size (approx. 500nm) vesicles were detected.

5.3.2. Exosome marker detection through flow cytometry

The presence of the exosome specific markers (CD63, CD82 and CD9) was assessed by flow cytometry in the EVs secreted by healthy and diseased hMSCs and hCPCs. This antibody panel was put together based on evidence found in the literature which state that EVs derived from the bone marrow hMSCs are CD63$^+$/CD81$^+$/CD9$^{+/-}$. 10 µg of each representative sample was incubated with antibodies against CD9, CD63 and CD81. An extra centrifugation (13,300 x g for 30 minutes) step was introduced in the washing of the samples, by comparison with the general protocol used in the flow cytometry analysis, with the aim to retain the EVs.

The graphs in Fig. 5.4 present the outcome of EV flow cytometry analysis. For the visualisation of the data in forward/side scatter plots, please see the supplementary data provided in the appendixes.
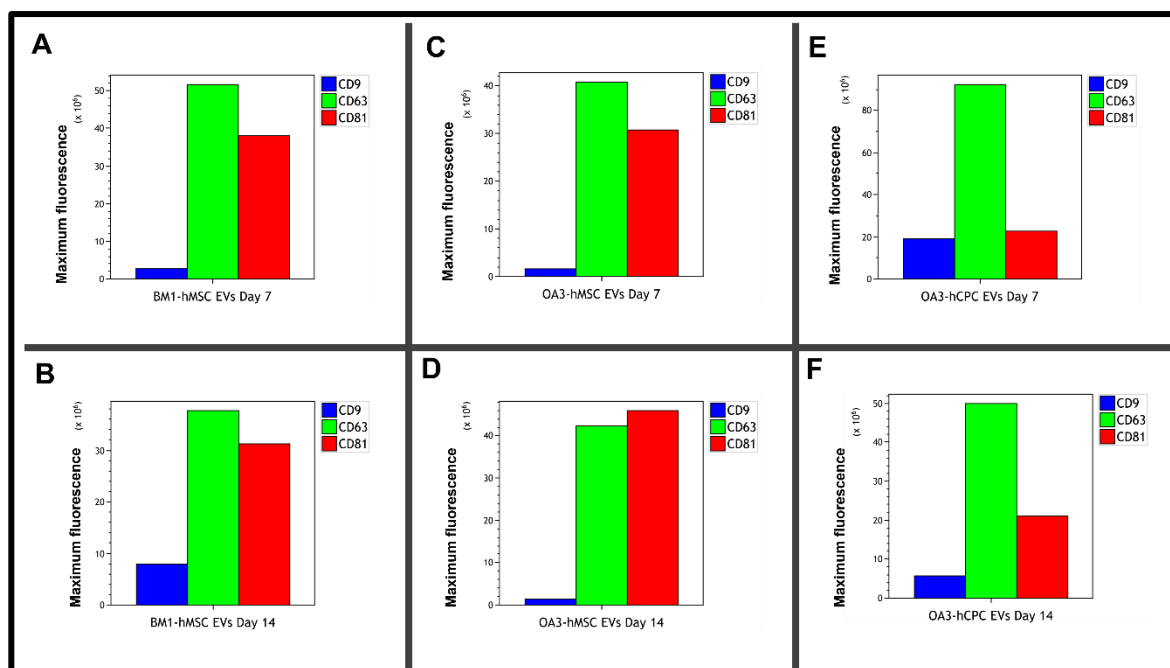
Figure 5. 4. Flow cytometry analysis of representative EV samples Maximum fluorescence detected in representative EV samples (A. BM1-hMSCs EVs collected at day 7, B. BM1-hMSC-EVs collected at day 14, C. OA3-hMSC-EVs collected at day 7, D. OA3-hMSC-EVs collected at day 4, E. OA3-hCPC-EVs collected at day 7 and F. OA3-hCPC-EVs collected at day 14) stained with antibodies against CD9, CD63 and CD81.

CD63 is the highest present exosome marker out of all tested exosome markers in our EVs samples included in this analysis. It is present in high levels compared with CD9 and CD81 in all the samples. Its highest maximum percentage was recorded in the healthy MSC derived EVs population.

CD81 presence varies across the samples. In EVs derived from healthy MSCs, analysis of the samples at day 7 indicates a low presence by comparison with CD63. The levels of CD81+ EVs increased at day in the secretion of healthy MSCs. Similar effect is observed in diseased bone derived MSCs. On the other hand, in the secretion of hCPCs (diseased) this trend is the total opposite. The CD81+ EVs are secreted less in day 14 post isolation compared with day 7.

By looking at the fluorescent intensity of the EVs samples stained with anti-CD9 antibody, a difference is observable between the healthy and diseased tissue derived EVs. The level of CD9 is higher in the healthy EVs compared with the diseased EVs. This difference in the levels of CD9 antigen between the healthy cells originated EVs and diseased cells originated EVs can constitute a diagnosis marker.

5.3.3. Analysis of EVs protein content.

SDS-Page analysis was carried out to confirm the presence of proteins in the purified EVs. Representative samples for each sample group have been included.

We can see on Fig. 5.5 that a protein or cluster of proteins with size of approximately 47 kDa is present in all the samples, including the +ve control (human plasma derived EVs). This is also present in the EVs purified from FBS enriched cell culture media, which can indicate a universal EVs peptide.

The data presented in Fig. 5.5 also indicates differences in the detected peptides between the samples. Higher protein content is available in the hCPC derived EVs than in the hMSC derived EVs. Differences between the EVs derived from the same cell population at different time points are also noticeable.

. Based on the above observations, it was decided to also include in the nano LC-MS/MS analysis the EVs isolated from the culture media where no cells were cultured, to avoid false detection of peptides present in the analysed hMSC and hCPC samples due to media serum carryover contamination. of.
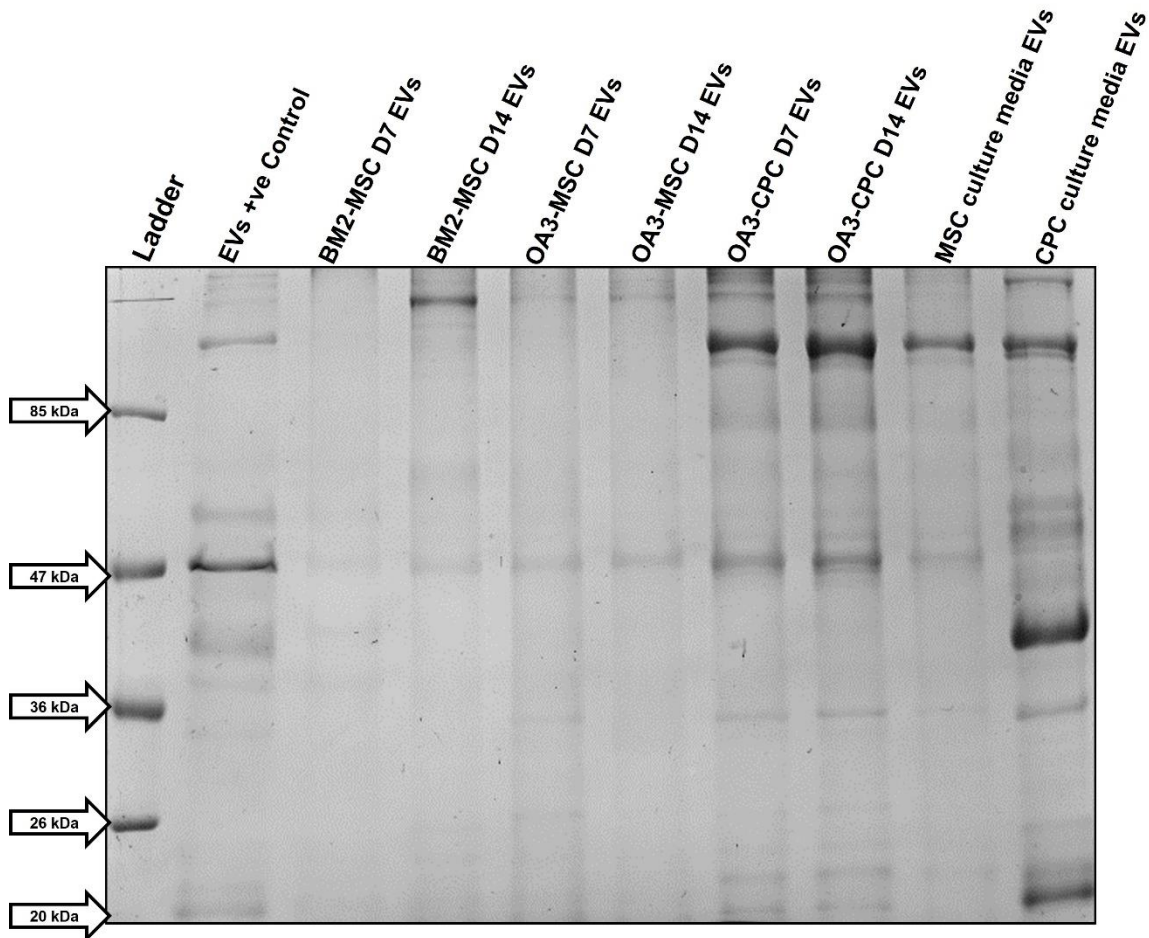
Figure 5. 5. Electrophoresis separation of the hMSCs and hCPCs derived EVs
Protein content from purified EVs isolated at culture day 7 and day 14 post-isolation for the bone marrow sample BM2, the OA bone sample 3 and the OA cartilage sample 3. EVs were lysed and their protein content separated on SDS-PAGE. The EV samples have been compared against the +ve control (confirmed EVs from human plasma), and against EVs from FBS enriched cell culture media.

5.3.4. The effect of PEG enrichment on Mass spectrometry

Nano LC-MS/MS is a sensitive proteomics method that relies on samples to be as clean as possible from contaminants, in order to correctly determine the right molecular components of the sample.

Our method of EV purification through density gradient centrifugation followed by polymer precipitation is thought to have impacted the detection of peptides through mass spectrometry (Fig. 5.4). Detected background ions are suspected to have originated from remaining PEG in the sample. As an additional control step, purified EV samples were separated by sonication and cleaned up before mass spectrometry. Unfortunately, not all contaminants resulted from the PEG enrichment steps were removed.
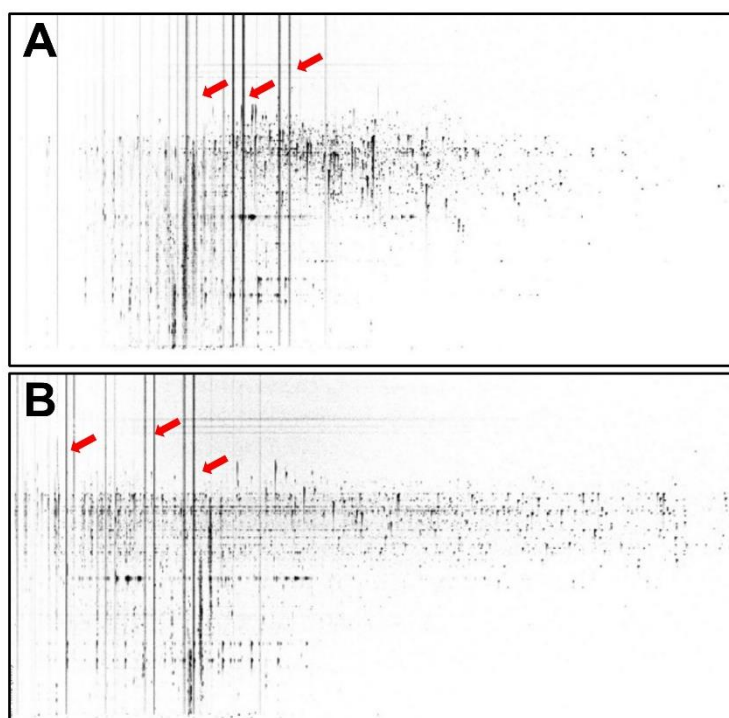
Figure 5. 6. The effect of PEG enriched EV purification on mass spectrometry.
The figure shows 2 examples (A. BM1-hMSC-EVs Day 7 sample at high energy and BM2-hMSC-EVs Day 7 at low energy) of the nano LC-MS/MS detection graphs. The vertical lines (marked with red arrows) present in the graphs indicate the presence of backgrounds ions. In our samples, the suspected contaminant is the PEG used for the EVs isolation from the culture media.

5.3.5. Peptide content identification in diseased and healthy human bone derived EVs

Nano LC-MS/MS was used to investigate the EVs in the secretome of primary isolated bone stroma cells during the expansion after the isolation. Samples were grouped as per collection time point and source. All technical replicates were run together.

The collected data was assessed with the Progenesis QI software, and the results were analysed against the Progenesis human database. Prior to the data analysis, an exclusion against serum enriched media EVs detected peptides was carried out. This was followed by selection of viable data based on the q-value and the number of unique peptide parameters. Detected proteins with less than 2 unique peptides and a q-value higher than 0.1 were excluded from the datasets.

For the interpretation of the data, the average amount of a peptide in fmol per sample was used.

Correlations between samples within the same group were established using Pearson correlation. Values of normal abundance were used for the calculation of the Z score per individual detected protein in each sample. The correlations were summarised though heatmap analysis.

Nano LC-MS/MS analysis of EVs secreted by the hMSC from healthy and diseased bone, indicate the presence of 87 proteins on day 7 post-isolation and 31 viable proteins on day 14 post-isolation, according to the data collected from groups 1 and 2.
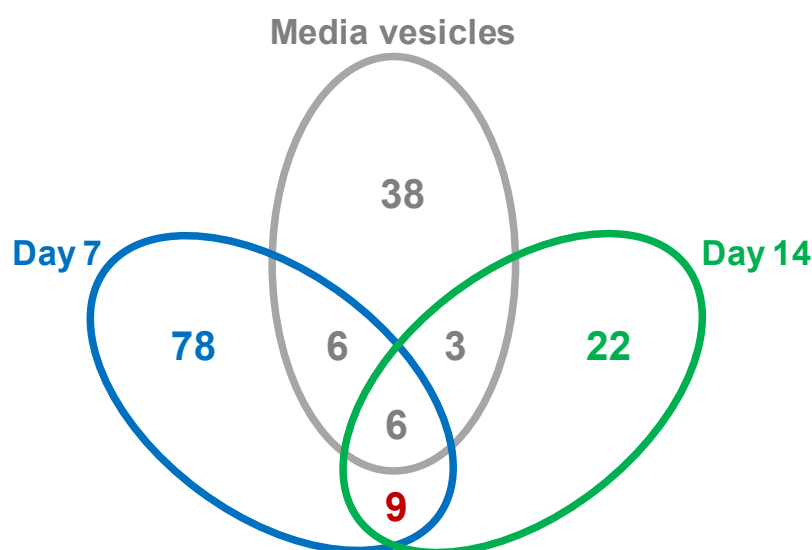
Figure 5. 7. Overlap analysis of hMSC secreted peptides.
Representative figure of the exclusion analysis carried out against EVs detected in expansion media in order to prevent false detection in bone stroma EVs analysis. Out of 53 detected proteins in serum, 15 were found in the representative samples for bone stroma EV secretion. These were treated as contaminants and excluded from the analysis.

Based on the number for unique peptides detected from samples at day 7 and day 14 post isolation, it has been recorded a 64.3% decrease in peptide secretion in day 14 compared with day 7.

The abundance (Z score) of the proteins detected on day 7 post isolation in purified EVs derived from hMSCs (healthy and diseased) is presented below in Fig. 5.8. The data was organised in a heatmap, where low abundance is represented in pink and high abundance in blue.

Analysing the abundance of the detected proteins across the samples collected from the expansion of OA-hMSCs at day 7 post isolation, correlations between the samples were identified (marked with red squares in Fig.5.8). Filamin-A, Neurabin-2 and Xin actin-binding-repeat containing protein 2, were detected as highly abundant in EVs purified from the healthy bone marrow samples, while Elongation factor 1-aplha-1 was also detected. Proteins detected in the purified EVs of bone stroma cells isolated from osteoarthritic patient no. 2 and patient no. 4 also share increased levels of hexokinase-3 and cathepsin G. Moreover, correlations have been found between all EVs samples

derived from diseased bone tissue, based on low levels of spectrin alpha chain, protein IWS1 homolog, tubulin beta-1 chain, synaptic vesicles membrane protein VAT-1 homolog, glycogen phosphorylase, xin actin-binding repeat-containing protein 2, neurabin-2, filamin-A, immunoglobulin heavy constant mu and cell division cycle protein 20 homolog.

High abundance of approximately 1/3 of the total peptides detected across the group, was found in the samples secreted by the hMSCs of the patient no. 5. These may imply a connection to other underlying disorders and may be unrelated to the condition on which this research is focused on, osteoarthritis.

From the data presented in Fig. 5.8, we can say that filamin-A, neurabin-2 and xin actin-binding-repeat-containing protein 2, while present in high abundance in the EVs secreted by healthy bone, these were detected as low abundant in the EVs secreted by osteoarthritic bone (Table 5.4).

Moreover, from the heatmap presented in Fig 5.8, considering the low protein levels (in pink) of BM-hMSC-EVs as baseline, the following proteins (Table 5.3.) are recorded with a higher abundance and can indicate OA. The table below that mentions them also summarised their already identified biological functions and possible implication in OA pathology (UniProt and PubMed).

Figure 5. 8. Heatmap analysis of the detected peptide content from EVs secreted during the first 7 days of expansion post-isolation for   bone stroma cells.
Samples were isolated from osteoarthritic human femoral head and bone marrow of healthy donors.   Data has been normalized and standardized in Excel and the presented heatmap and dendrogram were generated with OriginLab Software based on Pearson correlation analysis.

Table 5. 3. High abundant proteins in the OA-hMSC-EVs day 7 post isolation

Protein	Biological functions
Transmembrane protein KIAA1109	Phagocytosis, regulation of cell growth
Hexokinase-3	Cellular glucose homeostasis
Cathepsin	Potential cartilage degradation marker (Olszewska-Slonina *et al.*, 2013)
Annexin A1	Regulation of human fibroblasts from synovium (Sampey, Hutchinson and Morand, 2000)
Histone-lysine N-methyltransferase SETD2	Regulation of human fibroblasts from synovium (Araki *et al.*, 2018)
GRIP1-associated protein 1	Endocytic recycling in neurotransmission
Actin-depolymerizing factor	Actin filament binding

Table 5. 4. Low abundant proteins in the OA-hMSC-EVs compared with BM-hMSC-EVs, day 7 post isolation

Protein	Biological processes
Xin actin-binding protein	Actin filament organisation Negative regulation of protein binding
Neurabin-2	Cell migration Negative regulation of cell growth Negative regulation of phosphoprotein phosphatase activity Calcium-mediated signalling
Filamin-A	Wound healing (spreading of cells) Regulation of cell migration Positive regulation of integrin-mediated signalling pathway (cell adhesion) Positive regulation I-kappa B kinase/NF-kappa B signalling Negative regulation of apoptotic processes Epithelial to mesenchymal transition Angiogenesis
Immunoglobulin heavy constant mu	Primary immuno defence mechanism (early recognition of pathogens)
Cell division cycle protein 20	Cell differentiation Cell division Nervous system development Positive regulation of cell population proliferation

The abundance of the proteins detected in the EVs purified at day 14 post isolation from hMSCs is presented in Fig. 5.9 below.

The data collected from the nano LC-MS/MS analysis of the EVs content collected day 14 post isolation from   hMSCs (healthy and diseased) indicate a primary correlation between the healthy donor no.1 EVs and the patient no.4 EVs (marked with red squares in Fig. 5.9). This correlation is based on the high levels of collagen alpha 1(I), fibulin and tubulin present in both samples (marked with red shapes in Fig. 5.9). Similar levels of EMILIN-2 linked the EVs derived from the bone compartment of OA patient no.4 and the EVs from the bone marrow of the healthy donor no.2. According to this representation of the data, the content of the EVs derived from the hMSCs of the patient no.4, is more similar with the ones isolated from the healthy donors, rather than the diseased ones.

In addition to the data obtained from OA patient no.4, and the healthy donor, several differences in peptide abundance can be observed between the healthy and diseased EV samples. The EVs originated form diseased hMSCs 14 days after isolation, contain reduced levels of kinesin-like protein KIF1C, adenosyl homocysteinase, collagen alpha-1(I) and tubulin (circled in red on the peptide list, Fig. 5.9).

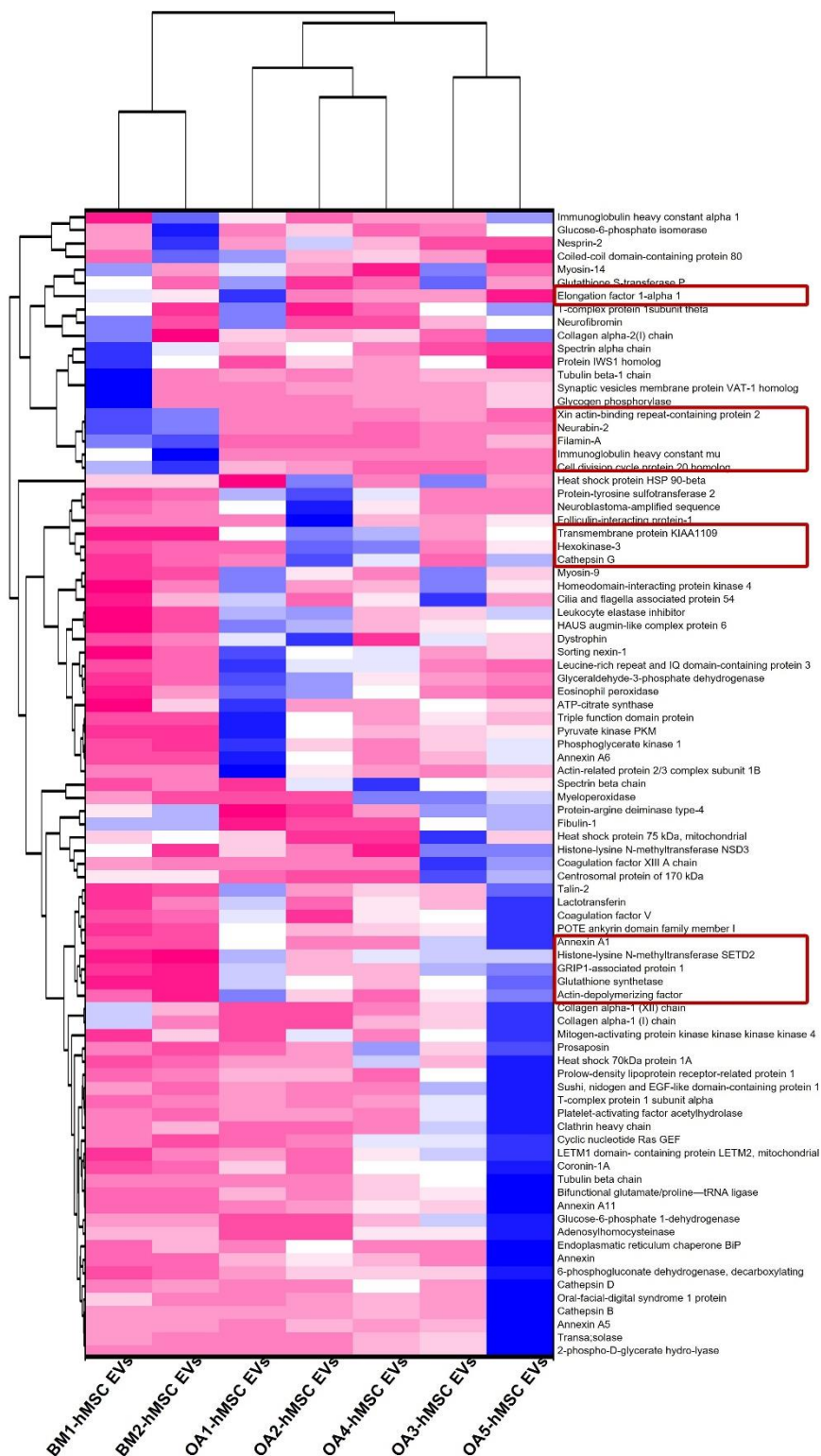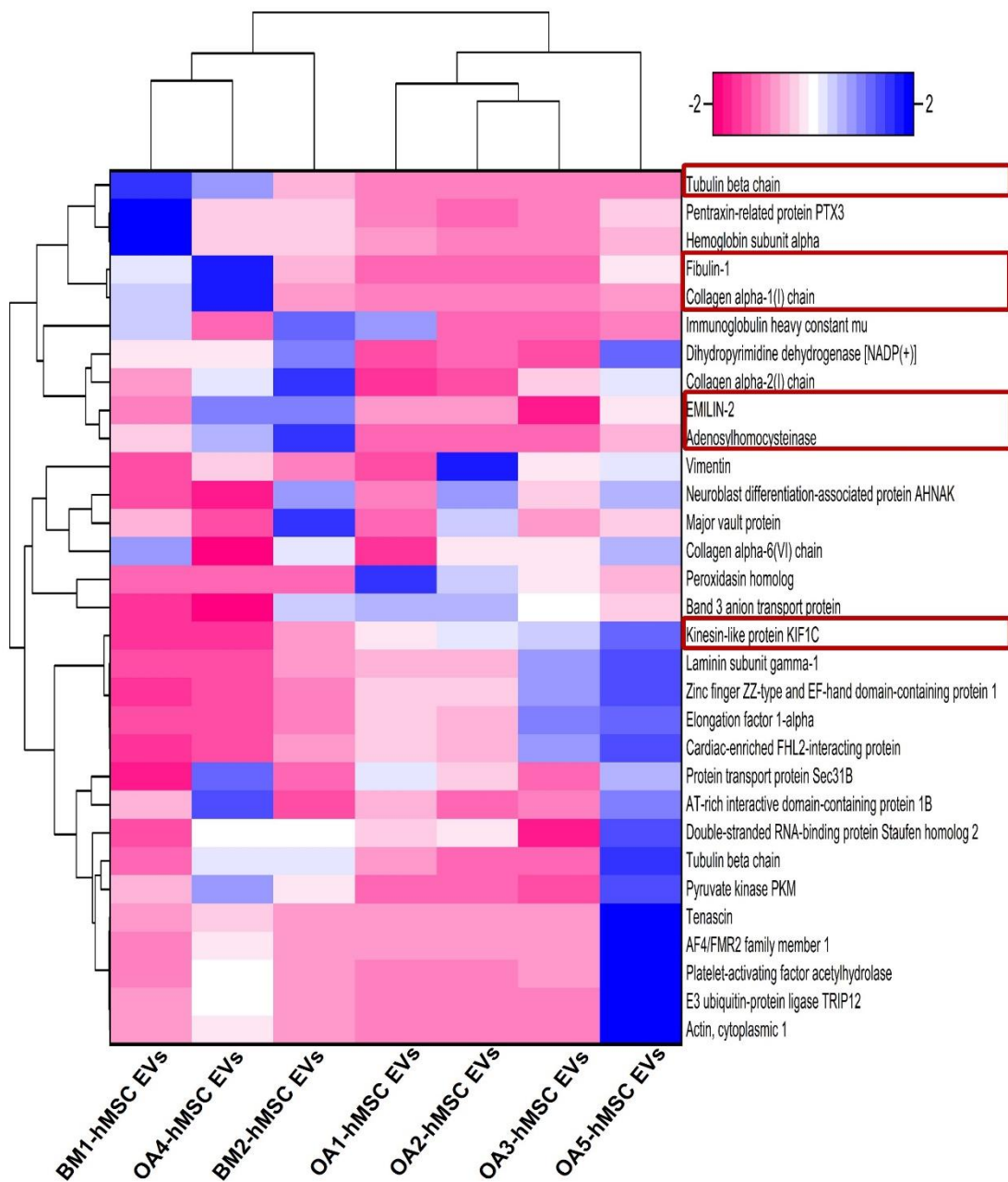**Figure 5. 9. Heatmap analysis of the detected peptide content from EVs secreted during the first 14 days of expansion post-isolation for bone stroma cells.**
Samples were isolated from osteoarthritic human femoral head and bone marrow of healthy donors s.   Data has been normalized and standardized in Excel and the presented heatmap and dendrogram were generated with OriginLab Software based on Pearson correlation analysis.

The comparison of the data from the day 7 time point and day 14 time point in EVs secreted by hMSCs purification, it appears that 9 proteins are maintained in the EVs population derived from both, healthy and diseased hMSCs: adenosyl homocysteinase, collagen alpha-1(I), collagen alpha-2(I), elongation factor 1-alpha 1, fibulin 1, immunoglobulin heavy constant mu, platelet-activating factor acetyl hydrolase, pyruvate kinase PKM and tubulin beta chain.

The quantitative analysis of the proteins that have been found maintained in the EVs secretion of hMSCs across the isolation period, shows that the majority of proteins presented in Fig. 5.10 are secreted in a higher amount on day 14 post isolation than in day 7 post isolation. Elongation factor 1, fibulin, platelet activating factor acetyl hydrolase, immunoglobulin heavy constant mu, pyruvate kinase PKM, tubulin β chain and collagen alpha 1(I) were recorded with a higher abundance in the EVs collected at day 14 by comparison with the day 7 collection. The levels of collagen alpha 1(I) were similar across the time points as well as in the healthy and diseased samples. Only the Adenosyl homocysteinase secretion seems to decrease on day 14 compared to day 7.
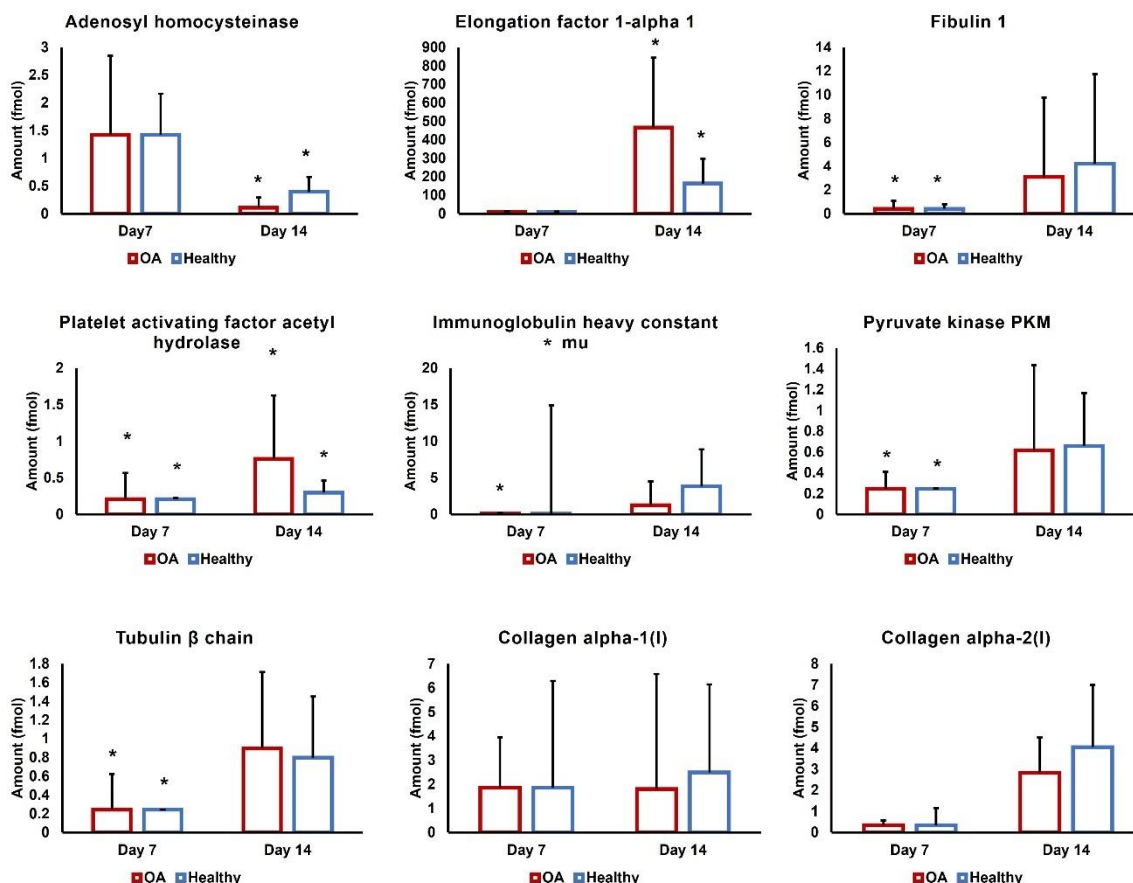
Figure 5. 10. Common peptides detected in the hMSC-EVs

This figure summarises the differences in the amount (fmol) (n=5 +/-SD per sample) of the peptides detected in both hMSC-EVs groups (day 7 and day 14 post isolation) for healthy and diseased (OA) bone hMSC. The data is organised in individual bar charts graphs that refer to each individual commonly found protein. Statistical significance was analysed in MiniTab Software (2-sample T test) and the significantly found groups are marked with *** for very significant (p-value<=0.001), ** for highly significant (p-value<=0.01), and * for significant (p-value<=0.05) data groups.

Out of all detected proteins, the top 10 in detected fmol per biological group have been summarised in Table 5.5, to assess the differences between the level of proteins detected in EVs secreted by BM-hMSCs vs. OA-hMSCs.

The detected amounts (fmol) of some of the proteins selected and presented in Table 5.5 in both, BM-hMSCs and OA-hMSCs are compared in the graphs presented in Fig. 5.11.

An overall trend of increased abundance for peptides detected in the OA-hMSC-EVs compared with BM-hMSCs is detected in the abundant proteins found at day 7 and day 14.

The only proteins that were similar in abundance in BM-hMSC-EVs and OA-hMSC-EVs are the heat shock 75kDa protein (HSP75), leucine-rich repeat and IQ domain-containing protein 3 and neuroblast differentiation-associated protein AHNAK.

Table 5. 5. Top 10 abundant proteins detected in the hMSC derived EVs from healthy and diseased bone

	Day 7 post isolation		Day 14 post isolation	
	Healthy	Diseased	Healthy	Diseased
1	Glyceraldehyde-3-phosphate dehydrogenase	Cilia- and flagella-associated protein 54	Elongation factor 1-alpha	Elongation factor 1-alpha
2	Cilia- and flagella-associated protein 54	Immunoglobulin heavy constant mu	Neuroblast differentiation-associated protein AHNAK	Cardiac-enriched FHL2-interacting protein
3	Eosinophil peroxidase	Eosinophil peroxidase	Cardiac-enriched FHL2-interacting protein	Laminin subunit gamma 1
4	Leucine-rich repeat and IQ domain-containing protein 3	Elongation factor 1-alpha 1	Laminin subunit gamma 1	Neuroblast differentiation-associated protein AHNAK
5	Elongation factor 1-alpha 1	Glyceraldehyde-3-phosphate dehydrogenase	Zinc finger ZZ-type and EF-hand domain-containing protein 1	Zinc finger ZZ-type and EF-hand domain-containing protein 1
6	Transmembrane protein KIAA1109	Nesprin-2	Kinesin-like protein KIF1C	Kinesin-like protein KIF1C
7	Homeodomain-interacting protein kinase 4	Leucine-rich repeat and IQ domain-containing protein 3	Major vault protein	Protein transport protein Sec31B
8	Heat shock protein 75 kDa, mitochondrial	Tubulin beta-1 chain	Collagen alpha 6(VI) chain	AT-rich interactive domain-containing protein 1B
9	Hexokinase-3	Heat shock protein 75 kDa, mitochondrial	Protein transport protein Sec31B	Peroxidasin homolog
10	Actin-related protein 2/3 complex subunit 1B	Neurofibromin	Haemoglobin subunit alpha	Tenascin
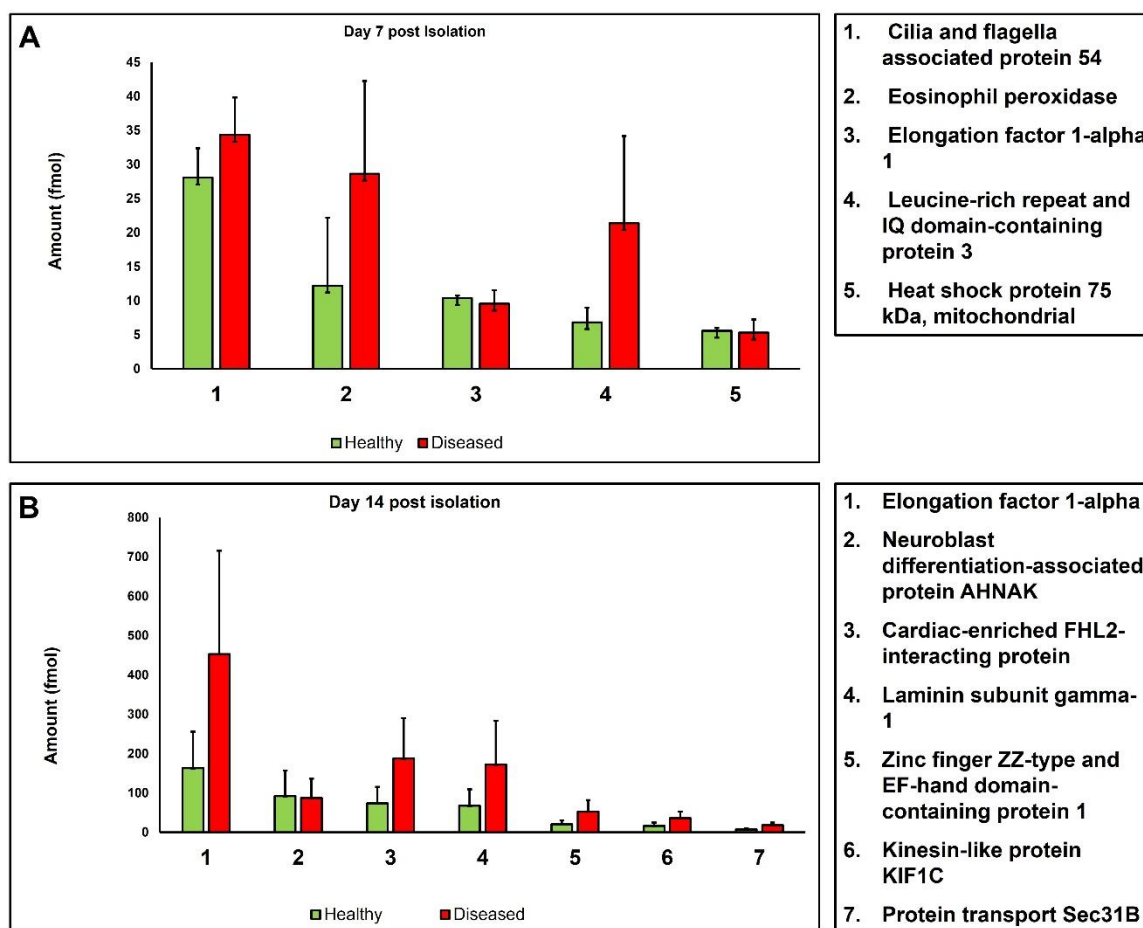
Figure 5. 11. Comparison between the most abundant proteins detected in group 1 (A) and group 2 (B).
BM-hMSCs-EV and OA-hMSC-EV detected proteins in group 1 and group 2, at day 7 (A) and at day 14 (B) post isolation. The mean (+/- SD) of the commonly found proteins in the top 10 most abundant proteins detected in the OA and healthy bone marrow subgroups detected on day 7 (A) and day 14 (B) post isolation are summarised and presented in the graphs A and B (n=5).

5.3.6. Peptide content identification in diseased cartilage derived EVs

Mass spectrometry analysis of the EVs secreted by cartilage derived progenitors indicate the presence of 68 unique proteins at day 7 post isolation and 69 unique proteins day 14 post isolation. Uniquely detected proteins were not present in the serum supplemented media sample. Fig. 5.12 shows the exclusion analysis carried out in order to remove from further analysis the proteins present in the serum of the cell culture media.
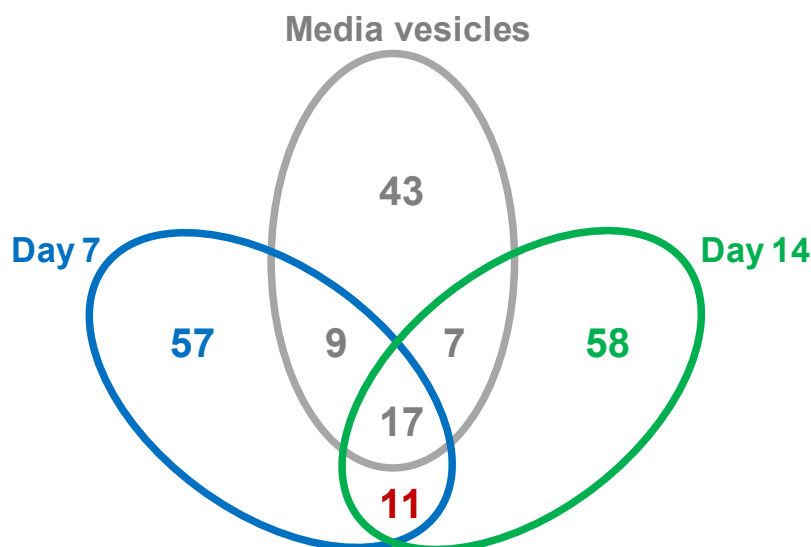
Figure 5. 12. Overlap analysis of peptides detected from the secretion of diseased human CPCs.
Comparative with secretion of bone originated progenitors, chondro- progenitors seem to keep a constant flow of secretion, with only 11 constant peptides expressed over the whole expansion period of time.

Compared with the bone derived EVs, cartilage derived EVs maintain the protein content, where 11 out of 68 at day 7 and 69 at day 14 proteins were found to be maintained in the content of the EVs. The amount of these identified proteins is compared in the graph from Fig. 5.15

In order to analyse the protein content of EVs derived from the cartilage tissue of the patients with osteoarthritis, the EVs secreted by CPCs at day 7 and day 14 post-isolation of 4 different patients were assessed by nano LC-MS/MS. The study intended to include the CPC-derived EVs from the tissue of the same patients presented in the analysis of bone stroma derived EVs. However, the isolation of CPCs from the articular cartilage of the femoral head collected from the osteoarthritic patient no.1 resulted in non-viable cells. In consequence the media collected at day 7, when this observation was made, was not processed further.

Furthermore, no healthy control was included in this group due to the lack of at least one source of healthy cartilage. All the articular cartilage tissue we had access to was considered osteoarthritic.

Peptides identified across the day 7 post-isolation EVs derived from the articular cartilage of patients with OA were characterised by variable abundance. The data summarised in Fig. 5.13 suggests that the EVs from each patient seem to vary in the abundance of detected peptides.

A correlation has been found between the data obtained from the CPC-EVs of patient no. 2 and patient no. 5 and between patient no.3 and patient no.4 (marked with red circles in Fig. 5.13). These correlations (marked with red squares in Fig. 5.13) appear to be distinctive between themselves, where low abundance in the first group (OA2-CPC and OA5-CPC) is paired by high abundance in the other group (OA3-CPC and OA4-CPC). These particular results made it difficult of reaching a conclusion regarding the identification of an OA disease marker across the examined samples.
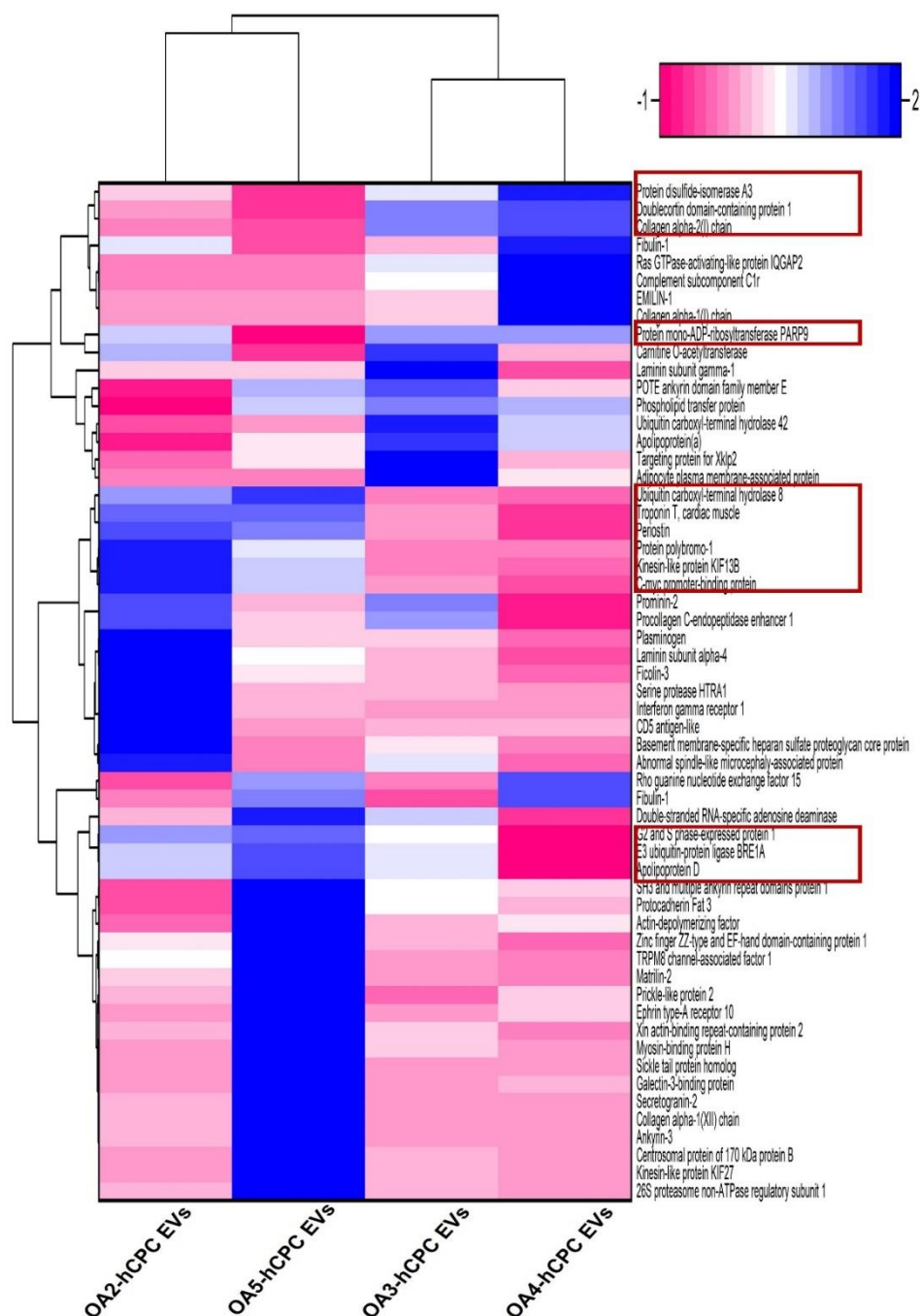
Figure 5. 13. Heatmap analysis of the detected peptide content from EVs secreted during the first 7 days of expansion post-isolation for diseased cartilage cells.
This heatmap summarises the standardised abundance of peptides detected in the secreted EVs of OA-hCPCs, 7 days post isolation, Pearson correlation was used to arrange and visualise the highest and the lowest abundance peptides across the sample group. Standardisation and arrangement were carried out in Excel and the heatmap was generated in OriginLab.

The analysis of peptide abundance across the OA-CPC derived EVs, 14 days post isolation showed no common abundance across the samples. However, a correlation was identified between the amount of EV peptides from OA patient no.3 and patient no.4, based on the high abundance of the peptides marked with red squares in Fig. 5.14.

Another correlation was found between the abundance of the detected peptides for patient no. 2 and patient no. 5 OA-CPC derived EVs, based on low abundance when compared to the patient no. 3 and patient no. 4 detected peptides from CPC derived EVs.
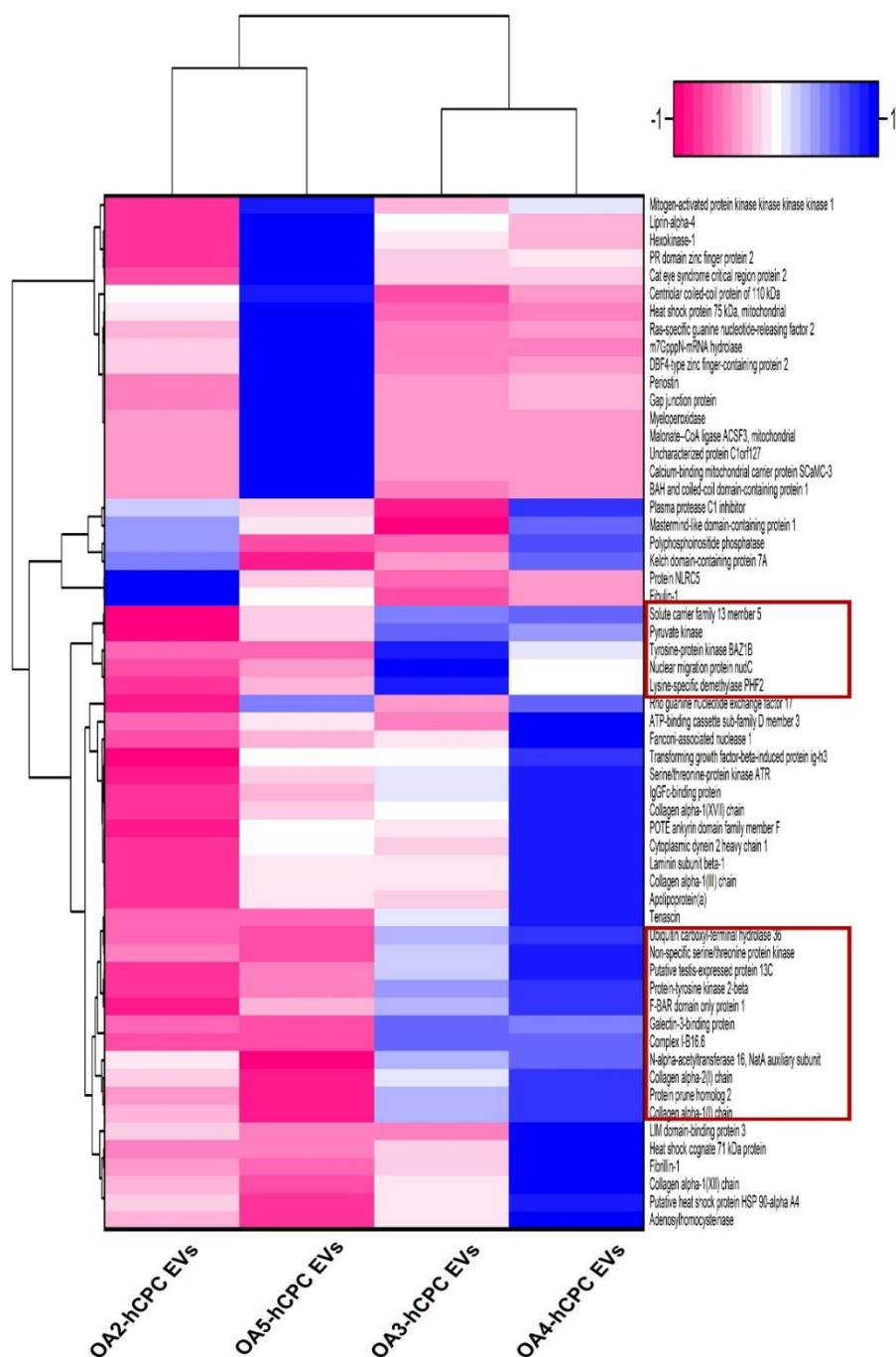
Figure 5. 14. Heatmap analysis of the detected peptide content from EVs secreted during the first 14 days of expansion post-isolation for diseased cartilage cells.
The heatmap summarises the standardised abundance of peptides detected in secreted EV ss from CPCs, 14 days post isolation. Pearson correlation was used to arrange and visualise the highest and the lowest concentrated peptides across the sample group. Standardisation and arrangement were carried out in Excel and the heatmap was generated in OriginLab.

Through overlap analysis, in the secretion of cartilage derived progenitors, 11 proteins appear to be present in the cell secreted EVs in both, day 7 and day 14 post-isolation. This detected number of common proteins in both groups (day 7 and day 14) is summarised across the samples and presented in the graph in Fig. 5.15.A significant increase was detected in the amount of apolipoprotein, collagen alpha-1(I), collagen alpha-2(I), POTE ankyrin domain family member, in day 14 compared with day 7 and a significant decrease in the amount of periostin.
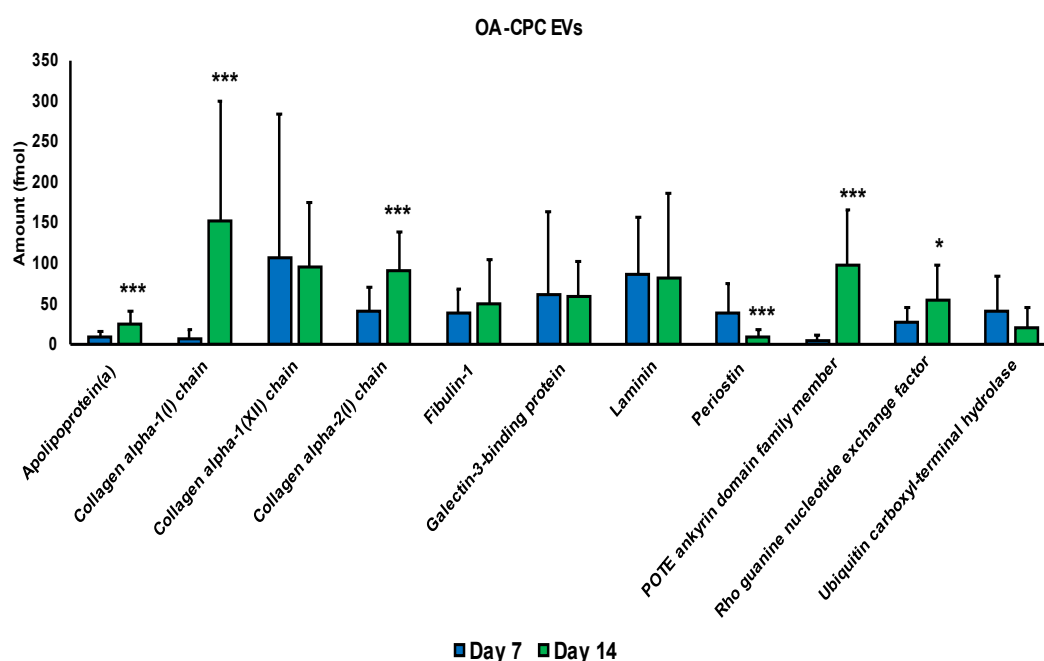
Figure 5. 15. Prevalent proteins detected in the secreted EVs from of OA-CPCs day 7 and day 14 post isolation.
The secreted peptides' amount detected in both stages of the cell expansion period has been analysed and represented in a bar chart in order to identify possible shifts in secretion. Statistical significance was analysed in MiniTab Software (2-sample T test) and the significantly found groups are marked with *** for very significant (p-value<=0.001), ** for highly significant (p-value<=0.01), * for significant (p-value<=0.05) data groups.

Table 5. 6. Top 10 most abundant proteins detected in EVs secreted from OA cartilage derived hCPCs.

	Day 7 post isolation	Day 14 post isolation
1	Sickle tail protein homolog	Calcium-binding mitochondrial carrier protein SCaMC-3
2	Ankyrin-3	Cytoplasmic dynein 2 heavy chain 1
3	Secretogranin-2	Fanconi-associated nuclease 1
4	Centrosomal protein of 170 kDa protein B	Tenascin
5	Abnormal spindle-like microcephaly-associated protein	Malonate--CoA ligase ACSF3, mitochondrial
6	Kinesin-like protein KIF27	Serine/threonine-protein kinase ATR
7	Protein polybromo-1	N-alpha-acetyltransferase 16, NatA auxiliary subunit
8	Serine protease HTRA1	Collagen alpha 1(I) chain
9	Matrilin-2	F-BAR domain only protein 1
10	Collagen alpha 1(XII) chain	Myeloperoxidase

In summary regarding the top 10 most abundant proteins detected in the OA-hCPC derived EVs there were no common proteins detected as present in day 7 and day 14 post isolation.

The common proteins presented in Fig. 5.15, are not between the most abundant proteins detected in group 3 and group 4 (Table 5.2).

5.4. Discussion:

Osteoarthritis (OA) is the most prevalent type of arthritis globally, and its incidence is rapidly increasing. According to the Lancet review summarised by ,Hunter, March and Chew, in 2020 OA was classified as the fifteenth most common cause of disability worldwide. During the on-set of OA, inflammatory mediators are released by the degraded ECM. The immune system is stimulated by these factors and start to produce pro-inflammatory cytokines (e.g., Tumor Necrosis Factor-α, Interleukin-1, Interleukin-6, Interleukin-15, Interleukin-10), proteases (matrix metalloproteinases (MMP) such MMP-1, MMP-3, MMP-13 and A disintegrin and metalloproteinase with thrombospondin motifs 5 (ADAMTS-5)) (Miller, Miller and Malfait, 2014; Malemud, 2019). The presence of these factors produced by the immune cells, subsequently will result in the structural degradation of cartilage ECM, damage of the subchondral bone and joint capsule hypertrophy, turning OA into a disease of the whole joint (Loeser *et al.*, 2012).

Diagnosis of OA is notoriously challenging, with the primary symptom of OA being chronic pain. At the on-set stages, this condition proves to be very hard to clinically diagnose. Currently, this relies on radiographic evidence (X-Ray, MRI) and exclusion of other potential joint pain linked conditions (synovitis, rheumatoid arthritis or infection).

In addition to diagnosis difficulties treatment of OA has also proved to be challenging. Currently, there is no gold standard therapy for OA, and current therapeutic strategies focus on managing disease-related symptoms rather than addressing the underlying cause.

Cell-based treatments, such as autologous MSC and chondrocyte transplantation, have emerged as a viable therapeutic option for OA in recent years. However, their restricted availability, the loss of function during *ex-vivo* expansion and reduced post-transplantation specificity limit their potential application in OA therapy (Steinert *et al.*, 2007). As a result, extracellular vesicles (EVs) produced by the cells in general, namely exosomes, are emerging as a unique and effective cell-free alternative to cell-based treatment for a variety of disease targets, including OA.

MSC are important for regenerative medicine research and clinical applications. They have been demonstrated to possess regenerative and immuno-modulatory effects in various disease models (e.g., wound healing, lung injury, liver injury, kidney injury, cardiovascular disease) (Frühbeis *et al.*, 2013; Rani *et al.*, 2015; Marote *et al.*, 2016).

MSCs actively secrete exosomes, and these can be easily isolated *in vitro* from the culture medium. Compared with other types of cells, MSCs secretion contains one of the highest amounts of exosomes (Yeo *et al.*, 2013).

Studies looking at the effects of MSC derived exosomes established that the administration of those instead of cell transplantation has similar beneficial effects to cell-based therapies (Clayton and Mason, 2009; Chen et al., 2011). They have been considered potent modulators of the immune response (Cossetti *et al.*, 2012).

Despite the fact that MSC-derived exosomes have shown significant improvements in a variety of disease models, they have just recently been considered for the treatment of OA. Inflammation is a significant factor in the pathogenesis of OA. MSC derived exosomes have been shown to inhibit the release of pro-inflammatory cytokines and increase the secretion of anti-inflammatory cytokines (Chen *et al.*, 2016). MSC derived exosomes not only suppress inflammation, but they also stimulate the repair of the damaged tissue by employment of the resident stem/progenitor population (Caplan and Dennis, 2006; S. Zhang *et al.*, 2016). The mechanism of action behind the MSC derived exosomes treatment in OA is mainly attributed to the delivery of miRNAs. For example, in OA, miR-140 and miR-320 are downregulated. They are involved in chondrogenesis and immune modulation by stimulation of IL-β1 secretion respectively. Therefore, treatment with MSC-derived exosomes is hypothesised to slow the progress of OA by delivery of the miRNA in deficit.

Differences in the content of exosomes in OA by comparison with the healthy stage can constitute a method for the diagnosis of OA. Potentially at the very early stages, by identification of the on-set stage specific bio factors.

In the incidence of OA, various studies have looked at biomarkers related with different processes and molecules involved in the pathophysiology of the disease. Biomarkers related to collagen metabolism, aggrecan metabolism, other proteins involved in joint homeostasis, inflammatory biomarkers, fibrosis indicating factors as well as bone cellular interactions related proteins have been investigated in clinical studies, with

little success. Despite the fact that a lot of promising research have been conducted in this area, no single biomarker has been identified that can be used in clinical diagnosis. All of the biomarkers assessed in OA patients and healthy individuals showed significant overlap (Garnero *et al.*, 2001; Lago *et al.*, 2008; Larsson *et al.*, 2012). More recent studies have correlated high levels of urinary C-terminal cross-linking telopeptide of type II collagen (CTX-II) and cartilage oligomeric matrix protein (COMP) with severe OA visible in radiographic evidence (Hao *et al.*, 2019; Arunrukthavon *et al.*, 2020). Therefore, they propose these 2 biomarkers as disease monitoring method.

Comparative with the above-mentioned studies, ours provides a more specific proteomic profile of the EVs derived from the stem/progenitor cells of the individual main tissues of the joint, bone and cartilage, rather than investigating the OA biomarkers in clinically available bodily fluids.

In this study we investigated the proteomic profile of the EVs isolated from the secretion of the *ex-vivo* culture of OA-hMSCs, OA-hCPCs and healthy BM-hMSCs. We focussed on the small EVs, known as exosomes, but non-specifically. We have found comparable differences in the phenotypic profile of the assessed EVs samples, differences in the levels of the peptide content of the healthy bone derived EVs and diseased bone derived EVs, and ultimately indications of disease markers in the protein cargo of the EVs secreted by the cells of the joint affected by OA.

SEM analysis has shown that the isolated EVs in our study present exosome like morphology. Exosomes are nano sized EVs characterised by spheroid appearance and a diameter of 30 to 300 nm (Jung and Mun, 2018). We have found EVs with these characteristics following the staining with glutaraldehyde, an exosome specific stain, and visualisation with SEM.

We also assessed the presence of the exosome specific markers. We achieved this by immuno staining with antibodies against CD9, CD63 and CD81, the tetraspanins widely used for the identification of bone marrow MSCs derived exosomes (Toh *et al.*, 2018). CD63 was found in all the representative samples we assessed, including the chondroprogenitors derived EVs. CD81 was also found present in all the assessed samples, with small variations. In BM-hMSC derived EVs at day 7 and OA-hCPC derived EVs at day 14 post isolation, the CD81 was recorded lower when compared

with the EVs isolated at the other available time point: day 14 post isolation for BM-hMSC-EVs and day 7 for OA-hCPC-EVs. Out of all investigated exosomes marker, the data recorded for the expression of CD9 appear to indicate an interesting result. The detection of CD9 is lower in the OA-hMSC-EVs and OA-hCPC-EVs than in BM-hMSC-EVs. All three types of cells were expanded in same conditions, without variations. Based on our observations, the lower expression of CD9 on the joint cells derived exosomes might constitute a criterion for OA diagnosis. The animal study presented by Sumiyoshi *et al.*, examined the implications of CD9 in the development of OA. They data correlated the low levels of CD9 with the progression of OA. Further investigations of CD9 in human cartilage tissue, are necessary to establish the full implications of CD9 in OA disease process.

Initial analysis of the proteomic content of EVs, by SDS-PAGE, indicated differences between the EVs samples derived from either the healthy vs diseased, or hMSC vs hCPC. An overall higher presence of the proteins was observed in hCPC derived EVs than in hMSC derived EVs. Based on previous studies that confirmed the presence of EVs in the serum used for supplementing the culture media, we decided to also include this type of control in our sample pool. EVs from standard medium batch, used for the *ex vivo* cell expansion, were isolated by the PEG enrichment isolation protocol. Separation of the EV protein content by SDS-PAGE, confirmed that indeed, there is a correlation between the serum supplemented medium EVs and EVs isolated from the secretion of the cells. As presented in Fig. 5.5, the proteins in EVs from serum supplemented media are present with a high intensity and not taking into consideration an exclusion of those prior to further investigation in the secretion of the cells expanded in that type of medium, can result in false peptide detection. An alternative approach would be the use of Knock-Out Serum (KOSR) instead of standard cell culture grade heat-inactivated FBS. While we need to investigate the viability of our primary cells in this cell culture supplement, we plan to explore this approach. Nevertheless, in our current study, to avoid false detection, we carried out exclusion analysis against the expansion culture media derived EVs, before proceeding with further analysis.

The nano LC-MS/MS analysis of our samples identified a lower number of proteins than expected. Under 100 viable proteins were detected in each of our biological groups (Table 5.2). In the utilised EVs isolation method, PEG enrichment, proved to be challenging for the analysis of the proteomic content by nano LC-MS/MS.

Considerable noise was observed while the data was acquired. This has been attributed to the remaining PEG. Preventive steps were taken to insure the elimination of contaminants. Unfortunately, the total clean-up of the samples was not optimal. While the PEG enrichment method has been reported as highly efficient for the isolation of EVs from various types of cells, we propose the use of different methods prior to mass spectrometry analysis.

Overall, the proteomic content of the hMSC-EVs derived from BM and OA-bone appears to decrease in terms of protein diversity the longer the cells are kept in culture. At day 7 post isolation, 87 different proteins were found in the content of the EVs, while only 31 different proteins were found at day 14 post isolation in the content of the EVs. This was observed across healthy and diseased EVs.

According to the concentration in fmol detected in the healthy EV samples (BM) and the diseased EVs samples (OA), the MSC specific EVs appear to be highly concentrated in the proteins such as cilia and flagella associated protein 54, eosinophil peroxidase and leucine-rich repeat and IQ domain-containing protein 3 at day 7 post isolation. Cilia is a protein associated with post-natal skeletogenesis (Moore, Yang and Jacobs, 2018). As the MSCs were isolated the bone compartment of the hip joints, the presence of this particular protein indicates the presence of spontaneous differentiation in the isolated cell population. At day 14, increased concentrations of elongation factor 1-alpha, cardiac-enriched FHL2-interacting protein, laminin subunit gamma 1, zinc finger ZZ-type and EF-hand domain-containing protein 1, kinesin-like protein KIF1C and protein transport Sec31B were detected in diseased MSC derived EVs in comparison with healthy MSC derived EVs.

Considering the origin of the cells that secreted EVs high in the above-mentioned proteins, the bone compartment of the hip joint, a correlation can be found between OA and the secretion of the resident MSCs in the affected joint. MSCs are known to have immuno-modulatory roles by secreting inhibitors of the immune response following injury. However, the proteins that are seen in increased concentrations in our datasets are not documented as being linked with the immune system. The presence of leucine-rich repeats might suggest biological processes that imply tyrosine kinase receptors.

It is possible that the increase in common immunomodulatory proteins secreted by diseased and healthy hMSCs is linked with the oxidative stress suffered by the cells in ex-vivo expansion culture. Their physiological micro-environment is known to be characterised by low levels of O_2.

We also found that MSCs secrete similar levels of collagen alpha 1 in both, diseased and healthy stages. The secretion of this protein was also constant in the culture of the hCPC, but in a considerably higher concentration (2-3 fmol in hMSCs and ~100 fmol in hCPCs).

Analysing the proteomic data organised in the heatmaps at Fig. 5.8 and Fig. 5.9, for the detection of an OA marker by taking into consideration the upregulated proteins in OA-hMSCs EVs compared with the BM-hMSCs EVs, cathepsin, annexin 1 and histone-lysine N-methyltransferase SETD2 proteins can be considered OA disease indicators. Their correlation with OA has been previously documented (Olszewska-Slonina *et al.*, 2013; Sampey *et al.*, 2000).

Secondly, comparative with the hMSCs, hCPCs are more consistent in their secretion as similar number of proteins were detected across the assessed time points post isolation (day 7 and day 14). With all of these no overall correlation was found across the EVs derived from all four hCPCs isolates. The heatmap analysis presented in Fig. 5.13 and Fig 5.14, shows a correlation between OA2-hCPC-EVs and OA5-hCPC-EVs and another one between OA3-hCPC-EVs and OA4-hCPC-EVs at both time points, day 7 and day 14, with no further correlation between these two subgroups.

The analysis of the common proteins secreted at both time points, day 7 and day 14 post isolation, indicate several proteins in the content of EVs derived from the CPC of the joint affected by OA. At day 14, in comparison with day 7, apolipoprotein, collagen alpha-1(I), collagen alpha-2(I), POTE ankyrin domain family member and Rho guanine nucleotide exchange factor are present in a higher concentration. Periostin is the only commonly detected protein across both time points that reduces its concentration the longer the cells are in *in vitro* culture. Periostin is a bone specific protein. Its presence in the secretion of cells isolated from the articular cartilage of individuals with OA suggests abnormal bone cell characteristics in the joint cartilage lining. This abnormal bone spurs form around the joints affected by OA. Unfortunately, we did not have access to the medical records of the patients included in this study, e.g. X-ray

diagnosis. However, considering the morphological appearance of the obtained hip joints, we can conclude that almost all of the femoral heads used for this study presented high bone density in the bone compartment and a thin smooth cartilage on the surface. No visible bone spurs were observed on the outside surface of the cartilage. Future studies were the presence of periostin in the cartilage tissue is assessed should be considered in the study of OA.

In conclusion, based on the results summarised in this chapter, we can assume that MSCs produced from OA hip joints have a higher level of secretory activity than healthy MSC derived from similar tissue structure. Although, the BM-hMSC utilised in this study as the healthy control, are derived from similar but not identical tissue are expected to have similar cellular characteristics. Moreover, the proteomic profile of EVs derived from the stem/progenitor component of the hip joint cartilage is distinct from that of EVs obtained from the stem/progenitor component bone compartment.

Ultimately, the presence of periostin in EVs produced from cartilage stem/progenitor cells together with the presence of cathepsin, annexin 1 and histone-lysine N-methyltransferase SETD2 in EVs produced from bone stem/progenitor cells may serve as a credible indicator of OA. Upon the latter finding, we propose that Periostin to be investigated in the secretion of hCPC under various *in vitro* conditions that replicate the OA mechanism of illness.

Chapter 6: Final Discussion

The aim of our study was to investigate the effect of neurotrophin 3 (NT-3) in bone and cartilage tissue regeneration through the modulation of resident stem/progenitor cell populations in joints affected by degenerative osteoarthritis (OA).

The work presented in this thesis discusses the presence of neurotrophin receptors in an OA animal model and primary cells isolated from patients with OA, the individual and combined effects of NGF effects and NT-3 on cellular maintenance, proliferation and differentiation and the protein/peptide content of EVs derived from the cartilage and bone compartments of human OA hip joints, in the search of disease markers.

OA is a complex degenerative disease with a strong inflammatory component that at first affects the articular cartilage inducing hypertrophy of the chondrocytes. The factor that causes this initial modification in tissue organisation, specific to onset of the OA is unknown (Chen *et al.*, 2017). In order to maintain its normal function, the cartilage in any synovial joint must be an elastic, well lubricated tissue without any major cellular processes taking place (Tamer, 2013). A hypertrophic cartilage is characterised by increased stiffness which results in poor functionality of the joint (Akkiraju and Nohe, 2015). Consequently, this will result in internal injury that will activate an immune response. A prolonged immune response impairs the tissue repair process and results in either augmentation of the injury or fibrosis induced by deficient tissue repair (Martel-Pelletier *et al.*, 2008) The presence of fibrosis will lead to future internal injury of the joint and will make this condition a 'self-sustained injury process' (Rim and Ju, 2021).

Even though the articular cartilage is the first joint tissue impacted by the onset of OA, this degenerative condition is a whole joint disease, as it induces modification and disruptions in all the structures of the affected joint (e.g., synovium and the synovial fluid, bone tissue, vascularisation, support structures) (Loeser *et al.*, 2012b). In order to have a broader investigation of this condition, we included in this study the stem/progenitor cells originated from the two main tissues of the human joint, the bone compartment, and the articular cartilage.

Some of the treatment approaches that rely on the MSC regenerative properties by inducing cartilage and tissue repair in joints affected by OA, imply autologous transplantation of *ex-vivo* expanded cultured MSCs from the bone marrow of the

patient to the site of injury, by intra-articular injections (Hwang *et al.*, 2021). In bone marrow, MSCs reside in a complex micro-environment known as the bone marrow niche (Ehninger and Trumpp, 2011). The disruption on that specific micro-environment and expansion in a new environment has the potential to induce morphological and phenotypical changes in the cell population prepared for transplantation (Kokkaliaris and Scadden, 2020). This will result in non-specificity and poor efficacy of the therapy. OA has a strong inflammatory component. In skeletal tissue, MSCs have immuno-modulatory roles by keeping under control the post-injury immune response. In advanced OA, MSC fail to fulfil this function, indicating that MSC's biology is also affected by OA (Najar *et al.*, 2020). Transplanting MSCs that have compromised immuno-modulatory capabilities and can bring significant non-specificity in the cellular micro-environment of the joint has the potential to induce an increase in inflammation (Musiał-Wysocka, Kot and Majka, 2019b).

Therefore, we hypothesised that regulation of bone and cartilage resident stem/progenitor cell maintenance, proliferation, differentiation, and secretion may result in improved tissue repair. p75NTR, a universal bone marrow MSC marker (CD271) (Jones *et al.*, 2002; Quirici *et al.*, 2002), with activating potential for the above-mentioned cellular processes, offers a potential tool for internal modulation of these cells. Regulating the resident stem/progenitor cells in the joints with the right modulation mechanism has the potential to induce healthy tissue repair and even to halt or reverse the OA degeneration.

A study by Cuthbert *et al*. has provided evidence in favour of the therapeutic use of p75NTR positively selected MSCs in the treatment of osteoarthritis, as being the more effective in the post-transplantation homing compared, with the standard practice.

6.1. Neurotrophin receptors in the OA joint (animal model)

The detection of neurotrophins receptors (p75NTR, Trk A, Trk B and Trk C) was reduced in rat joints affected by induced OA, according to the outcome of animal-based studies presented in Chapter 3. This observation indicates that in the pathophysiology of OA, the incidence of these neurotrophins receptors is reduced. This is true for the p75NTR in cartilaginous structures, such the growth plate and articular cartilage of the joint, for Trk A in the bone compartment of the joint in, for Trk B in the bone

compartment and the growth plate of the rat joint and for Trk C across all the structures of the joint.

6.2. NT-3 effects on *in vitro* cellular proliferation and differentiation

The *in vitro* assays carried out in rat and human cells, indicate that the effect of NT-3 on cellular maintenance, proliferation and differentiation could be modulated by the ratio of p75NTR/Trk C receptors on the cell membrane, as that was detected through a number of immunohistochemistry experiments on PC12 rat cells and primary human bone and cartilage stem/progenitor cells (hMSC and hCPC).

The NT-3 treatment in PC12 resulted in stimulation of proliferation and indications that differentiation is inhibited.

Clear results regarding the stimulation of proliferation by treatment with NT-3 were observed in PC12. But when investigated in hMSC and hCPCs, the results of NT-3 treatment showed inhibition of proliferation, with patient variability. By looking at the immunohistochemistry analysis that refers to the presence of NT-3 specific receptors, Trk C and p75NTR, comparable differences are noticed between PC12 and hMSC and hCPC. P75NTR was found present in all the assessed cells, while Trk C was found absent in healthy hMSC, with a reduced presence in diseased hMSC and it was only present in PC12 and hCPC with considerable intensity. The difference in cellular viability following NT-3 treatment could be correlated with the presence of Trk C on the cell membrane. Moreover, in the absence of Trk C, NT-3 appears to induce cell death by activation of p75NTR. We rely again on the results immuno staining carried out for the detection of p75NTR and Trk C across the investigated cell lines.

A stimulation of cellular viability was observed in the human cartilage derived stem/progenitors (hCPCs) treated with NT-3 in combination with NGF. The individual treatment with NGF and NT-3 resulted in inhibition of cellular viability. As hCPCs included in this study express p75NTR and Trk C, according to the immuno staining, we suspect that the enhancement of proliferation could have been the result of a cooperation between the NT-3 -Trk C and NGF – p75NTR activated signalling pathways.

The upregulated expression of Trk C in the OA-hCPCs compared with the BM-hMSCs, that were found negative for Trk C, suggests that Trk C might be linked with the OA disease mechanism. Additionally, NT-3 may be associated with chondro-hypertrophy. Or tissue degradation, as Trk C has been defined as a dependency receptor. In neuronal cells, Trk C induces proliferation when activated by NT-3. But it induces apoptosis on its own when NT-3 is not present (Tauszig-Delamasure *et al.*, 2007). This finding raises important questions about the NT-3 – Trk C – p75NTR signalling pathway in cartilage hypertrophy and tissue degeneration. This might get us closer to determining the cause of OA.

NT-3 and Trk C have been previously found involved in the differentiation of bone marrow originated MSC (Qiu *et al.*, 2015).

In our *in vitro* studies, combined NT-3 and NGF treatment of PC12 showed an inhibition of the differentiation potential by comparison with the NGF treatment. PC12 neurite outgrowth is mediated through p75NTR. The presence of NT-3 in the neurotrophic treatment of PC12 induced inhibition of this process, indicating that NT-3 either blocks p75NTR and as consequence differentiation is not induced, or the NT-3 mediated signalling pathway impairs the differentiation that is taking place in parallel through NGF – p75NTR mediated signalling.

Results that correlate only partially with the effects of NT-3 on PC12 differentiation, were observed in the assessment of NT-3 on the osteo-differentiation of hMSCs. The cells from 2 out of 4 tested patient samples showed an increase in osteo-differentiation when NT-3 was present, individually or in combination with NGF, while the rest of the patient sample as well as healthy donor sample showed no influence in cellular viability.

We recommend a future study where the differentiation potential of NT-3 is compared on positively selected cells with dual expression of Trk C and p75NTR, and single expression for either Trk C or p75NTR in order to describe the effect of NT-3 in osteo-differentiation in detail.

According to our results obtained from the *in vitro* assays and the immunostaining of the cells, in regard to the regeneration of bone and cartilage, it appears that NT-3 mediated signalling through Trk C – p75NTR could result in cell proliferation and inhibition of differentiation. Moreover, the NT-3 mediated signalling through p75NTR only, could result in the augmentation of osteo-differentiation and impairment of cellular viability.

In regard to bone and cartilage regeneration, our results gathered from the *in vitro* assays suggest that NT-3 could induce cell proliferation when both NT-3 specific receptors, p75NTR and Trk C, are available on the cell membrane. Moreover, the presence of p75NTR on the surface membrane of the cells treated with NT-3 appears to result in the augmentation of osteo-differentiation and impairment of cellular viability.

We anticipate that an *in vitro* evolution of the exogenous NT-3 on the proliferation and differentiation of the cells that are positively selected for p75NTR/Trk C and p75NTR only can confirmed the above suspected signalling mechanism.

Further *in vivo* evaluation of the exogenous NT-3 effects on tissue repair can be paired the above-recommended *in vitro* study in order to provide an overall understanding of the NT-3's role in skeletal tissue regeneration. Furthermore, we propose that a comprehensive gene expression analysis examining the status of active signalling pathways for cellular proliferation and differentiation will be able to elucidate the specific mechanism of action behind theNT-3 regenerative potential in bone and cartilage tissue regeneration.

Taking into consideration the results obtained in the animal study and in *in vitro* assays on primary human stem/progenitor cells from cartilage and bone, we can point out that neurotrophin signalling pathway, might be involved in key processes of the OA pathophysiology.

A full understanding of the neurotrophin signalling pathway in the human joints, can provide a strong basis for the development of the pharmacological strategies to treat degenerative conditions such OA. Moreover, a correct modulation of the neurotrophin mediated signalling in the resident stem/progenitor cell population, by exogenous over-expression, may enhance the tissue regeneration after mechanically induced injury of the cartilage and bone tissue in joints.

6.3. OA EVs proteomic analysis

The proteomic analysis of the EVs secreted by MSCs and CPCs from the human hip joint with advanced OA, resulted in identification of potential diseased markers or therapeutic targets. This was mainly established through comparison of the peptide abundance between BM-hMSCs derived EVs, OA-hMSCs and OA-hCPCs derived EVs. According to our investigation of the exosome specific membrane protein profile of the EVs, low levels of CD9 are specific to osteoarthritic tissue originated stem/progenitor cells (MSCs and CPCs). Additionally, the EVs secretion of CPCs was found more stable across the post—isolation expansion period, by comparison with the EVs secretion of MSCs. The heatmap analysis of detected proteins at day 7 post isolation, established comparative correlation that separated data in two subgroups based on the state of the source tissue (healthy and diseased). We were able to identify indicators of OA in the OA-hMSCs derived EVs, through the detection of proteins (cathepsin, annexin 1 and histone-lysine N-methyltransferase SETD2) previously linked with this condition. We also detection low level or absence of MSC specific proteins linked to normal functionality in OA-hMSCs derived EVs when compared with the BM-hMSCs derived EVs.

At day 14 post isolation, the proteomic analysis of the EVs derived from hMSCs showed non-specific correlation between all the samples, healthy and diseased, indicating that the secretion is influenced by the *in vitro* culture conditions, and it is not suitable for disease markers investigation. Because they have been removed from their natural micro-environment, it is possible that the cells have experienced changes in culture. And the new environment, culture media, has an impact on the cells and their secretion.

The proteomic analysis of OA-hCPCs derived EVs revealed expression of the bone specific protein, periostin. This can be correlated with the ossification of the cartilage reported in cases of advanced OA (Chen *et al.*, 2017).

Finally, rather than presenting a general disease marker for OA, the proteomic analysis of the EVs released by the joint cells afflicted by this condition reflects the deteriorated state caused by the progression of disease. The analysis of EVs derived from the joint tissue has the potential to indicate the cellular context of the joint structure and provide

the clinicians with a specific snapshot of the cellular processes taking place in the joint at the moment of investigation.

In regard to OA, researchers in the field agree that it has a complex pathophysiology and modifications taking place in the whole joint that are difficult to investigate separately. NGF -Trk A signalling is well described in this degenerative condition. The implications of other neurotrophins and their receptors is poorly explored currently. Our study proposes that neurotrophin signalling pathway mediated through Trk receptors in collaboration with p75NTR is the key in modulating not only the chronic pain afflicted by OA, but also the inflammation and the abnormal cell differentiation that are present in OA pathology. The whole-joint assessment of the neurotrophin receptor in the OA animal model, indicate that joint degeneration induces a decrease in the incidence of neurotrophin receptors. No similar studies in the current available specialist literature addresses this.

Neurotrophins, particularly NGF and BDNF, have been extensively studied in the intra-uterine and adult nervous system, which resulted in successful therapeutic strategies for nerve repair. Since its discovery, NT-3 has been found to induce cellular proliferation and maintenance of different populations of neurons. It also been found to be responsible of healthy differentiation with indirect implications (Houlton *et al.*, 2019; Kelamangalath & Smith, 2013; Miller & Kaplan, 2001; Su *et al.*, 2018).

Considering the potential of NT-3 in nerve repair and healthy differentiation, a translation of these properties into other systems has caught the attention of researchers lately. Studies that propose the usage of BM-MSCs, cells with regenerative properties, to enhance the neuro-differentiation by genetically induced NT-3 overexpression, have emerged (Yan *et al.*, 2016).

The influence of this particular neurotropic factor on the cell proliferation and differentiation was also translated in the musculo-skeletal system. NT-3 was found to influence BMP-2 and VEGF in bone injury promoting osteo-differentiation (Su *et al.*, 2016). The data in this study suggests that the most effective NT-3 promoted bone tissue repair is Trk C mediated. The findings of our study partially agree with the above-mentioned effects of NT-3. We found that NT-3 enhances the osteo-differentiation of human osteoarthritic bone derived stem/progenitor cells, as well as the proliferation, but the latter is dependent on the p75NTR/Trk C proportion.

The findings of this research project are based on data obtained from elderly (75-80 years old) patients with osteoarthritis and perhaps other illnesses. Because of patient variability, significant variability exists in the datasets presented in this work. For the interpretation of some of this project datasets we established the key findings mainly based on trends we have identified by analysing the data both in groups and individually. We believe that this is the most beneficial approach that has allowed us to retrieve all of the relevant information from the acquired data sets, to address the implication of neurotrophin signalling pathway in the pathophysiology of OA, as well as in tissue healing.

6.2. Summary of key findings:

- Downregulation of all neurotrophins (p75NTR and Trk receptors) receptors in the knee joints with OA pathophysiology (animal model-based results).

- Trk C is upregulated in the CPC and downregulated in MSC. Trk C has been found positively expressed only in the stem/progenitor cells from the cartilage of the hip joint affected by OA. The bone stem/progenitor cells were found negative with low expression of Trk C.

- NT-3 - p75NTR mediated signalling inhibits MSC cellular viability but promotes the osteo-differentiation.

- NT-3 + NGF may promote CPC proliferation through signalling mediated by p75NTR -Trk C.

- Human OA joint tissue derived EVs are characterised by atypical high concentrations of Periostin in the cartilage and reduction of MSC function indicators in the bone compartment.

In conclusion, and according to the data presented in this study, the neurotrophin signalling pathway could be an important player in the development of joint degenerative OA as well as in the bone and cartilage tissue regeneration. Moreover, the state of the cellular environment in the joints affected by OA can be described by the proteomic content of EVs, and constitute a potential approach in clinical diagnosis, as well as personalised treatment.

References

Aggarwal, S. and Pittenger, M.F. (2005) "Human mesenchymal stem cells modulate allogeneic immune cell responses," *Blood*, 105(4), pp. 1815–1822. doi:10.1182/blood-2004-04-1559.

Akkiraju, H. and Nohe, A. (2015) "Role of chondrocytes in cartilage formation, progression of osteoarthritis and cartilage regeneration," *Journal of Developmental Biology*. MDPI Multidisciplinary Digital Publishing Institute, pp. 177–192. doi:10.3390/jdb3040177.

Álvarez-Viejo, M. (2015a) "CD271 as a marker to identify mesenchymal stem cells from diverse sources before culture," *World Journal of Stem Cells*, 7(2), p. 470. doi:10.4252/wjsc.v7.i2.470.

Álvarez-Viejo, M. (2015b) "CD271 as a marker to identify mesenchymal stem cells from diverse sources before culture," *World Journal of Stem Cells*, 7(2), p. 470. doi:10.4252/wjsc.v7.i2.470.

Ammendrup-Johnsen, I. *et al.* (2015) "Neurotrophin-3 enhances the synaptic organizing function of trkc–protein tyrosine phosphatase σ in rat hippocampal neurons," *Journal of Neuroscience*, 35(36), pp. 12425–12431. doi:10.1523/JNEUROSCI.1330-15.2015.

Araki Y, Aizaki Y, Sato K, Oda H, Kurokawa R, Mimura T. Altered gene expression profiles of histone lysine methyltransferases and demethylases in rheumatoid arthritis synovial fibroblasts. Clin Exp Rheumatol. 2018 Mar-Apr;36(2):314-316. Epub 2018 Jan 31. PMID: 29465369.

Arunrukthavon, P. *et al.* (2020) "Can urinary CTX-II be a biomarker for knee osteoarthritis?," *Arthroplasty*, 2(1). doi:10.1186/s42836-020-0024-2.

Asaumi, K. *et al.* (2000) *Expression of Neurotrophins and Their Receptors (TRK) During Fracture Healing*.

Aslam, M. *et al.* (2009) "Bone marrow stromal cells attenuate lung injury in a murine model of neonatal chronic lung disease," *American Journal of Respiratory and Critical Care Medicine*, 180(11), pp. 1122–1130. doi:10.1164/rccm.200902-0242OC.

Attwood, S.W. and Edel, M.J. (2019) "ips-cell technology and the problem of genetic instability—can it ever be safe for clinical use?," *Journal of Clinical Medicine*. MDPI. doi:10.3390/jcm8030288.

Augello, A. *et al.* (2005) "Bone marrow mesenchymal progenitor cells inhibit lymphocyte proliferation by activation of the programmed death 1 pathway," *European Journal of Immunology*, 35(5), pp. 1482–1490. doi:10.1002/eji.200425405.

Bacakova, L. *et al.* (2018) "Stem cells: their source, potency and use in regenerative therapies with focus on adipose-derived stem cells – a review," *Biotechnology Advances*. Elsevier Inc., pp. 1111–1126. doi:10.1016/j.biotechadv.2018.03.011.

Baldwin, A.N. *et al.* (1992) "Studies on the structure and binding properties of the cysteine-rich domain of rat low affinity nerve growth factor receptor (p75(NGFR))," *Journal of Biological Chemistry*, 267(12), pp. 8352–8359. doi:10.1016/s0021-9258(18)42451-9.

Bamji, S.X. *et al.* (1998) *The p75 Neurotrophin Receptor Mediates Neuronal Apoptosis and Is Essential for Naturally Occurring Sympathetic Neuron Death*, *The Journal of Cell Biology*. Available at: http://www.jcb.org.

Barde, Y.-A., Edgar, D. and Thoenen, H. (1982) *Purification of a new neurotrophic factor from mammalian brain*, *The EMBO Journal*.

Barker, P., 2004. p75NTR Is Positively Promiscuous. *Neuron*, 42(4), pp.529-533.

Beattie, M.S. *et al.* (2002) *ProNGF Induces p75-Mediated Death of Oligodendrocytes following Spinal Cord Injury TrkA was not expressed in a cell. With the finding that proNGF can activate p75 regardless of the presence of TrkA, the ratio of proNGF to mature NGF now emerges as a critical regulatory factor for the maintenance of the*, *Neuron*.

Becerra, J., Andrades, J., Guerado, E., Zamora-Navas, P., López-Puertas, J. and Reddi, A., 2010. Articular Cartilage: Structure and Regeneration. *Tissue Engineering Part B: Reviews*, 16(6), pp.617-627.

Becker, J.A., Daily, J.P. and Pohlgeers, K.M. (2016) *Acute Monoarthritis: Diagnosis in Adults*. Available at: www.aafp.org/afp.

Becker, K. *et al.* (2018) "p75 Neurotrophin Receptor: A Double-Edged Sword in Pathology and Regeneration of the Central Nervous System," *Veterinary Pathology*. SAGE Publications Inc., pp. 786–801. doi:10.1177/0300985818781930.

Berkemeier, L.R. *et al.* (1991) *Neurotrophin-5: A Novel Neurotrophic Factor That Activates trk and trkB*.

Blom, A.B. *et al.* (2009) "Involvement of the Wnt signaling pathway in experimental and human osteoarthritis: Prominent role of Wnt-induced signaling protein 1," *Arthritis and Rheumatism*, 60(2), pp. 501–512. doi:10.1002/art.24247.

Bongso, A. and Fong, C.Y. (2013) "The Therapeutic Potential, Challenges and Future Clinical Directions of Stem Cells from the Wharton's Jelly of the Human Umbilical Cord," *Stem Cell Reviews and Reports*. Humana Press Inc., pp. 226–240. doi:10.1007/s12015-012-9418-z.

Bothwell, M. (1995) *FUNCTIONAL INTERACTIONS OF NEUROTROPHINS AND NEUROTROPHIN RECEPTORS*, *Annu. Rev. Neurosci*. Available at: www.annualreviews.org.

Boulet, A.M. *et al.* (2004) "The roles of Fgf4 and Fgf8 in limb bud initiation and outgrowth," *Developmental Biology*, 273(2), pp. 361–372. doi:10.1016/j.ydbio.2004.06.012.

Braun, H.J. and Gold, G.E. (2012) "Diagnosis of osteoarthritis: Imaging," *Bone*, 51(2), pp. 278–288. doi:10.1016/j.bone.2011.11.019.

Breeland G, Sinkler MA, Menezes RG. Embryology, Bone Ossification. [Updated 2021 May 8]. In: StatPearls [Internet]. Treasure Island (FL): StatPearls Publishing; 2022 Jan-. Available from: https://www.ncbi.nlm.nih.gov/books/NBK539718/

Bronfman, F.C. (2007) *Metalloproteases and c-secretase: new membrane partners regulating p75 neurotrophin receptor signaling?*, *J. Neurochem.*

Calabrese, G. *et al.* (2015) "Potential effect of CD271 on human mesenchymal stromal cell proliferation and differentiation," *International Journal of Molecular Sciences*, 16(7), pp. 15609–15624. doi:10.3390/ijms160715609.

Campbell, T.M. *et al.* (2016) "Mesenchymal Stem Cell Alterations in Bone Marrow Lesions in Patients With Hip Osteoarthritis," *Arthritis and Rheumatology*, 68(7), pp. 1648–1659. doi:10.1002/art.39622.

Caplan, A.I. (1991) *Mesenchymal Stem Cells**, *Journal of Orthopaedic Research*. Orthopaedic Research Society.

Caplan, A.I. (2017) "Mesenchymal stem cells: Time to change the name!," *Stem Cells Translational Medicine*, 6(6), pp. 1445–1451. doi:10.1002/sctm.17-0051.

Caplan, A.I. and Dennis, J.E. (2006) "Mesenchymal stem cells as trophic mediators," *Journal of Cellular Biochemistry*, pp. 1076–1084. doi:10.1002/jcb.20886.

Carter, B., Kaltschmidt, C., Kaltschmidt, B., Offenhäuser, N., Böhm-Matthaei, R., Baeuerle, P. and Barde, Y., 1996. Selective Activation of NF-κB by Nerve Growth Factor Through the Neurotrophin Receptor p75. *Science*, 272(5261), pp.542-545.

Catheline, S.E. *et al.* (2019) "Chondrocyte-Specific RUNX2 Overexpression Accelerates Post-traumatic Osteoarthritis Progression in Adult Mice," *Journal of Bone and Mineral Research*, 34(9), pp. 1676–1689. doi:10.1002/jbmr.3737.

Chen, D. *et al.* (2017a) "Osteoarthritis: Toward a comprehensive understanding of pathological mechanism," *Bone Research*. Sichuan University. doi:10.1038/boneres.2016.44.

Chen, D. *et al.* (2017b) "Osteoarthritis: Toward a comprehensive understanding of pathological mechanism," *Bone Research*. Sichuan University. doi:10.1038/boneres.2016.44.

Chen, T.S. *et al.* (2011) "Enabling a robust scalable manufacturing process for therapeutic exosomes through oncogenic immortalization of human ESC-derived MSCs," *Journal of Translational Medicine*, 9. doi:10.1186/1479-5876-9-47.

Chen, W. *et al.* (2016) "Immunomodulatory effects of mesenchymal stromal cells-derived exosome," *Immunologic Research*, 64(4), pp. 831–840. doi:10.1007/s12026-016-8798-6.

Cheng, J. and Abdi, S. (2007) *COMPLICATIONS OF JOINT, TENDON, AND MUSCLE INJECTIONS*.

Choi, Y., Halbritter, J., Braun, D., Schueler, M., Schapiro, D., Rim, J., Nandadasa, S., Choi, W., Widmeier, E., Shril, S., Körber, F., Sethi, S., Lifton, R., Beck, B., Apte, S., Gee, H. and Hildebrandt, F., 2019. Mutations of ADAMTS9 Cause Nephronophthisis-Related Ciliopathy. *The American Journal of Human Genetics*, 104(1), pp.45-54.

Christoffersen, J. and Landis, W.J. (1991) *A Contribution With Review to the Description of Mineralization of Bone and Other Calcified Tissues In Vivo*, THE ANATOMICAL RECORD.

Clary, D. 0 *et al.* (1994) *TrkA Cross-linking Mimics Neuronal Responses to Nerve Growth Factor*, *Molecular Biology of the Cell*.

Clayton phd, A. and md, M. (2009) *UPDATES AND DEVELOPMENTS IN ONCOLOGY Exosomes in tumour immunity*.

Cohen, S. (1960) *PURIFICATION OF A NERVE-GROWTH PROMOTING PROTEIN FROM THE MOUSE SALIVARY GLAND AND ITS NE URO-CYTOTOXIC ANTISER UM**, *Public Health Service*.

Cossetti, C. *et al.* (2012) "Extracellular membrane vesicles and immune regulation in the brain," *Frontiers in Physiology*, 3 MAY. doi:10.3389/fphys.2012.00117.

Cuevas-Diaz Duran, R. *et al.* (2013) "Age-related yield of adipose-derived stem cells bearing the low-affinity nerve growth factor receptor," *Stem Cells International* [Preprint]. doi:10.1155/2013/372164.

Cui Y, Luan J, Li H, Zhou X, Han J. Exosomes derived from mineralizing osteoblasts promote ST2 cell osteogenic differentiation by alteration of microRNA expression. FEBS Lett. 2016 Jan;590(1):185-92. doi: 10.1002/1873-3468.12024. Epub 2015 Dec 30. PMID: 26763102.

Curtis, E. *et al.* (2018) "A First-in-Human, Phase I Study of Neural Stem Cell Transplantation for Chronic Spinal Cord Injury," *Cell Stem Cell*, 22(6), pp. 941-950.e6. doi:10.1016/j.stem.2018.05.014.

Cuthbert, R.J. *et al.* (2015) "Examining the feasibility of clinical grade CD271+ enrichment of mesenchymal stromal cells for bone regeneration," *PLoS ONE*, 10(3). doi:10.1371/journal.pone.0117855.

Dai, L. *et al.* (2006) "Detection and initial characterization of synovial lining fragments in synovial fluid," *Rheumatology*, 45(5), pp. 533–537. doi:10.1093/rheumatology/kei206.

Dai, R. *et al.* (2018) "Intratracheal administration of adipose derived mesenchymal stem cells alleviates chronic asthma in a mouse model," *BMC Pulmonary Medicine*, 18(1). doi:10.1186/s12890-018-0701-x.

Dameshek, W., 1957. Editorial: Bone Marrow Transplantation—A Present-Day Challenge. *Blood*, 12(4), pp.321-323.

de Bernard B. Glycoproteins in the local mechanism of calcification. Clin Orthop Relat Res. 1982 Jan-Feb;(162):233-44. PMID: 6461463.

de Windt TS, Vonk LA, Slaper-Cortenbach IC, van den Broek MP, Nizak R, van Rijen MH, de Weger RA, Dhert WJ, Saris DB. Allogeneic Mesenchymal Stem Cells Stimulate Cartilage Regeneration and Are Safe for Single-Stage Cartilage Repair in Humans upon Mixture with Recycled Autologous Chondrons. Stem Cells. 2017 Jan;35(1):256-264. doi: 10.1002/stem.2475. Epub 2016 Aug 29. PMID: 27507787.

Deak, M. *et al.* (1998) *Mitogen-and stress-activated protein kinase-1 (MSK1) is directly activated by MAPK and SAPK2/p38, and may mediate activation of CREB*, *The EMBO Journal*.

Dechant, G. and Barde, Y.-A. (2002) *The neurotrophin receptor p75 NTR : novel functions and implications for diseases of the nervous system*. Available at: http://www.nature.com/natureneuroscience.

Defreitas, M.F., Mcquillen, P.S. and Shatz, C.J. (2001) *A Novel p75NTR Signaling Pathway Promotes Survival, Not Death, of Immunopurified Neocortical Subplate Neurons*.

Deponti, D. *et al.* (2009) "The Low-Affinity Receptor for Neurotrophins p75 NTR Plays a Key Role for Satellite Cell Function in Muscle Repair Acting via RhoA," *Molecular Biology of the Cell*, 20, pp. 3620–3627. doi:10.1091/mbc.E09.

Dezawa, M., Ishikawa, H., Itokazu, Y., Yoshihara, T., Hoshino, M., Takeda, S., Ide, C. and Nabeshima, Y., 2005. Bone Marrow Stromal Cells Generate Muscle Cells and Repair Muscle Degeneration. *Science*, 309(5732), pp.314-317.

di Maggio, N. *et al.* (2017) "Extracellular matrix and α 5 β 1 integrin signaling control the maintenance of bone formation capacity by human adipose-derived stromal cells," *Scientific Reports*, 7. doi:10.1038/srep44398.

di Nicola, V. (2020) "Degenerative osteoarthritis a reversible chronic disease," *Regenerative Therapy*. Japanese Society of Regenerative Medicine, pp. 149–160. doi:10.1016/j.reth.2020.07.007.

Dimicco, M.A. *et al.* (2002) "Integrative articular cartilage repair: Dependence on developmental stage and collagen metabolism," *Osteoarthritis and Cartilage*, 10(3), pp. 218–225. doi:10.1053/joca.2001.0502.

Ding, M. *et al.* (2012) "Targeting Runx2 expression in hypertrophic chondrocytes impairs endochondral ossification during early skeletal development," *Journal of Cellular Physiology*, 227(10), pp. 3446–3456. doi:10.1002/jcp.24045.

Distefano, P.S. *et al.* (1993) *Involvement of a Metalloprotease in Low-Affinity Nerve Growth Factor Receptor Truncation: Inhibition of Truncation ii, vitro and in vivo*, *The Journal of Neuroscience*.

Dolstra, H. *et al.* (2017) "Successful transfer of umbilical cord blood CD34+ hematopoietic stem and progenitor-derived NK cells in older acute myeloid leukemia

patients," *Clinical Cancer Research*, 23(15), pp. 4107–4118. doi:10.1158/1078-0432.CCR-16-2981.

Domenis, R. *et al.* (2017) "Characterization of the Proinflammatory Profile of Synovial Fluid-Derived Exosomes of Patients with Osteoarthritis," *Mediators of Inflammation*, 2017. doi:10.1155/2017/4814987.

Dominici, M. *et al.* (2006) "Minimal criteria for defining multipotent mesenchymal stromal cells. The International Society for Cellular Therapy position statement," *Cytotherapy*, 8(4), pp. 315–317. doi:10.1080/14653240600855905.

Dorsey J, Bradshaw M. Effectiveness of Occupational Therapy Interventions for Lower-Extremity Musculoskeletal Disorders: A Systematic Review. Am J Occup Ther. 2017 Jan/Feb;71(1):7101180030p1-7101180030p11. doi: 10.5014/ajot.2017.023028. PMID: 28027040.

Ebert, A.D., Liang, P. and Wu, J.C. (2012) "Induced pluripotent stem cells as a disease modeling and drug screening platform," *Journal of Cardiovascular Pharmacology*, pp. 408–416. doi:10.1097/FJC.0b013e318247f642.

Eger, W. *et al.* (2002) *Human knee and ankle cartilage explants: catabolic differences *, Joiirnal of Orthopaedic Research*. Available at: www.eisevier.com/locate/orthres.

Ehninger, A. and Trumpp, A. (2011) "The bone marrow stem cell niche grows up: Mesenchymal stem cells and macrophages move in," *Journal of Experimental Medicine*, pp. 421–428. doi:10.1084/jem.20110132.

Eichler, F. *et al.* (2017) "Hematopoietic Stem-Cell Gene Therapy for Cerebral Adrenoleukodystrophy," *New England Journal of Medicine*, 377(17), pp. 1630–1638. doi:10.1056/nejmoa1700554.

Eitner, A., Hofmann, G.O. and Schaible, H.G. (2017) "Mechanisms of osteoarthritic pain. Studies in humans and experimental models," *Frontiers in Molecular Neuroscience*. Frontiers Media S.A. doi:10.3389/fnmol.2017.00349.

Elliott, M.J. *et al.* (2012) "Stem-cell-based, tissue engineered tracheal replacement in a child: A 2-year follow-up study," *The Lancet*, 380(9846), pp. 994–1000. doi:10.1016/S0140-6736(12)60737-5.

Enomoto, M. *et al.* (2019) "Anti-nerve growth factor monoclonal antibodies for the control of pain in dogs and cats," *Veterinary Record*. British Veterinary Association. doi:10.1136/vr.104590.

Eskander, M.A. *et al.* (2015) "Persistent nociception triggered by nerve growth factor (NGF) is mediated by TRPV1 and oxidative mechanisms," *Journal of Neuroscience*, 35(22), pp. 8593–8603. doi:10.1523/JNEUROSCI.3993-14.2015.

Fan, G. *et al.* (2000) *Knocking the NT4 gene into the BDNF locus rescues BDNF deficient mice and reveals distinct NT4 and BDNF activities*. Available at: http://neurosci.nature.com.

Fan, T.M. *et al.* (2008) "Investigating TrkA expression in canine appendicular osteosarcoma," *Journal of Veterinary Internal Medicine*, 22(5), pp. 1181–1188. doi:10.1111/j.1939-1676.2008.0151.x.

Fernández, O. *et al.* (2018) "Adipose-derived mesenchymal stem cells (AdMSC) for the treatment of secondary-progressive multiple sclerosis: A triple blinded, placebo controlled, randomized phase I/II safety and feasibility study," *PLoS ONE*, 13(5). doi:10.1371/journal.pone.0195891.

Filardo, G. *et al.* (2021) "PRP Injections for the Treatment of Knee Osteoarthritis: A Meta-Analysis of Randomized Controlled Trials," *Cartilage*, 13(1), pp. 364S-375S. doi:10.1177/1947603520931170.

Flores-Torales, E. *et al.* (2010) "The CD271 expression could be alone for establisher phenotypic marker in Bone Marrow derived mesenchymal stem cells," *Folia Histochemica et Cytobiologica*, 48(4), pp. 682–686. doi:10.2478/v10042-010-0063-6.

Frade, J.M. and Barde, Y.-A. (1998) *Nerve growth factor: two receptors, multiple functions*, *BioEssays*. John Wiley & Sons, Inc.

Friedenstein AJ, Chailakhjan RK, Lalykina KS. The development of fibroblast colonies in monolayer cultures of guinea-pig bone marrow and spleen cells. *Cell Tissue Kinet.* 1970;3(4):393-403. doi:10.1111/j.1365-2184.1970.tb00347.x

Frühbeis, C. *et al.* (2013) "Extracellular vesicles as mediators of neuron-glia communication," *Frontiers in Cellular Neuroscience* [Preprint]. doi:10.3389/fncel.2013.00182.

Ganguly, P. *et al.* (2017) "Age-related Changes in Bone Marrow Mesenchymal Stromal Cells: A Potential Impact on Osteoporosis and Osteoarthritis Development," *Cell Transplantation*. SAGE Publications Ltd, pp. 1520–1529. doi:10.1177/0963689717721201.

Gao, K. *et al.* (2020) "Association between cytokines and exosomes in synovial fluid of individuals with knee osteoarthritis," *Modern Rheumatology*, 30(4), pp. 758–764. doi:10.1080/14397595.2019.1651445.

Gao, M. *et al.* (2018) "Exosomes—the enigmatic regulators of bone homeostasis," *Bone Research*. Sichuan University. doi:10.1038/s41413-018-0039-2.

Garnero, P. *et al.* (2001) *Cross sectional evaluation of biochemical markers of bone, cartilage, and synovial tissue metabolism in patients with knee osteoarthritis: relations with disease activity and joint damage*. Available at: www.annrheumdis.com.

Gazdic, M. *et al.* (2015) "Mesenchymal Stem Cells: A Friend or Foe in Immune-Mediated Diseases," *Stem Cell Reviews and Reports*, 11(2), pp. 280–287. doi:10.1007/s12015-014-9583-3.

Ge M, Ke R, Cai T, Yang J, Mu X. Identification and proteomic analysis of osteoblast-derived exosomes. Biochem Biophys Res Commun. 2015 Nov 6;467(1):27-32. doi: 10.1016/j.bbrc.2015.09.135. Epub 2015 Sep 28. PMID: 26420226.

Geetha-Loganathan, P., Nimmagadda, S. and Scaal, M. (2008) "Wnt signaling in limb organogenesis," *Organogenesis*. Landes Bioscience, pp. 109–115. doi:10.4161/org.4.2.5857.

Gelse, K., Pöschl, E. and Aigner, T. (2003) "Collagens - Structure, function, and biosynthesis," *Advanced Drug Delivery Reviews*, 55(12), pp. 1531–1546. doi:10.1016/j.addr.2003.08.002.

Giannotti, S. *et al.* (2013) "Use of Autologous Human mesenchymal Stromal Cell/Fibrin Clot Constructs in Upper Limb Non-Unions: Long-Term Assessment," *PLoS ONE*, 8(8). doi:10.1371/journal.pone.0073893.

Gigante, Antonio *et al.* (2002) *Expression of NGF, Trka and p75 in human cartilage*, *European Journal of Histochemistry*.

Gilbert SF. Developmental Biology. 6th edition. Sunderland (MA): Sinauer Associates; 2000. Formation of the Limb Bud. Available from: https://www.ncbi.nlm.nih.gov/books/NBK10003/

Ginty,'t Axad Bonni, D.D. and Greenberg', M.E. (1994) *Nerve Growth Factor Activates a Ras-Dependent Protein Kinase That Stimulates c-fos Transcription via Phosphotylation of CREB*, *Cell*.

Glassberg, M.K. *et al.* (2017) "Allogeneic Human Mesenchymal Stem Cells in Patients With Idiopathic Pulmonary Fibrosis via Intravenous Delivery (AETHER): A Phase I Safety Clinical Trial," in *Chest*. Elsevier Inc, pp. 971–981. doi:10.1016/j.chest.2016.10.061.

Glyn-Jones, S. *et al.* (2015) "Osteoarthritis," in *The Lancet*. Lancet Publishing Group, pp. 376–387. doi:10.1016/S0140-6736(14)60802-3.

Gnecchi, M. *et al.* (2006) "Evidence supporting paracrine hypothesis for Akt-modified mesenchymal stem cell-mediated cardiac protection and functional improvement," *The FASEB Journal*, 20(6), pp. 661–669. doi:10.1096/fj.05-5211com.

Goldring, M.B. and Marcu, K.B. (2009) "Cartilage homeostasis in health and rheumatic diseases," *Arthritis Research and Therapy*. doi:10.1186/ar2592.

Goolaerts, A. *et al.* (2014) "Conditioned media from mesenchymal stromal cells restore sodium transport and preserve epithelial permeability in an *in vitro* model of acute alveolar injury." doi:10.1152/ajplung.00242.2013.-Mesenchy.

Gordon, J., Amini, S. and White, M.K. (2013) "General overview of neuronal cell culture," *Methods in Molecular Biology*, pp. 1–8. doi:10.1007/978-1-62703-640-5_1.

Götherström, C. *et al.* (2014) "Pre- and Postnatal Transplantation of Fetal Mesenchymal Stem Cells in Osteogenesis Imperfecta: A Two-Center Experience," *Stem Cells Translational Medicine*, 3(2), pp. 255–264. doi:10.5966/sctm.2013-0090.

Gowrishankar, K., Zeidler, M.G. and Vincenz, C. (2004) "Release of a membrane-bound death domain by γ-secretase processing of the p75NTR homolog NRADD," *Journal of Cell Science*, 117(18), pp. 4099–4111. doi:10.1242/jcs.01263.

Grässel, S. and Muschter, D. (2020) "Recent advances in the treatment of osteoarthritis," *F1000Research.* F1000 Research Ltd. doi:10.12688/f1000research.22115.1.

Grills BL, Schuijers JA. Immunohistochemical localization of nerve growth factor in fractured and unfractured rat bone. Acta Orthop Scand. 1998 Aug;69(4):415-9. doi: 10.3109/17453679808999059. PMID: 9798454.

Gronthos, S. and Simmons, P.J. (1995) *The Growth Factor Requirements of STRO-I-Positive Human Bone Marrow Stromal Precursors Under Serum-Deprived Conditions In Vitro.* Available at: https://ashpublications.org/blood/article-pdf/85/4/929/615261/929.pdf.

Gruen, M.E., Myers, J.A.E. and Lascelles, B.D.X. (2021) "Efficacy and Safety of an Anti-nerve Growth Factor Antibody (Frunevetmab) for the Treatment of Degenerative Joint Disease-Associated Chronic Pain in Cats: A Multisite Pilot Field Study," *Frontiers in Veterinary Science*, 8. doi:10.3389/fvets.2021.610028.

Gs, M. and Mologhianu G (2014) *Osteoarthritis pathogenesis-a complex process that involves the entire joint, Journal of Medicine and Life.*

Gu, Y. zheng *et al.* (2013) "Different roles of PD-L1 and FasL in immunomodulation mediated by human placenta-derived mesenchymal stem cells," *Human Immunology*, 74(3), pp. 267–276. doi:10.1016/j.humimm.2012.12.011.

Gupta, V.K. *et al.* (2013) "TrkB receptor signalling: Implications in neurodegenerative, psychiatric and proliferative disorders," *International Journal of Molecular Sciences.* MDPI AG, pp. 10122–10142. doi:10.3390/ijms140510122.

Halliday, D.A. *et al.* (1998) *Elevated Nerve Growth Factor Levels in the Synovial Fluid of Patients with Inflammatory Joint Disease, Neurochemical Research.*

Han, L., Grodzinsky, A.J. and Ortiz, C. (2011) "Nanomechanics of the cartilage extracellular matrix," *Annual Review of Materials Research*, 41, pp. 133–168. doi:10.1146/annurev-matsci-062910-100431.

Hao, H.Q. *et al.* (2019) "Cartilage oligomeric matrix protein, C-terminal cross-linking telopeptide of type II collagen, and matrix metalloproteinase-3 as biomarkers for knee and hip osteoarthritis (OA) diagnosis: a systematic review and meta-analysis," *Osteoarthritis and Cartilage.* W.B. Saunders Ltd, pp. 726–736. doi:10.1016/j.joca.2018.10.009.

Harrell, C. *et al.* (2019) "Molecular Mechanisms Responsible for Therapeutic Potential of Mesenchymal Stem Cell-Derived Secretome," *Cells*, 8(5), p. 467. doi:10.3390/cells8050467.

Harrington, A.W. *et al.* (2004) *Secreted proNGF is a pathophysiological death-inducing ligand after adult CNS injury.* Available at: www.pnas.orgcgidoi10.1073pnas.0305755101.

Hassanzadeh, A. *et al.* (2021) "Mesenchymal stem/stromal cell-derived exosomes in regenerative medicine and cancer; overview of development, challenges, and

opportunities," *Stem Cell Research and Therapy*. BioMed Central Ltd. doi:10.1186/s13287-021-02378-7.

Hauge, E.M. *et al.* (2001) *Cancellous Bone Remodeling Occurs in Specialized Compartments Lined by Cells Expressing Osteoblastic Markers.*

He, X.L. and Garcia, K.C. (2004) "Structure of Nerve Growth Factor Complexed with the Shared Neurotrophin Receptor p75," *Science*, 304(5672), pp. 870–875. doi:10.1126/science.1095190.

Hefti, F.F. *et al.* (2006) "Novel class of pain drugs based on antagonism of NGF," *Trends in Pharmacological Sciences*, pp. 85–91. doi:10.1016/j.tips.2005.12.001.

Hempstead, B.L. (2002) "The many faces of p75NTR," *Current Opinion in Neurobiology*. Elsevier Ltd, pp. 260–267. doi:10.1016/S0959-4388(02)00321-5.

Hermida-Gómez, T. *et al.* (2011) "Bone marrow cells immunomagnetically selected for CD271+ antigen promote *in vitro* the repair of articular cartilage defects," *Tissue Engineering - Part A*, 17(7–8), pp. 1169–1179. doi:10.1089/ten.tea.2010.0346.

Hernigou, P.H. *et al.* (2005) *PERCUTANEOUS AUTOLOGOUS BONE-MARROW GRAETING EOR NONUNIONS INFLUENCE OF THE NUMBER AND CONCENTRATION OF PROGENITOR CELLS*. Available at: www.jbjs.org.

Herrup, K. and Shooter, E.M. (1973) *Properties of the 3 Nerve Growth Factor Receptor of Avian Dorsal Root Ganglia (iodination/membrane)*, *Part*. Available at: https://www.pnas.org.

Hiyama, E. and Hiyama, K., 2007. Telomere and telomerase in stem cells. *British Journal of Cancer*, 96(7), pp.1020-1024.

Houlton, J. *et al.* (2019a) "Therapeutic potential of neurotrophins for repair after brain injury: A helping hand from biomaterials," *Frontiers in Genetics*. Frontiers Media S.A. doi:10.3389/fnins.2019.00790.

Houlton, J. *et al.* (2019b) "Therapeutic potential of neurotrophins for repair after brain injury: A helping hand from biomaterials," *Frontiers in Genetics*. Frontiers Media S.A. doi:10.3389/fnins.2019.00790.

Hu, H. *et al.* (2021) "Endogenous repair and regeneration of injured articular cartilage: A challenging but promising therapeutic strategy," *Aging and Disease*. International Society on Aging and Disease, pp. 886–901. doi:10.14336/AD.2020.0902.

Huang, E.J. and Reichardt, L.F. (2001a) *NEUROTROPHINS: Roles in Neuronal Development and Function* *. Available at: www.annualreviews.org.

Huang, E.J. and Reichardt, L.F. (2001b) *NEUROTROPHINS: Roles in Neuronal Development and Function* *. Available at: www.annualreviews.org.

Huang, E.J. and Reichardt, L.F. (2003) "Trk receptors: Roles in neuronal signal transduction," *Annual Review of Biochemistry*, pp. 609–642. doi:10.1146/annurev.biochem.72.121801.161629.

Huang, Z. and Kraus, V.B. (2016) "Does lipopolysaccharide-mediated inflammation have a role in OA?," *Nature Reviews Rheumatology*. Nature Publishing Group, pp. 123–129. doi:10.1038/nrrheum.2015.158.

Hui, A.Y. *et al.* (2012) "A systems biology approach to synovial joint lubrication in health, injury, and disease," *Wiley Interdisciplinary Reviews: Systems Biology and Medicine*, pp. 15–37. doi:10.1002/wsbm.157.

Hunter, D.J., March, L. and Chew, M. (2020) "Osteoarthritis in 2020 and beyond: a Lancet Commission," *The Lancet*, 396, pp. 1711–1712. doi:10.1016/10.1001/jamapediatrics.2020.4573.

Hunter, D.J., Schofield, D. and Callander, E. (2014) "The individual and socioeconomic impact of osteoarthritis," *Nature Reviews Rheumatology*. Nature Publishing Group, pp. 437–441. doi:10.1038/nrrheum.2014.44.

Hutchison, M.R. (2012) "BDNF alters ERK/p38 MAPK activity ratios to promote differentiation in growth plate chondrocytes," *Molecular Endocrinology*, 26(8), pp. 1406–1416. doi:10.1210/me.2012-1063.

Hutchison, M.R., Bassett, M.H. and White, P.C. (2010) "SCF, BDNF, and Gas6 are regulators of growth plate chondrocyte proliferation and differentiation," *Molecular Endocrinology*, 24(1), pp. 193–203. doi:10.1210/me.2009-0228.

Hwang, J.J. *et al.* (2021) "Recent Developments in Clinical Applications of Mesenchymal Stem Cells in the Treatment of Rheumatoid Arthritis and Osteoarthritis," *Frontiers in Immunology*. Frontiers Media S.A. doi:10.3389/fimmu.2021.631291.

Idrisova, K.F. *et al.* (2022) "Application of neurotrophic and proangiogenic factors as therapy after peripheral nervous system injury," *Neural Regeneration Research*. Wolters Kluwer Medknow Publications, pp. 1240–1247. doi:10.4103/1673-5374.327329.

jaber, H. *et al.* (2021) "The therapeutic effects of adipose-derived mesenchymal stem cells on obesity and its associated diseases in diet-induced obese mice," *Scientific Reports*, 11(1). doi:10.1038/s41598-021-85917-9.

Jacobson, M.D. and Weil, M. (1997) *Programmed Cell Death Review in Animal Development*, *Cell*.

Jaffe, A.B. and Hall, A. (2005) "Rho GTPases: Biochemistry and biology," *Annual Review of Cell and Developmental Biology*, pp. 247–269. doi:10.1146/annurev.cellbio.21.020604.150721.

Jahan, S. *et al.* (2017) "Neurotrophic factor mediated neuronal differentiation of human cord blood mesenchymal stem cells and their applicability to assess the developmental neurotoxicity," *Biochemical and Biophysical Research Communications*, 482(4), pp. 961–967. doi:10.1016/j.bbrc.2016.11.140.

Jiang, M.H. *et al.* (2015) "Nestin+ kidney resident mesenchymal stem cells for the treatment of acute kidney ischemia injury," *Biomaterials*, 50(1), pp. 56–66. doi:10.1016/j.biomaterials.2015.01.029.

Jones, E.A. *et al.* (2002) "Isolation and characterization of bone marrow multipotential mesenchymal progenitor cells," *Arthritis and Rheumatism*, 46(12), pp. 3349–3360. doi:10.1002/art.10696.

Jones, E.A. *et al.* (2004) "Enumeration and Phenotypic Characterization of Synovial Fluid Multipotential Mesenchymal Progenitor Cells in Inflammatory and Degenerative Arthritis," *Arthritis and Rheumatism*, 50(3), pp. 817–827. doi:10.1002/art.20203.

Jones, E.A. *et al.* (2006) "Optimization of a flow cytometry-based protocol for detection and phenotypic characterization of multipotent mesenchymal stromal cells from human bone marrow," *Cytometry Part B - Clinical Cytometry*, 70(6), pp. 391–399. doi:10.1002/cyto.b.20118.

Jung, K.M. *et al.* (2003) "Regulated Intramembrane Proteolysis of the p75 Neurotrophin Receptor Modulates Its Association with the TrkA Receptor," *Journal of Biological Chemistry*, 278(43), pp. 42161–42169. doi:10.1074/jbc.M306028200.

Jung, M.K. and Mun, J.Y. (2018) "Sample preparation and imaging of exosomes by transmission electron microscopy," *Journal of Visualized Experiments*, 2018(131). doi:10.3791/56482.

Karantalis, V. *et al.* (2014) "Autologous mesenchymal stem cells produce concordant improvements in regional function, tissue perfusion, and fibrotic burden when administered to patients undergoing coronary artery bypass grafting: The prospective randomized study of mesenchymal stem cell therapy in patients undergoing cardiac surgery (PROMETHEUS) trial," *Circulation Research*, 114(8), pp. 1302–1310. doi:10.1161/CIRCRESAHA.114.303180.

Kelamangalath, L. and Smith, G.M. (2013) "Neurotrophin treatment to promote regeneration after traumatic CNS injury," *Frontiers in Biology*. Higher Education Press Limited Company, pp. 486–495. doi:10.1007/s11515-013-1269-8.

Khursigara, G. *et al.* (2001) *A Prosurvival Function for the p75 Receptor Death Domain Mediated via the Caspase Recruitment Domain Receptor-Interacting Protein 2*.

Khursigara, G., Orlinick, J.R. and Chao, M. v. (1999) "Association of the p75 neurotrophin receptor with TRAF6," *Journal of Biological Chemistry*, 274(5), pp. 2597–2600. doi:10.1074/jbc.274.5.2597.

Kiani, C. *et al.* (2002) *Structure and function of aggrecan, Cell Research*. Available at: http://www.cell-research.com.

Kim, Y.C. *et al.* (2009) *The transcriptome of human CD34 hematopoietic stem-progenitor cells*. Available at: www.pnas.org/cgi/content/full/.

Knight RD, Schilling TF. Cranial neural crest and development of the head skeleton. Adv Exp Med Biol. 2006;589:120-33. doi: 10.1007/978-0-387-46954-6_7. PMID: 17076278.

Kokkaliaris, K.D. and Scadden, D.T. (2020) "Cell interactions in the bone marrow microenvironment affecting myeloid malignancies," *Blood Advances*. American Society of Hematology, pp. 3795–3803. doi:10.1182/bloodadvances.2020002127.

Kolesky, D.B. *et al.* (2016) "Three-dimensional bioprinting of thick vascularized tissues," *Proceedings of the National Academy of Sciences of the United States of America*, 113(12), pp. 3179–3184. doi:10.1073/pnas.1521342113.

Kolhe, R. *et al.* (2017) "Gender-specific differential expression of exosomal miRNA in synovial fluid of patients with osteoarthritis," *Scientific Reports*, 7(1). doi:10.1038/s41598-017-01905-y.

Kolios, G. and Moodley, Y. (2012) "Introduction to stem cells and regenerative medicine," *Respiration*, pp. 3–10. doi:10.1159/000345615.

Kolli, S. *et al.* (2019) "The Role of Nerve Growth Factor in Maintaining Proliferative Capacity, Colony-Forming Efficiency, and the Limbal Stem Cell Phenotype," *Stem Cells*, 37(1), pp. 139–149. doi:10.1002/stem.2921.

Kong, C.M. *et al.* (2019) "Changes in Stemness Properties, Differentiation Potential, Oxidative Stress, Senescence and Mitochondrial Function in Wharton's Jelly Stem Cells of Umbilical Cords of Mothers with Gestational Diabetes Mellitus," *Stem Cell Reviews and Reports*, 15(3), pp. 415–426. doi:10.1007/s12015-019-9872-y.

Kraus, V.B. *et al.* (2015) "Call for standardized definitions of osteoarthritis and risk stratification for clinical trials and clinical use," *Osteoarthritis and Cartilage*. W.B. Saunders Ltd, pp. 1233–1241. doi:10.1016/j.joca.2015.03.036.

Kuang MJ, Huang Y, Zhao XG, Zhang R, Ma JX, Wang DC, Ma XL. Exosomes derived from Wharton's jelly of human umbilical cord mesenchymal stem cells reduce osteocyte apoptosis in glucocorticoid-induced osteonecrosis of the femoral head in rats via the miR-21-PTEN-AKT signalling pathway. Int J Biol Sci. 2019 Jul 20;15(9):1861-1871. doi: 10.7150/ijbs.32262. PMID: 31523188; PMCID: PMC6743291.

Kuçi, Z. *et al.* (2011) "Mesenchymal stromal cells derived from CD271+ bone marrow mononuclear cells exert potent allosuppressive properties," *Cytotherapy*, 13(10), pp. 1193–1204. doi:10.3109/14653249.2011.605118.

Kuriyan, A.E. *et al.* (2017) "Vision Loss after Intravitreal Injection of Autologous 'Stem Cells' for AMD," *New England Journal of Medicine*, 376(11), pp. 1047–1053. doi:10.1056/nejmoa1609583.

Kuruvilla R, Ye H, Ginty DD. Spatially and functionally distinct roles of the PI3-K effector pathway during NGF signaling in sympathetic neurons. Neuron. 2000 Sep;27(3):499-512. doi: 10.1016/s0896-6273(00)00061-1. PMID: 11055433.

Lago, R. *et al.* (2008) "A new player in cartilage homeostasis: adiponectin induces nitric oxide synthase type II and pro-inflammatory cytokines in chondrocytes," *Osteoarthritis and Cartilage*, 16(9), pp. 1101–1109. doi:10.1016/j.joca.2007.12.008.

Lane, N.E. *et al.* (2007) "Wnt signaling antagonists are potential prognostic biomarkers for the progression of radiographic hip osteoarthritis in elderly Caucasian women," *Arthritis and Rheumatism*, 56(10), pp. 3319–3325. doi:10.1002/art.22867.

Larsson, S. *et al.* (2012) "The association between changes in synovial fluid levels of ARGS-aggrecan fragments, progression of radiographic osteoarthritis and self-reported outcomes: A cohort study," *Osteoarthritis and Cartilage*, 20(5), pp. 388–395. doi:10.1016/j.joca.2012.02.001.

Lee, S. *et al.* (2021) "NGF-TrkA signaling dictates neural ingrowth and aberrant osteochondral differentiation after soft tissue trauma," *Nature Communications*, 12(1). doi:10.1038/s41467-021-25143-z.

Levi-Montalcini, R. (1954) *EFFECTS OF MOUSE TUMOR TRANSPLANTATION ON THE NERVOUS SYSTEM.*

Lewin', G.R., Rueff, A. and Mendell, L.M. (1994) *Peripheral and Central Mechanisms of NGF-induced H yperalgesia*, *European Journul of Neuroscience. Wd.*

Li J, Wong WH, Chan S, Chim JC, Cheung KM, Lee TL, Au WY, Ha SY, Lie AK, Lau YL, Liang RH, Chan GC. Factors affecting mesenchymal stromal cells yield from bone marrow aspiration. Chin J Cancer Res. 2011 Mar;23(1):43-8. doi: 10.1007/s11670-011-0043-1. PMID: 23467386; PMCID: PMC3587522.

Li X, Sun DC, Li Y, Wu XY. Neurotrophin-3 improves fracture healing in rats. Eur Rev Med Pharmacol Sci. 2018 Apr;22(8):2439-2446. doi: 10.26355/eurrev_201804_14837. PMID: 29762846.

Li, J. *et al.* (2020) "p75NTR optimizes the osteogenic potential of human periodontal ligament stem cells by up-regulating α1 integrin expression," *Journal of Cellular and Molecular Medicine*, 24(13), pp. 7563–7575. doi:10.1111/jcmm.15390.

Li, Z.J. *et al.* (2021) "Application of adipose-derived stem cells in treating fibrosis," *World Journal of Stem Cells*, 13(11), pp. 1747–1761. doi:10.4252/wjsc.v13.i11.1747.

Lindsay, J.O. *et al.* (2017) "Autologous stem-cell transplantation in treatment-refractory Crohn's disease: an analysis of pooled data from the ASTIC trial," *The Lancet Gastroenterology and Hepatology*, 2(6), pp. 399–406. doi:10.1016/S2468-1253(17)30056-0.

Loeser, R.F. *et al.* (2012a) "Osteoarthritis: A disease of the joint as an organ," *Arthritis and Rheumatism*, pp. 1697–1707. doi:10.1002/art.34453.

Loeser, R.F. *et al.* (2012b) "Osteoarthritis: A disease of the joint as an organ," *Arthritis and Rheumatism*, pp. 1697–1707. doi:10.1002/art.34453.

Lu, P., Minowada, G. and Martin, G.R. (2006) "Increasing Fgf4 expression in the mouse limb bud causes polysyndactyly and rescues the skeletal defects that result from loss of Fgf8 function," *Development*, 133(1), pp. 33–42. doi:10.1242/dev.02172.

Lu, Y. *et al.* (2014) *Col10a1-Runx2 transgenic mice with delayed chondrocyte maturation are less susceptible to developing osteoarthritis*, *Am J Transl Res.* Available at: www.ajtr.org.

Lu, Z. *et al.* (2017) "Nerve Growth factor fromchinese cobravenom stimulates chondrogenic differentiation of mesenchymal stem cells," *Cell Death and Disease*, 8(5). doi:10.1038/cddis.2017.208.

Luyten, F.P., Tylzanowski, P. and Lories, R.J. (2009) "Wnt signaling and osteoarthritis," *Bone*, pp. 522–527. doi:10.1016/j.bone.2008.12.006.

Ma, Y. *et al.* (2006) "Reconstruction of Chemically Burned Rat Corneal Surface by Bone Marrow–Derived Human Mesenchymal Stem Cells," *Stem Cells*, 24(2), pp. 315–321. doi:10.1634/stemcells.2005-0046.

Maisonpierre PC, Belluscio L, Squinto S, Ip NY, Furth ME, Lindsay RM, Yancopoulos GD. Neurotrophin-3: a neurotrophic factor related to NGF and BDNF. Science. 1990 Mar 23;247(4949 Pt 1):1446-51. doi: 10.1126/science.247.4949.1446. PMID: 2321006.

Maldonado, M. and Nam, J. (2013) "The role of changes in extracellular matrix of cartilage in the presence of inflammation on the pathology of osteoarthritis," *BioMed Research International*. doi:10.1155/2013/284873.

Malemud, C.J. (2019) "Inhibition of MMPs and ADAM/ADAMTS," *Biochemical Pharmacology*. Elsevier Inc., pp. 33–40. doi:10.1016/j.bcp.2019.02.033.

Malfait, A.M., Miller, R.E. and Block, J.A. (2020) "Targeting neurotrophic factors: Novel approaches to musculoskeletal pain," *Pharmacology and Therapeutics*. Elsevier Inc. doi:10.1016/j.pharmthera.2020.107553.

Maloley, P.M. *et al.* (2021) "Performance of a commercially available multiplex platform in the assessment of circulating cytokines and chemokines in patients with rheumatoid arthritis and osteoarthritis," *Journal of Immunological Methods*, 495. doi:10.1016/j.jim.2021.113048.

Mamidipudi, V., Li, X. and Wooten, M.W. (2002) "Identification of interleukin 1 receptor-associated kinase as a conserved component in the p75-neurotrophin receptor activation of nuclear factor-κB," *Journal of Biological Chemistry*, 277(31), pp. 28010–28018. doi:10.1074/jbc.M109730200.

Marote, A. *et al.* (2016) "MSCs-derived exosomes: Cell-secreted nanovesicles with regenerative potential," *Frontiers in Pharmacology*. Frontiers Media S.A. doi:10.3389/fphar.2016.00231.

Martel-Pelletier, J. *et al.* (2008) "Cartilage in normal and osteoarthritis conditions," *Best Practice and Research: Clinical Rheumatology*, pp. 351–384. doi:10.1016/j.berh.2008.02.001.

Martel-Pelletier, J. *et al.* (2016) "Osteoarthritis," *Nature Reviews Disease Primers*. Nature Publishing Group. doi:10.1038/nrdp.2016.72.

Matthes, S.M. *et al.* (2013) "Intravenous transplantation of mesenchymal stromal cells to enhance peripheral nerve regeneration," *BioMed Research International*, 2013. doi:10.1155/2013/573169.

Meeker, R. and Williams, K. (2014) "Dynamic Nature of the p75 Neurotrophin Receptor in Response to Injury and Disease," *Journal of Neuroimmune Pharmacology*. Springer Science and Business Media, LLC, pp. 615–628. doi:10.1007/s11481-014-9566-9.

Mendelson, A. and Frenette, P.S. (2014) "Hematopoietic stem cell niche maintenance during homeostasis and regeneration," *Nature Medicine*. Nature Publishing Group, pp. 833–846. doi:10.1038/nm.3647.

Mendicino, M. *et al.* (2014) "MSC-based product characterization for clinical trials: An FDA perspective," *Cell Stem Cell*. Cell Press, pp. 141–145. doi:10.1016/j.stem.2014.01.013.

Merskey, H. and Watson *'~, G.D. (1979) *THE LATERALISATION OF PAIN*, *Pain*.

Michael, J.W.P., Schlüter-Brust, K.U. and Eysel, P. (2010) "Epidemiologie, ätiologie, diagnostik und therapie der gonarthrose," *Deutsches Arzteblatt*, pp. 152–162. doi:10.3238/arztebl.2010.0152.

Migliore, A. and Procopio, S. (2015) *Effectiveness and utility of hyaluronic acid in osteoarthritis*, *Clinical Cases in Mineral and Bone Metabolism*.

Miller, F.D. and Kaplan, D.R. (2001) *Neurotrophin signalling pathways regulating neuronal apoptosis*, *CMLS, Cell. Mol. Life Sci*.

Miller, R.E., Miller, R.J. and Malfait, A.M. (2014) "Osteoarthritis joint pain: The cytokine connection," *Cytokine*. Academic Press, pp. 185–193. doi:10.1016/j.cyto.2014.06.019.

Mitre, M., Mariga, A. and Chao, M. v. (2017) "Neurotrophin signalling: Novel insights into mechanisms and pathophysiology," *Clinical Science*. Portland Press Ltd, pp. 13–23. doi:10.1042/CS20160044.

Mödinger, Y. *et al.* (2019) "Reduced Terminal Complement Complex Formation in Mice Manifests in Low Bone Mass and Impaired Fracture Healing," *American Journal of Pathology*, 189(1), pp. 147–161. doi:10.1016/j.ajpath.2018.09.011.

Moore, E.R., Yang, Y. and Jacobs, C.R. (2018) "Primary cilia are necessary for Prx1-expressing cells to contribute to postnatal skeletogenesis," *Journal of Cell Science*, 131(16). doi:10.1242/jcs.217828.

Musiał-Wysocka, A., Kot, M. and Majka, M. (2019a) "The Pros and Cons of Mesenchymal Stem Cell-Based Therapies," *Cell Transplantation*. SAGE Publications Ltd, pp. 801–812. doi:10.1177/0963689719837897.

Musiał-Wysocka, A., Kot, M. and Majka, M. (2019b) "The Pros and Cons of Mesenchymal Stem Cell-Based Therapies," *Cell Transplantation*. SAGE Publications Ltd, pp. 801–812. doi:10.1177/0963689719837897.

Nagaya, N. *et al.* (2005) "Transplantation of mesenchymal stem cells improves cardiac function in a rat model of dilated cardiomyopathy," *Circulation*, 112(8), pp. 1128–1135. doi:10.1161/CIRCULATIONAHA.104.500447.

Najar, M. *et al.* (2020) "Mesenchymal Stromal Cell Immunology for Efficient and Safe Treatment of Osteoarthritis," *Frontiers in Cell and Developmental Biology*. Frontiers Media S.A. doi:10.3389/fcell.2020.567813.

Nakanishi T, Takahashi K, Aoki C, Nishikawa K, Hattori T, Taniguchi S. Expression of nerve growth factor family neurotrophins in a mouse osteoblastic cell line. Biochem Biophys Res Commun. 1994 Feb 15;198(3):891-7. doi: 10.1006/bbrc.1994.1127. PMID: 8117293.

Németh, K. *et al.* (2009) "Bone marrow stromal cells attenuate sepsis via prostaglandin E 2-dependent reprogramming of host macrophages to increase their interleukin-10 production," *Nature Medicine*, 15(1), pp. 42–49. doi:10.1038/nm.1905.

Nicodemou A, Danisovic L. Mesenchymal stromal/stem cell separation methods: concise review. Cell Tissue Bank. 2017 Dec;18(4):443-460. doi: 10.1007/s10561-017-9658-x. Epub 2017 Aug 18. PMID: 28821996.

Nicola, M. di *et al.* (2002) "Human bone marrow stromal cells suppress T-lymphocyte proliferation induced by cellular or nonspecific mitogenic stimuli," *Blood*, 99(10), pp. 3838–3843. doi:10.1182/blood.V99.10.3838.

Oegema, T.R. *et al.* (1997) *The Interaction of the Zone of Calcified Cartilage and Subchondral Bone in Osteoarthritis*. Wiley-Liss, Inc.

Olszewska-Slonina, D. *et al.* (2013) *The activity of cathepsin D and alpha-1 antitrypsin in hip and knee osteoarthritis*. Available at: www.actabp.pl.

Orozco, L. *et al.* (2011) "Intervertebral disc repair by autologous mesenchymal bone marrow cells: A pilot study," *Transplantation*, 92(7), pp. 822–828. doi:10.1097/TP.0b013e3182298a15.

Pan, J. *et al.* (2012) "Elevated cross-talk between subchondral bone and cartilage in osteoarthritic joints," *Bone*, 51(2), pp. 212–217. doi:10.1016/j.bone.2011.11.030.

Pittenger, M.F. *et al.* (1999) "Multilineage potential of adult human mesenchymal stem cells," *Science*, 284(5411), pp. 143–147. doi:10.1126/science.284.5411.143.

Qi X, Zhang J, Yuan H, Xu Z, Li Q, Niu X, Hu B, Wang Y, Li X. Exosomes Secreted by Human-Induced Pluripotent Stem Cell-Derived Mesenchymal Stem Cells Repair Critical-Sized Bone Defects through Enhanced Angiogenesis and Osteogenesis in Osteoporotic Rats. Int J Biol Sci. 2016 May 25;12(7):836-49. doi: 10.7150/ijbs.14809. PMID: 27313497; PMCID: PMC4910602.

Qi, X. *et al.* (2016) "Exosomes secreted by human-induced pluripotent stem cell-derived mesenchymal stem cells repair critical-sized bone defects through enhanced angiogenesis and osteogenesis in osteoporotic rats," *International Journal of Biological Sciences*, 12(7), pp. 836–849. doi:10.7150/ijbs.14809.

Qiu, X.C. *et al.* (2015) "Donor mesenchymal stem cell-derived neural-like cells transdifferentiate into myelin-forming cells and promote axon regeneration in rat spinal cord transection," *Stem Cell Research and Therapy*, 6(1). doi:10.1186/s13287-015-0100-7.

Quirici, N. *et al.* (2002) *Isolation of bone marrow mesenchymal stem cells by anti-nerve growth factor receptor antibodies*, *Experimental Hematology*.

Rani, S. *et al.* (2015) "Mesenchymal stem cell-derived extracellular vesicles: Toward cell-free therapeutic applications," *Molecular Therapy*. Nature Publishing Group, pp. 812–823. doi:10.1038/mt.2015.44.

Reichardt, L.F. (2006) "Neurotrophin-regulated signalling pathways," *Philosophical Transactions of the Royal Society B: Biological Sciences*. Royal Society, pp. 1545–1564. doi:10.1098/rstb.2006.1894.

Ren L, Song ZJ, Cai QW, Chen RX, Zou Y, Fu Q, Ma YY. Adipose mesenchymal stem cell-derived exosomes ameliorate hypoxia/serum deprivation-induced osteocyte apoptosis and osteocyte-mediated osteoclastogenesis *in vitro*. Biochem Biophys Res Commun. 2019 Jan 1;508(1):138-144. doi: 10.1016/j.bbrc.2018.11.109. Epub 2018 Nov 23. PMID: 30473217.

Rezza, A., Sennett, R. and Rendl, M. (2014) "Adult Stem Cell Niches. Cellular and Molecular Components.," in *Current Topics in Developmental Biology*. Academic Press Inc., pp. 333–372. doi:10.1016/B978-0-12-416022-4.00012-3.

Richard, D. *et al.* (2020) "Evolutionary Selection and Constraint on Human Knee Chondrocyte Regulation Impacts Osteoarthritis Risk," *Cell*, 181(2), pp. 362-381.e28. doi:10.1016/j.cell.2020.02.057.

Riegger, J., Palm, H.G. and Brenner, R.E. (2018) "The functional role of chondrogenic stem/progenitor cells: Novel evidence for immunomodulatory properties and regenerative potential after cartilage injury," *European Cells and Materials*, 36, pp. 110–127. doi:10.22203/eCM.v036a09.

Rim, Y.A. and Ju, J.H. (2021) "The role of fibrosis in osteoarthritis progression," *Life*. MDPI AG, pp. 1–13. doi:10.3390/life11010003.

Roccaro, A.M. *et al.* (2013) "BM mesenchymal stromal cell-derived exosomes facilitate multiple myeloma progression," *Journal of Clinical Investigation*, 123(4), pp. 1542–1555. doi:10.1172/JCI66517.

Rocco, M.L. *et al.* (2018) "Nerve Growth Factor: Early Studies and Recent Clinical Trials," *Current Neuropharmacology*, 16(10), pp. 1455–1465. doi:10.2174/1570159x16666180412092859.

Rodriguez-Tebar, A., Dechant, G. and Barde, Y. (1990) *Binding of Brain-Derived Neurotrophic Factor to the Nerve Growth Factor Receptor*, *Neuron*.

Rodriguez-Tebar', A. *et al.* (1992) *Binding of neurotrophin-3 to its neuronal receptors and interactions with nerve growth factor and brain-derived neurotrophic factor*, *The EMBO Journal*.

Rossi, D. *et al.* (2012) "Characterization of the Conditioned Medium from Amniotic Membrane Cells: Prostaglandins as Key Effectors of Its Immunomodulatory Activity," *PLoS ONE*, 7(10). doi:10.1371/journal.pone.0046956.

Roux, P.P. and Barker, P.A. (2002) *Neurotrophin signaling through the p75 neurotrophin receptor*, *Progress in Neurobiology*.

Sabri, M.I. and Ochs, S. (1971) *INHIBITION OF GLYCERALDEHYDE-3-PHOSPHATE DEHYDROGENASE IN MAMMALIAN NERVE BY IODOACETIC ACID*, *Journal of Neurochemistry*. Pergamon Press.

Salama-Cohen, P. *et al.* (2005) "NGF Controls Dendrite Development in Hippocampal Neurons by Binding to p75 NTR and Modulating the Cellular Targets of Notch," *Molecular Biology of the Cell*, 16, pp. 339–347. doi:10.1091/mbc.E04.

Sampey, A. v, Hutchinson, P. and Morand, E.F. (2000) *ANNEXIN I SURFACE BINDING SITES AND THEIR REGULATION ON HUMAN FIBROBLAST-LIKE SYNOVIOCYTES*, *ARTHRITIS & RHEUMATISM*.

Sarchielli, P. *et al.* (2001) "Levels of nerve growth factor in cerebrospinal fluid of chronic daily headache patients," *Neurology*, 57(1), pp. 132–134. doi:10.1212/WNL.57.1.132.

Secunda, R. *et al.* (2015) "Isolation, expansion and characterisation of mesenchymal stem cells from human bone marrow, adipose tissue, umbilical cord blood and matrix: a comparative study," *Cytotechnology*, 67(5), pp. 793–807. doi:10.1007/s10616-014-9718-z.

Setiawati, R. and Rahardjo, P. (2019) "Bone Development and Growth," in *Osteogenesis and Bone Regeneration*. IntechOpen. doi:10.5772/intechopen.82452.

Shang, X., Wang, Z. and Tao, H. (2017) "Mechanism and therapeutic effectiveness of nerve growth factor in osteoarthritis pain," *Therapeutics and Clinical Risk Management*, 13, pp. 951–956. doi:10.2147/TCRM.S139814.

Shen, L. *et al.* (2013) "Neurotrophin-3 accelerates wound healing in diabetic mice by promoting a paracrine response in mesenchymal stem cells," *Cell Transplantation*, 22(6), pp. 1011–1021. doi:10.3727/096368912X657495.

Sherbet, G.V. (2011) "Growth Factor Families," in *Growth Factors and Their Receptors in Cell Differentiation, Cancer and Cancer Therapy*. Elsevier, pp. 3–5. doi:10.1016/b978-0-12-387819-9.00002-5.

Silver, F.H., Bradica, G. and Tria, A. (2002) *Elastic energy storage in human articular cartilage: estimation of the elastic modulus for type II collagen and changes associated with osteoarthritis*, *Matrix Biology*.

Skriner, K. *et al.* (2006) "Association of citrullinated proteins with synovial exosomes," *Arthritis and Rheumatism*, 54(12), pp. 3809–3814. doi:10.1002/art.22276.

Soleimani, M. and Nadri, S. (2009) "A protocol for isolation and culture of mesenchymal stem cells from mouse bone marrow," *Nature Protocols*, 4(1), pp. 102–106. doi:10.1038/nprot.2008.221.

Sommerfeldt, D. and Rubin, C. (2001) "Biology of bone and how it orchestrates the form and function of the skeleton," *European Spine Journal*, 10(SUPPL. 2). doi:10.1007/s005860100283.

Soontornniyomkij, B. *et al.* (2011) "Tyrosine kinase B protein expression is reduced in the cerebellum of patients with bipolar disorder," *Journal of Affective Disorders*, 133(3), pp. 646–654. doi:10.1016/j.jad.2011.04.044.

Sophia Fox, A.J., Bedi, A. and Rodeo, S.A. (2009) "The basic science of articular cartilage: Structure, composition, and function," *Sports Health*, 1(6), pp. 461–468. doi:10.1177/1941738109350438.

Sperry, M.M. *et al.* (2017) "The Interface of Mechanics and Nociception in Joint Pathophysiology: Insights from the Facet and Temporomandibular Joints," *Journal of Biomechanical Engineering*, 139(2). doi:10.1115/1.4035647.

Squinto, S.P. *et al.* (1991) *t&B Encodes a Functional Receptor for Brain-Derived Neurotrophic Factor and Neurotrophin-3 but Not Nerve Growth Factor*, *Cell*.

Steinert, A.F. *et al.* (2007) "Major biological obstacles for persistent cell-based regeneration of articular cartilage," *Arthritis Research and Therapy*. doi:10.1186/ar2195.

Su, Y.W. *et al.* (2016) "Neurotrophin-3 Induces BMP-2 and VEGF Activities and Promotes the Bony Repair of Injured Growth Plate Cartilage and Bone in Rats," *Journal of Bone and Mineral Research*, 31(6), pp. 1258–1274. doi:10.1002/jbmr.2786.

Su, Y.W. *et al.* (2018) "Roles of neurotrophins in skeletal tissue formation and healing," *Journal of Cellular Physiology*. Wiley-Liss Inc., pp. 2133–2145. doi:10.1002/jcp.25936.

Sun H, Dai K, Tang T, Zhang X. Regulation of osteoblast differentiation by slit2 in osteoblastic cells. Cells Tissues Organs. 2009;190(2):69-80. doi: 10.1159/000178020. Epub 2008 Nov 25. PMID: 19033678.

Tamer, T.M. (2013) "Hyaluronan and synovial joint: Function, distribution and healing," *Interdisciplinary Toxicology*, pp. 111–125. doi:10.2478/intox-2013-0019.

Tang, K.C. *et al.* (2008) "Down-Regulation of MHC II in Mesenchymal Stem Cells at High IFN-γ Can Be Partly Explained by Cytoplasmic Retention of CIITA," *The Journal of Immunology*, 180(3), pp. 1826–1833. doi:10.4049/jimmunol.180.3.1826.

Tarafder, S. and Lee, C.H. (2016) "Synovial Joint: In Situ Regeneration of Osteochondral and Fibrocartilaginous Tissues by Homing of Endogenous Cells," in *In Situ Tissue Regeneration: Host Cell Recruitment and Biomaterial Design*. Elsevier Inc., pp. 253–273. doi:10.1016/B978-0-12-802225-2.00014-3.

Taruc-Uy, R.L. and Lynch, S.A. (2013) "Diagnosis and Treatment of Osteoarthritis," *Primary Care - Clinics in Office Practice*, pp. 821–836. doi:10.1016/j.pop.2013.08.003.

Tauszig-Delamasure, S. *et al.* (2007) *The TrkC receptor induces apoptosis when the dependence receptor notion meets the neurotrophin paradigm*. Available at: www.pnas.orgcgidoi10.1073pnas.0701243104.

Teitelbaum, S.L. (2000) "Bone resorption by osteoclasts," *Science*, pp. 1504–1508. doi:10.1126/science.289.5484.1504.

Teng, H.K. *et al.* (2005) "ProBDNF induces neuronal apoptosis via activation of a receptor complex of p75NTR and sortilin," *Journal of Neuroscience*, 25(22), pp. 5455–5463. doi:10.1523/JNEUROSCI.5123-04.2005.

Thakkar, U.G. *et al.* (2015) "Insulin-secreting adipose-derived mesenchymal stromal cells with bone marrow-derived hematopoietic stem cells from autologous and allogenic sources for type 1 diabetes mellitus," *Cytotherapy*, 17(7), pp. 940–947. doi:10.1016/j.jcyt.2015.03.608.

The STaTe of MuSculoSkeleTal healTh 2021 Arthritis and other musculoskeletal conditions in numbers (2021). Available at: www.versusarthritis.org.

Toh, W.S. *et al.* (2018) "MSC exosome works through a protein-based mechanism of action," *Biochemical Society Transactions*. Portland Press Ltd, pp. 843–853. doi:10.1042/BST20180079.

Tomlinson, R.E. *et al.* (2017) "NGF-TrkA signaling in sensory nerves is required for skeletal adaptation to mechanical loads in mice," *Proceedings of the National Academy of Sciences of the United States of America*, 114(18), pp. E3632–E3641. doi:10.1073/pnas.1701054114.

Ullah, I., Subbarao, R.B. and Rho, G.J. (2015a) "Human mesenchymal stem cells - Current trends and future prospective," *Bioscience Reports*. Portland Press Ltd. doi:10.1042/BSR20150025.

Ullah, I., Subbarao, R.B. and Rho, G.J. (2015b) "Human mesenchymal stem cells - current trends and future prospective," *Biosci. Rep. Bioscience Reports*, 35. doi:10.1042/BSR20150025.

Underwood, C.K. *et al.* (2008) "Palmitoylation of the C-terminal fragment of p75NTR regulates death signaling and is required for subsequent cleavage by γ-secretase," *Molecular and Cellular Neuroscience*, 37(2), pp. 346–358. doi:10.1016/j.mcn.2007.10.005.

Valfrè Di Bonzo, L. *et al.* (2008) "Human mesenchymal stem cells as a two-edged sword in hepatic regenerative medicine: Engraftment and hepatocyte differentiation versus profibrogenic potential," *Gut*, 57(2), pp. 223–231. doi:10.1136/gut.2006.111617.

van de Laar, M. *et al.* (2012) *Send Orders of Reprints at bspsaif@emirates.net.ae Pain Treatment in Arthritis-Related Pain: Beyond NSAIDs*, *The Open Rheumatology Journal*.

Vega, A. *et al.* (2015) "Treatment of knee osteoarthritis with allogeneic bone marrow mesenchymal stem cells: A randomized controlled trial," *Transplantation*, 99(8), pp. 1681–1690. doi:10.1097/TP.0000000000000678.

Veziroglu, E.M. and Mias, G.I. (2020) "Characterizing Extracellular Vesicles and Their Diverse RNA Contents," *Frontiers in Genetics*. Frontiers Media S.A. doi:10.3389/fgene.2020.00700.

Vilar, M. (2017) "Structural Characterization of the p75 Neurotrophin Receptor: A Stranger in the TNFR Superfamily," in *Vitamins and Hormones*. Academic Press Inc., pp. 57–87. doi:10.1016/bs.vh.2016.10.007.

Vilar, M. *et al.* (2009) "Ligand-independent signaling by disulfide-crosslinked dimers of the p75 neurotrophin receptor," *Journal of Cell Science*, 122(18), pp. 3351–3357. doi:10.1242/jcs.055061.

Volosin, M. *et al.* (2008) "Induction of proneurotrophins and activation of p75NTR-mediated apoptosis via neurotrophin receptor-interacting factor in hippocampal neurons after seizures," *Journal of Neuroscience*, 28(39), pp. 9870–9879. doi:10.1523/JNEUROSCI.2841-08.2008.

Wagers, A.J. (2012) "The stem cell niche in regenerative medicine," *Cell Stem Cell*, pp. 362–369. doi:10.1016/j.stem.2012.02.018.

Walter, S.G.; Randau, T.M.; Hilgers, C.; Haddouti, E.-M.; Masson, W.; Gravius, S.; Burger, C.; Wirtz, D.C.; Schildberg, F.A. Molecular and Functional Phenotypes of Human Bone Marrow-Derived Mesenchymal Stromal Cells Depend on Harvesting Techniques. *Int. J. Mol. Sci.* **2020**, *21*, 4382. https://doi.org/10.3390/ijms21124382

Wang, M., Yuan, Q. and Xie, L. (2018) "Mesenchymal stem cell-based immunomodulation: Properties and clinical application," *Stem Cells International*. Hindawi Limited. doi:10.1155/2018/3057624.

Wang, S. *et al.* (2013) "Umbilical cord mesenchymal stem cell transplantation significantly improves neurological function in patients with sequelae of traumatic brain injury," *Brain Research*, 1532, pp. 76–84. doi:10.1016/j.brainres.2013.08.001.

Watson, J.T. *et al.* (2013) "CD271 as a marker for mesenchymal stem cells in bone marrow versus umbilical cord blood," *Cells Tissues Organs*, 197(6), pp. 496–504. doi:10.1159/000348794.

Webber, (D J *et al.* (2012) "Autologous mesenchymal stem cells for the treatment of secondary progressive multiple sclerosis: an open-label phase 2a proof-of-concept study," *The Lancet Neurology*, 11, pp. 150–156. doi:10.1016/S1474.

Wehling, P. *et al.* (2017) "Effectiveness of intra-articular therapies in osteoarthritis: a literature review," *Therapeutic Advances in Musculoskeletal Disease*. SAGE Publications Ltd, pp. 183–196. doi:10.1177/1759720X17712695.

Wiatrak, B. *et al.* (2020) "PC12 Cell Line: Cell Types, Coating of Culture Vessels, Differentiation and Other Culture Conditions," *Cells*, 9(4). doi:10.3390/cells9040958.

Wise, B.L., Seidel, M.F. and Lane, N.E. (2021) "The evolution of nerve growth factor inhibition in clinical medicine," *Nature Reviews Rheumatology*. Nature Research, pp. 34–46. doi:10.1038/s41584-020-00528-4.

Woldeyesus, M.T. *et al.* (1999) *Peripheral nervous system defects in erbB2 mutants following genetic rescue of heart development.* Available at: www.genesdev.org.

Wolff, S.N. (2002) "Mini-review Second hematopoietic stem cell transplantation for the treatment of graft failure, graft rejection or relapse after allogeneic transplantation," *Bone Marrow Transplantation*, 29, pp. 545–552. doi:10.1038/sj/bmt/1703389.

Wu, P. *et al.* (2018) "MSC-exosome: A novel cell-free therapy for cutaneous regeneration," *Cytotherapy.* Elsevier B.V., pp. 291–301. doi:10.1016/j.jcyt.2017.11.002.

Xie X, Zhang C, Tuan RS. Biology of platelet-rich plasma and its clinical application in cartilage repair. Arthritis Res Ther. 2014 Feb 25;16(1):204. doi: 10.1186/ar4493. PMID: 25164150; PMCID: PMC3978832.

Xing J, Ginty DD, Greenberg ME. Coupling of the RAS-MAPK pathway to gene activation by RSK2, a growth factor-regulated CREB kinase. Science. 1996 Aug 16;273(5277):959-63. doi: 10.1126/science.273.5277.959. PMID: 8688081.

Yagami, K. *et al.* (1999) *Matrix GLA Protein Is a Developmental Regulator of Chondrocyte Mineralization and, When Constitutively Expressed, Blocks Endochondral and Intramembranous Ossification in the Limb*, *The Journal of Cell Biology.* Available at: http://www.jcb.org.

Yamashiro, T. *et al.* (2001) *Gene and Protein Expression of Brain-Derived Neurotrophic Factor and TrkB in Bone and Cartilage*.

Yan, Y. hui *et al.* (2016) "Neurotrophin-3 promotes proliferation and cholinergic neuronal differentiation of bone marrow- derived neural stem cells via notch signaling pathway," *Life Sciences*, 166, pp. 131–138. doi:10.1016/j.lfs.2016.10.004.

Yang, D. *et al.* (2013) "Stromal cell-derived factor-1 receptor CXCR4-overexpressing bone marrow mesenchymal stem cells accelerate wound healing by migrating into skin injury areas," *Cellular Reprogramming*, 15(3), pp. 206–215. doi:10.1089/cell.2012.0046.

Yang, J., Plikus, M. v. and Komarova, N.L. (2015) "The Role of Symmetric Stem Cell Divisions in Tissue Homeostasis," *PLoS Computational Biology*, 11(12). doi:10.1371/journal.pcbi.1004629.

Yang, Y.H.K. *et al.* (2018) "Changes in phenotype and differentiation potential of human mesenchymal stem cells aging *in vitro*," *Stem Cell Research and Therapy*, 9(1). doi:10.1186/s13287-018-0876-3.

Yao, Q. *et al.* (2017) "Neurotrophin 3 upregulates proliferation and collagen production in human aortic valve interstitial cells: A potential role in aortic valve sclerosis," *American Journal of Physiology - Cell Physiology*, 312(6), pp. C697–C706. doi:10.1152/ajpcell.00292.2016.

Yeiser, E.C. *et al.* (2004) "Neurotrophin signaling through the p75 receptor is deficient in traf6-/-mice," *Journal of Neuroscience*, 24(46), pp. 10521–10529. doi:10.1523/JNEUROSCI.1390-04.2004.

Yeo, R.W.Y. *et al.* (2013) "Mesenchymal stem cell: An efficient mass producer of exosomes for drug delivery," *Advanced Drug Delivery Reviews*, pp. 336–341. doi:10.1016/j.addr.2012.07.001.

Zhan, X. *et al.* (2019) "Comparative profiling of chondrogenic differentiation of mesenchymal stem cells (MSCs) driven by two different growth factors," *Cell Biochemistry and Function*, 37(5), pp. 359–367. doi:10.1002/cbf.3404.

Zhang Y, Cai F, Liu J, Chang H, Liu L, Yang A, Liu X. Transfer RNA-derived fragments as potential exosome tRNA-derived fragment biomarkers for osteoporosis. Int J Rheum Dis. 2018 Sep;21(9):1659-1669. doi: 10.1111/1756-185X.13346. PMID: 30345646.

Zhang, K. *et al.* (2016) "Chondrogenic cells respond to partial-thickness defects of articular cartilage in adult rats: an *in vivo* study," *Journal of Molecular Histology*, 47(3), pp. 249–258. doi:10.1007/s10735-016-9668-1.

Zhang, S. *et al.* (2016) "Exosomes derived from human embryonic mesenchymal stem cells promote osteochondral regeneration," *Osteoarthritis and Cartilage*, 24(12), pp. 2135–2140. doi:10.1016/j.joca.2016.06.022.

Zhang, Y. and Jordan, J.M. (2010) "Epidemiology of osteoarthritis," *Clinics in Geriatric Medicine*, pp. 355–369. doi:10.1016/j.cger.2010.03.001.

Zhang, Y. *et al.* (2018) "Transfer RNA-derived fragments as potential exosome tRNA-derived fragment biomarkers for osteoporosis," *International Journal of Rheumatic Diseases*, 21(9), pp. 1659–1669. doi:10.1111/1756-185X.13346.

Zhang, Y. *et al.* (2020) "Intravenous infusion of human umbilical cord Wharton's jelly-derived mesenchymal stem cells as a potential treatment for patients with COVID-19 pneumonia," *Stem Cell Research and Therapy*, 11(1). doi:10.1186/s13287-020-01725-4.

Zhou, Z. *et al.* (2018) "Adipose-derived stem-cell-implanted poly(ϵ-caprolactone)/chitosan scaffold improves bladder regeneration in a rat model," *Regenerative Medicine*, 13(3), pp. 331–342. doi:10.2217/rme-2017-0120.

Zhu, J. *et al.* (2015) "Enhanced angiogenesis promoted by human umbilical mesenchymal stem cell transplantation in stroked mouse is Notch1 signaling associated," *Neuroscience*, 290, pp. 288–299. doi:10.1016/j.neuroscience.2015.01.038.

Appendix

Patient Consent Form

Lab Ref:
DP_ILL_CCCU

PATIENT INFORMATION

USE OF HUMAN MATERIAL SURPLUS TO CLINICAL
REQUIREMENT FOR RESEARCH OR TRAINING

In the operation you will shortly have, some tissue may be removed. Normally this would be discarded. Scientists and surgeons working with Queen Mary's Hospital/Darent Valley Hospital and Canterbury Christ Church University (CCCU) may be able to use this tissue to develop new techniques in regenerating tissue damaged by disease or injury.

- No additional tissue will be taken during the operation other than that required for your surgery.
- They are asking for your permission to take this surplus tissue after your operation and use it for research or training purposes.
- The tissue will only be used for training surgeons and scientists or in research projects which will have been ethically approved by an NHS Research Ethics Committee.
- The tissue will not be sold for profit.
- The tissue will not be subject to any diagnostic testing.
- The tissue will not be used for the treatment of any other patient.
- Your tissue sample will be given a code number to make it anonymous for all research or training purposes.
- To comply with the Human Tissue Act (2004) to ensure all donated human tissues are used only for the purposes for which consent was given, a secure record will link your identity with the anonymous code. This will be made prior to the sample being used for research or training and will be identified thereafter by only the code number.
- After being used any remaining tissue will be disposed of in a dignified manner in accordance with the CCCU policy for the disposal of human tissue.
- If you do not wish to donate your surplus tissue, this will not affect your treatment in any way whatsoever
- If you are willing to donate your surplus tissue, please tick the "Agree" box below.
- If you do not wish your tissue to be used for research or training, please make sure you tick the "Do Not Agree" box.
- If you are not sure, please discuss with your surgeon before the procedure. This will not affect your treatment in any way.

☐ I have read and understand the above

☐ I have read the statements and have more question to ask
(In this case do not tick either box below, and discuss with Surgeon at time of surgery)

☐ ☐ Agreement to donate any tissue that would otherwise be thrown away to be used for research. PLEASE TICK APPROPRIATE BOX

AGREE   DO NOT AGREE

Signed
....

Date
....

Figure 7. 1. **Patient consent form**

UN3373

Biological Substance
Category B

From:
Queen Mary's Hospital
Sidcup / Darent Valley
Hospital, Dartford

To:
CCCU Industry Liaison Lab
Discovery Park, Sandwich
CT13 9FF

Comments:

Lab Ref:

This number MUST be copied into notes and on 3 consent forms

Date:

Consultant:

Age group:

Specimen:

Gender:

Check this box if patient is allergic to penicillin or streptomycin

This patient has no known Hazardous Pathology (check box)

Category B Specimens only
For samples being transferred to Discovery
Park Industry Liaison Lab
Canterbury Christ Church University

Figure 7. 2. Sample transportation form

Patient information

Table 7. 1.Summary of the patient data we were allowed to record

Sample Ref.	Sex	Age Group	Condition
OA1	M	75 - 80	Advanced hip OA
OA2	F	75 - 80	Advanced hip OA
OA3	F	45 - 50	Advanced hip OA
OA4	F	75 - 80	Advanced hip OA
OA5	F	45 - 50	Advanced hip OA
BM1	M	20 - 25	Healthy
BM2	F	20 - 25	Healthy

Standard curve for Alamar Blue cell viability assay in PC12

For the quantification of PC12 viability in order to observe the effects on NT-3 on the proliferation of these cells, PC12 at different densities (all the numbers on the y axis in the Fig. 7.1) were plated in 96 well culture dishes. Alamar Blue solution was added to each well at a final concentration of 1.6mM. The plate was incubated at 37°C, 5% CO_2. Measurement of the fluorescence at 544 nm were taken at every hour for a total of 6 hours. The time point when the highest density of cells reached maximisation was used for plotting the Standard Curve for this particular assay.

Based on this standard curve we calculated the number of cells with the below equation:

PC12 cell number = (Fluoresce recorder at 544 nm – 31853) / 0.1742

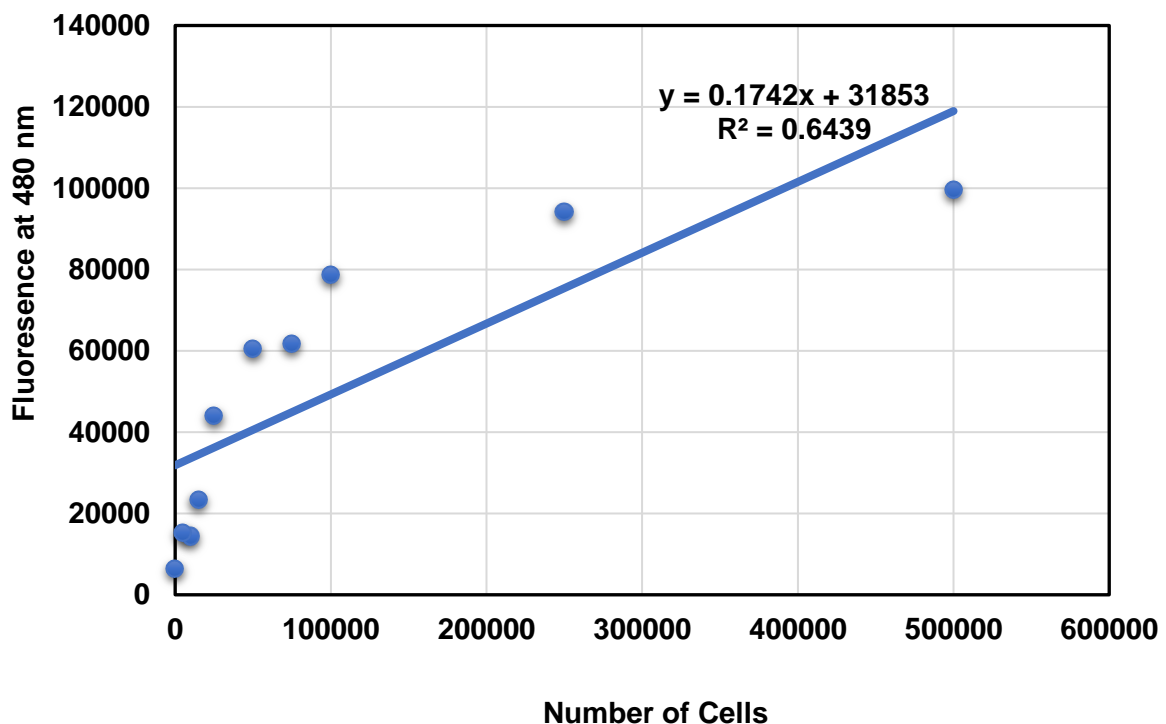**Alamar Blue assay Standard Curve for PC12**

Figure 7. 3. Alamar Blue assay Standard Curve
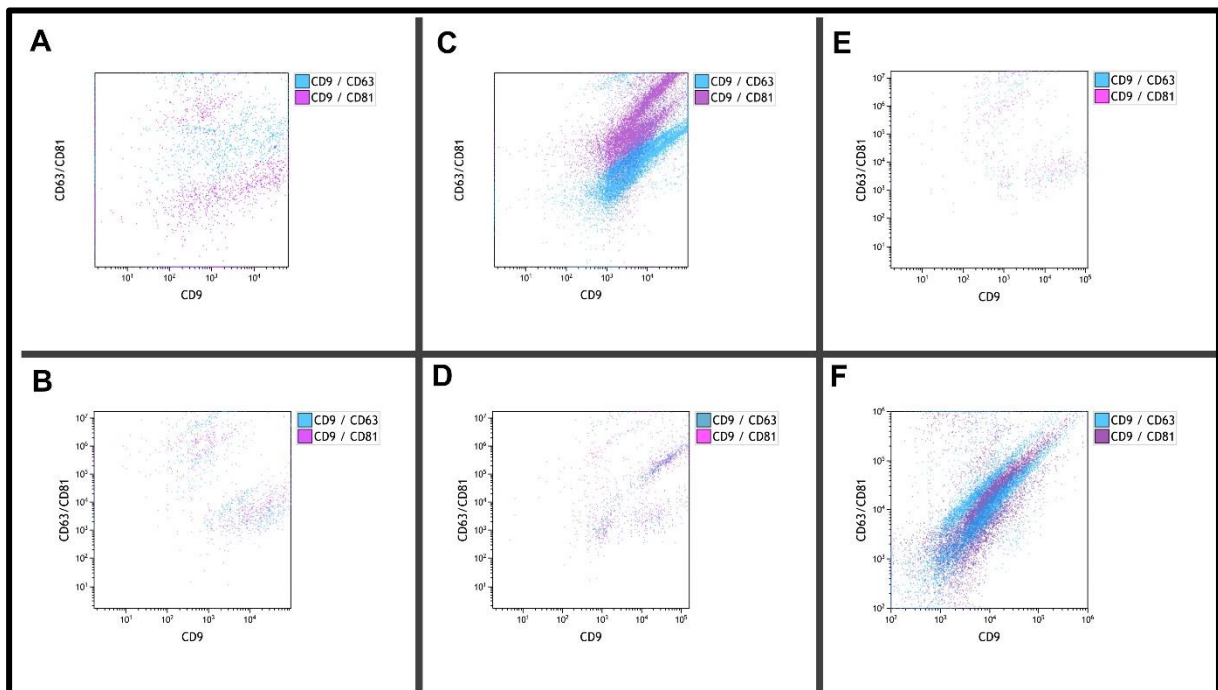
EVs flow cytometry dot plots

Figure 7. 4*. **The dot plots showing the maximum recorded fluorescence for CD9, CD63 and CD81 antibodies in the flow cytometry***
A. BM-hMSC-EVs at day 7, B. BM-hMSC-EVs at day 14, C. OA-hMSC-EVs at day 7, D. OA-hMSC-EVs at day 14, E. OA-hCPC-EVs at day 7 and F. OA-hCPCs at day 14
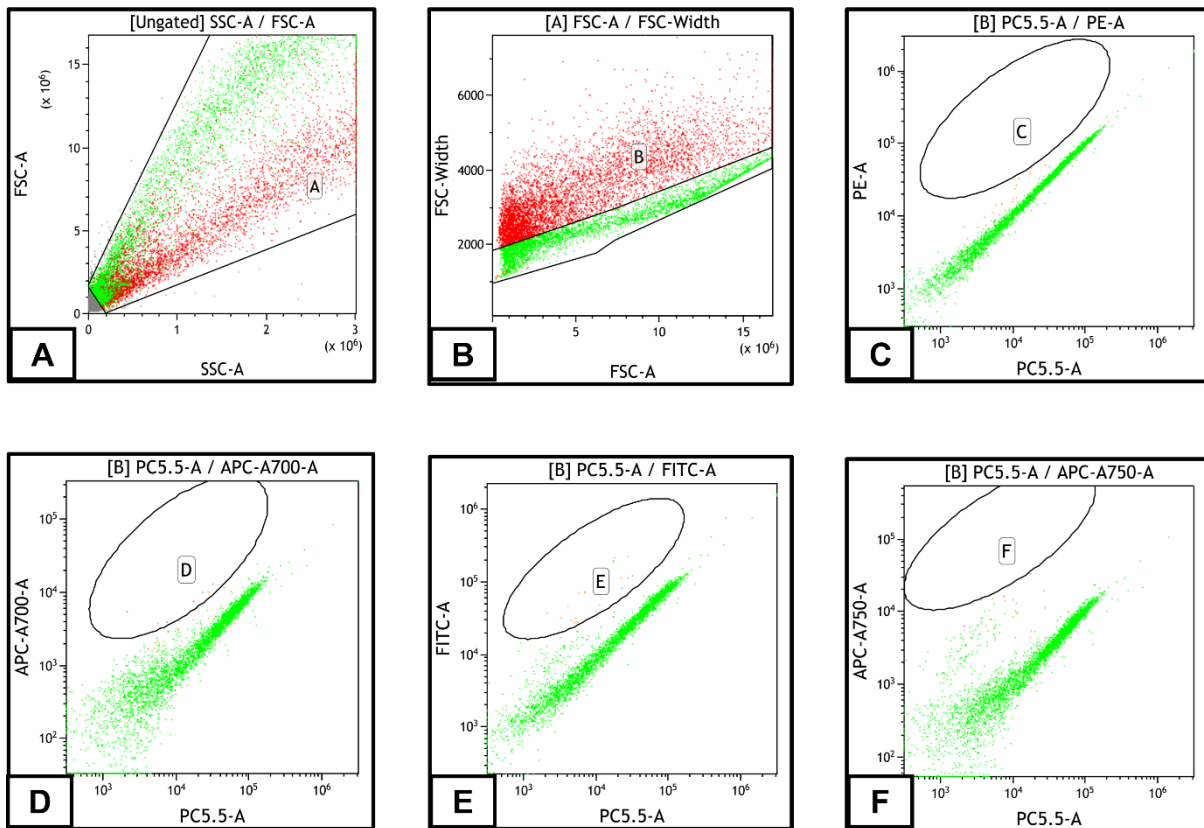
Figure 7.5. Gating strategy example applied in Flow Cytometry data analysis
This figure shows representatives dot plots including all the steps followed in order to establish the gating strategy for analysing the MSC immunophenotype in BM2-hMSC. To the above presented analysis, unstained BM2-hMSCs were used. (A). dot plot where the debris or unwanted cells are removed by Gate A; (B). dot plot where only the single recorded events are separated by gate B; (C) dot plot where the position of gate C for the detection of CD105+/CD45- events is determined; (D). dot plot where the position of gate D for the detection of CD90+/CD45- events is determined; (E.). dot plot where the position of gate E for the detection of CD271+/CD45- events is determined; (F). dot plot where the position of gate F for the detection of CD146+/CD45- events is determined.
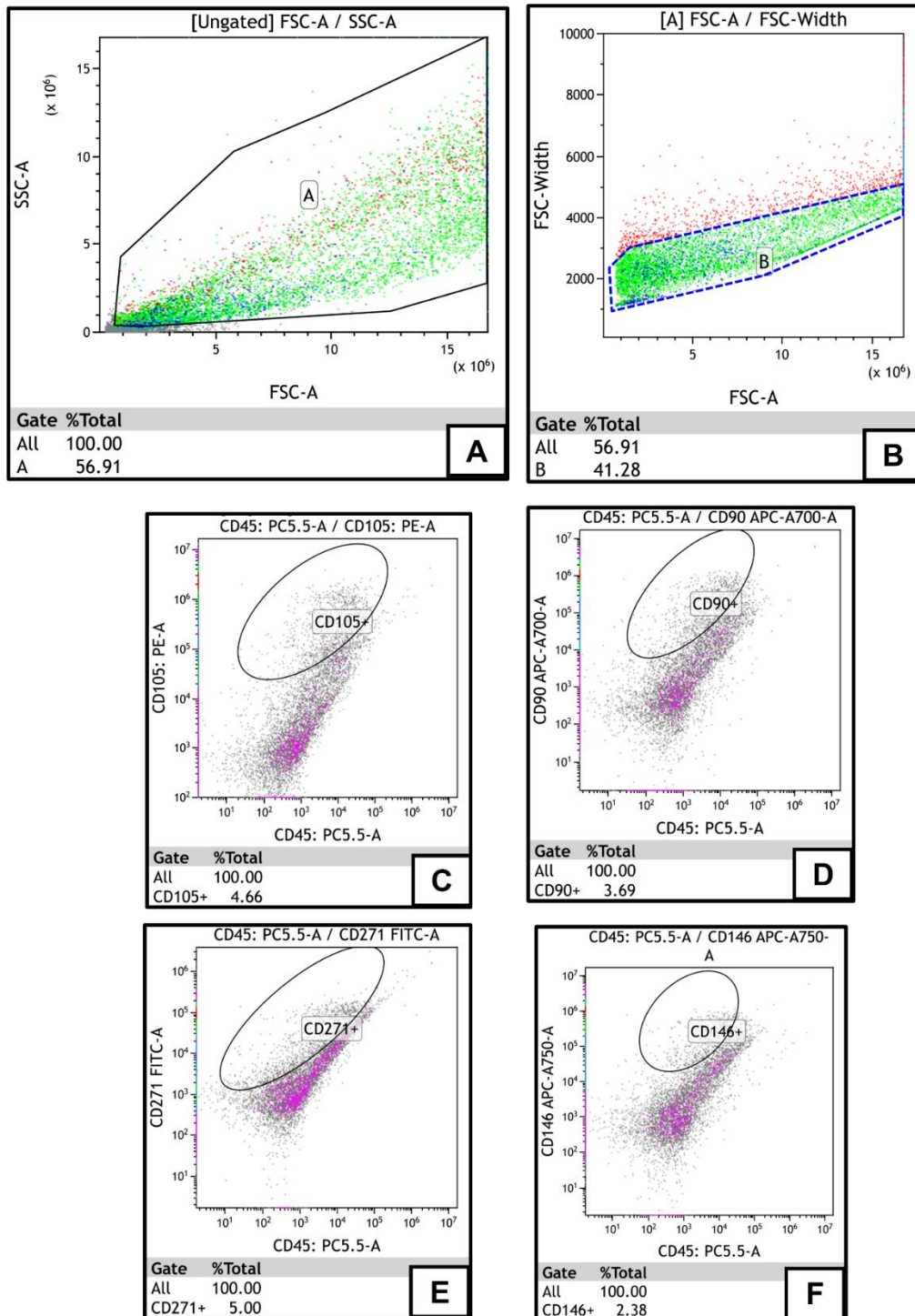
Figure 7.6. Detailed analysis of flow cytometry data for the assessment of MSC immunophenotype in BM2-hMSC

In the current figure, representative dot plots with all the steps included in the flow cytometry analysis are shown as following: (A). dot plot where the debris or unwanted cells are removed by gate A; (B). dot plot where only the events determined by gate A are shown. Gate B separates only the single recorded events; (C,D,E,F). events analysed based on the fluorescence intensity.